HIGH PERFORMANCE ALLOY ELECTROFORMING

FINAL REPORT

BAT REPORT NO. 8874-927001

PREPARED BY:

G. A. MALONE
AND
D. M. WINKELMAN

BELL AEROSPACE TEXTRON
DIVISION OF TEXTRON, INC.
POST OFFICE BOX ONE
BUFFALO, NEW YORK 14240-0001

PREPARED FOR:

NATIONAL AERONAUTICS AND SPACE ADMINISTRATION
NASA MARSHALL SPACE FLIGHT CENTER
CONTRACT NAS8-35817
DOUGLAS FRANKLIN, PROJECT MANAGER

Bell Aerospace TEXTRON
Division of Textron Inc.

Bell Aerospace TEXTRON

Bell Aerospace Textron
Division of Textron Inc.

Post Office Box One
Buffalo, New York 14240-0001
716/297-1000

HIGH PERFORMANCE ALLOY ELECTROFORMING

FINAL REPORT

BAT REPORT NO. 8874-927001

PREPARED BY:

G. A. MALONE
AND
D. M. WINKELMAN

BELL AEROSPACE TEXTRON
DIVISION OF TEXTRON, INC.
POST OFFICE BOX ONE
BUFFALO, NEW YORK 14240-0001

PREPARED FOR:

NATIONAL AERONAUTICS AND SPACE ADMINISTRATION
NASA MARSHALL SPACE FLIGHT CENTER
CONTRACT NAS8-35817
DOUGLAS FRANKLIN, PROJECT MANAGER

TABLE OF CONTENTS

1.0 SUMMARY

Electroformed copper and nickel are presently used in structural applications for advanced propellant combustion chamber applications. An improved process has been developed by BELL AEROSPACE TEXTRON, INC. wherein electroformed nickel-manganese alloy has demonstrated superior mechanical and thermal stability when compared to previously reported deposits from known nickel plating processes. Solution chemistry and parametric operating procedures are now established and material property data is established for deposition of thick, large complex shapes such as the Space Shuttle Main Engine.

The critical operating variables are those governing the ratio of codeposited nickel and manganese. The deposition uniformity which in turn affects the manganese concentration distribution is affected by solution resistance and geometric effects as well as solution agitation.

The manganese concentration in the deposit must be between 2000 ppm and 3000 ppm for optimum physical properties to be realized.

The study also includes data regarding deposition procedures for achieving excellent bond strength at an interface with copper, nickel-manganese or INCONEL 718.

Applications for this electroformed material include fabrication of complex or re-entry shapes which would be difficult or impossible to form from high strength alloys such as INCONEL 718.

2.0 INTRODUCTION

The main propulsion system of the reusable Space Shuttle Transportation System consists of three liquid propellant engines which provide the primary thrust during the initial ascent phase of vehicle launch. Upon ignition, the propellants partially burn at high pressure and low temperature in two preburners, and then are completely combusted at high temperature and pressure in a cylindrical structural chamber. This main combustion chamber (MCC) consists of a regeneratively fuel-cooled, NARloy-Z (copper alloy) coolant liner and a structural jacket. The liner of the MCC is manufactured by an electroforming process that deposits a barrier layer of copper followed by a thicker layer of nickel onto the NARloy-Z base. The liner must be structurally supported by a nickel-base alloy jacket.

The structural jacket of the MCC is produced from formed wrought metal segments which require numerous weldments. These weldments alter the mechanical properties of the base metal through heat affected zones. This requires strengthening of the alloy where joints are to be made to meet the structural requirements of the shroud.

The use of electroformable alloys with high temperature strength and ductility would have the potential for simplifying fabrication procedures for structural jackets. The overall weight would also be reduced by removing the weldments. This would lead to a structural improvement in the MCC, since the jacket would have less critical strength and thickness requirements. In addition, such an electroformable alloy has the potential for use in advanced engines where light weight and strength at high temperatures are necessary.

The following report is broken into three phases. Phase A consists of a literature survey in order to select the most promising structural alloy candidate. Optimization studies are performed on this alloy to develop deposition parameters by which alloys of consistently high strength and ductility can be produced. Phase B is concerned with application of the optimized alloy to a subscale version of the SSME main combustion chamber structural jacket presently fabricated by welded Inconel 718 sections. Phase C includes property and performance information beyond conventional properties. Mandrel shielding and bath parameters are studied further to provide more consistent high mechanical properties over complex hardware configurations. Design changes necessary to change from the presently welded SSME structural shrouds to an electroformed counterpart are examined.

3.0 PHASE A - SELECTION AND CHARACTERIZATION OF A HIGH PERFORMANCE ELECTROFORMABLE ALLOY

3.1 Introduction

The first major division of the program to study high performance alloy electroforming was Phase A. This phase was divided into two parts composed of literature and material characterization programs. The main purpose of the literature survey was to substantiate the selection of an electroformable alloy system from several potential candidates having the greatest potential for Space Shuttle Main Engine (SSME) application. The material characterization program was intended to demonstrate the ability of the selected alloy to provide improved high temperature strength and ductility for use in fabricating prototype components similar to SSME hardware and other advanced design engine parts.

At the time this contractual effort was initiated, a number of knowledgeable investigators were, or had been, examining electroformable alloys and dispersion strengthened materials in the following categories:

(1) Nickel and manganese (Ni-Mn)
(2) Nickel and cobalt (Ni-Co)
(3) Nickel, cobalt, and manganese (Ni-Co-Mn)
(4) Nickel and tungsten (Ni-W)
(5) Nickel and a dispersion strengthening material (Ni-D.S.)

Most recent studies, for which some elevated temperature mechanical property data was available, involved the nickel-manganese and nickel-cobalt systems. The most current studies of electrodeposited nickel-cobalt were directed at achieving an alloy competitive to Inconel 718 in a limited temperature range useful in SSME structural applications. Work with electroformed nickel-manganese alloy was primarily for the purpose of overcoming "hot-shortness" in conventional electrodeposited nickel due to the presence of sulfur as an impurity. The introduction of small amounts of manganese in the deposited nickel provided a benefit of improved mechanical properties at elevated test temperatures as high as 538^{o}C.

Since characterization and optimization of electrodeposited alloy compositions, thermal aging treatments, and elevated temperature mechanical properties is very time consuming and expensive, the importance of a most thorough literature review and critique cannot be over emphasized. It was anticipated that elevated and ambient temperature mechanical property data might be available for more than one alloy system, and benefits in strength retention might exist in different temperature ranges for the candidate alloys. Although mechanical properties competitive to those of Inconel 718 in the solution aged condition were sought for the temperatures expected for SSME structural shrouds (jackets), there was an interest in how these electrodeposited alloys performed against conventional electroformed nickel. This was based on the fact that the SSME inner liner, a high temperature copper base alloy, is cooled by hydrogen flowing through channels which are closed externally with conventional electrodeposited nickel. Capability to

electroform both components with a high performance alloy might provide additional benefits in weight savings.

Pulsed deposition has recently been utilized to produce improved alloy deposits due to the ability to better control electrolyte composition through diffusion at the cathode surface (region at which plating is taking place). It was expected that any benefits to the candidate alloys through pulsed deposition would be lacking in the literature and mechanical property data would need to be generated.

Electrodeposited metals in the "as deposited" condition usually contain imperfect atomic lattice structures. These lattice faults consist of atomic vacancies, absorbed gases, and trace impurity elements or compounds. Most electrodeposited alloys are internally stressed due to this imperfect lattice structure. Even low stressed conventional sulfamate nickel deposits usually contain 2.8 to about 33 MPa (0.4 to 5 ksi) residual tensile stress. Alloy deposits may contain much more stress since the primary element composing the deposit is being made impure by the alloying element or elements. Excessive stresses can lead to cracking of the alloy itself or to deformation of any underlying structure or basis metal - particularly when the basis metal has less strength.

In conventional sulfamate nickel deposits this stress is relieved by a treatment at about 343^{o}C (650^{o}F) for one hour or longer. It may be necessary to heat treat alloy deposits at higher temperatures or longer times at lower temperatures for proper stress relief. Such treatments for alloys may also be necessary to provide adequate ductility in the metal. Such heat treatments may require special modifications so that useful ductility is obtained without significant loss of ultimate and yield strengths. It is also necessary to consider the effect of the heat treatment cycle on other, more sensitive, components that may be present with the alloy electroform - for example, one must consider how the heat treatment will affect the copper alloy liner and electroformed nickel close-out in the case of the SSME.

An overview of Phase A efforts is shown below:

Literature Review

A. Review and Update - Gather significant information from studies of potential electroformable nickel based alloys and dispersion strengthened systems.

B. Survey Report - Issue a limited distribution report detailing the findings and conclusions drawn from the literature search.

Alloy Characterization and Optimization

A. Optimize Alloying Parameters for the Selected System (Nickel-Manganese) - Produce samples of conventionally deposited and pulse plated alloy for comparison in mechanical property tests.

B. Characterize Heat Treatment Effects - Investigate the ability of heat treatments to enhance ambient temperature strength retention and improve ductility.

C. Elevated Temperature Testing - Alloys showing best combinations of strength and ductility will be tested for mechanical properties at selected elevated temperatures to establish a performance criteria for further narrowing of the deposition parameters essential to producing the optimum material.

D. Test Bars - Test specimens are to be made per Federal Test Method Standard No. 151 for testing by NASA-MSFC for acceptability of mechanical property performance.

3.2 Literature Review

3.2.1 Introduction

A literature review and critique was performed as part of a broad scoped program to develop and demonstrate a system for electroforming materials with improved strength and high temperature properties. Studies of this nature usually evolve from an immediate, or near future, need for a specific material or process technology advancement. The basis for this study as an interest in fabricating structural components offering potential weight reductions and subsequent payload-fuel economies in connection with NASA-Marshall Space Flight Center's responsibilities in support of the Space Shuttle Program. A specific application of such an electroformable alloy might be in the SSME structural shroud currently produced by welding several wrought Inconel 718 sections to construct this jacket. Since welding produces a heat affected zone and mechanical properties are compromised elimination of welds by making an electroformed single piece structure could result in significant metal weight savings while retaining equivalent structural strength.

Nickel, as deposited from the low-stress sulfamate bath, has been universally accepted as the material for electroforming structures such as regeneratively cooled thrust chamber outer shells and high energy chemical laser components where good mechanical properties at temperatures to 482^{o}C (900^{o}F) are often desired. However, nickel deposits lose strength rapidly as temperature increases, and the ductility deteriorates within certain elevated temperature ranges. Several electroformable alloy systems have been developed and characterized to a point where practical hardware applications might be considered.

The properties of electrodeposited alloys are of particular interest because an alloy must possess significantly better properties for a particular application than a pure electrodeposit to compensate for the increased difficulty involved in operating the alloy plating process. Electrodeposited alloys frequently have certain enhanced properties - often they are stronger, have finer grain structure, or are harder than the individual parent metals. Although an electroformed (EF) alloy competitive with solution aged Inconel 718 is sought in the primary application of this effort, it is also appropriate to compare the alloy developed with conventional EF nickel as a

baseline for measuring improvement. This may prove helpful to the designer or materials engineer in developing new hardware in which wrought alloys such as Inconel 718 cannot be used.

3.2.2 EF Nickel

3.2.2.1 General

Nickel can be electroformed to produce a wide range of hardnesses, densities, tensile strengths, and internal stresses by proper selection of the electrolyte and operating conditions. Diggen (1) noted six basic types of nickel electrolytes being used for nondecorative nickel deposits. These are the Watts (sulfate) bath with or without addition agents, the hard nickel baths, the chloride nickel solution, the cobalt-nickel electrolyte, the fluoborate nickel bath, and the sulfamate nickel solution. The cobalt-nickel bath will be discussed under that particular alloy system. The hard nickel baths will be ignored because of the presence of chemically free sulfur and organic by-products in uncontrolled amounts in the deposits. These substances lead to catastrophic grain boundary failures under stress after exposure to temperatures exceeding 232^{o}C (450^{o}F). Such deposits also exhibit unacceptably low ductility for structural use.

3.2.2.2 EF Nickel - Watts Type Electrolytes

Watts baths were the primary solutions for nickel plating and electroforming prior to the development of the nickel sulfamate electrolyte. These solutions contain nickel sulfate, nickel chloride, and boric acid. The nickel sulfate to nickel chloride ratio by weight in a true Watts type solution is usually between 7.5:1 and 3.5:1. References to use of Watts type baths to electroform structural components for aerospace components are rare: however, Savage and Bommerscheim (2) reported the use of this solution to electroform supersonic pitot-static tubes. Diggen (1) reported mechanical properties typical for a low pH Watts bath, and International Nickel Company (3) has published data for deposit properties from pH 2.5 to 4.0. Table 3.2-1 summarizes properties from these references.

Brenner, Jennings, and Zentner (4) investigated the physical properties of the Watts bath deposits and studied the effects of bath modifications where nickel chloride was either decreased or increased in concentration. The chloride-free modification is called the all-sulfate bath while the bath with higher than normal nickel chloride is known as the chloride-sulfate bath. Data for the properties for deposits from these baths are shown in Table 3.2-2. The chloride-sulfate bath has a higher conductivity and a higher throwing power (ability to plate into recessed areas) than the conventional Watts bath. However, it has a major disadvantage of high internal stress.

ASTM Committee B-8 (5) implied that the best ductility of Watts bath deposits occurs at a bath temperature of 54.4^{o}C (130^{o}F). Mechanical strength from this bath is relatively independent of bath temperature, current density, and pH, but increases with increasing nickel or chloride content. The increase in chloride content also increases stress. This is in agreement with

TABLE 3.2-1. COMPOSITION, OPERATION, AND DEPOSIT MECHANICAL PROPERTIES FROM TYPICAL COMMERCIAL WATTS BATHS

Composition and Operating Conditions	Reference (1)	Reference (2)	Reference (3)
Nickel Sulfate, g/l	329.5	337	299.6
Nickel Chloride, g/l	44.9	44.9	59.9
Boric Acid, g/l	37.4	37.4	30
pH (Acidity)	1.5 - 4.5	2.0 - 2.3	3
Temperature, °C	46.1 - 60.0	54.4 - 57.2	60
Current Density, A/dm^2	2.69 - 10.76	3.23	5.38
Antipit Agent	Hydrogen Peroxide		
Mechanical Properties at Room Temperature			
Tensile Strength, MPa (ksi)	351.6 (51)	358.5 - 365.4 (52) - (53)	379.2 - 413.7 (55) - (60)
Yield Strength, MPa (ksi)	No Data	No Data	No Data
Elongation in 5.08 cm, %	30	36	25 - 30
Hardness	140 - 160 Vickers	No Data	150 DPN
Stress, MPa (ksi)	124.1 (18.0)	No Data	No Data
Mechanical Properties at Elevated Temperature			
Test Temperature, °C	No Data	537.8	No Data
Tensile Strength, MPa (ksi)	No Data	220.6 - 234.4 (32) - (34)	No Data
Yield Strength, MPa (ksi)	No Data	No Data	No Data
Elongation in 5.08 cm, %	No Data	33 - 36	No Data

TABLE 3.2-2. BATH COMPOSITIONS AND PROPERTIES OF NICKEL DEPOSITS FROM THE ALL-SULFATE, WATTS TYPE, AND CHLORIDE-SULFATE BATHS (4)

Bath Symbol	Bath Type	Nickel Sulfate g/l	Nickel Chloride g/l	Boric Acid g/l
S	All-Sulfate	280	0	30
S3-C1	Watts Type	210	60	30
S3-C1-1	Watts Type	105	30	30
S3-C1-4N	Watts Type	420	120	30
S1-C13	Chloride-Sulfate	140	120	30
S1-C1	Chloride-Sulfate	70	180	30

Bath Symbol	Bath Temp., °C	Current Density A/dm^2	pH	Tensile Strength MPa	Tensile Strength (ksi)	Elongation in 5.08 cm %	Stress MPa	Stress (ksi)	Density g/cm^3	Young's Modulus PSI x 10^6
S	30	5	1.5	558.5	81	14	No Data		No Data	No Data
	55	5	1.5	565.4	82	20	137.9	20	8.91	No Data
	55	5	3.0	455.1	66	20	117.2	17	8.92	23.5
	55	5	5.0	717.1	104	6	No Data		8.92	23.0
	80	5	1.5	413.7	60	18	No Data		No Data	No Data
S3-C1	30	2	5.0	517.1	75	18	No Data		No Data	No Data
	30	5	1.5	724.0	105	11	No Data		No Data	No Data
	30	5	3.0	517.1	75	15	241.3	35	No Data	23.8
	30	5	5.0	496.4	72	19	No Data		No Data	No Data
	40	5	3.0	517.1	75	19	No Data		No Data	No Data
	55	1	3.0	530.9	77	27	206.9	30	No Data	23.6
	55	2	1.5	510.2	74	22	No Data		No Data	No Data
	55	2	3.0	386.1	56	23	186.2	27	8.92	No Data
	55	5	1.5	462.0	67	28	165.5	24	No Data	No Data
	55	5	3.0	386.1	56	28	117.2	17	8.91	24.1
	55	5	5.0	406.8	59	25	172.4	25	No Data	23.7
S3-C1-1N	55	5	3.0	448.2	65	18	No Data		8.90	No Data
	55	5	5.0	441.3	64	19	137.9	20	8.91	19.7
S3-C1-4N	55	5	3.0	565.4	82	8	No Data		8.91	No Data
	55	5	5.0	799.8	116	2	193.1	28	8.88	27.2
S1-C1	55	2	3.0	579.2	84	18	No Data		No Data	No Data
	55	2	5.0	641.2	93	3	No Data		No Data	No Data
	55	5	1.5	503.3	73	23	193.1	28	No Data	No Data
	55	5	3.0	510.2	74	20	213.7	31	8.91	25.1
	55	5	5.0	717.1	104	8	234.4	34	8.91	28.2
	80	5	3.0	572.3	83	5	No Data		No Data	No Data
S1-C3	55	2	3.0	710.2	103	8	No Data		No Data	No Data
	55	5	3.0	634.3	92	11	262.0	38	8.90	20.8
	55	5	5.0	868.8	126	7	255.1	37	No Data	No Data
	80	5	3.0	620.6	90	4	No Data		No Data	No Data

stress data reported by other investigators (1, 3, 6) for the all sulfate, Watts, and chloride-sulfate baths. It was also noted (4) that chloride content in the series of baths reported in Table II had an effect on tensile strength and elongation. When about 25 percent of the total nickel content of the bath is present as nickel chloride salt, tensile strength is lowest and elongation is highest. Tensile strength and elongation properties of all sulfate bath deposits are roughly equivalent to those in deposits from baths with 50 percent of the nickel present as the chloride salt (chloride-sulfate type). The concentration of nickel in the bath showed significant effects on mechanical properties.

Brenner, Jennings, and Zentner (4) investigated the effects of annealing on mechanical properties of deposits from the all-sulfate, Watts type, and chloride-sulfate baths Table 3.2-3. Mechanical property data for wrought forms of nickel (7) are shown at the foot of Table 3.2-3 for comparison.

TABLE 3.2-3. MECHANICAL PROPERTIES OF ALL-SULFATE, WATTS TYPE, AND CHLORIDE-SULFATE BATH DEPOSITS AFTER ANNEALING (6)

Bath* Symbol	Bath Temp., °C	Current Density, A/dm^2	pH	Tensile Strength, MPa (ksi) As Deposited	Annealed 400°C	Annealed 1000°C	Elongation in 5.08 cm, % As Deposited	Annealed 400°C	Annealed 1000°C
S	55	5	1.5	565.4 (82)	530.9 (77)	262.0 (38)	20	22	14
S3-C1	30	5	3.0	517.1 (75)	427.5 (62)	324.1 (47)	15	39	37
	55	5	1.5	462.0 (67)	399.9 (58)	268.9 (39)	28	35	25
	55	5	3.0	386.1 (56)	365.4 (53)	241.3 (35)	28	39	17
	80	5	3.0	537.8 (78)	489.5 (71)	248.2 (36)	28	27	23
S1-C1	55	5	3.0	510.2 (74)	441.3 (64)	275.8 (40)	20	30	32
S1-C3	55	5	3.0	634.3 (92)	537.8 (78)	296.5 (43)	11	26	22
Nickel, Wrought Annealed (10)				363.4 (53)			56		
Nickel, Cold Drawn, 40% R.A. (10)				562.6 (82)			19		

* Bath symbols are the same as described in Table 3.2-2.

Sample and Knapp (8) examined mechanical properties of Watts bath nickel at various test temperatures, Table 3.2-4. Composition of the bath was 300 g/l nickel sulfate, 60 g/l nickel chloride, and 37.5 g/l boric acid. The bath pH was 3.0, temperature was 60°C, and current density was 4.3 A/dm^2.

TABLE 3.2-4. MECHANICAL PROPERTIES OF WATTS BATH NICKEL DEPOSITS AT VARIOUS TEST TEMPERATURES (11)

Test Temperature °C	Test Temperature °F	Average Tensile Strength MPa	Average Tensile Strength ksi	Average Yield Strength MPa	Average Yield Strength ksi	Average Elongation in 5.08 cm,%
-196	-320	586.8	85.1	277.9	40.3	48
- 73	-100	479.9	69.6	257.9	37.4	33
20	68	410.3	59.5	223.4	32.4	30
204	400	334.4	48.5	No Data		25
427	800	222.7	32.3	154.4	22.4	29
649	1200	127.6	18.5	82.1	11.9	13
760	1400	79.3	11.5	No Data		6
871	1600	47.6	6.9	No Data		8

3.2.2.3 EF Nickel - Nickel Chloride Electrolytes

Greenwood (9) noted the all-chloride solution to provide faster plating speeds than possible with the Watts type baths. The operating pH range is narrower than for the Watts type solutions and frequent pH checks are needed. The deposits are smoother than the Watts type but they are more highly stressed. Diggen (1), Safranek (10), and Brenner (4) reported compositions, operating conditions, and mechanical properties of deposits as shown in Table 3.2-5. Sample and Knapp (8) investigated the mechanical properties of the chloride deposits over a range of test temperatures as shown in Table 3.2-6.

TABLE 3.2-5. COMPOSITION, OPERATING CONDITIONS, AND MECHANICAL PROPERTIES OF ALL CHLORIDE NICKEL BATHS (1), (6), (13)

Compositions:	Reference (1)	Reference (6)	Reference (13)
Nickel Chloride, g/l	300	240	180
Boric Acid, g/l	30	30	36

Ref. No.	Bath Temp., °C	Current Density A/dm²	pH	Tensile Strength MPa	Tensile Strength ksi	Yield Strength MPa	Yield Strength ksi	Elongation in 5.08 cm %	Stress MPa	Stress ksi	Density g/cm³
(1)	40 - 70	2.7 - 10.8	5.4 - 5.8	681.9	98.9	No Data		21	275.8 - 344.8	40 - 50	No Data
(6)	30	5	3.0	606.8	88	No Data		14	282.7	41	No Data
	30	5	5.0	944.6	137	No Data		5	No Data		No Data
	55	1	5.0	910.1	132	No Data		4	No Data		No Data
	55	5	1.5	634.3	92	No Data		15	317.2	46	No Data
	55	5	3.0	703.3	102	No Data		14	289.6	42	8.90
	55	5	5.0	930.8	135	No Data		6	379.2	55	8.84*
(13)	60	4	3.0	744.7-855.0	108-124	634.3	92	8	No Data		No Data

*Density changed with heat treatment as follows:

Temperature, °C	Density, g/cm³
400	8.88
1000	8.23

TABLE 3.2-6. NICKEL DEPOSIT MECHANICAL PROPERTIES FROM THE ALL-CHLORIDE BATH AT VARIOUS TEST TEMPERATURES (11)

Bath Composition and Operation Conditions:

Nickel Chloride, g/l	300
Boric Acid, g/l	37.5
pH	3.0
Temperature, ^{o}C	60
Current Density, A/dm^2	4.3

Test Temperature ^{o}C	Test Temperature ^{o}F	Average Tensile Strength MPa	Average Tensile Strength ksi	Average Yield Strength MPa	Average Yield Strength ksi	Average Elongation in 5.08 cm,%
-196	-320	1062.5	154.1	697.8	101.2	22
- 73	-100	927.4	134.5	639.9	92.8	15
20	68	799.8	116.0	630.9	91.5	8
204	400	615.7	89.3	495.1	71.8	11
427	800	207.5	30.1	122.7	17.8	20
649	1200	60.0	8.7	No Data		10
760	1400	45.5	6.6	No Data		7

Yang (11) found that the all-chloride bath produces a deposit of nickel containing the face-centered-cubic (FCC) and hexagonal-close-packed (HCP) structures with current densities over 0.2 A/dm^2. Bath pH had no effect on the structures obtained. At bath temperatures of $40^{o}C$, or higher, the hexagonal structure was not obtained. High hydrogen concentration in the deposit was associated with the hexagonal structure. Heating in vacuum at $600^{o}C$ converted all hexagonal nickel to the normal face-centered-cubic form.

3.2.2.4 EF Nickel - Nickel Fluoborate Electrolytes

Nickel fluoborate electrolytes are simple to control and highly buffered - pH changes during operation are not rapid (12). Nickel fluoborate is highly soluble, making it possible to operate at greater nickel metal concentrations that in the Watts and chloride-sulfate baths. The fluoborate bath operates with high conductivity and good anode corrosion characteristics. The deposits are bright, smooth, and do not tend to form nodules in high current density areas. The internal stress is lower than in deposits from the Watts bath. Struyk and Carlson (13) presented several bath compositions, operating conditions, and mechanical properties for nickel fluoborate baths and deposits, Table 3.2-7. For baths of the medium nickel content defined in Table 3.2-7, Diggen (1) shows internal tensile stresses ranging from 110.3 to 179.3 MPa (16 to 26 ksi).

Brenner, Jennings, and Zentner (4) included nickel fluoborate deposits in their investigation of mechanical and other physical properties of electrodeposited nickel, Table 3.2-8.

3.2.2.5 EF Nickel - Nickel Sulfamate Electrolytes Without Chloride

The sulfamate electrolyte is the most widely used solution for electroforming nickel. According to Barrett (14) this electrolyte has advantages over other nickel plating solutions in that:

TABLE 3.2-7. TYPICAL NICKEL FLUOBORATE BATH COMPOSITIONS, OPERATING CONDITIONS, AND DEPOSIT MECHANICAL PROPERTIES (16)

Bath Composition and Operating Variables:

	Low Nickel	Medium Nickel	High Nickel
Nickel Fluoborate, g/l	220	300	440
Nickel Metal, g/l	55	75	110
Free Fluoboric Acid, g/l	4 to 38	4 to 38	4 to 38
Free Boric Acid, g/l	30	30	30
pH (Colorimetric)	2.0 to 3.5	2.0 to 3.5	2.0 to 3.5
Temperature, °C	37.8 to 76.7	37.8 to 76.7	37.8 to 76.7

Mechanical Property Data:

Nickel Metal, g/l	pH	Bath Temp., °C	Current Density, A/dm²	Tensile Strength MPa	Tensile Strength ksi	Yield Strength MPa	Yield Strength ksi	Elongation in 5.08 cm, %	Vickers Hardness
110	2.0	54.4	8.1	377.8	54.8	277.9	40.3	20.4	164
75	2.5	54.4	8.1	513.7	74.5	363.4	52.7	16.6	183
75	3.5	54.4	8.1	481.3	69.8	307.5	44.6	13.0	159
55	2.5	54.4	8.1	561.3	81.4	402.0	58.3	14.4	204
55	2.5	32.2	5.4	686.7	99.6	572.3	83.0	10.4	270
55	3.5	32.2	5.4	692.9	100.5	579.2	84.0	13.5	243
55	4.0	32.2	5.4	735.0	106.6	546.8	79.3	7.6	280
55	3.5	32.2	2.7	832.9	120.8	456.4	66.2	5.5	305

TABLE 3.2-8. TABLE NICKEL FLUOBORATE DEPOSIT PROPERTIES AND ELECTROLYTE COMPOSITION-OPERATING CONDITIONS (6)

Electrolyte Composition:

Nickel Fluoborate, g/l	232
Boric Acid, g/l	30

Properties of Deposits:

Bath Temp., °C	Current Density, A/dm²	Bath pH	Density, g/cm³ As Deposited	Density, g/cm³ Heat Treated 400°C	Density, g/cm³ Heat Treated 1000°C	Tensile Strength MPa	Tensile Strength ksi	Elongation in 5.08 cm, %	Stress MPa	Stress ksi
55	5	3.0	8.91	8.91	8.90	427.5	62	30	No Data	
55	5	4.5	8.92	No Data		475.8	69	22	No Data	
55	5	2.0	No Data	No Data		No Data		No Data	206.9	30

1. low stress deposits are obtained,
2. the bath can operate at higher current density at lower temperatures,
3. bath composition, control, and maintenance is simple,
4. deposits of high purity are obtained,
5. a wide range of easily reproducible properties of the deposits are possible,
6. excellent grain structure and ductility are produced,
7. fatigue strength of the base metal is improved, and
8. the bath operates over a wide range of conditions.

The low stress and resulting improved fatigue performance of deposits from sulfamate baths has led to adoption of these baths for nickel electroforming of hardware for the aerospace industry. Barrett's (14) recommended electrolyte composition, operating conditions, and deposit mechanical properties are shown in Table 3.2-9. Boric acid control is said to be not critical and can be analyzed infrequently. The pH is preferably checked daily; it will tend to rise slowly with use and may be quickly adjusted with additions of sulfamic acid. Barrett notes that filtration should be continuous. Activated carbon treatment to remove organic impurities is not recommended on a continuous basis as it will remove any wetting agent present. Barrett states that anode corrosion is 100 percent efficient without the use of chloride ion to promote dissolution. He advises that anodes must be 99 percent plus in purity and of rolled depolarized or electrolytic sheet. It has since been shown that this is not correct since the bath must either contain some chlorides or sulfur depolarized anodes to maintain active anode surfaces for proper corrosion.

TABLE 3.2-9. COMPOSITION, OPERATING RANGES, AND AVERAGE DEPOSIT MECHANICAL PROPERTIES FROM THE CHLORIDE-FREE SULFAMATE ELECTROLYTE (17)

Composition and Operating Conditions:

Nickel Sulfamate, g/l	449.3
Nickel Metal Content, g/l	76.4
Boric Acid, g/l	30.0
Anti-pit Agent, g/l	0.37
Temperature Range, ^{o}C	37.8 - 60.0
pH Range	3.0 - 5.0
Density, ^{o}Baumè	29 - 31
Anodes	99% plus, rolled depolarized
Maximum Cathode Current Density, A/dm^2	32.3 (at 60^{o}C) 16.1 (at 37.8^{o}C)
Agitation	Cathode bar movement or Solution circulation
Tank Voltage	6 - 9 volts
Anode Efficiency	100 percent
Cathode Efficiency	98 - 100 percent

Average Mechanical Properties

Hardness, Vickers	250 - 350
Tensile Strength, MPa (ksi)	620.6 (90)
Elongation in 5.08 cm, %	20 - 30
Internal Stress (Tensile), MPa (ksi)	3.45 (0.5)

There is considerable controversy over the employment of chlorides in sulfamate nickel solutions. The main objection is based on the introduction of stress into the deposits. Very low chloride concentrations do not seem to impart any significant stresses beyond those found in chloride-free sulfamate bath deposits.

Barrett advises that excessive internal stresses can cause peeling, cracking, crazing, warping, blistering, distortion, and even complete destructive failure of deposits. Stresses of a tensile nature can produce premature fatigue failure of the underlying metal to which the deposit is bonded. The effects of bath variables on stress are summarized as:

pH - Stress has a slight minimum at pH 4.0. It rises slowly at lower pH values and sharply at values above 6.0.

Metal Content - No appreciable effect on stress.

Temperature - Stress decreases with increase in bath temperature and increases with temperature drop, usually not more than a total of $\pm$ 34.5 MPa (5 ksi) for the extremes.

Chlorides - Stress rises sharply and linearly with increasing chloride content - approximately 20.7 MPa (3 ksi) for each ten percent increase in chloride as nickel chloride.

Current Density - Stress increases gradually with increase of current density.

Agitation - Agitation reduces the rate of increase of stress with increase of current density.

Boric Acid - This has no appreciable effect between 15.0 and 37.4 g/l.

Wetting Agents - These act slightly as stress reducers.

Asher and Harding (15) determined the mechanical properties of nickel sulfamate bath deposits when no chlorides were added. Their test samples were 0.0254 to 0.0381 cm thick. The bath composition, operating conditions, and deposit test results are shown in Table 3.2-10. (The elongation results in this work appear low for deposits from this type of electrolyte. It is possible that the use of depolarized nickel anodes at these current densities in the absence of chloride contributed to the problem. It has also been shown by Brenner that deposits this thin do no always afford representative ductility data.) Asher and Harding concluded that:

1. The strength decreases with increasing current density.
2. The elongation increases with increasing current density but at a gradual rate.
3. The strength increases as the temperature increases to around 48.9^{o}C and then decreases.
4. The ductility decreases rapidly with increasing bath temperature.
5. Raising the pH from 3.5 to 4.0 increases the strength at 37.8^{o}C bath temperature but has little effect at 48.9^{o}C and 60^{o}C.

Klingenmeier (16) and Knapp (17) investigated the effects of anode behavior on the internal stress and mechanical properties of chloride-free sulfamate bath deposits. Each investigator found that poor anode efficiency

in the absence of chlorides in the bath promoted solution instability wherein a product identified as azodisulfonate formed. This substance acts as a stress reducing agent leading to compressive stresses and higher sulfur content in the deposit. This would account, in some part, for the low ductility noted in Asher and Harding's data in Table 3.2-10. The ultimate solution to this problem because the use of sulfur depolarized anodes in place of depolarized nickel, cast nickel, or rolled nickel for sulfamate baths without chlorides. Klingenmeier noted that sulfur depolarized anodes resulted in greater tensile stress in deposits than was found with depolarized nickel, but the reduction of sulfur content was more desirable.

TABLE 3.2-10. RESULTS OF ASHER AND HARDING (15) INVESTIGATION OF NICKEL SULFAMATE DEPOSIT MECHANICAL PROPERTIES

Bath Composition and Operating Conditions:

Nickel Sulfamate, g/l	449.3
Boric Acid, g/l	Saturated
Anti-pit, g/l	0.37
Anodes	Depolarized nickel bagged in Dynel
Filtration	Continuous at .757 to 1.136 liters per minutes
Bath Volume, Liters	17.03
Agitation	Mechanical (Propellor)

Mechanical Properties of Test Samples:

Bath pH	Bath Temp °C	Current Density A/dm^2	Tensile Strength MPa	Tensile Strength ksi	Yield Strength MPa	Yield Strength ksi	Elongation in 5.08 cm %
3.5	37.8	1.938	462.0	67	303.4	44	22
		2.045	517.1	75	344.8	50	11
		3.229	434.4	63	303.4	44	18
		5.167	448.2	65	275.8	40	15
		6.997	482.7	70	310.3	45	16
3.5	48.9	1.507	675.7	98	482.7	70	4
		1.722	786.0	114	641.2	93	4
		2.045	744.7	108	572.3	83	4
		3.337	530.9	77	393.0	57	5
		7.104	689.5	100	524.0	76	8
		7.212	399.9	58	268.9	39	24
		9.257	627.4	91	441.3	64	10
3.5	60.0	2.583	717.1	104	524.0	76	3
		3.229	634.3	92	468.9	68	2
		3.552	689.5	100	551.6	80	2
		6.459	503.3	73	344.8	50	3
4.0	37.8	2.045	655.0	95	462.0	67	10
		2.906	675.7	98	427.5	62	5
		5.813	517.1	75	282.7	41	13
		7.535	779.1	113	448.2	65	6
4.0	48.9	1.292	758.5	110	No Data		3
		2.583	661.9	96	655.0	95	3
		6.674	586.1	85	448.2	65	4
4.0	60.0	2.260	710.2	103	599.9	87	2

Rocketdyne Division of North American Rockwell (18) uses the chloride-free nickel sulfamate electrolyte to electroform the outer shells of regeneratively cooled thrust chambers. This deposit may be applied directly over wax-filled and conductivized coolant passages or after a preliminary close-out of the channels with electroformed copper. Procurement requirements are placed on the nickel sulfamate concentrate used to prepare the electrolyte. No additives or brighteners are permitted. The chemical purity requirements are as follows:

pH	4.3 - 4.7
Nickel as metal	150 g/l minimum
Sulfate ion	0.5 percent by weight maximum
Ammonium ion	300 ppm maximum
Iron	6 ppm maximum
Copper	6 ppm maximum
Lead	1 ppm maximum
Zinc	6 ppm maximum
Chromium	1 ppm maximum
Chloride	100 ppm maximum

For newly formulated nickel sulfamate baths, Rocketdyne (19) requires that the bath and the deposits meet the requirements shown in Table 3.2-11. For electrodeposition of structural nickel closures, for thrust chamber coolant passages, Rocketdyne (24) requires that the bath and the deposits meet the requirements given in Table 3.2-12. The reference to SNAP (sulfamate nickel anti-pit) and SNAC (sulfamate nickel acid controller) in these tables and the impurity limits imposed on the sulfamate concentrate indicate that the Barrett sulfamate bath (Allied Kelite Products Division, The Richardson Company) is being used.

Rocketdyne (21) has determined the minimum expected properties of deposits from their sulfamate nickel baths, Table 3.2-13. Some of their test data (22) from Space Shuttle Main Combustion Chamber (MCC) samples of electroformed nickel are shown in Table 3.2-14.

Messerschmitt-Bolkow-Blohm of Munich, West Germany, has provided the author extensive data on their thrust chamber electroforming capability. They use the sulfamate nickel electrolyte. This solution is employed to electroform aerospace products such as satellite components, heat exchangers, and rocket engines. They electroformed the HM7 thrust chamber for the Ariane Third Stage Propulsion System. Although no information was supplied concerning the chloride-free nature of their sulfamate electrolyte, it is highly probable that no such additions were made. According to MBB representatives, they participated in a cooperative program with Rocketdyne in the early 1960s which evolved the non-chloride formulation presently used by both parties. This association also may have contributed to the discovery of xylose as an additive for Rocketdyne's acid copper bath to electroform copper channel closures with deposits free of harmful oxygen for elevated temperature use. This discovery is believed to have resulted from the fact that many European plating facilities used caulked oak tanks from which extracts became electrolyte additions. Copper plated from these solutions exhibited excellent properties after thermal exposures; it was relatively simple to isolate the derivative that led to this performance.

TABLE 3.2-11. ROCKETDYNE NICKEL SULFAMATE "NEW ELECTROLYTE" MAKE-UP, OPERATING, AND DEPOSIT REQUIREMENTS (19)

Composition and Operating Conditions:	Requirements
Nickel Content, g/l	72 - 85
Boric Acid, g/l	37 - 45
Sulfamate Nickel Anti-Pit (SNAP), g/l	.65 - .75 as measured by 15 second minimum bubble retention time on a 7.62 cm diameter ring
Specific Gravity	1.26 - 1.30
Anodes	Nickel chips in titanium baskets with polypropylene cover bags
Make-up Water	Minimum specific resistance of 1 megohm/cm
Temperature, ^{o}C	48.9 $\pm$ 2.8
pH	3.8 - 4.2*
Filtration	10 micron polypropylene cores
Filtration Rate	1.5 tank volumes per hour minimum
Current Density, A/dm^2 (ASF)	2.15 $\pm$ .22 (20 $\pm$ 2)
Agitation	Cathode

Required Properties (New Electrolytes):

Ultimate Strength, MPa (ksi)	As Deposited	586.1 (85)
Yield Strength, MPa (ksi)	As Deposited	379.2 (55)
Elongation in 1.27 cm	As Deposited	20 percent minimum
	Stress Relieved**	40 percent minimum
Microstructure	As Deposited	Uniform and clean
	Annealed***	Free from grain boundary inclusions

* - pH will initially be 3.4 and will increase upon electrolysis of the bath
** - Stress relieved by holding at 343.3 + 8.3^{o}C for one hour in argon
*** - Annealed by holding at 982.2 $\pm$ 13.9^{o}C for one hour in hydrogen

TABLE 3.2-12. ROCKETDYNE REQUIREMENTS FOR ELECTROFORMING STRUCTURAL NICKEL FROM THE SULFAMATE BATH - BATH COMPOSITION, OPERATING CONDITIONS, AND REQUIRED MECHANICAL PROPERTIES (20)

Composition and Operating Conditions:	Requirement
Nickel Metal Content, g/l	72 - 80
Boric Acid, g/l	27 Minimum
Iron, ppm	6 Maximum
Copper, ppm	6 Maximum
Zinc, ppm	6 Maximum
Lead, ppm	6 Maximum
Chromium, ppm	2 Maximum
Chloride, ppm	500 Maximum
Sulfamate Nickel Anti-pit (SNAP)	As required to obtain 15 sec. minimum bubble on 7.62 cm diameter ring
Anodes	SD nickel chips in titanium baskets with polypropylene covers
Water	Minimum specific resistance 1 megohm/cm
Temperature, ^{o}C	46.1 - 51.7
Specific Gravity	1.25 - 1.30
pH (Adjust with Sulfamate Nickel Acid Controller - SNAC)	3.8 - 4.2
Filtration	10 micron polypropylene core and element
Filtration Rate	2 tank volumes per hour minimum
Current Density, A/dm^2 (ASF)	$2.153 \pm .22$ (20 ± 2)
Agitation	Cathode and electrolyte flow
Minimum Mechanical Properties of Deposits:	
Ultimate Strength, MPa (ksi)	620.6 (90)
Yield Strength, MPa (ksi)	413.7 (60)
Elongation in 1.27 cm, %	16
Hardness, R_b	90
As Deposited Microstructure	Columnar, no lamination striations, banding, or voids. Uniform and clean.
Annealed Microstructure	Free from grain bounding inclusions

TABLE 3.2-13. EXPECTED MINIMUM PROPERTIES OF ROCKETDYNE ELECTRODEPOSITED NICKEL FROM THE CHLORIDE-FREE SULFAMATE BATH (21)

	As Deposited		Stress Relieved[1]	
Tensile Ultimate Strength, MPa (ksi) Expected Minimum	530.9	(77)	448.2	(65)
Tensile Yield Strength, MPa (ksi) Expected Minimum	372.3	(54)	268.9	(39)
Tensile Elongation, % Expected Minimum	10		36	
Reduction in Area, % Predicted Minimum			50	
Thermal Conductivity, Cal.-cm/sec-cm^2-^{o}C Typical	0.14		-	
Elastic Modulus, MPa (10^6 psi) Typical	180,649	(26.2)	-	
Poisson's Ratio Typical	0.34		-	
Density, g/cm^3 (lb/in^3) Typical	8.86	(0.32)	-	

(1) Stress Relief at 343.3^{o}C (650^{o}F)

TABLE 3.2-14. TENSILE STRENGTH - ELECTRODEPOSITED NICKEL FROM SPACE SHUTTLE MAIN COMBUSTION CHAMBER SAMPLES - ROCKETDYNE (22)

(EDNi STRESS RELIEVED AT 343.3^{o}C 1 HOUR)

Type Bar	Ultimate Strength MPa	ksi	Yield Strength MPa	ksi	Reduction of Area, %	Panel No.
Min. Reqmnts.	448.2	65	268.9	39	50	-
TR 125	579.2	84	427.5	62	90	MTD-4
TR 125	572.3	83	427.5	62	92	MTD-4
TRC 210	530.9	77	379.2	55	98	MTD-4
TRC 210	537.8	78	406.8	59	97	MTD-4
TR 125	544.7	79	399.9	58	90	9001-4
TRC 210	586.1	85	420.6	61	96	9001-4
TRC 210	586.1	85	393.0	57	96	9001-4
TR 125	579.2	84	420.6	61	87	0001-4
TR 125	572.3	83	413.7	60	89	0001-4
TRC 210	544.7	79	441.3	64	97	0001-4
TRC 210	537.8	78	386.1	56	97	0001-4

TR 125 - Tensile round with electrodeposited nickel structure perpendicular to direction of loading (hoop direction). No bonds in samples.

TRC 210 - Tensile round, conical heat, with electrodeposited nickel parallel to direction of loading. All bond interfaces are included. No bond interface failure in tests.

NOTE: TR 125 samples are from a specific electrodeposited nickel layer while TRC samples test all electrodeposited nickel layers. Thus lower values for TRC 210 samples reflect the strength of the weakest electrodeposited nickel layer

Messerschmitt-Bolkow-Blohm (23) electroforms flat tensile test bars which are approximately 0.25 cm thick. The mechanical properties at two different current densities are shown in Table 3.2-15 for a range of test temperatures.

TABLE 3.2-15. NICKEL SULFAMATE BATH DATA AND DEPOSIT MECHANICAL PROPERTIES - MESSERSCHMITT-BOLKOW-BLOHM (23)

Bath Composition:

Nickel Sulfamate, g/l	450
Boric Acid	No Data
Wetting Agent	No Data

Operating Conditions:

Temperature, ^{o}C		50
Current Density,	A/dm^2	3 to 5
	ASF	28 to 46.5

Mechanical Properties (Average):

Current Density A/dm^2	Test Temperature ^{o}C	Ultimate Strength MPa	Ultimate Strength ksi	Yield Stregth 0.2% Offset MPa	Yield Stregth 0.2% Offset ksi	Elongation in 1 cm %
5	-196	743.3	106.5	421.3	61.1	28
5	20	548.2	79.5	352.3	51.1	18.5
5	200	410.9	59.6	284.1	41.2	15
5	400	235.1	34.1	176.5	25.6	43
5	600	107.6	15.6	68.3	9.9	16
3	-196	655.7	95.1	362.0	52.5	33
3	20	470.2	68.2	323.4	46.9	18
3	200	382.0	55.4	264.1	38.3	11
3	400	254.4	36.9	195.8	28.4	27
3	600	97.9	14.2	58.6	8.5	7

It is appropriate to mention that the sulfamate nickel bath can be operated with stress reducing additives which impart a compressive stress in the deposits (1), (24), (25). Although these references name several organic chemicals useful for stress reduction, the most commonly used substance is the sodium salt of saccharine. These additives also promote a finer grain size in the nickel microstructure; however, they normally increase the sulfur content of the deposits (24), (26), (27). This leads to reduced ductility, poorer notch sensitivity, and unsatisfactory performance at elevated temperatures. Such deposits would be inappropriate for use at elevated temperatures or where welding or brazing might be required as secondary fabrication operations after electroforming. Means to overcome the detrimental effects of sulfur will be discussed in a later section.

3.2.2.6 EF Nickel - Nickel Sulfamate Electrolytes with Chloride

Available literature reveals that most sulfamate nickel electrolytes used to produce electrodeposits for engineering applications are operated with some nickel present as the chloride salt. The requirement that chloride be present is based on the types of anodes available for use. Without chloride ions or some other ion (e.g. - bromide) capable of dissolving the nickel anode at a suitably controlled rate, there is a tendency for the bath to become unstable and produce deposits with higher sulfur contents (16), (17). The use

of sulfur depolarized anode chips has made chloride additions no longer necessary, but many sulfamate bath users continue to maintain a low chloride content so that other types of anodes may be employed or bath loads may be varied with respect to anode surface area without risking operation of the anodes at current densities too low to promote acceptable dissolution.

Klingenmeier (16) found that air agitation of the sulfamate bath using depolarized anodes contributed to anode passivity. When mechanical agitation was used, good bath stability with depolarized nickel anodes required 2.4 to 4.8 g/l of nickel chloride. His findings also disclosed a tensile stress in deposits of 13.8 to 20.7 MPa (2 to 3 ksi) with nickel chloride concentration at 2.4 g/l and about 68.9 MPa (10 ksi) with nickel chloride levels of 4.8 g/l. Using sulfur depolarized anodes, chloride was not necessary, but tensile stress was present. Addition of 0.8 g/l of nickel chloride increased stress about 20 percent.

In similar work, Knapp (17) reported that sulfur depolarized nickel and rolled depolarized nickel anodes remained active with as little as 0.2 g/l of chloride. He also found that all commercially available anodes corroded properly at chloride concentrations of 1.5 g/l.

Diggen (1) presented data from the work of Fanner and Hammond which showed the effect of chloride concentration on internal stress of nickel sulfamate deposits based on bath temperature and current density, Table 3.2-16. From this data it appears that tensile stress is not excessive in the bath temperature range of 45^{o} to $50^{o}C$ and at current densities ranging from 2.15 to 6.46 A/dm^2.

Typical compositions, operating conditions, and deposit mechanical properties for sulfamate nickel baths with varied amounts of chloride content are found in the literature. Suggested formulations by ASTM Committee B-8 (5), Diggen (1), and International Nickel (28) are shown in Table 3.2-17.

Camin Laboratories (29) reported the use of sulfamate nickel electrolyte containing chloride to electroform injectors for rocket engines. Their data concerning the bath composition, operating conditions, and deposit mechanical properties at room and elevated temperature is shown in Table 3.2-18. Machined round test bars were used as deposit test specimens. The 42 percent elongation reported at a test temperature of $537.8^{o}C$ ($1000^{o}F$) is rather high compared with any data reported elsewhere in the literature for sulfamate nickel metal deposits. This would indicate that special precautions and controls were exercised to remove sulfur from the bath before electroforming the test specimens. This can be done by high current density treating the bath at about 10.8 A/dm^2. The author doubts that sulfur could be consistently maintained at such a low level to promote this great an elongation over a long production electroforming operation.

TABLE 3.2-16. DATA FOR INTERNAL STRESS OF NICKEL SULFAMATE DEPOSITS FROM ELECTROLYTES CONTAINING NICKEL CHLORIDE (1)

Electrolyte Composition:

Nickel Sulfamate, g/l	Not given
Nickel Chloride, g/l	5
Boric Acid, g/l	Not given
pH	4.0 ± 0.1

Effect of Bath Temperature on Internal Stress, Hardness, and Cathode Efficiency at a Current Density of 0.43 A/dm^2 (40 ASF):

Temperature, °C	Tensile Stress MPa	Tensile Stress ksi	Vickers Diamond Hardness	Cathode Efficiency, %
30	74.5	10.8	204	99.3
35	51.0	7.4	170	99.4
40	51.0	7.4	168	99.4
45	30.3	4.4	No Data	No Data
50	20.7	3.0	174	99.4
55	31.7	4.6	No Data	No Data
60	40.0	5.8	173	99.3

Effect of Current Density in Sulfamate Bath on Stress, Hardness, and Cathode Efficiency (pH 4.0, Temperature 50.6 °C):

Cathode Current Density, A/dm^2	Tensile Stress MPa	Tensile Stress ksi	Vickers Diamond Hardness	Cathode Efficiency, %
2.15	15.2	2.2	168	99.1
3.23	22.1	3.2	166	99.2
4.31	20.7	3.0	166	99.2
5.38	24.8	3.6	166	99.4
6.46	27.6	4.0	168	99.4

TABLE 3.2-17. TYPICAL SULFAMATE NICKEL BATH (WITH CHLORIDE) COMPOSITIONS, OPERATING CONDITIONS AND DEPOSIT MECHANICAL PROPERTY RANGES (1), (8), (32)

Composition Range:	Reference (1) Range	Reference (1) Optimum	Reference (5) Range	Reference (28) Range
Nickel Sulfamate, g/l	225-405	338	315-450	300-450
Nickel Metal, g/l	52-94	77	73-104	69-104
Nickel Chloride, g/l	6-30	6-15	0-22.5	0-15
Boric Acid, g/l	30-45	30	30-45	30-45
Operating Conditions:				
Temperature, ^{o}C	28-60	49	32-60	38-60
pH (Electrometric)	3.5-4.2		3.5-4.5	3.5-4.5
Cathode Current Density				
A/dm^2	2.2-6.5	4.3	0.5-32	2.7-10.8
(ASF)	(20-140)	(40)	(5-300)	(25-100)
Agitation	Air preferred; cathode movement or electrolyte flow		Air or mechanical	Air, solution pumping, cathode movement
Mechanical Properties (Typical):				
Tensile Strength, MPa	744.7		413.7-1310.1	413.7-758.5
(ksi)	(108)		(60-190)	(60-110)
Elongation in 5.08 cm, %	15-20		10-25	5-30
Stress (Tensile), MPa	10.3-69.0		0-55.2	6.9-41.4
(ksi)	1.5-10.0		0-8.0	1.0-6.0
Vickers Hardness	140-190		170-230	140-250

TABLE 3.2-18. NICKEL SULFAMATE ELECTROLYTE COMPOSITION, OPERATING RANGE AND DEPOSIT MECHANICAL PROPERTIES - CAMIN LABORATORIES (29)

Bath Composition and Operating Range:

Nickel Sulfamate, g/l	337
Nickel Metal Content, g/l	76.4
Nickel Chloride, g/l	6 - 15
Boric Acid, g/l	30
Temperature, ^{o}C	37.8 - 60
pH (Electrometric)	3.5 - 5.0
Density, ^{o}Baumè	29 - 31
Tank Voltage, Volts	6 - 9

Mechanical Property Data:

	Test Temperature		
	Room	260^{o}C	537.8^{o}C
Ultimate Strength, MPa	743.3	493.0	190.3
ksi	106.5	71.5	27.6
Elongation in 5.08 cm, %	20	25	42

Electro-Optical Systems (30) developed procedures for electroforming cryogenic pressure vessels and large mass solar panel structures for aerospace applications. For pressure vessels, the nickel sulfamate bath with chloride for anode corrosion was selected. This formulation was chosen as typical for a bath which must produce a heavy wall electroform requiring high elongation. Temperature and current density were monitored hourly and other conditions daily. For solar panel structures, a sulfamate bath with lower chloride content was used. Operating data and some mechanical property test results were reported, Table 3.2-19. The author has noted that compressive stresses were reported for the low chloride bath. This is rather unexpected, since use of stress reducing additives was not reported. The selection of a sulfamate bath containing chloride to produce high elongation deposits is in conflict with the statement by Such (31) that use of chloride in a sulfamate bath reduces ductility.

TABLE 3.2-19. SULFAMATE NICKEL BATH COMPOSITION, OPERATING CONDITIONS, AND DEPOSIT MECHANICAL PROPERTIES - ELECTRO-OPTICAL SYSTEMS, PASADENA, CA (30)

	Structural Application:	
	Cryogenic Tanks	Solar Panels
Electrolyte Composition:		
Nickel Metal Content, g/l	62	70
Nickel Chloride, g/l	28	3.1
Boric Acid, g/l	37	40
Operating Conditions:		
pH (Electrometric)	3.0 to 3.7	4.2 to 4.8
Temperature, ^{o}C	38	54 to 57
Current Density, A/dm^2	2.1	2.1
ASF	20	20
Mechanical Property Results:		
Stress, Tensile, MPa (ksi)	34.5-69.0 (5-10)	-
Stress, Compressive, MPa (ksi)	-	0-34.5 (0-5)
Before Electroforming:		
Ultimate Strength, MPa (ksi)	552.7 (80.16)	No Data
Yield Strength, MPa (ksi)	388.9 (56.40)	Reported
Elongation in 5.08 cm, %	13.5	-
Modulus of Elasticity, MPa	149.6×10^3	-
After Electroforming:		
Ultimate Strength, MPa (ksi)	562.2 (81.54)	-
Yield Strength, MPa (ksi)	380.7 (55.22)	-
Elongation in 5.08 cm, %	12.0	-
Modulus of Elasticity, MPa	150.3×10^3	-

McCandless and Davies (32) investigated techniques for electroforming stronger nickel to allow a fuller utilization of electroforming as a reliable and low cost fabrication technique for regeneratively cooled thrust chambers. The target mechanical properties sought were 689.5 MPa (100 ksi) tensile strength with 10 percent elongation in a 5.08 cm gauge length. It was reported that the electrolyte was a Barrett (Allied-Kelite Division, The Richardson Company) sulfamate nickel plating solution. Although the Barrett bath normally is "chloride-free", the formulation used in this work contained 3.7 g/l chloride as the nickel salt. The chloride presence enabled the investigators to use rolled depolarized nickel anodes without danger of electrolyte instability.

During the first 4800 ampere-hours of bath operation, the deposits had a tensile strength of 689.5 MPa or greater, but the elongation was below 10 percent. During the next 15000 ampere-hours of operation, the mechanical properties changed to exhibit an elongation greater than 10 percent, but the tensile strength decreased to below 689.5 MPa. To increase tensile strength, small additions of chloride ion were made to bring the total chloride content of the bath to 8.25 g/l. The bath composition, operation conditions, and deposit mechanical properties, including testing performed by NASA-Lewis Research Center, are summarized in Table 3.2-20.

Sample and Knapp (8) included the nickel sulfamate bath with low chloride content in their study of the mechanical properties of nickel electrodeposits at various test temperatures. The chloride content was 1.3 g/l and the tensile stress in the deposits was reported as 57.9 MPa (8.4 ksi) for a current density of 4.31 A/dm^2 (40 ASF) and a bath temperature of 57.2°C. The bath composition, operating conditions, and deposit mechanical properties are summarized in Table 3.2-21. This data indicates that tensile strength and ductility increase with the thickness of the deposit.

Bell Aerospace Textron (33) normally uses the nickel sulfamate bath with very small chloride additions for electroforming structural hardware, including regeneratively cooled thrust chamber outer shells. In a past program to study response of such structures to nondestructive evaluation techniques, this bath was used to produce coolant passage closures of differing mechanical strengths. One such bath had been in operation for over six years with minimal routine maintenance to provide closely controlled mechanical properties. Bell has operated these electrolytes with, and without, wetting agents. The bath is continuously filtered and, where wetting agent is not employed, continuously carbon treated. The electrodeposits can be welded or heat treated with no detrimental effects.

Bell normally operates the sulfamate bath in the temperature range of 40.5° to 48.9°C to minimize expansion of wax filler materials used in recesses or coolant passages of chamber liners or other devices employing heat exchangers such as high energy laser devices. Agitation of the solution is provided by two separate circulation systems. One system contains a filter pump with the primary filter system. The other system provides the main electrolyte flow system in which electrolyte is pumped through sprays against the surfaces being electroformed. Periodic clean-up of the electrolyte is

TABLE 3.2-20. NICKEL SULFAMATE-CHLORIDE ELECTROLYTE COMPOSITION, OPERATING CONDITIONS, AND DEPOSIT MECHANICAL PROPERTIES - GENERAL TECHNOLOGIES CORPORATION (32)

Electrolyte Composition:

Nickel Sulfamate, g/l	450
Nickel Metal, g/l	76.5
Nickel Chloride, g/l	8.25
Boric Acid, g/l	39.4
Anti-pit Agent, g/l	0.38

Bath Operating Conditions:

pH (Electrometric)	4.0 ± 0.2
Temperature, ^{o}C	50 ± 2
Current Density, A/dm^2 (ASF)	4.3 (40)

Mechanical Property Test Data:

Results of General Technologies Corporation Tests:

Test No.	Tensile Strength MPa	Tensile Strength ksi	Yield Strength MPa	Yield Strength ksi	Elongation in 2.54 cm, %	Elongation in 5.08 cm, %
1	687.4	99.7	Not Determined		Not Determined	10.6
2	675.0	97.9	-		-	11.3
3	667.4	96.8	-		-	11.1
4	696.4	101.0	-		-	10.4

Results of NASA-Lewis Research Center Tests:

1	696.4	101.0	479.2	69.5	17	Not Determined
2	689.5	100.0	479.9	69.6	16	-
3	697.8	101.2	461.3	66.9	16	-

Results from Specimen Annealed at 815.6^{o}C:

4	353.0	51.2	44.5	6.45	47	Not Determined

TABLE 3.2-21. DATA FROM SAMPLE AND KNAPP (8) ON ELECTRODEPOSITED NICKEL FROM THE SULFAMATE ELECTROLYTE CONTAINING LOW CHLORIDE CONTENT

Electrolyte Composition and Operating Conditions:

Nickel Sulfamate, g/l	450
Nickel Chloride, g/l	1.3
Boric Acid, g/l	30
pH (Electrometric)	4.5
Temperature, ^{o}C	57
Current Density, A/dm^2 (ASF)	4.3 (40)
Anodes	Rolled Depolarized Nickel

Mechanical Properties at Various Test Temperatures:

Test Temp ^{o}C	Deposit Thickness cm	Tensile Strength MPa	Tensile Strength ksi	Yield Strength MPa	Yield Strength ksi	Elongation in 5.08 cm, %
-196	0.0686	996.3	144.5	619.9	89.9	13
	0.1321	1003.9	145.6	617.8	89.6	21
	0.2388	1027.4	149.0	657.1	95.3	22
- 73	0.0686	854.3	123.9	548.8	79.6	6
	0.1321	879.1	127.5	576.4	83.6	14
	0.2388	889.5	129.0	581.2	84.3	17
20	0.0686	765.3	111.0	541.3	78.5	7
	0.1321	779.1	113.0	506.8	73.5	12
	0.2388	821.9	119.2	No Data		14
204	0.0686	601.2	87.2	408.2	59.2	11
	0.1321	579.9	84.1	No Data		14
	0.2388	593.0	86.0	No Data		18
427	0.0686	311.7	45.2	182.0	26.4	15
	0.1321	313.0	45.4	193.7	28.1	24
	0.2388	276.5	40.1	No Data		36
649	0.0686	101.4	14.7	74.5	10.8	3
	0.1321	84.8	12.3	59.3	8.6	10
	0.2388	104.1	15.1	No Data		15
760	0.0686	No Data		No Data		No Data
	0.1321	44.8	6.5	No Data		9
	0.2388	No Data		No Data		No Data
871	0.0686	No Data		No Data		No Data
	0.1321	35.2	5.1	No Data		2
	0.2388	No Data		No Data		No Data

accomplished by filtering the entire tank volume through special stacked disk filters having filter elements as fine as 0.45 micron. With this electrolyte it is possible to use sulfur depolarized, rolled depolarized, or combination anodes. Most of Bell's nickel sulfamate plating capability has been replaced by the nickel-manganese system due to improved elevated temperature mechanical properties.

Table 3.2-22 presents bath composition, operating conditions, and mechanical properties for low strength and high strength sulfamate nickel from Bell's conventional sulfamate electrolytes.

TABLE 3.2-22. ELECTROFORMED NICKEL MECHANICAL PROPERTIES AND ELECTROLYTE DATA FOR THE SULFAMATE NICKEL BATH WITH CHLORIDE (33)

Bath Composition:

Nickel Metal, g/l	74.2
Nickel Chloride, g/l	3.1
Boric Acid, g/l	33.0
Wetting Agent*	None

*0.37 g/l wetting agent is used in some electrolytes when continuous carbon treatment is not employed.

Bath Operation:	High Strength	Low Strength
pH (Electrometric)	4.2	4.2
Temperature, ^{o}C	40.6	43.3
Current Density, A/dm^2	3.23	7.53
Nickel Anodes	Sulfur Depolarized	Sulfur Depolarized
Agitation	10 micron polypropylene filters with an integral pumping system; a 1136 l/hr. circulation pumping system; a carbon treatment system with integral pump.	

Deposit Mechanical Properties:	High Strength	Low Strength
Ultimate Strength, MPa (ksi)	697 (101)	524 (76)
Yield Strength, MPa (ksi)	462 (67)	331 (49)
Elongation in 5.08 cm, %	9	12

Table 3.2-23 presents additional mechanical property data for nickel deposits from Bell Aerospace Textron (34) sulfamate electrolytes over widely different deposition conditions. In general, decreasing current density results in higher tensile strength and yield strength, but elongation is decreased. Similar effects were noted when the bath temperature was increased while maintaining the current density constant. Minimum deposit thickness was 0.036 cm (0.014 in.) It should be noted that elongation results for Bell's electrodeposited nickel are based on tests of flat strips using a standard

5.08 cm gauge length. Unlike most wrought metals and alloys which elongate through plastic deformation at a fairly uniform rate over a long length, electrodeposited metals and alloys tend to undergo most of their deformation in a relatively short distance. This is due to several causes:

1) Electrodeposited metals in the "as deposited" condition are usually characterized by a microstructure with very fine grains. Often these grains are sufficiently small so as to permit grain sliding, rather than entirely dislocation movement, when deformation stresses are imposed.

2) Typical Watts type and sulfamate nickel deposits, in addition to being fine grained, have columnar grains. The columnar axis is in the direction of plating. Specimens subjected to tensile testing will thus stress the "short transverse" direction of these grains.

3) Because of the nature of electrodeposition, deposits will contain absorbed or entrapped gases, lattice vacancies, and distortions caused by occasional impurities that find their way into the electrolyte. Until normalized by some form of heat treatment such as stress relieving, these materials will not elongate in the same fashion as a wrought metal which has been produced from a melt or heat treated.

TABLE 3.2-23. MECHANICAL PROPERTIES FROM BELL AEROSPACE NICKEL SULFAMATE ELECTRODEPOSITS (34)

Nickel Metal, g/l	Nickel Chloride, g/l	Boric Acid, g/l	pH	Bath Temp., °C	Current Density, A/dm²	Ultimate Strength MPa	Ultimate Strength ksi	Yield Strength MPa	Yield Strength ksi	Elongation in 5.08 cm, %	Deposition Rates cm/hour
80.9	10.5	41.2	3.7	40.6	8.07	406.8	59	262.0	38	23	.0064
(Using mild air agitation.)			3.9	48.9	8.07	434.4	63	289.6	42	23	.0064
			3.9	57.2	8.07	496.4	72	324.1	47	13	.0064
77.1	12.0	34.4	3.9	43.3	3.23	724.0	105	482.7	70	11	.0025
(Using air and pumped electrolyte agitation.)			4.0	43.3	5.38	503.3	73	317.2	46	13	.0043
68.9	11.2	34.4	3.9	48.9	1.94	792.9	115	510.2	74	6	.0015
(Using air and pumped			3.9	48.9	3.01	772.2	112	482.7	70	10	.0025
electrolyte agitation.)			3.9	48.9	5.92	599.9	87	379.2	55	9	.0051
72.6	7.5	33.7	3.9	48.9	11.30	482.7	70	310.3	45	13	.0089
(Using high velocity electrolyte pumping.)			3.9	48.9	15.61	468.9	68	296.5	43	14	.0127

As a result of this ductility behavior in electrodeposited metals and alloys, many investigators and contractors have elected to present elongation data in terms of shorter gauge lengths - lengths which reflect the span over which nearly all of the elongation takes place. Table 3.2-11 shows that Rocketdyne employs a gauge length of 1.27 cm (1 in.) Messerschmitt-Bolkow-Blohm, Table 3.2-15, used a gauge length of only 1 cm (0.39 in.) Table 3.2-20 illustrates elongation comparisons where gauge lengths of 2.54 cm and 5.08 cm have been used on samples from the same deposits. Each 50 percent reduction of gauge length appears to increase the elongation by about 50 percent.

3.2.2.7 Selecting an Optimum Electroformed Nickel for Elevated Temperature Mechanical Properties

We have surveyed and examined the mechanical properties and some of the other physical properties of deposits from all of the nickel electrolytes of practical importance for structural applications. In some cases data was lacking for elevated temperature performance - a factor of prime concern in this investigation. It is difficult to compare materials investigated by so many individuals using electrolytes of varied composition and operating conditions. Fortunately, Sample and Knapp (8) presented data suitable for this comparison in Tables 3.2-4, 3.2-6, and 3.2-21 for Watts type, chloride, and sulfamate nickel. Figure 3.2-1 shows a graphic comparison of these properties.

From Figure 3.2-1, sulfamate nickel appears to be the optimum deposit for selection for reasonable performance at elevated temperatures. Chloride nickel shows slightly better ultimate strength to about 288°C (550°F) and better yield strength to about 371°C (700°F); however, it has an inferior ductility - particularly in the range of -46°C to 260°C (-60°F to 500°F) which is critical with respect to use on structural applications for Space Shuttle Main Engines. Also, chloride deposits contain some of the highest stresses found in electrodeposited nickel. Watts deposits reflect excellent ductility but lack good mechanical strength. They too are highly stressed in comparison with sulfamate deposits.

It would be desirable to compare Sample and Knapp's data with that of Rocketdyne over an inclusive elevated temperature range, since Rocketdyne has had responsibility for the applications of nickel electroforming to Space Shuttle Main Engine. This can be done, at least for ultimate strength, based on Moeller and Schulers' (35) paper dealing with the tensile behavior of bonded electrodeposits used on the main combustion chamber (MCC). Samples for this study consisted of conical head test specimens pulled in a direction parallel to the direction of electroform growth. The material contained a "core" sheet of Rocketdyne electroformed sulfamate nickel sandwiched between two bonded sulfamate nickel layers. The conical head configuration (also used by Bell Aerospace Textron for bond evaluation) is shown in Figure 3.2-2 with the results of the Rocketdyne testing.

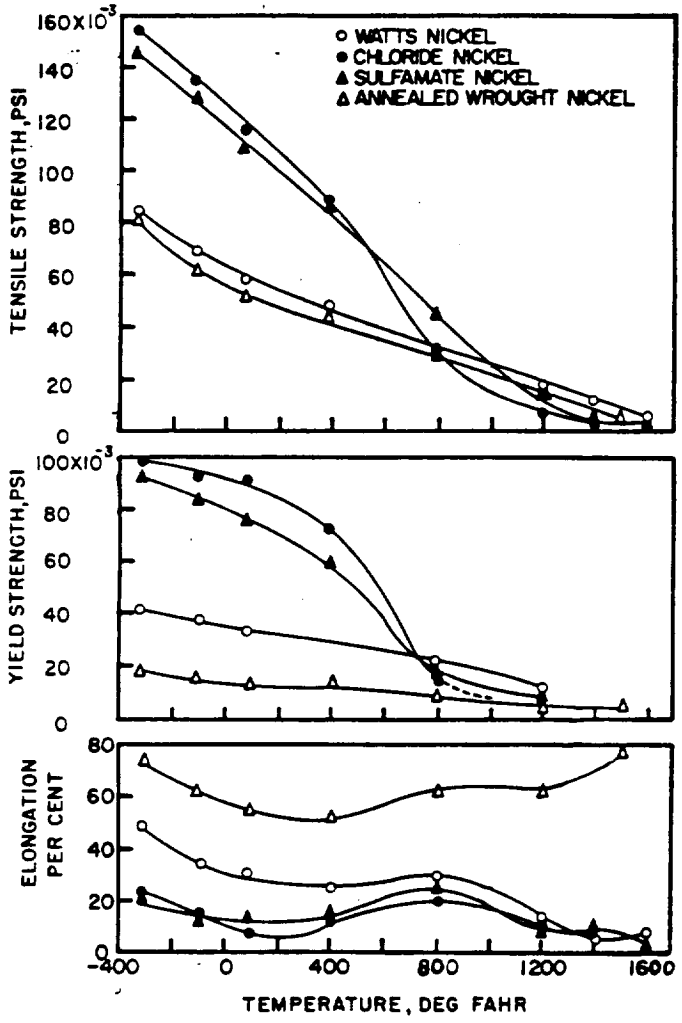

Figure 3.2-1. A Comparison of Mechanical Properties of Watts, Chloride, and Sulfamate Nickel Electrodeposits - Sample and Knapp (8)

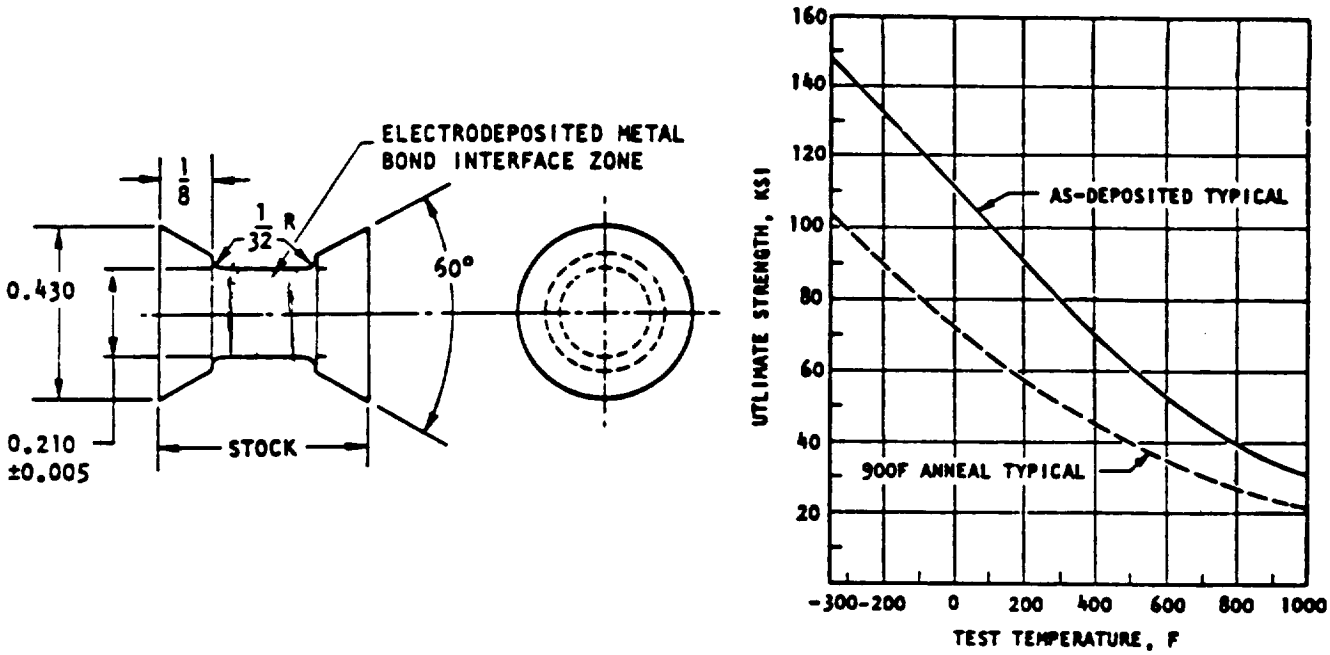

Figure 3.2-2. Illustration of Conical Head Test Specimens and Bond Strength (Rocketdyne Sulfamate Nickel Ultimate Strength) Results (35).

A comparison of the Rocketdyne data for ultimate strength of sulfamate nickel deposits with that of Sample and Knapp, Figure 3.2-1, shows reasonably good agreement, although that of the latter exhibits higher values in the intermediate temperature range. This would provide further evidence, in support of McCandless and Davies (32), that the presence of some chlorides promotes higher mechanical strength. We can thus conclude that the mechanical properties of sulfamate nickel over the test range investigated by Sample and Knapp represent the baseline, or control, from which we wish to make improvements. It is now necessary to establish a goal by which these improvements can be measured.

Structural shrouding for the Space Shuttle MCC is composed of a nickel base superalloy such as Inconel 718. As shown in Table 3.2-24 (36), this alloy has excellent mechanical properties over a wide temperature range. However, fabrication of the shroud structure requires many weldments which substantially reduce joint strength. Heavier plate thicknesses must be employed to obtain desired strength and the result is the addition of weight penalty requiring more propellant to accelerate the vehicle during launch.

From the above discussion, it follows that an electroformed metal or alloy would be desired to fabricate the shroud and avoid weldments. Such an electroformed material need not possess the Inconel 718 mechanical properties at temperatures much in excess of 204°C (400°F), since the main combustion chamber is regeneratively cooled and the shroud temperature is unlikely to experience higher temperatures.

TABLE 3.2-24. INCONEL 718 - COMPOSITION AND MECHANICAL PROPERTIES OF MILL ANNEALED SHEET, AGED AT 718.3°C (1325°F) FOR 16 HOURS (36)

Composition:

Carbon	0.10 Max.	Columbium*	4.5-5.75
Silicon	0.75 Max.	Molybdenum	2.8-3.3
Manganese	0.50 Max.	Aluminum	0.2-1.0
Copper	0.75 Max.	Titanium	0.3-1.3
Nickel	50.0-55.0	Iron	Remainder
Chromium	17.0-21.0	*Plus incidental	Tantalum

Test Temp °C	Tensile Strength MPa	Tensile Strength ksi	Yield Strength MPa	Yield Strength ksi	Elongation in 5.08 cm, %
20	1275.6	185	999.8	145	22
93.3	1241.1	180	951.5	138	22
204.4	1192.8	173	910.1	132	22
315.6	1172.2	170	882.6	128	22
426.7	1158.4	168	868.8	126	22
537.8	1103.2	160	855.0	124	22
648.9	1130.8	164	882.6	128	22
760	827.4	120	717.1	104	26

3.2.3 EF Nickel-Manganese Alloy

3.2.3.1 General

Brenner (37) has extensively surveyed the deposition of manganese and its alloys over the period to about 1962. He noted that manganese alloys of several metals could be deposited in a fairly smooth, coherent form, but none of the processes was wholly satisfactory. Alloys of manganese over the complete range of manganese content cannot be deposited in a sound condition. Those that are satisfactory usually contain either 90 percent or more of the alloying metal or 90 percent or more of manganese. Manganese has been codeposited with nickel, iron, cobalt, zinc, tin, and tungsten. The electrodeposition of manganese with the iron group metals has received the most attention.

The primary difficulty in the deposition of manganese alloys lies in the very negative (unnoble) potential of the metal in aqueous solutions. Its standard electrode potential is -1.18 volt. It is the most electronegative metal that has been deposited from aqueous solution. Brenner further advises that the highly negative potential of manganese in solutions of its simple salts makes the deposition of alloys difficult, because this potential is so far removed from the potentials of the other depositable metals. The use of complexing agents to shift the potential of the more noble metal closer to manganese would have limited value since such agents would likely inhibit the deposition of manganese altogether.

The potential of electrodeposited nickel-manganese for elevated temperature applications was not realized until 1965 when Stephenson disclosed the results of his investigation of nickel codeposits containing low contents of manganese from a sulfamate electrolyte. Since then, only a handful of investigators have examined this alloy from a standpoint of bath control, deposit composition, and elevated temperature mechanical properties. The current state of art for depositing such alloys is best discussed by the work of individual investigators.

3.2.3.2 EF Nickel-Manganese Alloy - Farmer and Stephenson

These investigators (38) were seeking an electrodeposited alloy that would equal the mechanical properties of Stainless Steel 410 from room temperature to 193°C (380°F) and withstanding heating to 260°C (500°F) for a short time without losing its capabilities at room temperature. The minimum properties were defined as:

Ultimate Tensile Strength, MPa (ksi)	1103.2	(160)
Tensile Yield Strength, 0.2%, MPa (ksi)	896.4	(130)
Elongation in 5.08 cm, % Minimum	6	
Hardness, R_C Minimum	34	

From an extensive review of then current literature (1965), cobalt-tungsten, nickel-tungsten, iron-tungsten, cobalt-molybdenum, nickel-molybdenum, iron-molybdenum, iron-chromium, nickel-chromium, nickel-cobalt, nickel-iron, nickel-manganese, nickel-cobalt-manganese, and nickel-iron-manganese-cobalt baths were investigated. From the aspects of bath control and deposit properties, the nickel-cobalt and nickel-manganese electrolytes appeared most promising.

Farmer and Stephenson employed a sulfamate electrolyte for their work with nickel-manganese composed and operated as follows:

Nickel Sulfamate (As Nickel Metal), g/l	80	
Manganese Sulfamate (As Manganese Metal), g/l	30	
Boric Acid, g/l	30	
Wetting Agent, g/l	0.375	
pH	3.5	
Temperature, °C (°F)	60	(140)
Current Density, A/dm^2 (ASF)	5	(50)
Anodes	Depolarized Nickel	

They prepared the manganese sulfamate by reacting chemical reagent grade manganese carbonate with sulfamic acid. They commented that this solution showed good promise from the start. With less than one percent manganese in the deposit, the hardness and heat stability of the nickel were changed very markedly. At 0.1 percent manganese, the "as deposited" hardness was R_C 20, and the plate had practically no stress. At 0.75 percent manganese, the hardness was R_C 44 and stress was sufficient to cause some fine cracks. The practical upper limit for a sound plate was found to be R_C 40. They cited the deposit as stable up to 400-450°C (750-850°F) with no loss in room temperature

hardness. Table 3.2-25 shows the effects of changes in manganese content of the solution, current density, temperature, and pH on the deposits.

TABLE 3.2-25. NICKEL-MANGANESE BATH COMPOSITION, OPERATING CONDITIONS, AND DEPOSIT CHARACTERISTICS AS DETERMINED BY FARMER AND STEPHENSON (38)

Electrolyte (g/l)			Bath Temp.	Current Density		Deposit Manganese,	Deposit Characteristics		
Ni	Mn	pH	°C	A/dm²	ASF	%	Stress	Hardness, R_C	Physical Appearance
Effects of Manganese Content of Electrolyte:									
88	64	3.5-4.0	54	3.7	35	1.15	High	51	Cracked and brittle
88	46	3.5-4.0	54	3.7	35	1.2	High	47	Cracked and brittle
86	39	3.5-4.0	54	3.7	35	.78	Moderate	43	Fine edge cracks
88	29	3.5-4.0	54	3.7	35	.59	Slight	36	Sound
88	24	3.5-4.0	54	3.7	35	.49	Slight	34	Sound
88	24	3.5-4.0	54	3.7	35	.25	Very slight	20	Sound
Effects of Current Density:									
88	29	3.5-4.0	54	2.1	20	.11	Very slight	26	Sound
88	29	3.5-4.0	54	5.4	50	.65	Moderate	37	Sound
Effects of Temperature:									
90	30	3.5-4.0	32	3.7	35	4.5	High	-	Many cracks
88	29	3.5-4.0	49	3.7	35	.93	High	43	Cracked and brittle
88	29	3.5-4.0	60	3.7	35	.56	Slight	34	Sound
88	29	3.5-4.0	66	3.7	35	.15	Slight	31	Sound
88	29	3.5-4.0	71	3.7	35	.025	Slight	29	Sound
Effects of pH:									
90	30	5.0	54	3.7	35	.56	Moderate	41	Slightly brittle
88	29	3.0	54	3.7	35	.44	Slight	34	Sound
90	30	2.0	54	3.7	35	.49	Slight	37	Sound
90	30	1.0	54	3.7	35	-	Very slight	-	Gas pits, soft and granular
Effects of High Current Density:									
88	29	3.5	60	5.4	50	.37	Slight	26	Sound
90	30	3.5	60	8.1	75	.40	Slight	28	Sound

Farmer and Stephenson concluded that the percentage of manganese in the deposit decreased with temperature, increased with current density increase, but fluctuations in pH caused little change in manganese content. The most important factor was the ratio of manganese to nickel in the electrolyte. They observed that the ratio of manganese in solution to that in the deposit was relatively large and concluded that the manganese concentration in the bath would not change rapidly, making it easier to control. They also noted that anode corrosion was good and the bath efficiency was close to 100 percent; oxidation resistance of the alloy was about the same as nickel.

These investigators studied the effect on deposits from heat treating at various temperatures. Comparisons were based on hardness changes for various manganese contents in samples. This data is shown in Table 3.2-26. A patent (39) was granted on this alloy in 1966 wherein some mechanical property data was supplied, Table 3.2-27.

TABLE 3.2-26. EFFECTS OF VARIOUS HEAT TREATMENTS ON HARDNESS OF NICKEL MANGANESE DEPOSITS (38)

Deposit % Manganese	Hardness Results, R_C Heat Treatment* Temp., °C Initial	260	398	482	538
.78	43	40	40	39	36
.59	36	36	36	35	33
.25	20	20	20	20	20
.11	26	22	20	20	20
.57	37	37	37	35	35
.025	29	24	20	20	20
.44	34	34	34	30	28
.49	37	37	37	31	29
.44	36	35	32	24	20
.40	38	37	35	24	23

*Heat treatments were at indicated temperature for 16 hours. All hardness testing was at room temperature.

TABLE 3.2-27. MECHANICAL PROPERTIES OF NICKEL-MANGANESE DEPOSITS AT ELEVATED TEMPERATURE (39)

Test Temperature °C	Average Ultimate Strength MPa	ksi	Average Elongation in 5.08 cm, %	Average Hardness R_C
20	1234.2	179	5.4	39
93	1137.7	165	4.0	37
204	896.4	130	5.6	36
316	682.6	99	18.0	37

3.2.3.3 EF Nickel-Manganese Alloy - Dini, Johnson, and Helms

Dini, Johnson, and Helms (40) investigated means of joining two vastly dissimilar metals - aluminum and stainless steel - by electroforming so as to avoid the thermal effects of conventional welding or brazing techniques. They sought the strongest practical electroformable metal or alloy. A literature review indicated three potential candidates, including stress reduced nickel, nickel-cobalt, and nickel-manganese. For the nickel-manganese evaluation, the bath suggested by Farmer and Stephenson (38) was selected:

Nickel (As Nickel Sulfamate), g/l	80
Manganese (As Manganese Sulfamate), g/l	30
Boric Acid, g/l	30
Wetting Agent (Surface Tension), dynes/cm	43

Since it was not possible to purchase manganese sulfamate, they used Farmer and Stephenson's procedure of mixing manganese carbonate with sulfamic acid.

Using varied conditions of pH and temperature, 0.0508 cm thick deposits were electroformed. Material from a bath at 48.^{o}C (120^{o}F), as well as those under most other conditions, were highly stressed and brittle. Efforts to electroform acceptable specimens at 60^{o}C (140^{o}F) met with failure due to high stress, so the initial work with this alloy was abandoned. Those samples that could be tested revealed the results shown below for a bath pH of 3.1:

Sample Code	Manganese in Deposit	Tensile Strength
MF	0.65%	855.0 MPa (124 ksi)
MG	0.31%	910.1 MPa (132 ksi)

In 1977, Dini and Johnson (41) again examined nickel-manganese electroforming in conjunction with a program to investigate and improve high-temperature ductility in electrodeposited nickel. This work was undertaken for the use of electroformed nickel on throat nozzle sections for the thermal protective system test facility at NASA Langley Research Center. They compared high temperature ductility between Nickel 201 and electrodeposited nickel from the sulfamate bath. It was deduced that the greatly superior performance of Nickel 201 was due to the presence of manganese which chemically combined with any sulfur present to prevent formation of nickel sulfide, a eutectic (Ni-Ni_3S_2) at 643^{o}C. Since manganese is a strong desulfurizer, Dini and Johnson re-examined the work of Farmer and Stephenson - noting that they had deposited as much as 5000 ppm manganese with nickel and obtained excellent ductility at temperatures as high as 400^{o}C.

Dini and Johnson investigated electrodeposited nickel-manganese alloy using a 40 liter bath with manganese additions, as manganese sulfamate, from 1 to 5 g/l. Round tensile specimens were made from thick electrodeposits and tested at 22^{o}C and 538^{o}C. Some specimens were tested in the "as deposited" condition, others after heating at 538^{o}C for one day, and a third set after heating at 538^{o}C for one week. Results of their mechanical property testing are shown in Table 3.2-28.

The investigators stated that for deposits containing no manganese, the typical decrease in reduction of area (RA) values expected occurred at 538^{o}C. Heating these deposits for one week at 538^{o}C before testing improved the room temperature elongation and RA but did not influence these properties at 538^{o}C. Tensile properties at 538^{o}C were considerably improved by codepositing manganese. Elongation and RA values were significantly higher than for specimens containing no manganese; quite often this improvement was close to 100 percent.

Dini and Johnson reported that there were some inconsistencies in the data which could not be explained. The 700 ppm manganese deposit exhibited an 83 percent RA at 538^{o}C in the "as deposited" condition - a value much higher than that for all other data at this test temperature. The author of this survey is of the opinion that the 700 ppm manganese concentration was sufficient to chemically combine with all sulfur present, but the excess manganese was insufficient to form appreciable amounts of the Ni_3Mn intermetallic phase which inhibits ductility to some degree as will be explained later. Dini and

TABLE 3.2-28. MECHANICAL PROPERTIES DATA FOR "AS DEPOSITED" AND HEAT TREATED NICKEL WITH AND WITHOUT MANGANESE ADDITIONS, AT ROOM AND ELEVATED TEMPERATURE (41)*

System	Test Temp °C	Tensile Strength MPa	Tensile Strength ksi	Yield Strength MPa	Yield Strength ksi	Elongation %	Reduction in Area %
"As Deposited" Specimen Data:							
No Manganese	22	790	114.5	566	82.1	21.1	76.7
	538	283	41.0	242	35.1	22.0	29.6
700 ppm Mn	22	856	124.3	714	103.6	15.0	65.0
	538	228	33.1	166	24.0	39.0	82.9
1800 ppm Mn	22	779	112.9	577	83.7	12.2	47.8
	538	245	35.5	177	25.7	22.0	47.6
Heat Treated One Day at 538°C Specimen Data:							
No Manganese	22	503	82.9	280	40.5	33.7	88.1
	538	178	25.8	143	20.7	17.1	23.8
700 ppm Mn	22	447	64.7	224	32.4	39.3	94.1
	538	171	24.8	126	18.2	32.0	43.4
1800 ppm Mn	22	646	93.7	506	73.3	21.4	92.4
	538	249	36.1	200	29.0	26.1	37.8
Heat Treated One Week at 538°C Specimen Data:							
No Manganese	22	535	77.5	297	43.1	41.1	88.4
	538	182	25.4	165	23.9	19.3	25.0
700 ppm Mn	22	448	64.9	212	30.8	49.8	92.1
	538	165	23.9	112	16.2	35.5	40.1
1800 ppm Mn	22	610	88.4	448	64.9	24.8	91.1
	538	243	35.2	222	32.2	34.6	47.3

*Round tensile specimens with a reduced section 0.2 cm in diameter and 2 cm long. Average of 2 specimens.

Johnson concluded comments on this particular investigation with the statement that adding 700 ppm manganese affected neither yield nor tensile strengths, but adding 1800 ppm of manganese increased both of these mechanical properties at high temperatures.

3.2.3.4 EF Nickel-Manganese Alloy - Wearmouth and Belt

Wearmouth and Belt (42) investigated the addition of manganese to nickel deposits produced from electrolytes containing organic stress reducing agents. Such deposits without manganese contain abnormal amounts of sulfur which makes them susceptible to catastrophic embrittlement on exposure to elevated temperatures. They determined the effect of codeposited manganese on the hardness and ductility of sulfur-containing nickel deposits as deposited and after heat treatment at temperatures up to 500°C (932°F). Their results indicated that in the presence of greater than 0.1 weight percent manganese, there is no

catastrophic embrittlement on heat treatment. Metallographic evidence was presented to show that manganese preferentially combined with sulfur on heat treatment and prevented the formation of brittle grain boundary films of nickel sulfide. The high levels of sulfur present in their deposits was due to the use of stress reducing agents to promote a compressive stress in the electroform for easier separation from the mandrel.

Wearmouth and Belt noted that sulfur brittleness in wrought nickel is eliminated by additions of manganese or magnesium to the molten nickel just prior to casting. The chemical combination of manganese with sulfur forms a high melting point eutectic which melts at 1325°C and is precipitated as globules along the grain boundaries. Although most work with nickel-manganese was previously performed in sulfate or chloride baths, Wearmouth and Belt employed the sulfamate bath and operated it in much the same manner as Dini, Johnson, and West (43). The included deposits from the Watts and Ni-speed sulfamate solutions in their study, operating all baths at 60°C. The sodium salt of o-benzoic sulfamide (sodium saccharine) was used as the stress reducer in a concentration of 0.25 g/l. Baths were maintained at a pH of 4.0. Table 3.2-29 presents other electrolyte data and manganese and sulfur compositions of the deposits at various current densities.

TABLE 3.2-29. NICKEL-MANGANESE ELECTROLYTE COMPOSITIONS AND DEPOSIT COMPOSITIONS USING VARIOUS CURRENT DENSITIES (42)

Solution Compositions:

Solution Type	Concentration, g/l				
	Nickel Sulfate	Nickel Sulfamate	Nickel Chloride	Manganese*	Boric Acid
Watts	285	-	26	15	38
Conventional Sulfamate	-	280	5	13	33
NI-Speed	-	560	8	14	33

*Manganese was added as manganese sulfate.

Effect of Current Density on Deposit Composition:

Current Density A/dm^2	Solution Type					
	Watts		Conventional Sulfamate		NI-Speed	
	% Mn	% S	% Mn	% S	% Mn	% S
4.3	0.03	0.024	0.02	0.040	0.03	0.018
6.5	0.05	0.030	0.06	0.037	0.06	0.022
8.6	0.16	0.033	0.10	0.040	0.10	0.023
10.8	0.20	0.034	0.12	0.033	0.11	0.023
12.9	0.22	0.035	0.18	0.031	0.17	0.026

From the above table it can be seen that the deposit manganese concentration increases with increase in current density with more manganese being deposited from the Watts electrolyte than from the sulfamate solutions at current densities higher than 6.5 A/dm^2. The effect of current density on hardness and stress of deposits from the three different electrolytes with sodium saccharine addition is shown in Table 3.2-30. At the lower current densities, the differences in hardness values are believed related more to the types of solutions used. At the higher current densities, the hardnesses are more similar - probably due to the increased influence of the saccharine additive. The deposit stress from all three electrolyte deposits remains compressive up to a current density of 10.8 A/dm^2.

TABLE 3.2-30. EFFECT OF CURRENT DENSITY ON HARDNESS AND STRESS OF NICKEL-MANGANESE DEPOSITS FROM VARIOUS ELECTROLYTES (42)

Current Density A/dm^2	Watts			Conventional Sulfamate			NI-Speed		
	Mn %	Vickers Hardness	Stress MPa	Mn %	Vickers Hardness	Stress MPa	Mn %	Vickers Hardness	Stress MPa
4.3	0.03	240	-43	0.02	295	-95	0.03	398	-86
6.5	0.05	274	-62	0.06	333	-98	0.06	405	-80
8.6	0.16	408	-59	0.10	378	-100	0.10	405	-91
10.8	0.20	418	-56	0.12	420	-94	0.11	410	-62
12.9	0.22	437	-53	0.18	420	+17	0.17	443	+36

Note No. 1 - Vickers Hardness tests were with 1 kg load.
Note No. 2 - Negative stress values indicate a compressive stress.

Wearmouth and Belt examined the effect of heat treatment on the mechanical properties of sulfur-containing nickel-manganese electrodeposits. Several samples of various manganese contents were prepared from Watts and conventional sulfamate nickel solutions, together with a control specimen from the conventional bath without manganese addition. Table 3.2-31 displays the hardness and ductility data for these materials as deposited and after various time-temperature heat treatments.

These investigators noted that above 200^{o}C the deposits softened appreciably - the largest decrease in hardness occurring after heat treatment at 300^{o}C, a behavior previously noted for nickel and nickel-cobalt alloy electrodeposits. At temperatures in excess of 300^{o}C, all deposits were softened, regardless of type of electrolyte employed or length of heat treatment. They observed that at 300^{o}C, the time of heat treatment has a marked effect on hardness with values generally being much lower for the longer heat treatment times. At 200^{o}C, an increase hardness was found after the four hour heat treatment, and little change was seen after the 22 hour treatment. This was surprising to Wearmouth and Belt in that such performance had not been noted for nickel or nickel-cobalt deposits subjected to similar heat treatments.

TABLE 3.2-31. EFFECT OF HEAT TREATMENT ON HARDNESS AND DUCTILITY OF DEPOSITS FROM WATTS AND CONVENTIONAL SULFAMATE BATHS (42)

Sample Preparation Data:

Solution Type	Current Density A/dm^2	Deposit Sulfur Concentration % by Wt.	Manganese Concentration Solution g/l	Manganese Concentration Deposit % by Wt
Watts	6.5	0.026	5	0.02
	12.9	0.031	5	0.10
	10.8	0.033	20	0.20
	12.9	0.036	20	0.27
Conventional Sulfamate	5.4	0.024	5	0.04
	10.8	0.025	5	0.12
	12.9	0.027	5	0.18
	7.5	0.032	20	0.23
	10.8	0.032	Nil	Under 0.01

Effect of Heat Treatment on Hardness and Ductility - Watts Deposits:

		Vickers Hardness, 1 kg Load							
Deposit	As	200°C		300°		400°C		500°C	
% Mn	Plated	4 Hrs	22 Hrs	4 Hrs	22 Hrs	4 Hrs	22 Hrs	4 Hrs	22 Hrs
0.02	287	301	298	283	214	165	129	127	143
0.10	405	428	445	205	178	186	168	178	178
0.20	405	454	445	245	156	159	138	145	150
0.27	420	445	463	368	153	168	143	129	140
		Ductility, 90° Reverse Bends to Failure							
0.02	8	7	6	8	5	<1	<1	<1	<1
0.10	4	2	3	3	3	<1	1	1	1
0.20	3	3	3	3	3	2	3	3	4
0.27	3	2	2	2	7	6	6	9	9

Effect of Heat Treatment on Hardness and Ductility - Conventional Sulfamate Deposits:

		Vickers Hardness, 1 kg Load							
Deposit	As	200°C		300°		400°C		500°C	
% Mn	Plated	4 Hrs	22 Hrs	4 Hrs	22 Hrs	4 Hrs	22 Hrs	4 Hrs	22 Hrs
0.04	338	338	333	210	165	153	145	143	143
0.12	390	428	420	175	165	168	175	175	165
0.18	428	483	483	165	172	150	182	159	165
0.23	445	493	493	378	131	148	156	148	131
<0.01	445	483	320	239	251	165	159	140	159
		Ductility, 90° Reverse Bends to Failure							
0.04	5	4	5	5	3	<1	<1	<1	<1
0.12	4	3	3	4	4	2	3	3	4
0.18	3	2	2	3	4	3	4	8	9
0.23	3	3	2	3	5	5	5	9	11
<0.01	2	<1	<1	<1	<1	<1	<1	<1	<1

Wearmouth and Belt suggested that the transitory behavior of hardness in the manganese-free" deposit of Table 3.2-31 would indicate that the more permanent hardening effect in the manganese-containing deposits may be due to the dispersion and size characteristics of the manganese sulfide particles, compared with the nickel sulfide grain boundary film in the control sample. The investigators concluded that the as-plated ductility decreased with increasing manganese content, although the decrease was small above 0.1 percent manganese (1000 ppm by weight). They further stated that the ductility after heat treatment is dependent on the manganese content of the deposit and the heat treatment temperature; the time of heat treatment having little effect on ductility, except at levels of manganese less than 0.1 percent.

A most interesting aspect of this work was the investigators observation that at 300°C, the ductility is adversely affected by increased time of heat treatment, and embrittlement occurs after heat treatment for four hours at 400°C and 500°C. To prevent embrittlement at temperatures higher than 300°C, they recommended a manganese content in excess of nominally 0.1 percent manganese - and, preferably, a manganese content of at least 0.2 percent for maximum ductility.

Wearmouth was granted a British patent (44) and a U.S. patent (45) from results of the foregoing work. Both are pertinent to additions of manganese to nickel electrodeposits having high sulfur levels for purpose of alleviating embrittlement at elevated temperature. Working with a nickel-manganese alloy with normal sulfur levels for the purpose of improving elevated temperature strength with reasonable ductility does not appear to violate these patents. The U.S. patent has been assigned to International Nickel Company.

3.2.3.5 EF Nickel-Manganese Alloy - Lichtenberger

As a result of sulfur induced hot shortness in electroformed nickel for high energy chemical laser applications, Bell Aerospace Textron converted many conventional sulfamate nickel baths to contain modest amounts of manganese sulfamate. Many of the conventional nickel specimens had been analyzed to show sulfur contents in the range of 40 to 60 ppm. Metallurgical evaluation of such samples revealed brittle fractures to be occurring at mechanical property test temperatures in the region of 538°C. Although colloidal sulfides leading to high sulfur contents in electrodeposits can be removed by frequent chemical cleaning of anode chips and high current density treating the electrolyte overnight, the recurrence of the problem is not readily detected - particularly if a critical and expensive piece of hardware is being electroformed. The ultimate solution appeared to be the incorporation of manganese in the deposit to chemically combine with sulfur and prevent grain boundary wetting from nickel sulfide at high temperature. This was essentially the same philosophy proposed by Dini and Wearmouth to improve nickel ductility in severe thermal environments.

Using a production sized electroforming facility with a capacity of 950 liters (approximately 250 gallons), Lichtenberger (46) investigated the effects of current density and electrolyte temperature on manganese content of the deposited alloy. His findings, Figure 3.2-3, indicated that manganese

content of the deposit increases exponentially with increasing current density while decreasing with increase in temperature of the electrolyte. Although the exact details of this work - particularly the control of manganese concentration in the electrolyte - are proprietary for the particular application to high energy laser components, it can be revealed that manganese was at a sufficiently low level in the bath as to introduce no significant stress in the electroformed test samples. This concentration was less than one-third of that used by Stephenson and Farmer (30 g/l). Lichtenberger attributed the decrease in manganese content with increase of bath temperature as due to the lowering of the deposition overpotential with the increasing temperature.

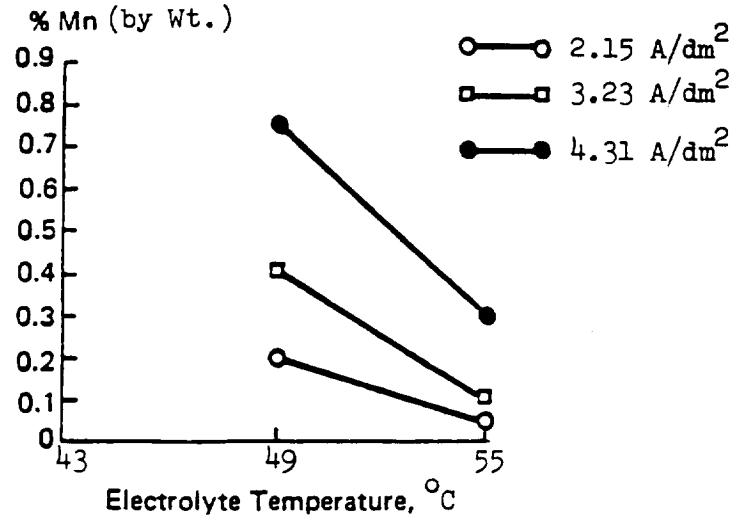

Figure 3.2-3. Manganese Concentration in Codeposits as Functions of the Electrolyte Temperature and Current Density

Figure 3.2-4 provides mechanical property data for sulfamate nickel deposits containing manganese over a range of test temperatures. All data in this figure is from specimens produced from an electrolyte operated at 48.8°C and a pH range of 4.0 to 4.1. The data indicates that manganese content of the deposit increased with increasing current density. The increase in tensile and yield strengths with increasing manganese content confirms that manganese exerts a significant effect on mechanical properties over a rather broad temperature range. Most surprising was the fact that most of the improvement in mechanical strength over conventional nickel electrodeposits (11) was achieved with as little as 0.19 percent manganese.

From the data in Figure 3.2-4 it is readily apparent that conventional electrodeposited nickel has better ductility than the nickel-manganese alloy at temperatures below about 475°C. At higher temperatures, the alloy exhibits far superior ductility. It should be noted that none of the electrodeposited metals or alloys used in constructing the data in Figure 3.2-4 had been subjected to stress relieving or other thermal treatments. Since electrodeposited alloys may be expected to have a greater degree of lattice disordering than nearly pure metal deposits, it is not surprising to note the inferior ductility of the nickel-manganese in the "as deposited" condition. As the

Figure 3.2-4. A Comparison of Mechanical Properties of Electrodeposited Nickel and Nickel-Manganese Alloys from Sulfamate Electrolytes for Various Test Temperatures. (Alloy Bath Temperature, 48.8°C Nickel Bath Temperature, 57°C) (All Specimens "As Deposited")

(a) Ultimate Strength

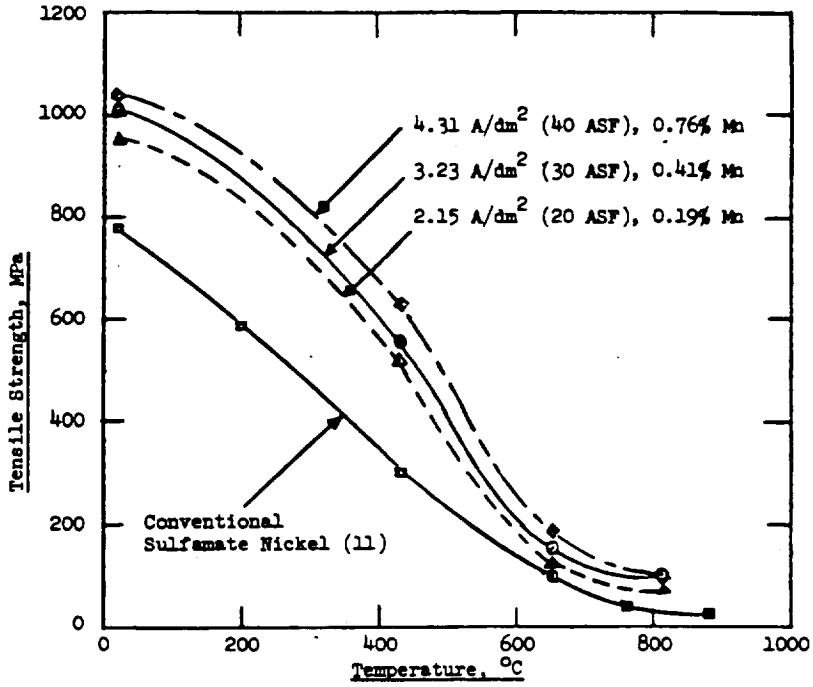

(b) Yield Strength

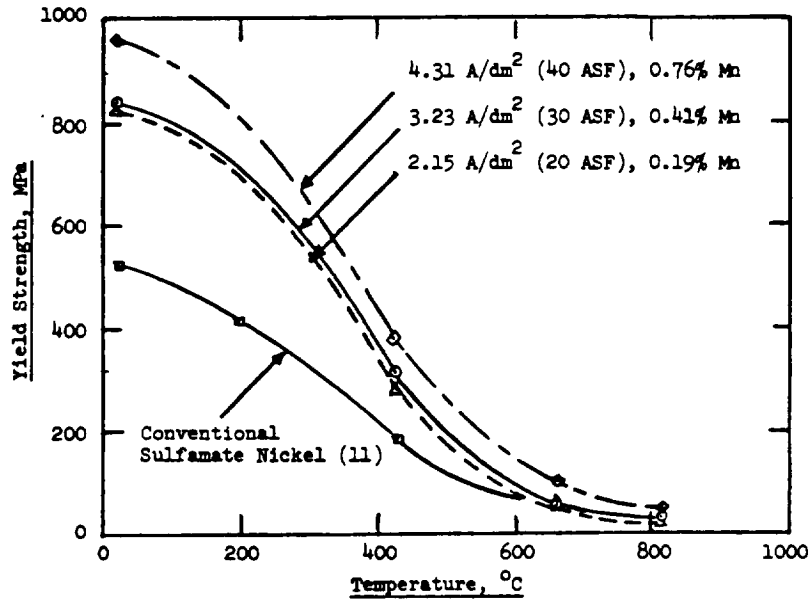

(c) Elongation

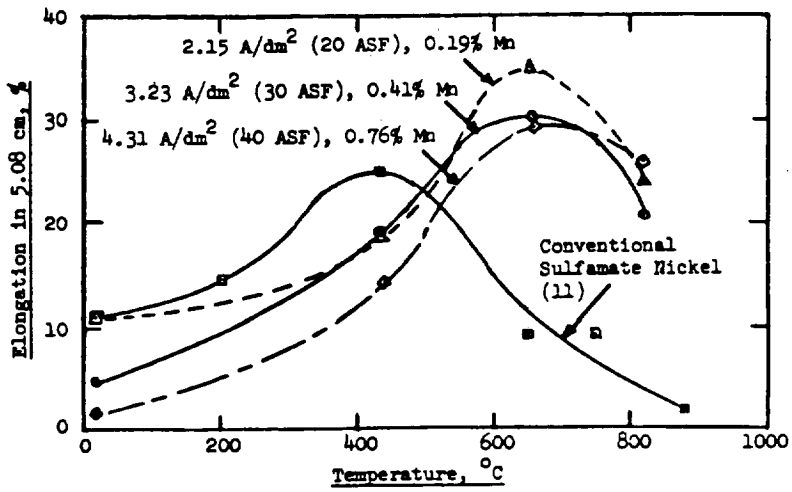

test temperature is increased beyond 400°C, it is evident that chemical and metallurgical changes are taking place which result in improved ductility performance. Much of this improvement may be attributed to manganese forming a relatively inactive solidus phase of manganese sulfide and preventing formation of a mobile liquidus phase of nickel sulfide which wets intergranular surfaces.

Lichtenberger investigated similar nickel-manganese alloys deposited from the same electrolyte at a higher temperature of 54.4°C and a pH range of 4.1 to 4.2 Similar current densities were used as in the previous study. Figure 3.2-5 presents the mechanical property test results at various test temperatures for these specimens. These results confirm the observations of Farmer and Stephenson (51) that manganese content in the deposit decreases with an increase in bath temperature. A direct comparison of the effect of bath temperature on mechanical properties is difficult to make based on the data in Figures 3.2-4 and 3.2-5 due to the great differences in deposit manganese content. However, the 3.23 A/dm^2 current density specimens from Figure 3.2-4 contain manganese in reasonably close proximity to that in 4.31 A/dm^2 current density samples tested and reported in Figure 3.2-5. Comparing these results, the alloy from the 54.4°C electrolyte exhibits higher "as deposited" ultimate and yield strengths than the material from the 48.8°C bath. However, at elevated temperature the material from the lower temperature electrolyte exhibits slightly better ultimate and yield strengths. The higher operating temperature bath also appears to yield material with better ductility over the entire range of test temperatures.

From Figure 3.2-5 it was noted that the ductility of electrodeposited nickel was greatly improved, except at room temperature, by the addition of as little as 0.06 percent manganese. Similar improvements in ultimate and yield strengths were realized at this low manganese level. However, improved yield strength was only maintained to a test temperature of about 452°C while material with significantly greater manganese concentrations appeared to retain improved yield strengths to at least 600°C.

3.2.3.6 EF Nickel-Manganese - Malone

During 1979, Malone investigated and developed procedures for producing highly reliable bonds of electrodeposited nickel-manganese alloy on age-hardened Inconel 718. The electrolyte used to deposit the nickel manganese alloy was essentially the same as used by Lichtenberger in previous studies. Bond strength test samples consisted of conical-head specimens fabricated from a thick plate containing center stock of Inconel and nickel-manganese plated on both faces. Bond test temperatures ranged from ambient to 816°C. At all temperatures below 427°C, except at room temperature, samples failed in the electrodeposited nickel-manganese in a brittle mode. It thus appeared that "as deposited" nickel-manganese alloy was subject to an unfavorable ductility transition phenomenon in this temperature range. This had not been detected in any prior work by Lichtenberger, since the alloy application was for high energy laser components where mechanical properties at temperatures over 427°C were of primary concern. As a result, the test temperatures used by Lichtenberger did not encompass the region of poor ductility performance; it was erroneously assumed that ductility behavior was normal in this regime.

Figure 3.2-5. A Comparison of Mechanical Properties of Electrodeposited Nickel and Nickel-Manganese Alloys from Sulfamate Electrolytes for Various Test Temperatures. (Alloy Bath Temperature, 54.5°C Nickel Bath Temperature, 57°C) (All Specimens "As Deposited")

(a) Ultimate Strength

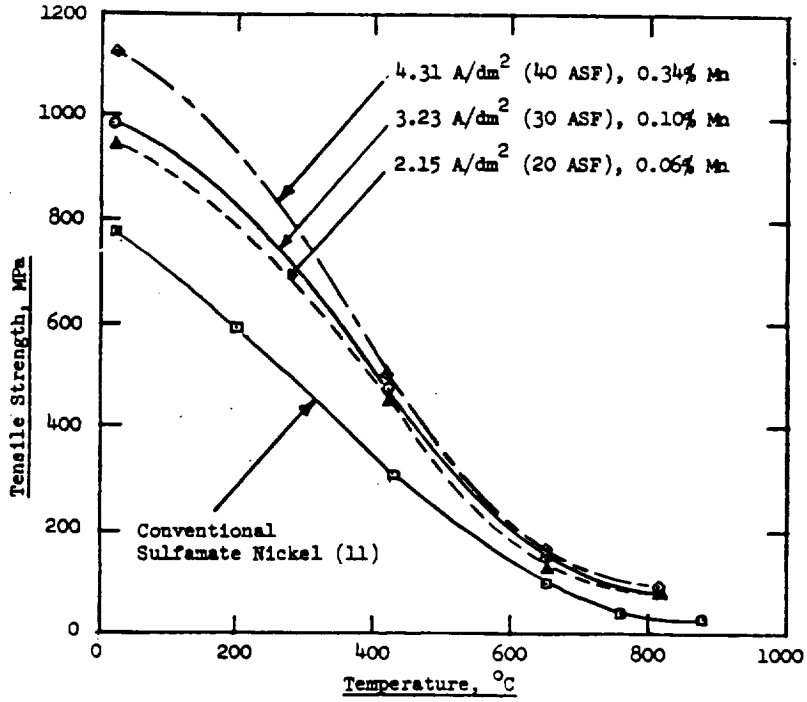

(b) Yield Strength

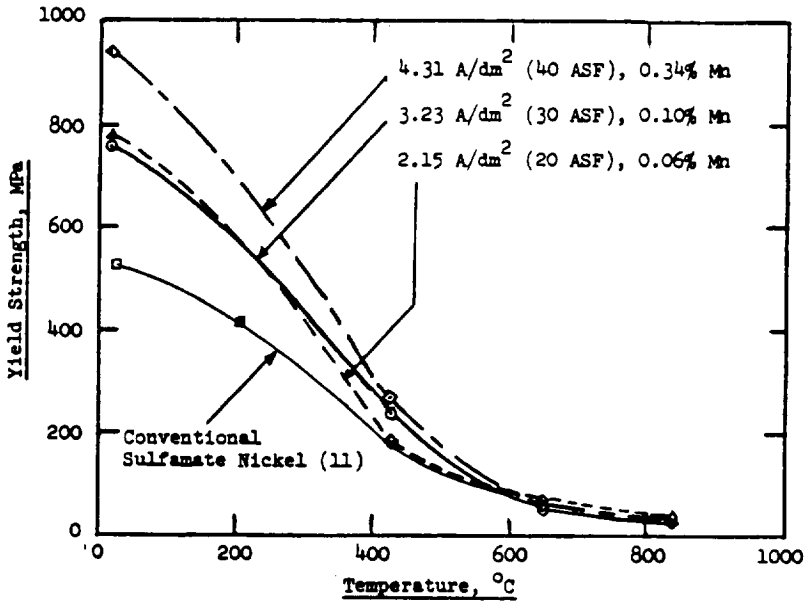

(c) Elongation

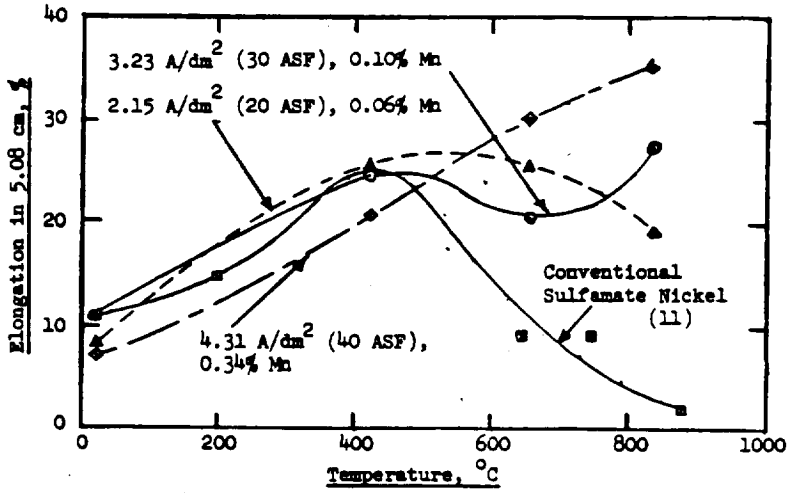

To better understand the severity of this peculiarity, Malone evaluated mechanical properties of electrodeposited nickel with varied manganese contents over more numerous test temperatures than previously employed (47). The results are shown in Figure 3.2-6, and it was confirmed that there is a decrease in ductility through a temperature range between 20°C and 427°C. Good ductility is obtained as test temperatures exceed 350°C, and it is coincidental to note that this is the temperature recommended for stress relieving conventional electrodeposited nickel. At higher temperatures (over 415°C) the nickel-manganese alloys investigated in Figure 3.2-6 exhibited very different ductility performances. The alloy deposited at a current density of 2.15 A/dm^2 contained only 0.01 percent manganese and elongated in a manner similar to conventional sulfamate nickel - i.e., it exhibited hot shortness at temperatures approaching 600°C. However, ductility improved at higher temperatures. This would indicate that very low manganese contents can have significant effects in controlling sulfides at grain boundaries. For the alloy deposited at 3.23 A/dm^2 and containing 0.07 percent manganese, the data indicates that the increased manganese content simply shifts the ductility curve to the higher temperature region and provides a higher maximum ductility "peak". Increasing manganese still higher (sample deposited at 4.31 A/dm^2, with 0.11 percent manganese) resulted in generally lower, but acceptable, ductility.

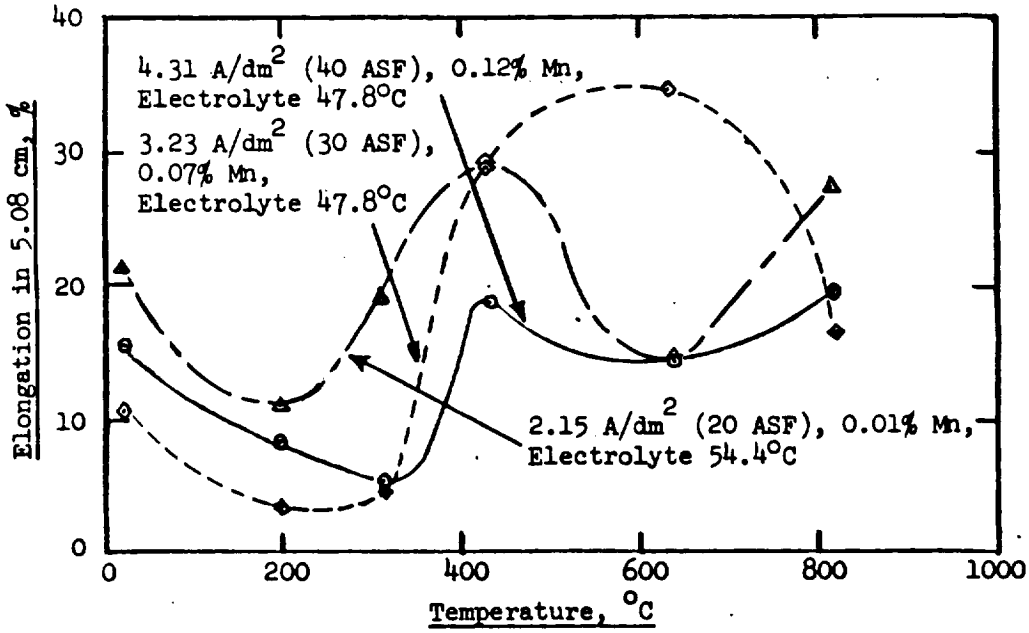

Figure 3.2-6. Ductility Transitions in Nickel-Manganese Alloys at Various Test Temperatures (61)

Malone attributed the lower ductility of the higher manganese alloy to the influence of (a) an excess of manganese over that stoichiometrically required to combine with all sulfur present and (b) to the fact that lack of

prior heat treatments resulted in short term normalization effects during thermal testing. In other words, the presence of manganese in some critical amount beyond that required to control sulfur has a profound influence on lattice slip planes or dislocation movement mechanics which govern ductility. Fully heat treated deposits would have such preferential slip planes restored for optimum ductility.

Recognizing that manganese additions to electrodeposited nickel were resulting in benefits beyond inhibition of hot shortness, Malone continued the characterization of nickel-manganese from 1981 to the present. 1981-82 efforts centered on determining how and why manganese resulted in higher ultimate strengths in electrodeposited nickel and what conditions favored retention of strength at elevated temperatures.

Malone (48) investigated pulsed current deposition of nickel-manganese alloy as a means of overcoming the problems of a diffusion controlled plating process. An array of samples was produced in 1981 and 1982 which contained nickel-manganese electrodeposits utilizing various conditions of conventional and pulse plating, various current densities, and two different low levels of manganese concentration in the electrolyte. Eight replicate tensile test strips, generally 1.78 cm in thickness, were machined from each set of electroformed plates produced for a given set of operating conditions. To evaluate the effects of heat treatment, one set of specimens was tested in the "as deposited" condition, one set after heat treating at 537.8^{o}C for two hours, and one set after exposure to 760^{o}C for twenty hours. Table 3.2-32 provides a tabulation of all mechanical property test data and corresponding sulfur and manganese contents of the alloys. The pulse duty cycle is defined as the percentage of total pulse duration time in which deposition is taking place. Thus, 100 percent would represent conventional plating while 33 percent would mean that plating was occurring during only one-third of the pulse time - the pulse is null for two-thirds of the time. Rather long pulse cycles were used such as five milliseconds on, five milliseconds off or five milliseconds on, ten milliseconds off, etc.

The data in Table 3.2-32 for mechanical properties of "as deposited" nickel-manganese alloy does not show any significant benefits attributable to pulse plating, except for the case of using a very low pulse duty cycle of 20 percent. The high mechanical strength in this instance is likely due to formation of an ultrafine grain structure, since the high properties are not retained to any significant degree after heat treatment. The one case of using a low electrolyte plating temperature (40.6^{o}C) resulted in higher manganese content as expected, but the room temperature mechanical properties were not outstanding - nor were they particularly noteworthy after heat treatment. However, a careful examination of the data for specimens heat treated at 760^{o}C for 20 hours indicates slight improvement in yield strength retention based on the amount of manganese present in the alloy. Provided sufficient manganese is present to exert an influence on mechanical properties, low pulse duty cycles appear to improve yield strength retention to some degree following heat treatment. This may be due to more uniform dispersion of the manganese in the deposit.

TABLE 3.2-32. EFFECTS OF HEAT TREATMENT ON ROOM TEMPERATURE MECHANICAL PROPERTIES OF PULSE CURRENT DEPOSITED NICKEL-MANGANESE ALLOYS (48)

Pulse Duty Cycle %	Peak Current Density A/dm^2	Average Current Density A/dm^2	Bath Temp. °C	Alloy Manganese Content % by Wt.	Alloy Sulfur Content % by Wt.	Mechanical Properties: Ultimate Str. MPa	Ultimate Str. ksi	Yield Str. MPa	Yield Str. ksi	Elongation in 5.08 cm, %
Electrodeposited Alloys Without Heat Treatment:										
100	2.15	2.15	47.8	0.102	0.018	1025.7	148.8	803.5	116.5	12
100	2.15	2.15	47.8	0.148	0.004	1114.4	161.6	868.4	125.9	10
100	2.87	2.87	47.2	0.253	0.004	1103.3	160.0	885.6	128.4	4
67	5.38	3.58	46.7	0.203	0.003	1046.0	151.7	828.1	120.1	7
67	3.23	2.15	46.7	0.129	0.005	1034.3	150.0	818.6	118.7	7
67	4.31	2.87	47.2	0.178	0.003	1170.6	169.8	875.9	127.0	5
50	4.31	2.15	40.6	0.310	0.003	943.0	136.8	721.1	104.6	8
50	4.31	2.15	47.8	0.129	0.005	1101.1	159.7	791.8	114.8	10
50	4.31	2.15	47.8	0.093	0.002	950.2	137.8	767.1	111.3	11
33	5.17	1.72	47.8	0.100	0.003	1141.2	165.5	938.9	136.2	10
33	3.23	1.08	47.8	0.028	0.002	1141.2	165.5	762.4	110.6	7.5
33	8.61	2.87	46.7	0.118	0.004	1051.6	152.5	843.2	122.3	6.5
33	5.17	1.72	46.7	0.039	0.004	1054.6	152.9	757.4	109.8	10
20	5.38	1.08	46.7	0.077	0.007	1409.4	204.4	1006.4	146.0	7
Companion Samples Heat Treated at 537.8°C for 2 Hours:										
100	2.15	2.15	47.8	0.102	0.018	711.2	103.1	569.3	82.6	20
100	2.15	2.15	47.8	0.148	0.004	879.0	127.5	788.9	114.4	10
100	2.87	2.87	47.2	0.253	0.004	965.0	140.0	827.2	120.0	10
67	5.38	3.58	46.7	0.203	0.003	834.7	121.1	709.5	102.9	8
67	3.23	2.15	46.7	0.129	0.005	804.5	116.7	716.2	103.9	10
67	4.31	2.87	47.2	0.178	0.003	909.7	131.9	765.5	111.0	10
50	4.31	2.15	40.6	0.310	0.003	790.4	114.6	707.7	102.6	8
50	4.31	2.15	47.8	0.129	0.005	764.0	110.8	689.9	100.1	11
50	4.31	2.15	47.8	0.093	0.002	653.0	94.7	498.4	72.3	21
33	5.17	1.72	47.8	0.100	0.003	717.5	104.1	673.5	97.7	16
33	3.23	1.08	47.8	0.028	0.002	510.6	74.1	368.7	53.5	32
33	8.61	2.87	46.7	0.118	0.004	740.5	107.4	619.6	89.9	2.5
33	5.17	1.72	46.7	0.039	0.004	623.2	90.4	561.8	81.5	6
20	5.38	1.08	46.7	0.077	0.007	673.8	97.7	648.4	94.0	19.5
Companion Samples Heat Treated at 760°C for 20 Hours:										
100	2.15	2.15	47.8	0.102	0.018	425.5	61.7	154.6	22.4	42
100	2.15	2.15	47.8	0.148	0.004	426.9	61.9	204.2	29.6	40
100	2.87	2.87	47.2	0.253	0.004	499.6	72.5	288.3	41.8	34
67	5.38	3.58	46.7	0.203	0.003	468.8	68.0	262.8	38.1	24
67	3.23	2.15	46.7	0.129	0.005	436.5	63.3	220.3	32.0	39
67	4.31	2.87	47.2	0.178	0.003	478.8	69.4	260.6	37.8	36
50	4.31	2.15	40.6	0.310	0.003	442.0	64.1	254.1	36.9	30
50	4.31	2.15	47.8	0.129	0.005	495.3	71.8	264.1	38.3	39
50	4.31	2.15	47.8	0.093	0.002	425.3	61.7	154.6	22.4	42
33	5.17	1.72	47.8	0.100	0.003	423.2	61.4	169.1	24.5	41
33	3.23	1.08	47.8	0.028	0.002	392.8	57.0	92.2	13.4	43
33	8.61	2.87	46.7	0.118	0.004	440.9	64.0	201.9	29.3	32
33	5.17	1.72	46.7	0.039	0.004	410.2	59.5	136.7	19.8	33
20	5.38	1.08	46.7	0.077	0.007	422.4	61.3	159.1	23.1	32

Malone also investigated the mechanical property performance of many of these specimens at elevated temperatures. He was aware that room temperature properties of heat treated specimens do not always provide reliable indications of how a material will perform at higher temperatures. This data has been assembled in Table 3.2-33 and can be directly related to data in Table 3.2-32 by the descriptions of pulse duty cycle and alloy manganese content. At the test temperature of 315.6°C there is a clear indication that decreasing the pulse plating duty cycle and increasing the pulse peak current density leads to improved mechanical properties over conventionally plated alloy, providing the manganese contents of the specimens being compared are roughly equivalent. Most noticed is the fact that yield strength is equal or better than that of the conventionally plated alloy. Moreover, mechanical strength and yield strength are significantly improved over those of conventional electrodeposited nickel.

This improvement over conventional plated nickel becomes more pronounced as the test temperature increases to 426.7°C. From the data for this test temperature, nickel-manganese alloys have greatly improved mechanical properties than conventional sulfamate nickel deposits, provided that reasonable amounts of manganese are present. At test temperatures as high as 537.8°C, the benefits of pulse plating over conventional plating are clearly seen. Less manganese is required in the alloy to maintain equivalent, and in most cases better, mechanical properties than obtained through conventional plating.

It will be observed that the yield strength of conventional (manganese-free) electrodeposited nickel is much higher than that of the alloy at 537.8°C test temperature. This is not necessarily so for ultimate strength comparisons for the two materials. This may well be due to how the heat treatments used affect grain size and structure. For conventional sulfamate nickel, a long soak at 537.8°C will produce rather large grain sizes. Conversely, the presence of manganese in the electrodeposited alloy inhibits grain growth significantly at temperatures as high as 982°C. Even small amounts of manganese exert this influence. Under these circumstances, and at elevated temperature, it is possible for fine grained electrodeposits to plastically deform and fail through a grain boundary sliding mode (50).

Malone (48) suggested that part of the strengthening effect of manganese in electrodeposited nickel might be due to formation of manganese sulfide which exists in the face-centered-cubic (FCC) cell structure having a cell (edge length) parameter of "a" = 5.224 Å. Compared with an FCC nickel cell with "a" = 3.524 Å and FCC Ni_3Mn with "a" = 3.57 Å, the larger FCC manganese sulfide cell would be expected to prevent complete lattice structure reordering upon thermal exposure. If the energy of formation of MnS were sufficiently high, such cells should act much in the manner of refractory oxide crystallites in dispersion strengthening. These large cells might retard, or at least delay, dislocation movement along primary slip planes.

TABLE 3.2-33. MECHANICAL PROPERTIES AT VARIOUS TEST TEMPERATURES OF PULSE CURRENT DEPOSITED AND HEAT TREATED NICKEL-MANGANESE ALLOYS (48)

All specimens heat treated at 537.8°C for 2 hours.

Pulse Duty Cycle %	Peak Current Density A/dm^2	Average Current Density A/dm^2	Bath Temp. °C	Alloy Manganese Content % by Wt.	Alloy Sulfur Content % by Wt.	Mechanical Properties: Ultimate Str. MPa	Ultimate Str. ksi	Yield Str. MPa	Yield Str. ksi	Elongation in 5.08 cm, %
Specimens Tested at 315.6°C (600°F):										
100	2.15	2.15	47.8	0.102	0.018	468.9	68.0	347.8	50.4	21.5
100	2.15	2.15	47.8	0.148	0.004	Not tested at this temperature.				
100	2.87	2.87	47.2	0.253	0.004	Not tested at this temperature.				
67	5.38	3.58	46.7	0.203	0.003	Not tested at this temperature.				
67	3.23	2.15	46.7	0.129	0.005	Not tested at this temperature.				
67	4.31	2.87	47.2	0.178	0.003	Not tested at this temperature.				
50	4.31	2.15	40.6	0.310	0.003	Not tested at this temperature.				
50	4.31	2.15	47.8	0.129	0.005	Not tested at this temperature.				
50	4.31	2.15	47.8	0.093	0.002	483.0	70.0	358.0	51.9	22
33	5.17	1.72	47.8	0.100	0.003	467.1	67.7	362.0	52.5	23
33	3.23	1.08	47.8	0.028	0.002	336.2	48.8	263.6	38.2	29.5
33	8.61	2.87	46.7	0.118	0.004	504.5	73.2	373.7	54.2	17.5
33	5.17	1.72	46.7	0.039	0.004	422.5	61.3	321.7	46.7	21.5
20	5.38	1.08	46.7	0.077	0.007	435.5	63.2	347.6	50.4	26
Conventional ED Nickel (315.6°C Soak for 24 Hours) (Reference 49)						344.8	50.0	241.3	35.0	34
Specimens Tested at 426.7°C (800°F):										
100	2.15	2.15	47.8	0.102	0.018	Not tested at this temperature.				
100	2.15	2.15	47.8	0.148	0.004	Not tested at this temperature.				
100	2.87	2.87	47.2	0.253	0.004	Not tested at this temperature.				
67	5.38	3.58	46.7	0.203	0.003	Not tested at this temperature.				
67	3.23	2.15	46.7	0.129	0.005	Not tested at this temperature.				
67	4.31	2.87	47.2	0.178	0.003	Not tested at this temperature.				
50	4.31	2.15	40.6	0.310	0.003	Not tested at this temperature.				
50	4.31	2.15	47.8	0.129	0.005	Not tested at this temperature.				
50	4.31	2.15	47.8	0.093	0.002	405.8	58.9	263.1	38.2	31
33	5.17	1.72	47.8	0.100	0.003	467.1	67.7	362.0	52.5	23
33	3.23	1.08	47.8	0.028	0.002	238.6	34.6	146.0	21.2	41
33	8.61	2.87	46.7	0.118	0.004	401.4	58.2	286.2	41.5	26.5
33	5.17	1.72	46.7	0.039	0.004	296.3	43.0	198.5	28.8	34
20	5.38	1.08	46.7	0.077	0.007	315.1	45.7	185.3	26.9	36
Conventional ED Nickel (426.7°C Soak for 24 Hours) (Reference 49)						248.2	36.0	165.5	24.0	37
Specimens Tested at 537.8°C (1000°F):										
100	2.15	2.15	47.8	0.102	0.018	Not tested at this temperature.				
100	2.15	2.15	47.8	0.148	0.004	181.8	26.4	40.9	5.9	30
100	2.87	2.87	46.7	0.253	0.004	Not tested at this temperature.				
67	5.38	3.58	46.7	0.203	0.003	Not tested at this temperature.				
67	3.23	2.15	46.7	0.129	0.005	Not tested at this temperature.				
67	4.31	2.87	47.2	0.178	0.003	Not tested at this temperature.				
50	4.31	2.15	40.6	0.310	0.003	228.1	33.1	80.8	11.7	28
50	4.31	2.15	47.8	0.129	0.005	201.1	29.2	59.1	8.6	38
50	4.31	2.15	47.8	0.093	0.002	Not tested at this temperature.				
33	5.17	1.72	47.8	0.100	0.003	267.3	38.8	98.0	14.2	34
33	3.23	1.08	47.8	0.028	0.002	169.3	24.6	116.4	16.9	35
33	8.61	2.87	46.7	0.118	0.004	276.4	40.1	93.1	13.5	27.5
33	5.17	1.72	46.7	0.039	0.004	213.3	30.9	104.8	15.2	25.5
20	5.38	1.08	46.7	0.077	0.007	194.8	28.3	74.5	10.8	34
Conventional ED Nickel (537.8°C Soak for 24 Hours) (Reference 49)						213.7	31.0	179.3	26.0	37

To pursue this hypothesis, Malone (48) investigated sulfur additions to electrodeposited nickel-manganese alloys and the effects on mechanical properties at various temperatures. The addition of sulfur was accomplished through the use of sodium o-benzoic sulfimide (sodium saccharin). Such compounds would normally be catastrophic regarding high temperature properties of electrodeposited nickel. However, the presence of manganese permits their use; all sulfur is chemically combined with manganese. An advantage with adding sodium saccharin is the ability to reduce tensile stress in deposits. Since codeposition of large amounts of manganese in nickel is accompanied by greatly increased tensile stress, the saccharine additive should permit codeposition of much higher manganese contents without distortion of the alloy.

Table 3.2-34 lists mechanical property test results at room temperature for specimens included in the sulfur addition study. Replicate test strips were heat treated at various temperatures to evaluate mechanical property changes and strength retention resulting from these thermal exposures. From "as deposited" and 537.8^{o}C heat treated specimens, direct comparison with similar conditions can be made from Table 3.2-32 (assuming manganese contents are roughly equivalent). In the "as deposited" condition, mechanical strength appears to be improved by incorporating more sulfur in the deposit. Ultimate strength values appear to be as equally related to increasing sulfur content as with increasing manganese content. Realizing that agents introducing sulfur into the deposits also act as stress reducers and grain refiners, Malone concentrated attention to the effects of heat treatment on ultimate strength and yield strength retention.

From Table 3.2-34 an examination of data for alloy heat treated at 204.4^{o}C shows the sample containing 0.199% by weight manganese and 0.011% by weight sulfur to have higher room temperature ultimate and yield strengths than for the following sample containing 0.251% by weight manganese and 0.004% by weight sulfur. For alloys heat treated at 537.8^{o}C, the sample containing 0.542% by weight manganese and 0.009 by weight sulfur had ultimate and yield strengths almost identical to the following sample containing 0.590% by weight manganese and 0.004% by weight sulfur. In other words, the fact that the former sample contained more than double the sulfur of the latter did not seem to influence mechanical properties after this higher temperature soak. The only conclusion drawn was that manganese sulfide may exert some strengthening effect, such effect is very minor. It must be remembered that manganese is not chemically combined with the sulfur until a temperature-time relationship is established which provides the atomic mobility and energy of formation required. Experience has shown that this formation occurs to an adequate degree by heat treating at 454.4^{o}C (850^{o}F) for two hours. Lower temperatures require longer treating times.

Some of the replicate specimens for alloys listed in Table 3.2-34 were heat treated and tested for mechanical properties at elevated temperatures. High temperature mechanical properties of these samples are of special interest because of the higher manganese contents present in certain examples. Table 3.2-35 presents the results of these tests.

TABLE 3.2-34. EFFECTS OF HEAT TREATMENTS ON ROOM TEMPERATURE MECHANICAL PROPERTIES OF PULSE CURRENT DEPOSITED, SULFUR-HARDENED NICKEL-MANGANESE ALLOYS (48)

Pulse Duty Cycle %	Peak Current Density A/dm^2	Average Current Density A/dm^2	Bath Temp. °C	Alloy Manganese Content % by Wt.	Alloy Sulfur Content % by Wt.	Mechanical Properties: Ultimate Str. MPa	Ultimate Str. ksi	Yield Str. MPa	Yield Str. ksi	Elongation in 5.08 cm, %
Electrodeposited Alloys Without Heat Treatment:										
100	2.15	2.15	49.4	0.026	0.011	1102.9	160.0	756.4	109.7	8(12)
100	2.15	2.15	49.4	0.118	0.006	1008.9	146.3	779.9	113.1	8(12)
100	3.23	3.23	49.4	0.199	0.011	1313.4	190.5	1053.4	152.8	1(3)
100	3.23	3.23	48.9	0.251	0.004	1171.8	170.0	872.0	126.5	6(11)
100	3.23	3.23	48.9	0.542	0.009	1159.2	168.1	Not determined		1
100	3.23	3.23	48.9	0.590	0.004	1419.9	205.9	1087.7	157.7	2.5
50	4.31	2.15	49.4	0.035	0.009	1079.2	156.5	775.5	112.5	8(11)
50	6.46	3.23	48.3	0.097	0.010	1377.0	199.7	920.8	133.5	4
50	6.46	3.23	47.8	0.126	0.021	1704.4	247.2	1085.8	157.5	8(12)
50	6.46	3.23	48.9	0.164	0.019	1702.2	246.9	1049.8	152.3	9
50	6.46	3.23	48.6	0.240	0.010	1283.2	186.1	907.8	131.7	6
Companion Samples Heat Treated at 204.4°C (400°F) for 72 Hours:										
100	2.15	2.15	49.4	0.026	0.011	1105.0	160.3	826.4	119.9	8.5(12)
100	2.15	2.15	49.4	0.118	0.006	1055.5	153.1	870.8	126.3	6(11)
100	3.23	3.23	49.4	0.199	0.011	1353.8	196.4	1154.7	167.5	1(1)
100	3.23	3.23	48.9	0.251	0.004	1272.0	184.5	1119.3	162.3	5.5(8)
100	3.23	3.23	48.9	0.542	0.009	Not heat treated at this temperature.				
100	3.23	3.23	48.9	0.590	0.004	Not heat treated at this temperature.				
50	4.31	2.15	49.4	0.035	0.009	1042.6	151.2	798.3	115.8	5.5(10)
50	6.46	3.23	48.3	0.097	0.010	Not heat treated at this temperature.				
50	6.46	3.23	47.8	0.126	0.021	Not heat treated at this temperature.				
50	6.46	3.23	48.9	0.164	0.019	Not heat treated at this temperature.				
50	6.46	3.23	48.6	0.240	0.010	Not heat treated at this temperature.				
Companion Samples Heat Treated at 315.6°C (600°F) for 24 Hours:										
100	2.15	2.15	49.4	0.026	0.011	Not heat treated at this temperature.				
100	2.15	2.15	49.4	0.118	0.006	724.9	105.1	701.3	101.7	11(3¼*)
100	3.23	3.23	49.4	0.199	0.011	Not heat treated at this temperature.				
100	3.23	3.23	48.9	0.251	0.004	1017.6	147.6	916.7	133.0	1.5
100	3.23	3.23	48.9	0.542	0.009	Not heat treated at this temperature.				
100	3.23	3.23	48.9	0.590	0.004	1496.4	217.0	1189.6	172.5	6(1¼*)
50	4.31	2.15	49.4	0.035	0.009	Not heat treated at this temperature.				
50	6.46	3.23	48.3	0.097	0.010	Not heat treated at this temperature.				
50	6.46	3.23	47.8	0.126	0.021	Not heat treated at this temperature.				
50	6.46	3.23	48.9	0.164	0.019	Not heat treated at this temperature.				
50	6.46	3.23	48.6	0.240	0.010	Not heat treated at this temperature.				
Companion Samples Heat Treated at 426.7°C (800°F) for 4 Hours:										
100	2.15	2.15	49.4	0.026	0.011	Not heat treated at this temperature.				
100	2.15	2.15	49.4	0.118	0.006	Not heat treated at this temperature.				
100	3.23	3.23	49.4	0.199	0.011	Not heat treated at this temperature.				
100	3.23	3.23	48.9	0.251	0.004	Not heat treated at this temperature.				
100	3.23	3.23	48.9	0.542	0.009	1564.4	226.9	1356.8	196.8	4(1¼*)
100	3.23	3.23	48.9	0.590	0.004	1436.8	208.4	1268.4	184.0	5(1¼*)
50	4.31	2.15	49.4	0.035	0.009	Not heat treated at this temperature.				
50	6.46	3.23	48.3	0.097	0.010	545.2	79.1	512.1	74.3	25(30*)
50	6.46	3.23	47.8	0.126	0.021	630.9	91.5	625.3	90.7	30(40*)
50	6.46	3.23	48.9	0.164	0.019	599.7	87.0	541.5	78.5	29
50	6.46	3.23	48.6	0.240	0.010	1214.5	176.1	1082.2	157.0	6(3¼*)
Companion Samples Heat Treated at 537.8°C (1000°F) for 2 Hours:										
100	2.15	2.15	49.4	0.026	0.011	457.9	66.4	447.6	64.9	5(6)
100	2.15	2.15	49.4	0.118	0.006	726.4	105.4	664.1	96.3	12.5(26)
100	3.23	3.23	49.4	0.199	0.011	828.4	120.2	Not determined		7.5(15)
100	3.23	3.23	48.9	0.251	0.004	1118.1	162.2	1008.9	146.3	5(10)
100	3.23	3.23	48.9	0.542	0.009	1357.0	196.8	1206.6	175.0	6(1¼*)
100	3.23	3.23	48.9	0.590	0.004	1363.8	197.8	1204.7	174.7	6(16*)
50	4.31	2.15	49.4	0.035	0.009	500.5	72.5	353.5	51.3	40.5(50)
50	6.46	3.23	48.3	0.097	0.010	Not heat treated at this temperature.				
50	6.46	3.23	47.8	0.126	0.021	Not heat treated at this temperature.				
50	6.46	3.23	48.9	0.164	0.019	Not heat treated at this temperature.				
50	6.46	3.23	48.6	0.240	0.010	859.4	124.6	810.0	117.5	11(3¼*)

NOTE: Elongation values in () are 2.54 cm gauge length; values with * are 1.27 cm gauge length.

TABLE 3.2-35. MECHANICAL PROPERTIES AT VARIOUS TEST TEMPERATURES OF PULSE CURRENT DEPOSITED AND HEAT TREATED SULFUR-HARDENED NICKEL-MANGANESE ALLOYS (48)

Pulse Duty Cycle %	Peak Current Density A/dm²	Average Current Density A/dm²	Bath Temp. °C	Alloy Manganese Content % by Wt.	Alloy Sulfur Content % by Wt.	Mechanical Properties: Ultimate Str. MPa	Ultimate Str. ksi	Yield Str. MPa	Yield Str. ksi	Elongation in 5.08 cm, %
Specimens Heat Treated at 537.8°C (1000°F) for 2 Hours:										
Specimens Tested at 426.7°C (800°F):										
100	2.15	2.15	49.4	0.026	0.011	241.0	35.0	179.9	26.1	5.5(6)
100	2.15	2.15	49.4	0.118	0.006	372.7	54.1	257.1	37.3	13.5(18)
100	3.23	3.23	49.4	0.199	0.011	371.4	53.9	290.3	42.1	13(18)
100	3.23	3.23	48.9	0.251	0.004	503.7	73.1	290.1	42.1	7(13)
50	4.31	2.15	49.4	0.035	0.009	246.4	35.7	201.1	29.2	19(23)
Specimens Tested at 648.9°C (1200°F):										
100	2.15	2.15	49.4	0.026	0.011	Brittle failure early in test.				
100	2.15	2.15	49.4	0.118	0.006	138.0	20.0	38.3	5.6	11(17)
100	3.23	3.23	49.4	0.199	0.011	112.7	16.3	27.2	4.0	15(22)
100	3.23	3.23	48.9	0.251	0.004	138.3	20.1	42.3	6.1	22.5(34)
50	4.31	2.15	49.4	0.035	0.009	113.9	16.5	47.0	6.8	5(6)
Specimens Heat Treated at 426.7°C (800°F) for 4 Hours:										
Specimens Tested at 315.6°C (600°F):										
100	3.23	3.23	48.9	0.542	0.009	971.0	140.8	586.1	85.0	4.5
100	3.23	3.23	48.9	0.590	0.004	952.1	138.1	659.9	95.7	9
50	6.46	3.23	48.3	0.097	0.010	381.0	55.3	351.7	51.0	9
50	6.46	3.23	47.8	0.126	0.021	423.6	61.4	389.6	56.5	16.5(23)
50	6.46	3.23	48.9	0.164	0.019	413.7	60.0	358.9	52.1	23(27)
50	6.46	3.23	48.6	0.240	0.010	732.9	106.3	541.3	78.5	6.8(8.2)
Specimens Tested at 537.8°C (1000°F):										
100	3.23	3.23	48.9	0.542	0.009	315.7	45.8	150.7	21.9	9.6
100	3.23	3.23	48.9	0.590	0.004	362.7	52.6	150.9	21.9	10.5
50	6.46	3.23	48.3	0.097	0.010	215.6	30.8	84.4	12.2	12.5(19)
50	6.46	3.23	47.8	0.126	0.021	205.7	29.8	66.7	9.7	15.5(20)
50	6.46	3.23	48.9	0.164	0.019	203.7	29.6	85.4	12.4	16.5(24)
50	6.46	3.23	48.6	0.240	0.010	258.2	37.5	98.3	14.3	8.5

NOTE: Elongation values in () are 2.54 cm gauge length.

The data in Table 3.2-35 shows conclusively that ultimate strength and yield strength of nickel-manganese alloys are, at elevated temperatures, closely related to manganese content. The fact that such low concentrations of manganese can have such a profound effect is surprising.

Since Ni_3Mn and nickel are both face-centered-cubic (FCC) with similar "a" values for cell dimensions, we still need a mechanism for elevated temperature strengthening due to the manganese. If one examines the binary phase diagram for nickel-manganese, Figure 3.2-7, it can be seen that Ni_3Mn lies in a region where peritectic transformations might occur. Should this be correct, it is probable that two adjacent Ni_3Mn cells undergo a thermally induced transformation to produce one FCC cell of nickel and one face-centered-tetragonal (FCT) cell of Ni-Mn. An alternate possibility is the codeposition of manganese rich atomic layers which order into FCT NiMn cells upon heat

treatment. In either event, NiMn will be FCT and exert the effects of such a cell on mechanical performance of surrounding FCC cells. One would then anticipate impediments to climb whereby dislocation movements cross grain boundaries - leading to coalescence and grain growth - on heat treating, and delays in slip plane movements under stress wherein higher yield strengths would be evident.

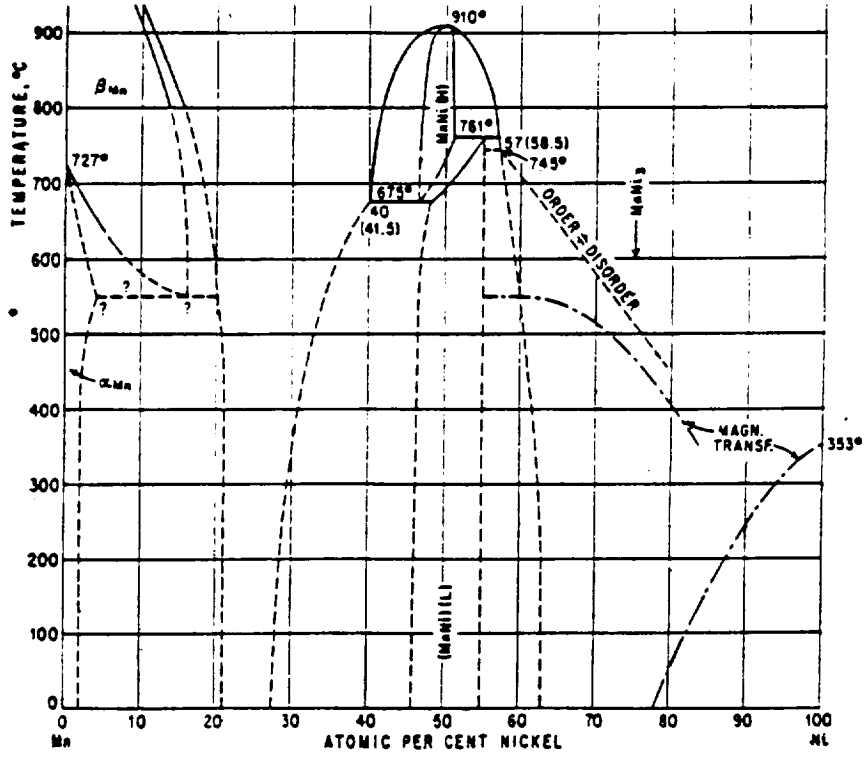

Figure 3.2-7. Nickel-Manganese Phase Diagram

3.2.3.7 Conclusions - Electrodeposited Nickel-Manganese Alloys

Nickel-manganese alloys are relatively easy to electrodeposit in a low stress condition. However, high manganese contents in deposits (over 0.5 percent by weight) are accompanied by visible signs of stress. Unless manganese contents are low (sufficient only to chemically combine with sulfur to overcome hot-shortness), it is necessary to heat treat the alloy in order to assure suitable ductility. Nickel-manganese electrodeposits are exceptionally stronger than conventional nickel deposits over a wide thermal test range. Strength appears directly related to manganese content. Manganese content can be increased while internal stress is minimized by the addition of stress reducing agents to the electrolyte. The deleterious effects of sulfur thus induced is offset by heat treating the alloy to combine sulfur with manganese.

Nickel-manganese has an added advantage in that many severe thermal treatments or exposures do not lead to excessive grain growth. This

contributes to excellent strength retention in such alloys - even after brazing or welding operations. The bath is very simple to operate; manganese is supplied through an infrequent addition of manganous ion. Manganese content of the alloy can be adjusted through control of electrolyte temperature and current density. Large changes can be made by increasing the concentration of manganese ion in the bath. Internal stress can be minimized by very small additions of sodium saccharin without increasing sulfur to a great degree.

A primary disadvantage of electrodeposited nickel-manganese is the fact that "as deposited" material, like most electroplated alloys, shows poor ductility at moderate temperatures unless a heat treatment is performed. Ductility is quickly restored by a two hour soak at 454.4°C; longer times are required at lower temperatures. The user must consider the consequences of such heat treatments on the electroformed item - particularly where a thermally sensitive component may form part of the end item.

3.2.4 EF Nickel-Cobalt Alloys

3.2.4.1 General

Brenner (51) points out that nickel and cobalt, both metals of the iron group, are easily deposited as an alloy. This ease of codeposition is due to the facts that the standard potentials of the two metals are close together and the metals deposit with a high polarization. Nickel, the more noble metal, has a standard potential of -0.250 volt, while cobalt has a standard potential of -0.277 volt. Alloy plating baths are easily prepared by mixing simple salt baths of the individual metals together. Although nickel-cobalt alloys have many useful properties, such as high strength, hardness, and unusual magnetic properties, it is only within the last 30 years that the applications of these alloys began to attract much interest.

Codeposition of nickel and cobalt follows a process of the anomalous type; however, this phenomenon is not as pronounced as with other alloys such as nickel-zinc. Brenner notes that anomalous codepositions are characterized by the peculiarity that the less noble metal deposits preferentially. He also advises that anomalous behavior may only occur over certain ranges of the plating conditions imposed on a bath. As an example, the most important aspect of anomalous codeposition is the unusual variation of alloy composition with current density. At very low current densities, the system may behave in a normal manner with the more noble metal being preferentially deposited. As the current density is increased, the system goes through a transition where both metals are deposited in the same ratio as present in the bath. Further increase in current density results in anomalous behavior where the less noble metal is preferentially plated. In this survey we will be concerned with nickel-cobalt as an anomalous plating system.

Barrett (52) included nickel-cobalt alloy in his discussion of plating various metals from the sulfamate solution. He provided information on bath composition, operating conditions, and effects of changing operating conditions on alloy composition as shown in Table 3.2-36.

TABLE 3.2-36. SULFAMATE COBALT-NICKEL ALLOY PLATING BATH COMPOSITION, OPERATING PARAMETERS, AND EFFECTS OF PARAMETER CHANGES IN ALLOY COMPOSITIONS (52)

Bath Composition and Operating Parameters:

Cobalt Sulfamate, g/l	225
Nickel Sulfamate, g/l	225
Boric Acid, g/l	30
Magnesium Chloride, g/l	15
Anti-pit Agent, mg/l	375
Cobalt: Nickel Metal Ratio	1:1 (approximate)
Cobalt: Nickel Plating Ratio	80% Co, 20% Ni
Anodes (Special Cast)	80% Co, 20% Ni
pH (Electrometric)	2.0 - 4.0
Temperature, ^{o}C	25
Average Current Density, A/dm^2	1.61 - 3.23
Agitation	Cathode Movement
Cathode Efficiency, %	98 - 99
Anode Efficiency, %	100
Stress, MPa	100.7

General Effects of Operating Parameter Changes on Alloy:

Variable	Direction of Change	Effect
Temperature	Increase	Increase in Co Content
pH	Increase	Decrease in Co Content
Agitation	Increase	Increase in Co Content
Cathodic Current Density	Increase	Decrease in Co Content
Boric Acid	Increase, Decrease	No effect on Co Content
Magnesium	Increase, Decrease	No effect on Co Content

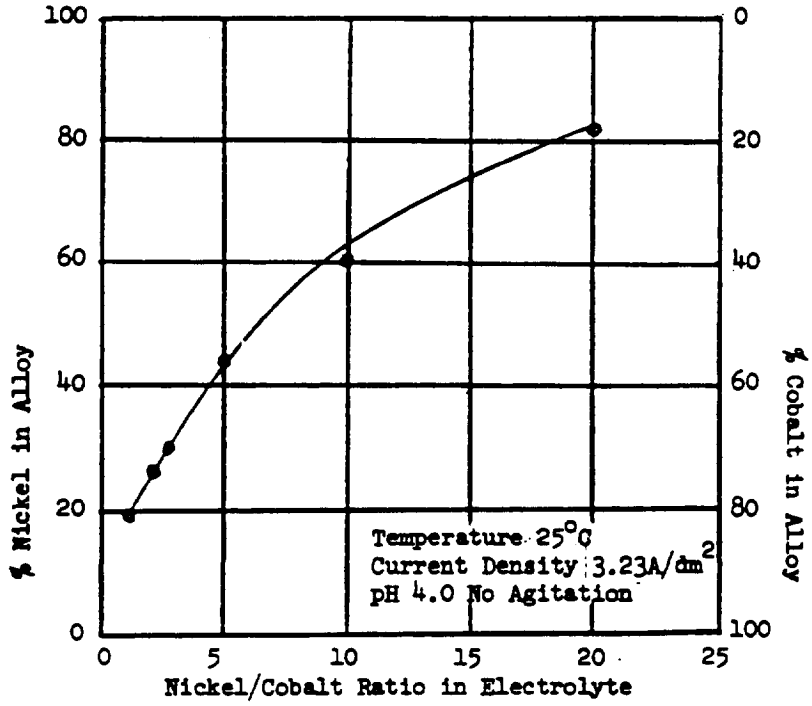

Barrett advises that the high tensile stress found in cobalt deposits is not consistent with the low stress in nickel from the sulfamate solution. He suggests that this anomaly may be due to the fact that electrodeposited cobalt can exist in the stable, close-packed-hexagonal (HCP) lattice of crystallization as well as face-centered-cubic (FCC) while nickel crystallizes only in the FCC system. Stress can be relieved readily at relatively low temperatures of 204°C to 227°C.

Walker and Cruise (53) surveyed the use and production of electrodeposited cobalt. They point out a main advantage of nickel-cobalt alloy electroforms over nickel is that the cobalt content acts to strengthen the deposit without the need for the conventional sulfur-containing organic additives codeposited with pure nickel deposits. Such sulfur (when manganese is not present) tends to promote cracking in the range of 380°C to 420°C. They also state that the cathode efficiency of cobalt plating baths depends on variables such as pH, metal ion concentration, current density, etc. Often, a reduction of the pH of the solution results in an increase in the efficiency, but hydrogen uptake in the deposits increases. Incorporating hydrogen into the deposits increases stress. This can be reduced by using a wetting agent to release hydrogen gas bubbles from the cathode surface. This appears contrary to the statements of Morral (54) where data is presented showing the least absorbed hydrogen in the deposit when the electrolyte pH is 1.8. Both Morral and Walker and Cruise agree with Barrett in the situation of HCP and FCC cobalt being present with the amount dependent on operating conditions for the electrolyte.

With the great variety of electrolytes available for depositing nickel-cobalt alloys and the even greater multitude of operating conditions, it is best to survey the field from a standpoint of individual investigators.

3.2.4.2 EF Nickel-Cobalt Alloys - Endicott and Knapp

Endicott and Knapp (55) investigated nickel-cobalt alloys deposited from a sulfamate bath. They related solution operating variables to physical properties of the deposits and investigated effects of the solution metal ratios, anode characteristics, bath temperature, boric acid content, and current densities on alloy compositions. They correlated mechanical properties, hardness, and grain structures with compositions and heat treatments up to 620°C (1150°F). The sulfamate bath was selected because it has proven to be the most suitable for nickel electroforming and because cobalt additions are readily compatible.

To produce the pure nickel, pure cobalt, and nickel-cobalt alloy deposits, three plating set-ups were used. One system was conventional for plating the pure metals. A second system employed a current splitting device to divide current between the nickel and cobalt anodes. The third system incorporated a metering pump to maintain solution-metal balance by metered cobalt additions. No cobalt anodes were used in the latter set-up. Only the work with the alloy system is discussed in this survey. Their nickel-cobalt bath was composed and operated as follows:

Total Metal (Nickel + Cobalt)	82-94 g/l
Nickel/Cobalt Ratio	Varied from 1% to 90% by Weight Co (approx.)
Boric Acid	29.6 to 31.5 g/l
Nickel Bromine	12.4 to 15.2 g/l
or	
Cobalt Bromide	13.6 to 14.2 g/l
pH (Electrometric)	3.8 to 4.2
Surface Tension	26.4 to 31.1 dynes/cm
Temperature	49°C (120°F)
Anodes	Pure Ni and/or Pure Co

The nickel or cobalt bromide addition to the electrolyte was for the purpose of better anode corrosion without the great increases in internal stress normally associated with chloride as a corrosion aid.

Figure 3.2-8 illustrates the anomalous nature of nickel-cobalt codeposition based on the Endicott and Knapp investigation. These investigators also determined the effect of the nickel to cobalt ratio in the electrolyte on the deposit composition as a result of varying the current density, Figure 3.2-9. Figure 3.2-9 shows that increasing current density increases the nickel content of the alloy deposit. The investigators also commented that the deposition of alloys containing 5 to 35 percent cobalt require very close control of the electrolyte metal as is evident from Figure 3.2-8. They did not comment on the effects of agitation, although they employed agitation in each plating facility.

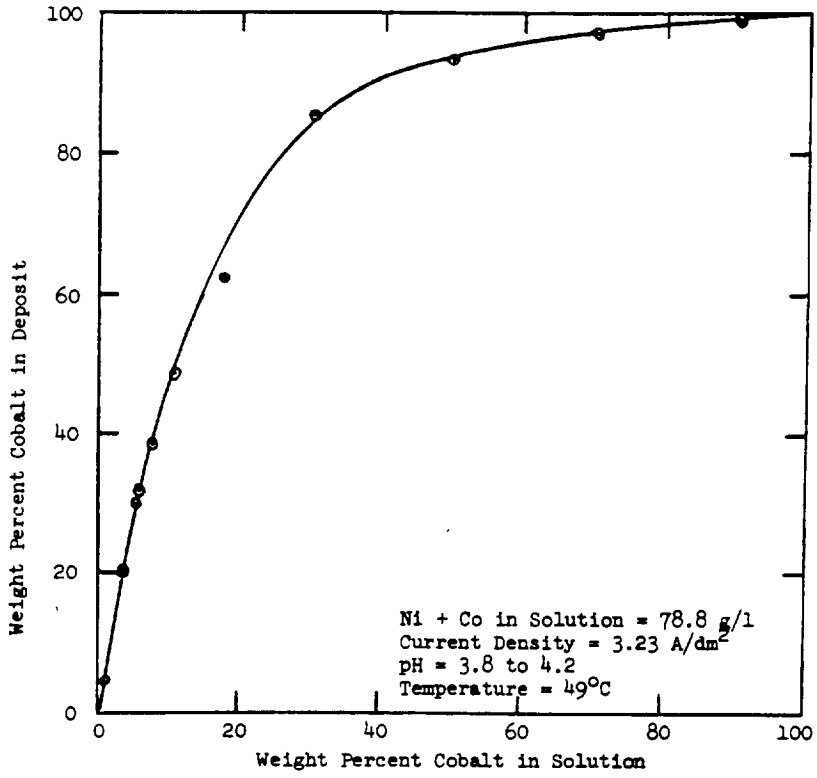

Figure 3.2-8. Deposit Composition as a Function of Solution Metal Ratio

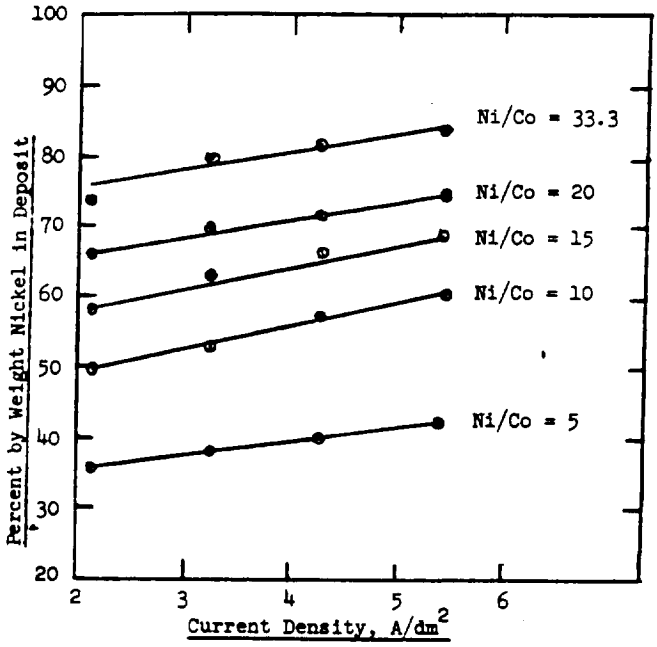

Figure 3.2-9. Effect of Bath Ni/Co Ratio and Current

Alloys of various compositions were electrodeposited for mechanical property, hardness, and microstructural evaluation at room temperature and at room temperature after various heat treatments. It should be pointed out that their tensile specimens were only 0.0178 cm (0.007 in.) thick. Many investigators prefer to use much thicker specimens to provide more representative data for yield strength and elongation in a given gauge length. Brenner (56) stated that the thickness of a deposit can have appreciable effect on the physical properties of the metal due to microstructural variations in the early stages of plating. Although a severe heat treatment will tend to normalize this structure, the influence of moderate heat treatments may not be sufficient to offset these anomalies. He preferred use of thicknesses of at least 0.030 cm (0.012 in.) Much of this abnormal initial microstructure may stem from the microstructure of the basis metal on which deposition is taking place. Mechanical properties for "as deposited" nickel-cobalt alloys have been replotted from Endicott and Knapp's reported data, Figure 3.2-10. It appears that best ultimate and yield strengths are obtained when the alloy nickel content is between 55 and 75 percent by weight.

These investigators applied various heat treatments to duplicate samples of the alloys investigated. Figure 3.2-11 represents a replot of their reported data for alloys heat treated at 232.2°C (450°F) for 10 minutes in a vacuum followed by an argon quench. Comparing mechanical properties in Figure 3.2-11 with those in Figure 3.2-10 discloses that few significant changes occurred. There is some improvement in ultimate and yield strengths for cobalt rich alloys but ductility remains poor. Yield strength is generally lower after this mild heat treatment, except for those alloys described as having lamellar or mixed lamellar-columnar structure. Although the

investigators did not comment on specific changes occurring at this heat treatment temperature, an examination of the binary alloy phase diagram for nickel-cobalt, Figure 3.2-12, will help to visualize allotropic changes (or lack of changes) and their effects on mechanical properties.

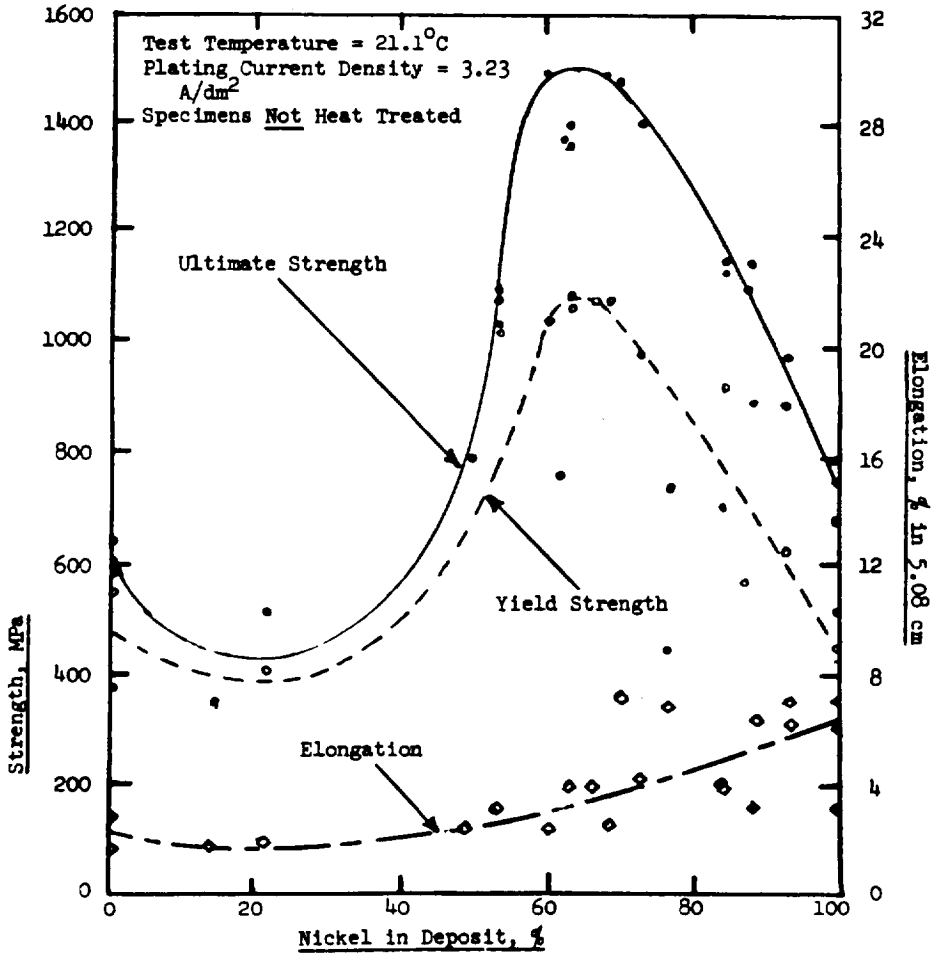

Figure 3.2-10. Effects of Nickel-Cobalt Electrodeposited Alloy Composition on Room Temperature Mechanical Properties of "As Deposited" Metal

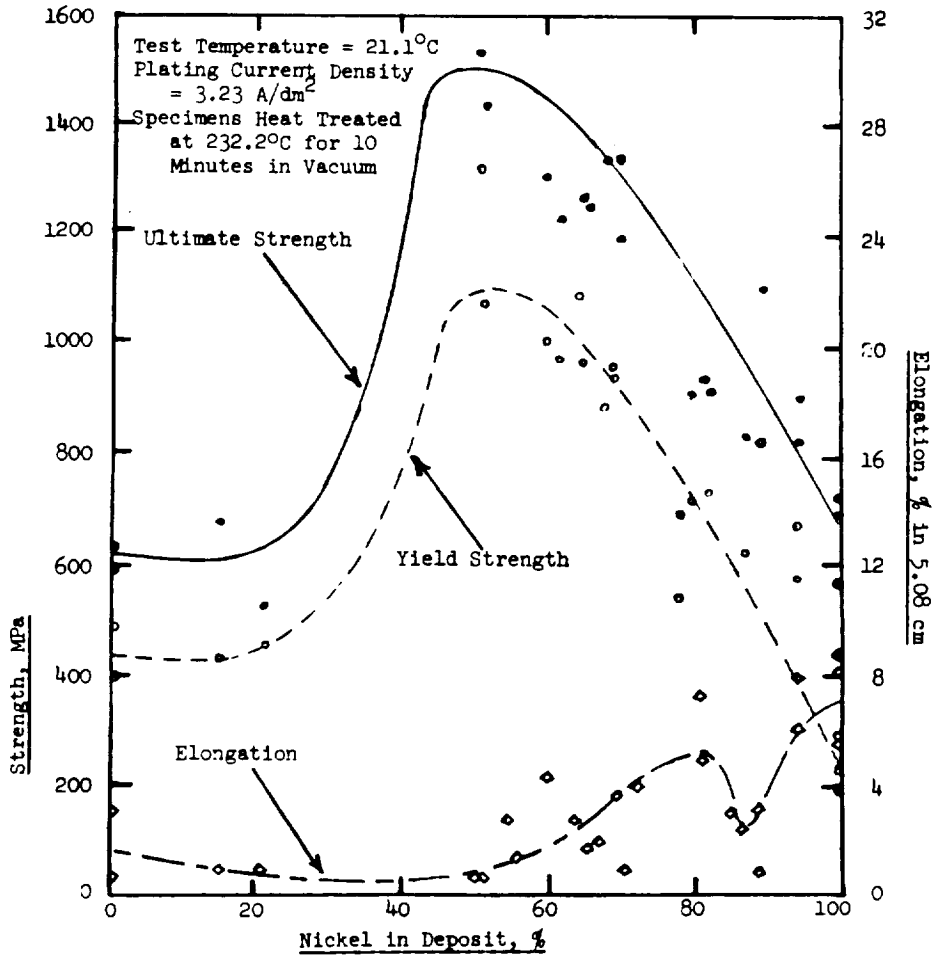

Figure 3.2-11. Effects of Heat Treating at 232.2°C for 10 Minutes on Room Temperature Mechanical Properties of Various Nickel-Cobalt Alloys

The ϵ' region for cobalt rich alloys is where cobalt-nickel exists with primarily hexagonal-close-packed (HCP) cell structure. On heating the metal to 420°C all existing HCP cells are transformed to face-centered-cubic (FCC) cells similar to those common to nickel - even the cell dimensions are very close to those for nickel. On cooling, the HCP structure is restored, but this is true only for pure cobalt. As nickel is added to the cobalt and temperature is applied, a region called the peritectic zone (shaded area in Figure 3.2-12) is encountered. In this region exists both HCP and FCC cellular systems. Peritectic reactions take place as temperature is increased and HCP cells are transformed into FCC counterparts. The temperature at which all HCP cells become FCC cells is decreased. More importantly, as temperature is again decreased, not all of the FCC structure is transformed back to HCP structure. Of equal importance to the alloy electroformer is the fact that these HCP-FCC mixtures are present throughout the electrodeposited alloy of nickel-cobalt. The amount of HCP cobalt or nickel-cobalt present is dependent on the cobalt content and the deposition conditions. Retention of these HCP

cells appears to be essential for maintaining outstanding mechanical strength in nickel-cobalt alloys.

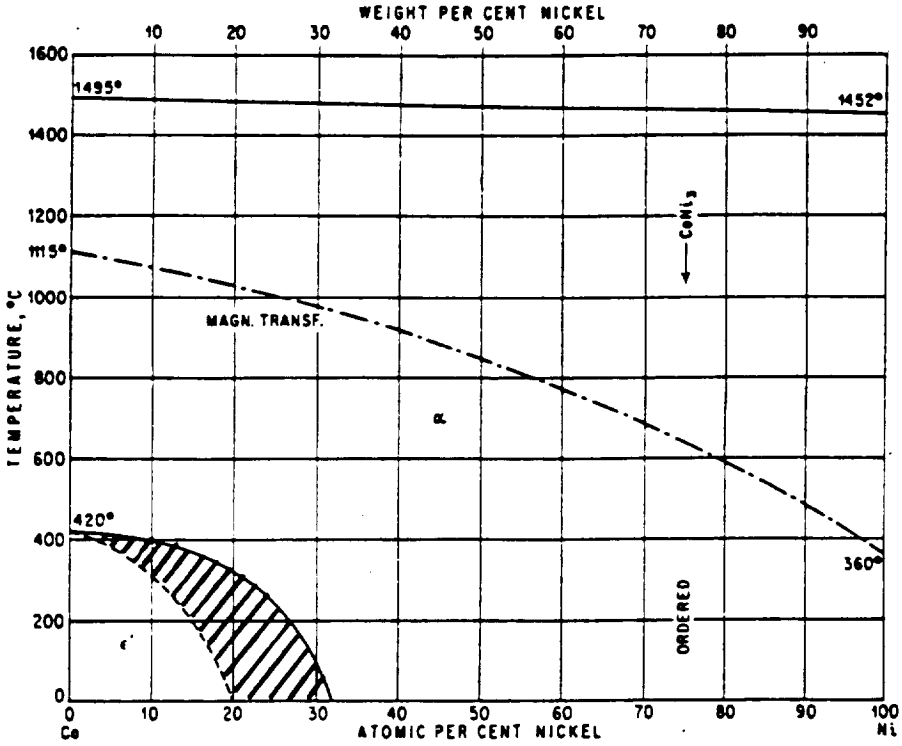

Figure 3.2-12. Nickel-Cobalt Binary Alloy Phase Diagram (57)

Looking again at Figure 3.2-11, the allotropic transformation of HCP to FCC nickel-cobalt is sluggish at 232.2°C. Peritectic reactions are temperature time dependent. The exposure of the specimens to 232.2°C for only 10 minutes was not sufficiently severe to convert much HCP structure. Mechanical property changes were likely due to some hydrogen relief and stress relief, although both reactions would not be expected to be complete. The fact that Endicott and Knapp observed a lamellar or mixed lamellar microstructure over cobalt concentration ranges corresponding to outstanding ultimate and yield strengths is of importance to the metallurgist, since such structures may indicate stacking faults typical of mixed HCP and FCC cells. It is not unusual to find such properties in this type of microstructure.

For specimens heat treated at 343.3°C (650°F) for 10 minutes, Endicott and Knapp obtained mechanical properties as shown in Figure 3.2-13. Although the heat treatment time was brief, the temperature was sufficient to cause some changes in the mechanical properties. Ultimate strengths decreased - especially those for alloy containing 40 to 80 percent nickel. Yield strengths showed no appreciable changes. Ductility was slightly improved but remained generally poor.

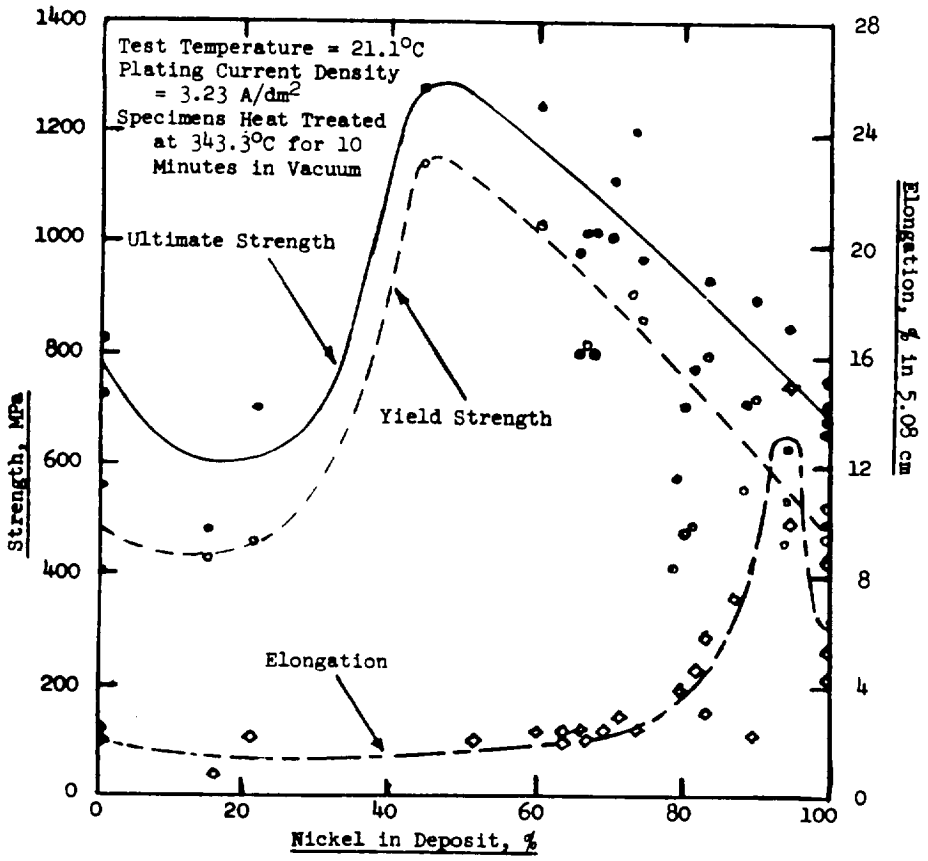

Figure 3.2-13. Effects of Heat Treating at 343.3°C for 10 Minutes on Room Temperature Mechanical Properties of Various Nickel-Cobalt Alloys

The tensile strength decrease was likely due to some degree of lattice reordering with further expulsion of hydrogen. The lack of major changes in yield strengths indicates that almost all HCP cobalt-nickel cell systems were restored after the allotropic transformation at 343.3°C. From photomicrographs in Endicott and Knapp's presentation, it was apparent that the lamellar banding described for certain cobalt concentration ranges was still present with about the same intensity. If these are indeed stacking faults due to mixed HCP and FCC cell systems, one would expect to see their effect manifested by good yield strength retention as is this case. This would also account for why no significant ductility improvement was noted. Again, the time factor in the heat treatment was probably too short to permit influential microstructural changes from occurring.

The investigators heat treated companion specimens at 454.4°C for 10 minutes and performed room temperature mechanical property tests. Although they presented data plots showing decreases in both ultimate and yield strengths, there are considerable data points indicating good property retention for alloys containing 45 to 60 percent nickel. From the data scattering it is difficult to reach any conclusion regarding the effects of this particular heat treatment. When the final heat treatment of 621.1°C (1150°F) for

10 minutes was employed, very pronounced mechanical property changes took place. Figure 3.2-14 shows the severity of strength loss in these alloys. Endicott and Knapp evaluated the microstructure of these samples after the 621.1°C treatment as follows.

a. Alloys containing 0 to 22 percent nickel undergo no recrystallization with heat treatments at 621°C.

b. Alloys containing about 53 percent nickel undergo fine-grain recrystallization with heat treatments at 621°C.

c. Alloys containing from 70 to 80 percent nickel have a grain size increasing with nickel content in the recrystallized heat treated condition.

d. Alloys containing 83 percent nickel show very little change in the modified columnar structure after heat treating at 621°C.

e. Alloys containing 95 percent nickel undergo complete recrystallization at 621°C.

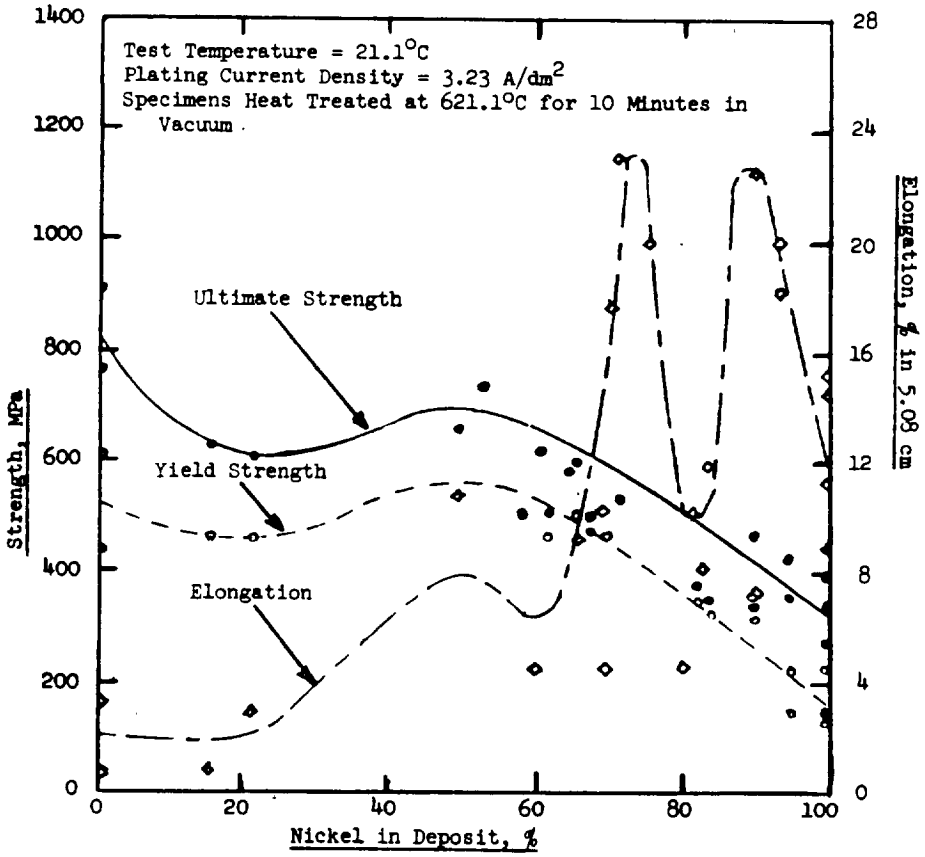

Figure 3.2-14. Effects of Heat Treating at 621.1°C for 10 Minutes on Room Temperature Mechanical Properties of Various Nickel-Cobalt Alloys

They also recognized that the lamellar structure was associated with high strength in the alloys and that this structure disappeared with the 621°C heat treatment. Although some HCP nickel-cobalt is probably still present after a severe heat treatment, the visible signs (as evidenced from the stacking faults making up the lamellar bands) are gone. It is possible that cobalt rich cells capable of transforming back to HCP systems can interchange atoms with cobalt deficient FCC cells (nickel rich cells) so that only the FCC structure can exist after the heat treatment. Endicott and Knapp did not report any elevated temperature testing for mechanical properties. They did perform Knoop hardness tests on most of the specimens. Changes in hardness with heat treatment followed similar trends to ultimate strength and yield strength - decreasing with increased heat treatment temperature.

3.2.4.3 EF Nickel-Cobalt Alloys - McFarlen

McFarlen (58) evaluated the properties of electroformed nickel-cobalt for application to the fabrication of elevated temperature structural components. He noted that structural electroforming has not been able to bridge the gap between experimental and production hardware due to the lack of high strength electrodeposits and the need for more sophistication in controlling the mechanical properties of the electroformed structure. In selecting a process for electroforming high strength deposits, McFarlen emphasized certain restrictions and goals on which his work was based. These included a minimum ultimate strength of 6895 MPa (100 ksi) in an operating range of 204°C to 316°C (400°F to 600°F) and the use of a plating solution operating at low temperature due to the implementation of low melting temperature proprietary waxes as nonmetallic filler materials (presumably for coolant passages such as found in regeneratively cooled thrust chambers).

McFarlen first examined the nickel-cobalt sulfate bath investigated by Safranek (59). This bath was composed and operated as follows

Cobalt Sulfate, $CoSO_4 \cdot 7H_2O$	29 g/l
Nickel Sulfate, $NiSO_4 \cdot 7H_2O$	300 g/l
Nickel Chloride, $NiCl_2 \cdot 6H_2O$	50 g/l
Boric Acid, H_3BO_3	30 g/l
Sulfuric Acid, H_2SO_4 to pH	3.7 to 4.0
Wetting Agent, $NaC_{12}H_{24}OSO_3$	0.5% by volume
Temperature	66°C (150°F)
Current Density	2.7 to 11 A/dm^2 (25 to 100 ASF)
Anodes	Nickel and cobalt

Sound deposits could not be produced from this bath owing to the cracked or brittle nature of the alloy. McFarlen then examined the bath suggested by Stephenson for nickel-cobalt alloy electroforming (38). This was a sulfamate bath composed and operated as follows:

Nickel Sulfamate (75 g/l Ni)	15 parts by volume
Cobalt Sulfamate (75 g/l Co)	1 part by volume
Boric Acid	30 g/l
Wetting Agent	375 mg/l

pH	4.0
Temperature	Room
Current Density	2 to 5 A/dm^2 (25 to 50 ASF)
Anodes	Depolarized nickel

This bath was reported to produce sound nickel-cobalt deposits over a current density range of 2.7 to 8.1 A/dm^2. McFarlen's main interest in this study was the effect of current density in the 2.7 to 8.1 A/dm^2 (25 to 75 ASF) range on alloy composition, and the effect of cobalt concentration in the alloy on tensile properties.

Replicate specimens were deposited at current densities of 2.7, 5.4, and 8.1 A/dm^2 (25, 50, and 75 ASF). Cobalt was analyzed in each sample. For the particular cobalt content of this electrolyte, McFarlen found that the maximum cobalt in the alloy was obtained at a current density of about 5 A/dm^2. At current densities of 2.7 to 8.1 A/dm^2, he found that the ultimate and yield strengths increased as the weight percent cobalt increased in the deposit. The highest room temperature tensile strength for "as deposited" alloy was 1951 MPa (283 ksi) with a cobalt content of 38.5 percent by weight. He reported a nominal deposition rate of 0.0025 mm per hour at a current density of 5.8 A/dm^2 (54 ASF). If correct, this would imply a cathode efficiency of less than fifty percent - in other words, there would have been significant hydrogen evolution.

McFarlen's tensile specimens were electroformed to a thickness of 0.0508 cm. Mechanical properties at room temperature of "as deposited" nickel-cobalt specimens were determined as tabulated in Table 3.2-37. This data indicates that as the cobalt concentration in the deposit increases, the strength increases, and the maximum cobalt concentration in the deposit occurs at about 5 A/dm^2. This statement by McFarlen requires modification in that strength will decrease above a certain cobalt content as demonstrated by Endicott and Knapp (55) and some subsequent investigators.

McFarlen evaluated the effects of heat treatments and soak times on the room temperature mechanical properties of electroformed nickel-cobalt. In the first study, tensile specimens were electroformed at 5.4 A/dm^2 and subjected to various elevated temperature treatments, holding each specimen for four hours at temperature. As shown in Figure 3.2-15, McFarlen found the ultimate tensile strength decreased from 1723.8 MPa (250 ksi) at room temperature to 613.7 MPa (89 ksi) after heat treating at 649°C (1200°F) for four hours. Based on desired optimum properties in the 204°C to 310°C range, 371°C (700°F) was selected as the heat treatment or thermal stabilization temperature. It can be seen that strength retention decreases at a rapid rate as temperatures in excess of 275°C are employed, Figure 3.2-15. For the alloy deposits subjected to the 371°C thermal stabilization treatment, it appeared that time dependent effects were eliminated after a 14 hour soak period. Ultimate strength and yield strength appeared to be similar to those noted in Figure 3.2-15 for alloy subjected to 427°C for four hours. Soak periods of up to 24 hours did not change these values to any appreciable degree. It should be noted that 371°C is considerably below the 420°C required to allotropically transform all HCP cells to FCC.

TABLE 3.2-37. AS-DEPOSITED MECHANICAL PROPERTIES OF NICKEL-COBALT SPECIMENS (58)

Current Density A/dm^2	Current Density ASF	Cobalt, % by Weight	Ultimate Strength MPa	Ultimate Strength ksi	0.2 % Offset Yield Strength MPa	0.2 % Offset Yield Strength ksi	Elongation in 5.08 cm %
2.69	25	-	1585.9	230	1227.3	178	3.0
		22.0	1689.3	245	1199.7	174	3.0
		-	1599.6	232	1475.5	214	4.5
		-	1592.7	231	1213.5	176	4.0
		24.8	1599.6	232	1185.9	172	4.0
		-	1537.6	223	1158.4	168	3.0
		-	1599.6	232	1254.9	182	4.5
		-	1689.3	245	1351.4	196	2.0
5.38	50	-	1647.9	239	1075.6	156	3.0
		-	1682.4	244	1158.4	168	4.0
		-	1689.3	245	1158.4	168	5.0
		-	1689.3	245	1213.5	176	3.0
		24.7	1668.6	242	1254.9	182	3.0
		-	1682.4	244	1268.7	184	5.0
		-	1696.2	246	1323.8	192	2.0
		-	1675.5	243	1344.5	195	3.0
8.07	75	-	1427.3	207	-	-	2.0
		-	1675.5	243	1248.0	181	2.0
		17.3	1475.5	214	1192.8	173	1.5
		16.2	1551.4	225	1172.2	170	2.5
		-	1620.3	235	1261.8	183	2.0
		-	1385.9	201	1213.5	176	1.5
		-	1627.2	236	1241.1	180	2.5

Figure 3.2-16 illustrates McFarlen's data for specimens electroformed at 5.4 A/dm^2, thermally stabilized at 371^{o}C for 16 hours, and tested for mechanical properties at various test temperatures. Prior to performing the actual tests, some specimens were given 15 minute or 30 minute thermal soak periods. Why the specimens given a 15 minute exposure at test temperature had the higher ultimate strength than those subjected to no soak is not clear.

McFarlen also compared elevated temperature mechanical properties of nickel-cobalt, conventional sulfamate nickel, and nickel-manganese deposits. The data used for nickel-0.5% manganese appears to be derived from the results published by Stephenson (38). The comparison is illustrated in Figure 3.2-17. Although the nickel-cobalt electrodeposited alloy appeared to have greatly improved mechanical strength over conventional electroformed nickel, it was not equivalent in mechanical strength to nickel-manganese. A comparison of these materials based entirely on ultimate strength is not recommended, since yield strength and elongation are two important considerations for structural applications.

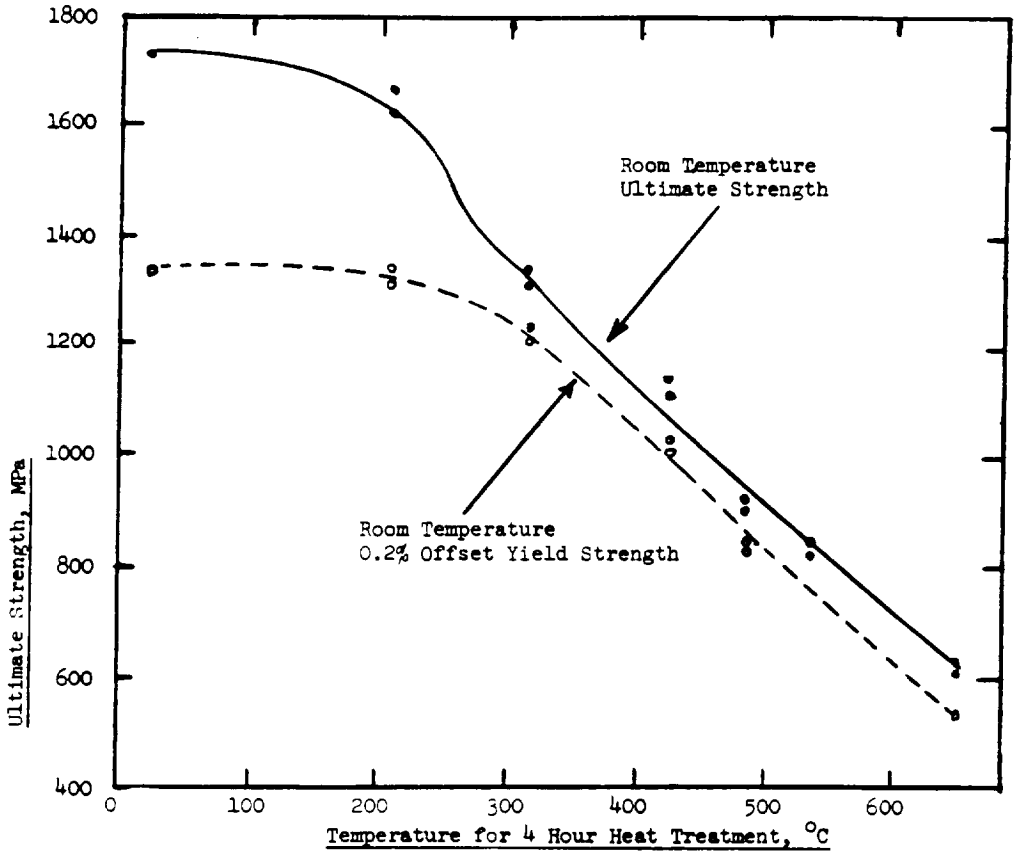

Figure 3.2-15. Ultimate and Yield Strength Retention of Electroformed Nickel-Cobalt Alloy After Various Thermal Treatments (58)

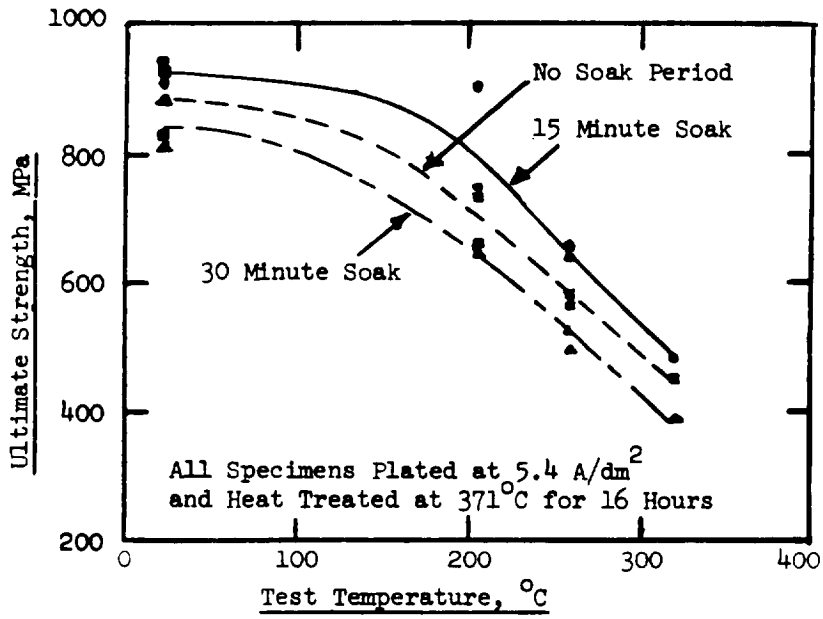

Figure 3.2-16. Effect of Temperature Stabilization Time on Ultimate Strength of Nickel-Cobalt Electroform Specimens Previously Heat Treated at 371°C for 16 Hours

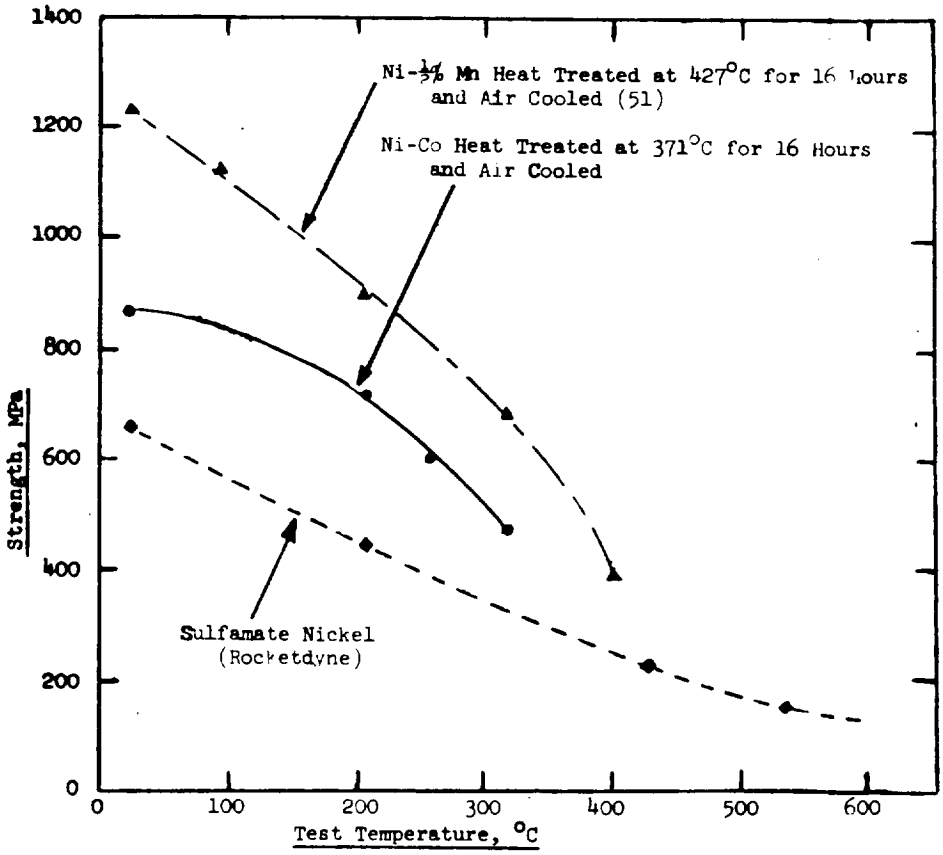

Figure 3.2-17. A Comparison of Ultimate Strengths of Ni-1/2% Mn, Ni-Co, and Conventional Sulfamate Nickel Deposits at Various Testing Temperatures

3.2.4.4 EF Nickel-Cobalt Alloys - Dini, Johnson, and Helms

These investigators (60) examined nickel-cobalt electrodeposits as possible materials for high strength plated joints. They noted that Belt (61) reported the use of nickel-cobalt deposits offered several advantages for engineering applications:

1. The deposits are sulfur-free and can be heated without becoming embrittled.

2. Control of the deposit properties is simple.

3. There is no accumulation of breakdown products such as normally occurs in electrolytes containing organic additives.

4. Hard deposits of the nickel-cobalt type are more ductile than those hardened by sulfur containing additives.

The bath formulation used and general operating conditions for the nickel-cobalt system were as shown below:

Nickel Sulfamate	490 ml/l
Nickel Metal (from Sulfamate)	73.5 g/l
Nickel Bromide	64 ml/l
Nickel Metal (from Bromide)	3.7 g/l
Cobalt Sulfamate	107 ml/l
Cobalt Metal (from Sulfamate)	8.0 g/l
Total Metal (Ni + Co)	85.2 g/l
Nickel/Cobalt Ratio	9.7
Boric Acid	30.0 g/l
Surface Tension	26-31 dynes/cm
Temperature	37.8-54.4^{o}C (100-130^{o}F)
Anodes	Pure Ni and Co

This formulation was used on the basis of the nickel-cobalt ratio giving Endicott and Knapp (55) the maximum strength properties. The bath volume was 105 liters.

The investigators evaluated the use of four different anode arrangements for plating:

1. Separate nickel and cobalt anodes operated without splitting the current between the anodes; this resulted in excessive amounts of cobalt going into solution.

2. Separate nickel and cobalt anodes operated with a current splitting device; this gave inconsistent results.

3. Nickel anodes used in conjunction with a metering pump that made controlled additions of cobalt in the form of sulfamate; this worked well and was used for most of the investigation.

4. Alloy anodes of the same composition as that desired in the deposit; this method produced the best results.

They examined the effects of current density, temperature, pH, and agitation on the constancy of the alloy composition and confirmed the same trends noted by other investigators (and previously discussed in this survey). The greatest influence on cobalt content of the alloy was found to occur as a result of electrolyte agitation. They noted that for a current density of 2.69 A/dm^{2}, a bath temperature of 48.9^{o}C, and a pH of 3.5, the cobalt content was only 28.5 percent with no agitation. Under the same conditions the cobalt increased to 50 percent with moderate agitation and to 53.5 percent with vigorous agitation. They recognized that this could pose a serious problem in electroforming complex shapes. Unless fairly uniform agitation were obtained, such electroforms could vary significantly in composition and properties.

Dini, Johnson, and Helms found that stress in nickel-cobalt deposits is fairly high - i.e., the range varied from 117.2 to 213.7 MPa (17 to 31 ksi) depending on the bath cobalt content and the operating conditions. Figure 3.2-18 illustrates that agitation significantly increases stress for a given cobalt concentration in the bath. Table 3.2-38 shows the influence of other

variables on internal stress. These investigators considered bath agitation to be the most important variable associated with increased stress, and they attributed this to the increase in cobalt content resulting from increased agitation.

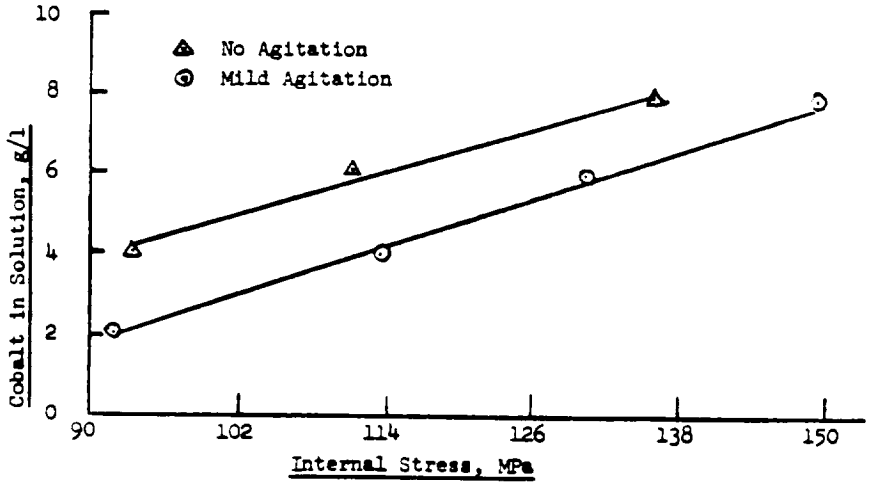

Figure 3.2-18. Influence of Cobalt on Deposit Stress for Nickel-Cobalt Alloy Electrodeposited at a Current Density of 2.69 A/dm^2, Bath Temperature of 48.9^{o}C, Bath pH of 3.5-4.0, and Bath Nickel Content of 77 g/l

TABLE 3.2-38. INFLUENCE OF OPERATING VARIABLES ON STRESS OF NICKEL-COBALT ELECTRODEPOSITS (60)

Variable	Range	Stress (Rigid Strip Technique) No Agitation MPa	ksi	Vigorous Agitation MPa	ksi
Current Density, A/dm^2 (Temperature 48.9^{o}C, pH 3.5)	1.07	121.4	17.6	193.1	28.0
	2.69	128.9	18.7	165.5	24.0
	5.38	101.4	14.7	147.6	21.4
pH (2.69 A/dm^2, Temperature 48.9^{o}C)	2.5	133.8	19.4	213.7	31.0
	3.5	128.9	18.7	165.5	24.0
	4.5	126.9	18.4	165.5	24.0
Temperature, ^{o}C (2.69 A/dm^2, pH 3.5)	37.8	122.7	17.8	179.3	26.0
	48.9	128.9	18.7	165.5	24.0
	60.0	117.2	17.0	165.5	24.0

Dini, Johnson, and Helms electroformed nickel-cobalt alloy specimens with a wide range of cobalt content for mechanical property testing in the "as deposited" condition. The test results are shown in Figure 3.2-19. The investigators cited the highest ultimate strengths as occurring in the alloys having cobalt contents between 30 and 60 percent. Best yield strengths were found for samples containing 40 to 60 percent cobalt.

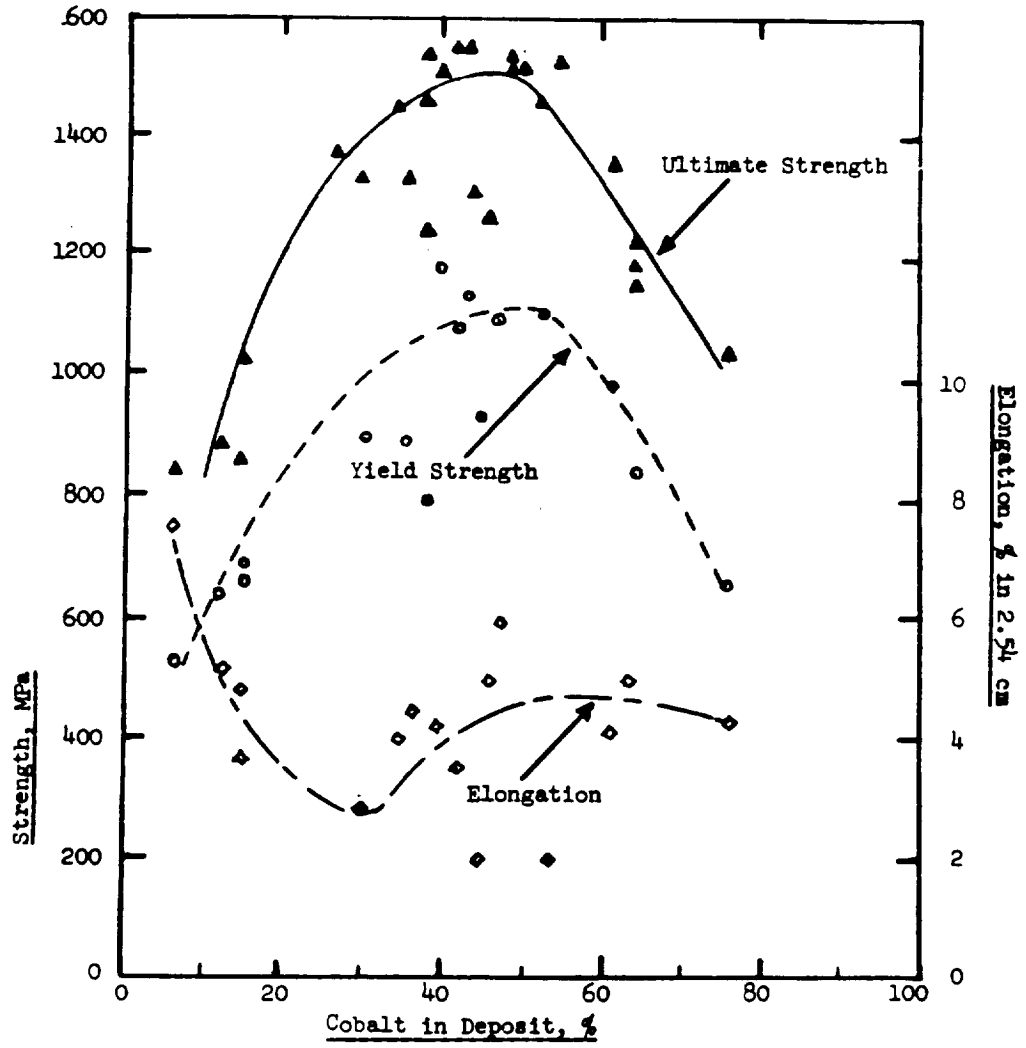

Figure 3.2-19. Mechanical Property Test Results (Room Temperature) for Nickel-Cobalt Specimens in the "As Deposited" Condition (84)

They also evaluated the influence of heat treatment upon elongation to determine if ductility could be improved without too drastic a reduction of tensile and yield strengths. Specimens used for this study contained 45 percent cobalt, since this was in the compositional region where maximum strength of the alloy occurred. Results of the tests and heat treating conditions are shown in Table 3.2-39. They observed that specimens heated to 371°C and 427°C for varying lengths of time showed a slight reduction in tensile strength but no significant improvement in elongation. For heat treatments above 427°C, both tensile and yield strengths decreased while elongation increased. The data for alloy heat treated at 621°C agreed well with that of McFarlen. Hardness for various nickel-cobalt alloy compositions were obtained on matallographic cross-sections. Hardnesses were found to range from 410 to 460 Knoop (300 gram load) for alloys containing 30 to 50 percent cobalt.

TABLE 3.2-39. INFLUENCE OF HEAT TREATMENT ON MECHANICAL PROPERTIES OF 55% Ni - 45% Co ALLOY

Heat Treatment Temperature, °C	Time, Hours	Ultimate Strength MPa	Ultimate Strength ksi	Yield Strength MPa	Yield Strength ksi	Elongation, % in 2.54 cm
None (Control)		1310.1	190	841.2	122	4
371.1	4	1172.2	170	882.6	128	2
371.1	16	1123.9	163	889.5	129	2
426.7	1	1061.8	154	820.5	119	6
482.2	1	951.5	138	786.0	114	5
537.8	1	799.8	116	717.1	104	10
537.8	2	799.8	116	724.0	105	8
621.1	4	682.6	99	627.4	91	25
704.4	2	586.1	85	517.1	75	35

3.2.4.5 EF Nickel Cobalt Alloys - Schuler

Schuler (62) investigated nickel-cobalt electrodeposited alloys with cobalt contents ranging from 22 to 50 percent by weight. His objective in this work was to determine if nickel-cobalt electroforming could provide a superior metal from a mechanical property standpoint for application to outer shells for high-performance thrust chamber liners. A goal in this study was to produce and evaluate electrodeposited nickel-cobalt alloys with minimum yield strengths of 689.5 MPa (100 ksi) after stress relief.

For an electrolyte, Schuler selected the nickel and cobalt sulfamate system maintained at a total metal content of 75 to 80 g/l. Varying cobalt content in the electrodeposited alloy was accomplished by changing nickel to cobalt ratios in the electrolyte and by depositing at very specific current densities. Anodes were sulfur depolarized (SD) nickel. Cobalt metal was continuously replenished using cobalt sulfamate metered to the bath. The electrolyte was maintained at a pH of 4 and the temperature controlled at 49°C. 10 micron nominal filtration was used on a continuous basis to keep the electrolyte clean. The bath volume was 60 liters.

Considerable efforts were required to establish the electrolyte cobalt consumption rates at different current densities. Once this was performed, deposits for testing were made containing 22 percent cobalt from an electrolyte containing 7 percent cobalt at a current density of 4.3 A/dm^2. Deposits containing 43 and 50 percent cobalt were electroformed from an electrolyte containing 8 and 10 percent cobalt metal, respectively, and at a current density of 1.4 A/dm^2. Some alloy with 28 percent cobalt was produced from a bath with 9 percent cobalt at 2.8 A/dm^2. Internal stress of electroformed nickel-cobalt was evaluated using strips plated on one side only. The degree of stress was determined by the amount of deflection of the strips.

Figure 3.2-20 shows ultimate yield strength test results for "as deposited" nickel-cobalt alloys of various cobalt contents and corresponding test data for companion samples subjected to stress relieving treatments at

345°C for one hour and 455°C for one hour. Significant decreases in these properties occurred which appeared directly related to the temperature at which stress relieving was conducted. Such performance is to be expected from the binary alloy phase diagram (57), since the stress relieving temperatures are either well into the peritectic reaction zone or above this zone (where a significant portion of the HCP cell structure transforms to FCC and may not be fully restored on return to room temperature).

Figure 3.2-21 illustrates the beneficial effects of heat treatments on ductility of nickel-cobalt electrodeposited alloys. From Figure 3.2-22 it is indicated that residual tensile stress in the alloy deposits is reduced by plating at higher current densities which also decrease the cobalt content of the deposits. Increasing the cobalt content in the electrolyte appeared to decrease these stresses while increasing the alloy cobalt content for corresponding current densities.

3.2.4.6 EF Nickel-Cobalt Alloys - Walter

Walter (63) examined the electrochemistry of alloy plating with an emphasis on the nickel-cobalt deposition system. Although much of his paper dealt with partial currents and overpotentials of mixed metal ions based on the text of Bockris and Reddy (64), some interesting results of nickel-cobalt alloy work at Rocketdyne were presented. Figure 3.2-23 shows the mechanical properties at various test temperatures of electrodeposited nickel containing 50 percent by weight cobalt after a preliminary stress relief at 204.4°C for 72 hours. Ultimate strengths and yield strengths are vastly superior to conventional electroformed nickel for temperatures from ambient to about 275°C. At higher temperatures the tensile and yield values tend to approximate those of conventional electrodeposited nickel. Elongation peaks to a maximum at temperatures beyond 420°C. These performances are easily explained by the allotropic nature of the HCP cobalt and cobalt-nickel cells as previously discussed.

It is the author's understanding that Rocketdyne no longer relies on metering cobalt sulfamate into the alloy electrolyte but uses separate nickel and cobalt anode arrays independently driven by two power supplies. This is a considerable improvement over cobalt additions by metering but still requires close control of nickel/cobalt ratio in the electrolyte as well as individual anode area. Any factor affecting anode corrosion rate would require critical control because of differing corrosion rates for cobalt and nickel.

3.2.4.7 Conclusions - Electrodeposited Nickel-Cobalt Alloys

The nickel-cobalt electroforming baths are more difficult to operate and control than either the conventional sulfamate nickel or sulfamate nickel-manganese baths. The highest tensile properties appear to occur at alloy cobalt contents between 45 and 50 percent by weight. Under these conditions, the alloy exhibits outstanding room temperature and moderate temperature strength. "As deposited" ductility is quite low, and some form of stress relief or normalizing treatment is necessary; however, this is true for most electrodeposited alloys.

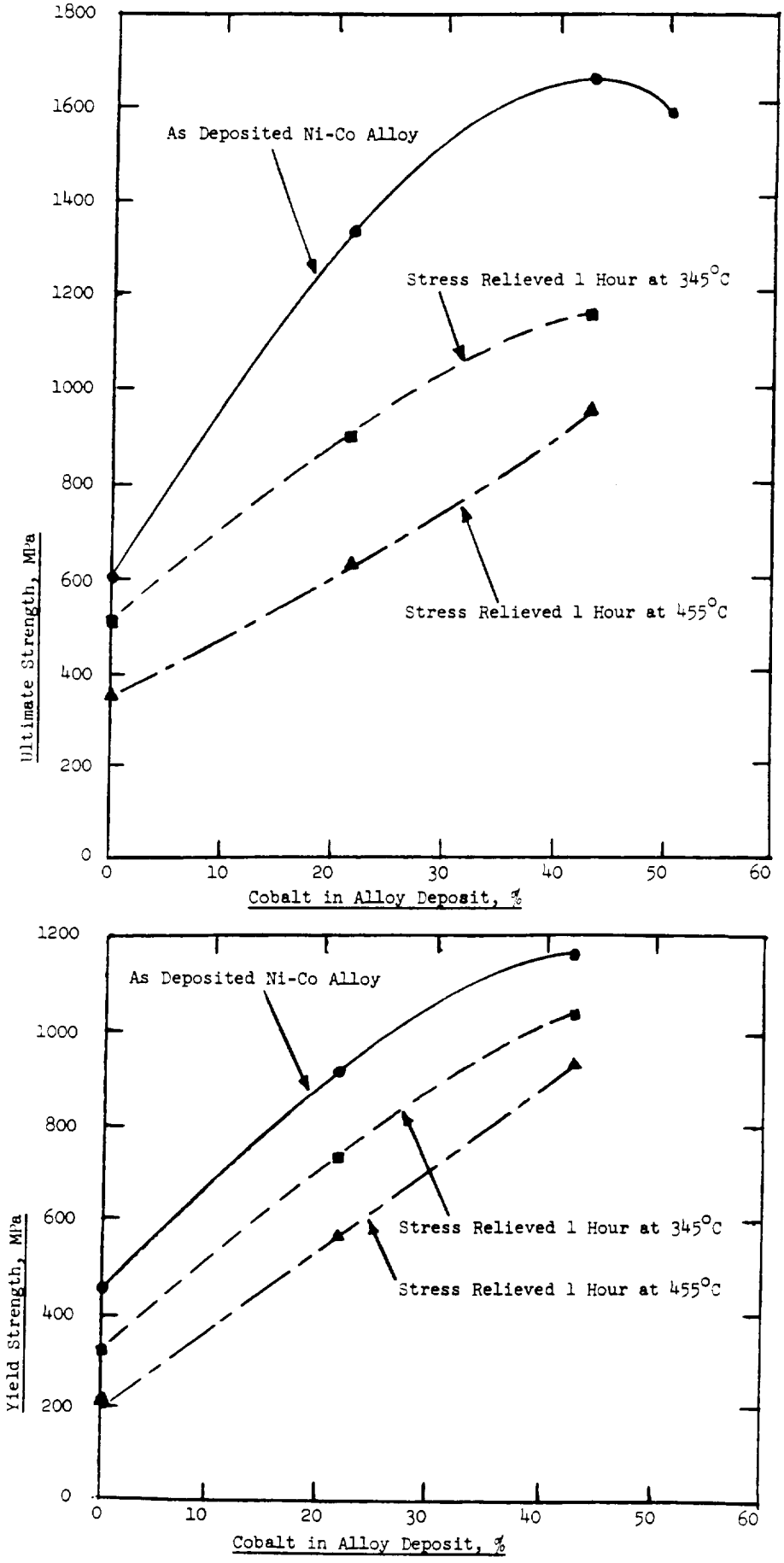

Figure 3.2-20. Influence of Cobalt Content on Ultimate and Yield Strengths of As Deposited and Heat Treated Nickel-Cobalt Deposits (62)

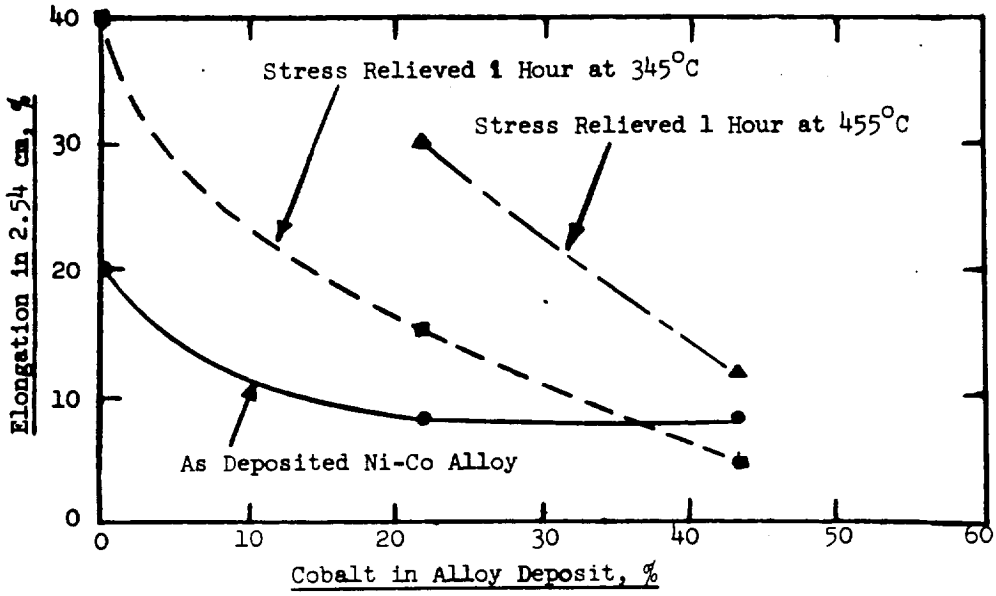

Figure 3.2-21. Influence of Cobalt Content on Elongation of As-Deposited and Heat Treated Nickel-Cobalt Deposits (62)

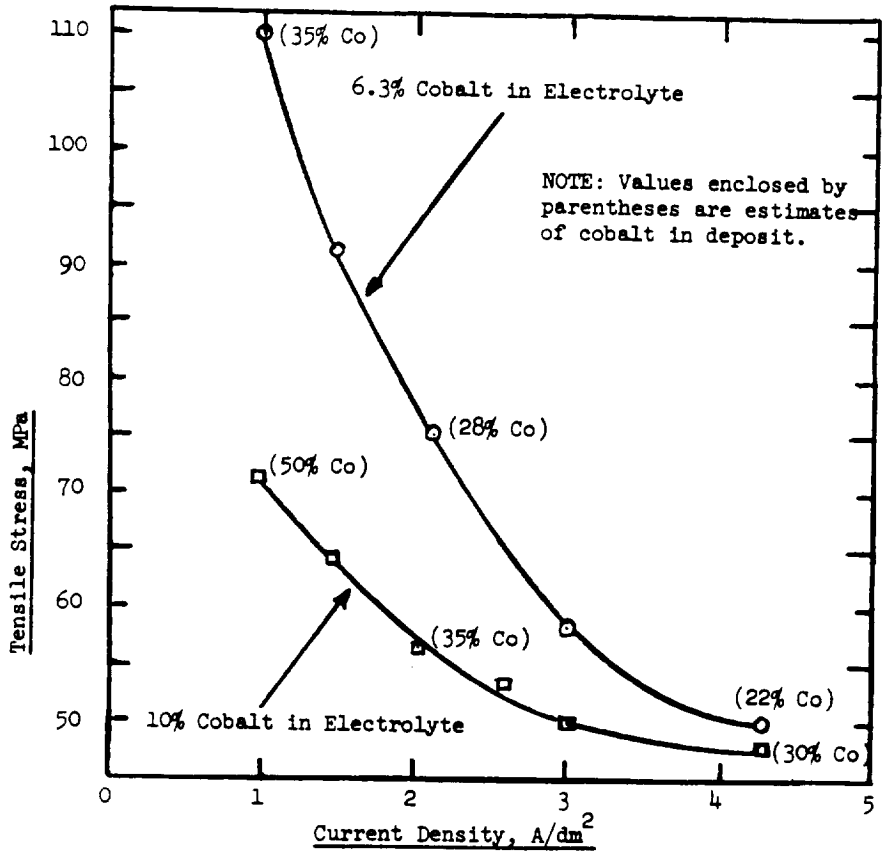

Figure 3.2-22. Effects of Current Density and Electrolyte Cobalt Content on Residual Stresses in Nickel-Cobalt Electrodeposits (62)

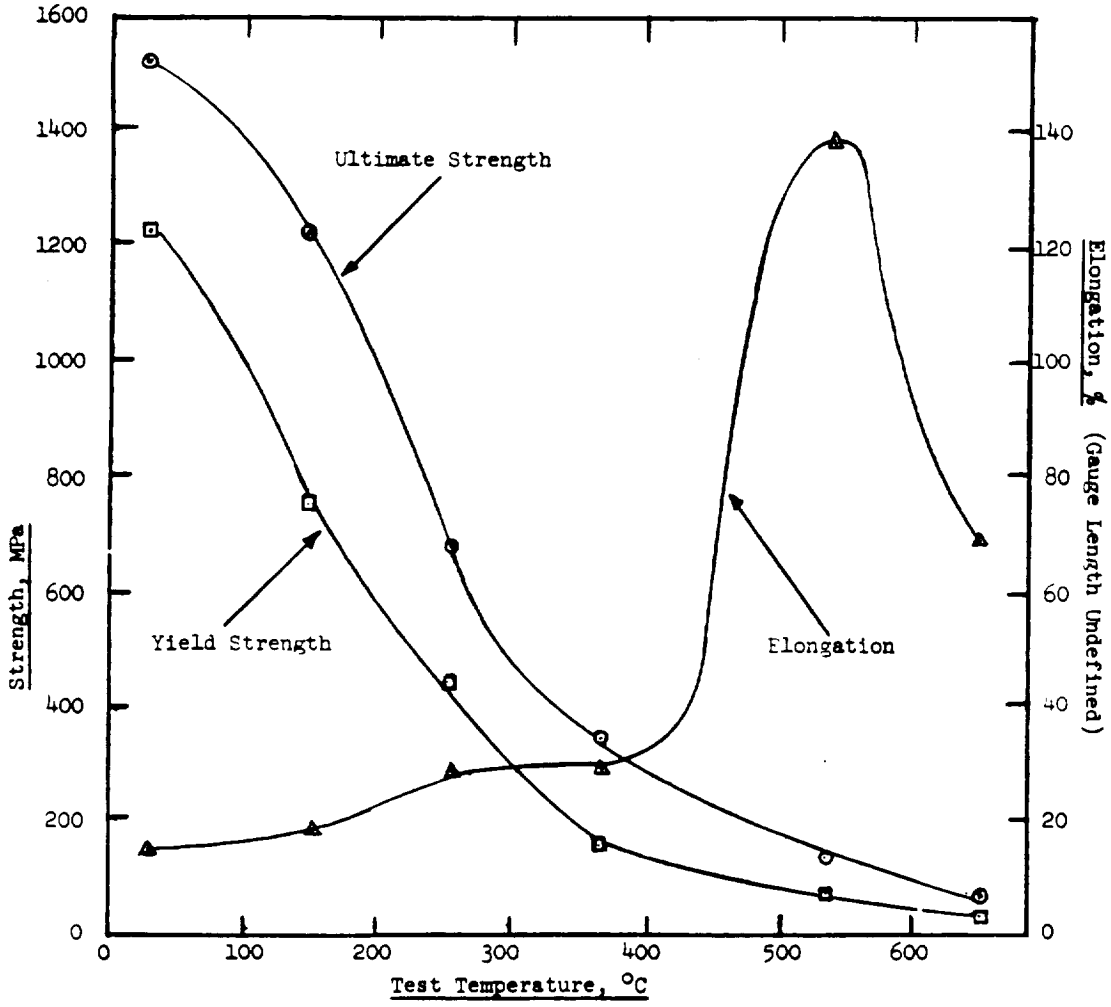

Figure 3-2.23. Typical Mechanical Properties of Electrodeposited Ni-50% at Various Test Temperatures After Stress Relief at 204.4°C for 72 Hours (63)

The high strength exhibited by electroformed nickel-cobalt is generally accepted as due to the mixed HCP and FCC cell structures present in the crystallographic lattice. Such cell mixture is often accompanied by lattice stacking faults. The lamellar banding noted in most nickel-cobalt alloys produced by plating is visual evidence that such faults are likely to be present. As long as these structures can be maintained, the metal will exhibit good mechanical strength with relatively high yield strength due to added resistance to plastic deformation. Unfortunately, the HCP cells in nickel-cobalt are susceptible to allotropic transformation to FCC cells as temperature is increased. At 420°C all HCP is converted to FCC and strength becomes similar to conventional sulfamate nickel. Peritectic reactions in which this transformation occurs start at even lower temperatures. This means that selection of electroformed nickel-cobalt for structural uses requires careful evaluation of such factors as:

1. Secondary fabrication operations where high temperatures may be involved such as welding, diffusion bonding, or brazing.

2. The highest temperature to which exposure is expected. As the temperature is increased, more HCP is transformed to FCC with strength loss. Not all HCP structure is restored on return to the starting temperature - hence, some strength may be permanently lost.

In addition to the fairly high internal stress present, electroforming with nickel-cobalt poses the problem of alloy compositional variation due to current density and electrolyte agitation fluctuations where parts of complex alloys but not necessarily to the same degree.

3.2.5 EF Nickel-Cobalt-Manganese Alloys

3.2.5.1 General

Stephenson (38) mentions efforts by himself and Farmer to electroform an alloy of nickel, cobalt, and manganese from a sulfamate bath composed and operated as follows:

Nickel Metal	80 g/l
Cobalt Metal	7.5 g/l
Manganese Metal	30 g/l
Boric Acid	30 g/l
Wetting Agent	0.375 g/l
Magnesium Chloride	15 g/l
pH	3.5
Current Density	5.4 A/dm^2 (50 ASF)
Anodes	Depolarized nickel

They claimed the deposit had a hardness of R_C 40 and started to anneal at 315^{o}C (600^{o}F). Chemical analysis revealed only a trace of manganese in the deposit which led these investigators to conclude that cobalt in the bath depresses the deposition of manganese. Unfortunately, Stephenson and Farmer did not investigate the alloy further to discover the significant effects of even a trace of manganese on mechanical properties of nickel-cobalt alloy.

3.2.5.2 EF Nickel-Cobalt-Manganese Alloys - Malone

Malone (65) investigated and characterized mechanical properties of nickel-cobalt-manganese alloy electrodeposits using conventional and pulsed current. The electrolyte being used is a sulfamate type operated at 48.9^{o}C to 54^{o}C and a pH range of 3.2 to 4.2. His purpose in evaluating this alloy was to obtain electroformable alloy which combines the advantages of nickel-cobalt and nickel-manganese alloys over a wide temperature range. Although nickel-cobalt electrodeposits exhibit the highest tensile and yield strengths at room and moderate temperatures, they do not have the mechanical strength performance of nickel-manganese at more severe thermal exposures.

Table 3.2-40 shows Malone's test results for his initial investigation of nickel-cobalt electroformed alloys with very minor manganese additions. In this study duplicate specimens were produced which were heat treated at fairly high temperatures - one temperature being below the Curie temperature and the

other at a higher temperature than that for magnetic transformation. A most interesting aspect of this study was the discovery that when even very small amounts of manganese were present, and the cobalt content was only 30 percent, mechanical strengths in the same range as 50-55 percent nickel-cobalt were obtained. Since most investigators have claimed that maximum strength of nickel-cobalt can only be obtained between 40 and 55 percent cobalt content, these results appear most encouraging.

TABLE 3.2-40. ROOM TEMPERATURE MECHANICAL PROPERTIES OF CONVENTIONAL AND PULSE CURRENT DEPOSITED NICKEL-COBALT-MANGANESE ALLOY CONTAINING 28-33% COBALT AND LESS THAN 0.08% MANGANESE - BEFORE AND AFTER HEAT TREATING (65)

Pulse Duty Cycle %	Peak Current Density A/dm^2	Average Current Density A/dm^2	Bath Temp. °C	Bath pH	Alloy Composition (Percent by Weight) Ni	Co	Mn	Electrolyte Ni/Co Ratio	Ultimate Strength MPa	ksi	Yield Strength MPa	ksi	Elongation Percent In 2.54 cm	5.08 cm
"As Deposited" Alloys:														
100	2.15	2.15	48.6	4.4	68.94	31.00	0.055	16.23	1692.0	245.4	1181.1	171.3	10	7.5
67	3.23	2.15	48.3	4.2	70.55	29.40	0.051	17.64	1689.3	245.0	1179.7	171.1	8	5
50	2.15	1.08	48.3	4.3	71.18	28.80	0.015	23.14	1527.2	221.5	1296.9	188.1	11	7
50	4.31	2.15	48.3	4.2	69.65	30.30	0.049	18.85	1650.7	239.4	1128.7	163.7	6	4
50	7.53	3.77	50.0	3.8	67.05	32.90	0.046	11.00	1312.1	190.3	859.8	124.7	7	5
33	6.46	2.15	48.6	4.2	69.52	30.40	0.079	20.10	1738.9	252.2	1346.6	195.3	7	4
Heat Treated at 621°C for 2 Hours:														
100	2.15	2.15	48.6	4.4	68.94	31.00	0.055	16.23	826.7	119.9	806.0	116.9	20	10
67	3.23	2.15	48.3	4.2	70.55	29.40	0.051	17.64	732.2	106.2	-----	-----	36	17
50	2.15	1.08	48.3	4.3	71.18	28.80	0.015	23.14	599.9	87.0	460.6	66.8	46	33
50	4.31	2.15	48.3	4.2	69.65	30.30	0.049	18.85	668.1	96.9	612.3	88.8	36	26
50	7.53	3.77	50.0	3.8	67.05	32.90	0.046	11.00	546.6	79.3	346.1	50.2	48	41.5
33	6.46	2.15	48.6	4.2	69.52	30.40	0.079	20.10	764.7	110.9	-----	-----	31	14
Heat Treated at 760°C for 20 Hours:														
100	2.15	2.15	48.6	4.4	68.94	31.00	0.055	16.23	541.9	78.6	252.4	36.6	39	34
67	3.23	2.15	48.3	4.2	70.55	29.40	0.051	17.64	535.1	77.6	259.3	37.6	51	39
50	2.15	1.08	48.3	4.3	71.18	28.80	0.015	23.14	502.6	72.9	177.9	25.8	57	48
50	4.31	2.15	48.3	4.2	69.65	30.30	0.049	18.85	526.8	76.4	204.1	29.6	55	47
50	7.53	3.77	50.0	3.8	67.05	32.90	0.046	11.00	492.3	71.4	140.7	20.4	58	47.5
33	6.46	2.15	48.6	4.2	69.52	30.40	0.079	20.10	532.3	77.2	233.1	33.8	55	44

Limited testing at elevated temperature was performed on extra specimens from the initial group of alloys. All material had received a preliminary heat treatment at 621°C for 2 hours. Mechanical property test results are shown in Table 3.2-41.

Malone observed that the manganese contents of the alloys shown in Table 3.2-41 were about one-half (or less) than those expected for the bath operating parameters used. Stephenson (38) had suggested that cobalt in the alloy electrolyte suppressed manganese codeposition. This now appears to be a false conclusion. A more likely reason for the lower manganese content of nickel-cobalt alloys, as opposed to nickel deposits for similar bath operating conditions and manganese ion concentration, appears to be the ability of cobalt to absorb monatomic hydrogen to a much greater degree than nickel which decreases the amount available to reduce manganese.

TABLE 3.2-41. MECHANICAL PROPERTIES AT ELEVATED TEMPERATURE OF CONVENTIONAL AND PULSE CURRENT DEPOSITED NICKEL-COBALT-MANGANESE ALLOY CONTAINING 28-33% COBALT AND LESS THAN 0.08% MANGANESE HEAT TREATED AT 621°C FOR 2 HOURS

Pulse Duty Cycle %	Peak Current Density A/dm²	Average Current Density A/dm²	Bath Temp. °C	Bath pH	Alloy Composition (Percent by Weight) Ni	Co	Mn	Electrolyte Ni/Co Ratio	Ultimate Strength MPa	ksi	Yield Strength MPa	ksi	Elongation Percent In 2.54 cm	5.08 cm
Specimens Tested at 621°C:														
100	2.15	2.15	48.6	4.4	68.94	31.00	0.055	16.23	313.7	45.5	116.5	16.9	9.2	6.7
67	3.23	2.15	48.3	4.2	70.55	29.40	0.051	17.64	246.8	35.8	101.4	14.7	23.4	21.3
50	2.15	1.08	48.3	4.3	71.18	28.80	0.015	23.14	208.5	30.2	97.9	14.2	39	30
50	4.31	2.15	48.3	4.2	69.65	30.30	0.049	18.85	218.6	31.7	99.3	14.4	42.8	32.2
50	7.53	3.77	50.0	3.8	67.05	32.90	0.046	11.00	Not tested at elevated temperature.					
33	6.46	2.15	48.6	4.2	69.52	30.40	0.079	20.10	277.9	40.3	99.3	14.4	45	35
Specimens Tested at 649°C:														
100	2.15	2.15	48.6	4.4	68.94	31.00	0.055	16.23	137.9	20.0	32.1	4.66	----	13
67	3.23	2.15	48.3	4.2	70.55	29.40	0.051	17.64	126.9	18.4	32.6	4.73	43	36
50	2.15	1.08	48.3	4.3	71.18	28.80	0.015	23.14	131.0	19.0	49.0	7.10	43	34
50	4.31	2.15	48.3	4.2	69.65	30.30	0.049	18.85	126.2	18.3	36.5	5.30	48	40
50	7.53	3.77	50.0	3.8	67.05	32.90	0.046	11.00	Not tested at elevated temperature.					
33	6.46	2.15	48.6	4.2	69.52	30.40	0.079	20.10	117.9	17.1	28.8	4.18	53	-----

In the next stage of his work, Malone considered that the shortcomings of nickel-cobalt alloy deposits - the allotropic transformation of HCP to FCC cells at 420°C or less - might be alleviated by blocking the cell change at temperatures higher than 420°C by the use of manganese. Although cobalt-manganese is normally of an FCC cell system at all atomic percentages of manganese expected in this work, the fact remains that insufficient manganese would be present to obstruct the deposition of cobalt rich HCP cells. The concept of several HCP cobalt or cobalt-nickel cells commonly sharing manganese atoms appeared to offer potential usefulness in improving elevated temperature strength as well as strength retention after heat treatment.

Table 3.2-42 summarizes test results from the second phase of Malone's investigation of the ternary nickel-cobalt-manganese electroformed alloy. The most interesting aspect of the data is the indication that unusually high yield strengths are achieved in the "as deposited" alloy with high levels of retention after heat treating. Equally remarkable is the fact that this was achieved with less than 40 percent by weight cobalt in the alloy. Although most elongation values are less than desired for engineering structural uses, it should be noted that these fine-grained, high yield strength alloys tend to elongate locally. They also appear to undergo a phenomenon similar to discontinuous yielding whereby plastic deformation is still occurring at a higher stress than that in existence at the time tensile failure takes place. While this behavior does not show the typical "sawtooth" stress-strain pattern of a work hardening carbon steel in the discontinuous yielding mode, it is difficult to give it any other description.

TABLE 3.2-42. ROOM TEMPERATURE MECHANICAL PROPERTIES OF CONVENTIONAL AND PULSE CURRENT DEPOSITED NICKEL-COBALT-MANGANESE ALLOY CONTAINING 26-38% COBALT AND MORE THAN 0.10% MANGANESE - BEFORE AND AFTER HEAT TREATING (65)

Pulse Duty Cycle %	Peak Current Density A/dm^2	Average Current Density A/dm^2	Bath Temp. °C	Bath pH	Alloy Composition (Percent by Weight) Ni	Co	Mn	Ultimate Strength MPa	ksi	Yield Strength MPa	ksi	Elongation Percent In 1.27 cm	5.08 cm
"As Deposited" Alloys:													
100	3.14	3.14	48.9	3.3	67.04	32.80	0.160	1670.0	242.2	1221.1	177.1	10	3
100	3.23	3.23	48.3	3.7	73.49	26.30	0.209	1570.7	227.8	1150.8	166.9	10	3.5
33	9.52	3.18	49.4	4.4	70.20	29.70	0.102	1801.0	261.2	1197.0	173.6	4	1.5
33	9.40	3.13	49.4	4.1	71.58	28.30	0.122	1451.4	210.5	1272.8	184.6	-----	1.5
33	9.68	3.23	48.9	3.7	73.79	26.00	0.206	1683.8	244.2	1237.7	179.5	4	1.5
33	9.58	3.20	48.3	3.3	61.98	37.80	0.215	Specimen fractured in machining tensile strip.					
33	9.61	3.21	48.9	4.5	67.08	32.70	0.219	1244.5	180.5	------	-----	-----	0.4
33	9.46	3.15	48.9	4.0	72.23	27.50	0.274	1642.4	238.2	1401.8	203.3	-----	1.5
Heat Treated at 315.6°C for 24 Hours:													
100	3.14	3.14	48.9	3.3	67.04	32.80	0.160	1679.6	243.6	1379.7	200.1	12	4
100	3.23	3.23	48.3	3.7	73.49	26.30	0.209	1460.4	211.8	1246.6	180.8	6	3.5
33	9.52	3.18	49.4	4.4	70.20	29.70	0.102	Not heat treated at this temperature.					
33	9.40	3.13	49.4	4.1	71.58	28.30	0.122	1134.2	164.5	1056.3	153.2	-----	3
33	9.68	3.23	48.9	3.7	73.79	26.00	0.206	1743.1	252.8	1449.3	210.2	5	3
33	9.58	3.20	48.3	3.3	61.98	37.80	0.215	1917.5	278.1	------	-----	8	3
33	9.61	3.21	48.9	4.5	67.08	32.70	0.219	Not heat treated at this temperature.					
33	9.46	3.15	48.9	4.0	72.23	27.50	0.274	1147.3	166.4	1088.0	157.8	-----	0
Heat Treated at 426.7°C for 4 Hours:													
100	3.14	3.14	48.9	3.3	67.04	32.80	0.160	1552.8	225.2	1308.7	189.8	6	3.5
100	3.23	3.23	48.3	3.7	73.49	26.30	0.209	1496.9	217.1	1272.1	184.5	6	3
33	9.52	3.18	49.4	4.4	70.20	29.70	0.102	Not heat treated at this temperature.					
33	9.40	3.13	49.4	4.1	71.58	28.30	0.122	1086.0	157.5	1023.9	148.5	-----	5
33	9.68	3.23	48.9	3.7	73.79	26.00	0.206	1518.3	220.2	1333.5	193.4	10	3.5
33	9.58	3.20	48.3	3.3	61.98	37.80	0.215	1796.8	260.6	1589.3	230.5	10	3
33	9.61	3.21	48.9	4.5	67.08	32.70	0.219	Not heat treated at this temperature.					
33	9.46	3.15	48.9	4.0	72.23	27.50	0.274	1363.8	197.8	1323.8	192.0	-----	0
Heat Treated at 537.8°C for 4 Hours:													
100	3.14	3.14	48.9	3.3	67.04	32.80	0.160	1126.6	163.4	1058.4	153.5	-----	4
100	3.23	3.23	48.3	3.7	73.49	26.30	0.209	1155.6	167.6	1076.3	156.1	-----	5
33	9.52	3.18	49.4	4.4	70.20	29.70	0.102	757.8	109.9	722.6	104.8	-----	14
33	9.40	3.13	49.4	4.1	71.58	28.30	0.122	846.7	122.8	839.8	121.8	-----	11
33	9.68	3.23	48.9	3.7	73.79	26.00	0.206	1179.0	171.0	1123.2	162.9	-----	4
33	9.58	3.20	48.3	3.3	61.98	37.80	0.215	1487.3	215.7	1401.1	203.2	-----	3
33	9.61	3.21	48.9	4.5	67.08	32.70	0.219	1486.6	215.6	1317.6	191.1	-----	2.6
33	9.46	3.15	48.9	4.0	72.23	27.50	0.274	1053.6	152.8	------	-----	-----	7.5
Heat Treated at 760°C for 15 Minutes:													
100	3.14	3.14	48.9	3.3	67.04	32.80	0.160	Not heat treated at this temperature.					
100	3.23	3.23	48.3	3.7	73.49	26.30	0.209	Not heat treated at this temperature.					
33	9.52	3.18	49.4	4.4	70.20	29.70	0.102	489.5	71.0	230.3	33.4	-----	40
33	9.40	3.13	49.4	4.1	71.58	28.30	0.122	518.5	75.2	277.9	40.3	-----	41.5
33	9.68	3.23	48.9	3.7	73.79	26.00	0.206	Not heat treated at this temperature.					
33	9.58	3.20	48.3	3.3	61.98	37.80	0.215	Not heat treated at this temperature.					
33	9.61	3.21	48.9	4.5	67.08	32.70	0.219	732.9	106.3	701.2	101.7	-----	12
33	9.46	3.15	48.9	4.0	72.23	27.50	0.274	608.1	88.2	476.4	69.1	-----	38

3.2.5.3 Conclusions - EF Nickel-Cobalt-Manganese Alloys

It is difficult to reach any definite conclusions regarding the high temperature strength capabilities of this alloy since only one investigator has attempted to characterize it and studies are incomplete. Test results for room temperature mechanical properties before and after heat treatment indicate it combines the best features of nickel-cobalt and nickel-manganese alloys and expands the temperature range for which each of these alloys display outstanding ultimate and yield strengths. Work remains to be performed to demonstrate that acceptual ductility can be obtained for structural applications. If this effort is successful, nickel-cobalt-manganese appears to be the only electroformable alloy of those considered which can be fully competitive with Inconel 718 over a wider service temperature range than expected for the Space Shuttle Main Combustion Chamber (MCC).

3.2.6 EF Nickel-Molybdenum, Nickel-Tungsten, Cobalt-Molybdenum, and Cobalt-Tungsten Alloys

3.2.6.1 General

Nearly all superalloys for elevated temperature use contain one or more elements from the iron group and at least one element from subgroup VI of the periodic table - chromium, molybdenum, and tungsten. It is easy to understand why these alloys perform well in severe thermal environments by examination of the binary phase diagrams of the iron group and subgroup VI elements. In the wrought alloys, many peritectic reactions through heat treatments or thermal service exposure occur which produce crystallographic cell configurations much different than those natural to the base iron group metal. The binary phase diagrams show many of these "alien" configurations to be stable to very high temperatures. Their influences on the base metal are profound and may persist to very high temperatures. This would be a most desired feature of any electroformed alloy expected to show outstanding mechanical properties under severe thermal conditions.

Investigators have been examining deposition of alloys of the iron group metals and subgroup VI elements for over 100 years. Although no process of practical commercial importance has been developed to electrodeposit these alloys, the progress on such processes is worth discussion in this survey. One of the problems confronting investigators has been a determination of the mechanism by which molybdenum or tungsten becomes plateable when an iron group metal is present. Brenner (66) calls molybdenum and tungsten "reluctant" metals since they cannot be deposited alone from aqueous solutions. He refers to the iron group metals in the alloy process as "inducing" elements because they will induce codeposition of the "reluctant" metals when present. The phenomenon involves additional peculiarities which show it to be different from ordinary alloy deposition:

1. There is a limited content of reluctant metal which can be deposited in an alloy.

2. Under some circumstances the reluctant metal deposits preferentially.

3. The current density-potential curves of alloy deposition are often situated at more noble (more positive) potentials than those of the inducing metal itself.

The single theory which appears to best explain the induced codeposition of tungsten and molybdenum with the iron group metals was advanced by Brenner (67). He suggests that the polarization involved in the deposition of the inducing metal (nickel, cobalt, or iron) assisted the codeposition of the reluctant element. He also considers hydrogen as an additional inducing element - particularly when it accompanies discharge of the iron group metal at the cathode.

Brenner (67) reported that a large variety of baths, both acid and alkaline, have been investigated for the deposition of molybdenum alloys. The acid baths were categorized as either wholly inorganic or containing organic acids (hydroxy acids as chelating agents). The alkaline baths were divided into several types such as ammoniacal (the most important), pyrophosphate, carbonate, and others containing organic complexing agents. He cited the nickel-molybdenum alloys as the soundest of those containing an iron group metal. In general, the alkaline baths were preferred for depositing the alloys, and most work was done with the ammoniacal baths containing citrate ion.

Brenner gave a general description of appearance, structure, and properties of iron group-molybdenum alloys. He noted that under best conditions the alloys were silvery white but unsound because they did not hold together when the basis metal was removed. Few measurements have been made of the mechanical properties of the electrodeposited molybdenum alloys due usually to the unsound character of thick deposits.

A review of Seim and Holts' (68) work to codeposit binary alloys of nickel-molybdenum and cobalt-molybdenum revealed no practical process for electroforming these materials. They used plating solutions composed of sulfates of the iron group metals, citric acid as a complexing agent, and sodium molybdate. A wide range of bath pH values, molybdate concentrations, temperatures, and current densities were evaluated. Current efficiencies were very low. With the nickel-molybdenum bath, satisfactory deposits were obtained and current efficiency increased with increasing pH. In the cobalt-molybdenum bath, satisfactory deposits under alkaline conditions could only be obtained at high current densities. Stephenson (38) examined these same baths and concluded that only the cobalt-molybdenum bath would provide sound deposits, but the bath efficiency was too low for practical applications.

Frantsevich, Zabludovskaya, and Zhelvis (69) codeposited nickel-molybdenum alloys from baths containing citrates and tartrates using anodes of 70 percent nickel and 30 percent molybdenum. They reported the efficiency of the bath increased with solution stirring and with higher ratios of nickel to molybdenum. Thicknesses up to 10 μm could be obtained. This would be unsatisfactory for electroforming. Later work was performed with nickel-molybdenum alloy deposition from an ammoniacal tartrate bath with sodium

chloride to increase conductivity. With the tartrate complexing agent at the same molar concentration as the bath metal content, higher cathode efficiencies (about 75 percent) were obtained.

Stephenson included the investigation of a pyrophosphate bath developed by Rama Char (70) in his search for electrodeposited alloys for elevated temperature use. This was a cobalt-molybdenum bath from which Stephenson could obtain no satisfactory deposits.

Brenner (71) notes the Armstrong-Menefee processes as some of the earliest commercially exploited techniques for plating tungsten alloys. The electrolyte involved acid fluoride solutions with various other additives such as phosphate ion, boric acid, or acetic acid. Deposits thicker than 1μm were cracked and exfoliated - presumably due to codeposited inclusions. The most significant early researches of tungsten alloy deposition were made by Gol'tz and Kharlamov (72). They developed practicable alloy plating baths by using ammoniacal electrolytes containing ammonium salts. Deposits up to 0.02 cm thick could be plated at current efficiencies to 30 percent. They noted that:

1. The soundest deposits and the highest cathode current efficiencies were obtained with baths operated at elevated temperatures.

2. Increasing the content of tungsten in the bath above a certain concentration did not result in an increase in the tungsten content of the deposit and lowered the cathode current efficiency.

3. The deposition potentials of the nickel-tungsten alloy were more noble than those for the deposition of nickel alone.

Their plating bath was not totally satisfactory because the thick deposits obtained were porous and weak. The poor quality arose from deposition at excessively high current densities for a bath containing only 12 g/l total metal. The deposits likely contained nonmetallic inclusions. The low metal content was necessary due to instability of ammoniacal solutions with higher metal content.

The work of Brenner and his associates at the National Bureau of Standards (73) is worthy of further discussion, since they considered the physical properties of the alloy deposits to a much greater degree than most investigators. They noted that:

1. The iron-group-tungsten deposit hardnesses were quite high as plates and that the hardnesses increased when subjected to suitable heat treatments. On heating to 600^{o}C and cooling, certain of these alloys exhibited hardness increases (Vickers) of over 100 points. The nickel alloys exhibited less tendency to increased hardening than the cobalt counterparts.

2. Precipitation hardening occurred with cobalt-tungsten alloys containing above 5 percent of tungsten and with nickel-tungsten alloys having over 17 percent of tungsten. There were some exceptions whereby some alloys with a high tungsten content softened on heating and others with low tungsten hardened.

3. Precipitation hardening occurs at lower tungsten contents in the electrodeposited alloys than in the metallurgical (wrought) alloys.

4. Hot-hardness of cobalt-tungsten electrodeposited alloys appeared to be comparable to that of stellite when the tungsten content was over 20 percent.

5. The nickel-tungsten and cobalt-tungsten deposits with not over 5 percent tungsten had slight ductility. At higher tungsten contents, there was no apparent ductility. Heating the nickel-tungsten alloys to 600°C, or above, and the cobalt-tungsten alloys to above 900°C lead to good ductility as determined by simple bend tests.

6. Very limited mechanical property testing showed nickel-tungsten alloys containing about 20 percent tungsten to have a tensile strength in the range of 765 to 1079 MPa (111 to 156.5 ksi). The electrodeposited cobalt-tungsten had a tensile strength of 539.4 MPa (78.2 ksi).

7. The oxygen content of all iron group-tungsten electrodeposits was slightly higher than that for the individual iron group metals plated separately. The citrate bath deposits had higher oxygen content than the tartrate alloy deposits.

Safranek (74) has presented mechanical property data for various cobalt-tungsten electrodeposited alloys resulting from the investigations of Turns and Hildebrand (75), Browning and Turns (76), and Browning, Leavenworth, Webster, and Dunkerley (83). Safranek notes that Turns and Hildebrand investigated cobalt-tungsten binary alloy deposits with tungsten contents from 20 to 35 percent and ternary alloy deposits of cobalt containing 30 percent tungsten with 5 percent nickel addition. The 20 percent tungsten binary alloy was deposited from an electrolyte composed and operated as follows:

Cobalt Chloride - $CoCl_2 \cdot 6H_2O$	160 to 200 g/l
Sodium Tungstate - $Na_2WO_4 \cdot 2H_2O$	27 to 36 g/l
Rochelle Salts (NaK Tartrates)	400 g/l
Ammonium Chloride - NH_4Cl	50 g/l
pH	8.5
Temperature	90°C
Cathode Current Density	5 A/dm^2

The "as deposited" ultimate strength of the cobalt alloy with 20 percent tungsten was 1068.7 MPa (155 ksi) with practically no ductility.

Turns and Hildebrand (75) used a sulfate-tartrate bath to deposit a cobalt-tungsten alloy containing 35 percent tungsten. This bath was of the following composition and operating conditions:

Cobalt Sulfate - $CoSO_4 \cdot 7H_2O$	120 g/l
Sodium Tungstate - $Na_2WO_4 \cdot 2H_2O$	30 g/l
Rochelle Salts (NaK Tartrates)	380 g/l
Ammonium Chloride - NH_4Cl	50 g/l
Wetting Agent	0.5 g/l
pH	8.0 to 9.0
Temperature	85°C
Cathode Current Density	5 A/dm^2

The deposit was (according to Safranek) heat treated at 1093°C for 16 hours prior to test. An ultimate strength of 803.3 MPa (116.5 ksi) was obtained with a reduction in area of only 1 percent. In further work, Turns and Hildebrand produced more 35 percent tungsten alloy from an identical bath, except for the increase of tungstate content to 43 g/l. This material was heat treated at 1122°C and aged at 1300°C. Samples were tested for mechanical properties at elevated temperatures and the results are shown in Figure 3.2-24.

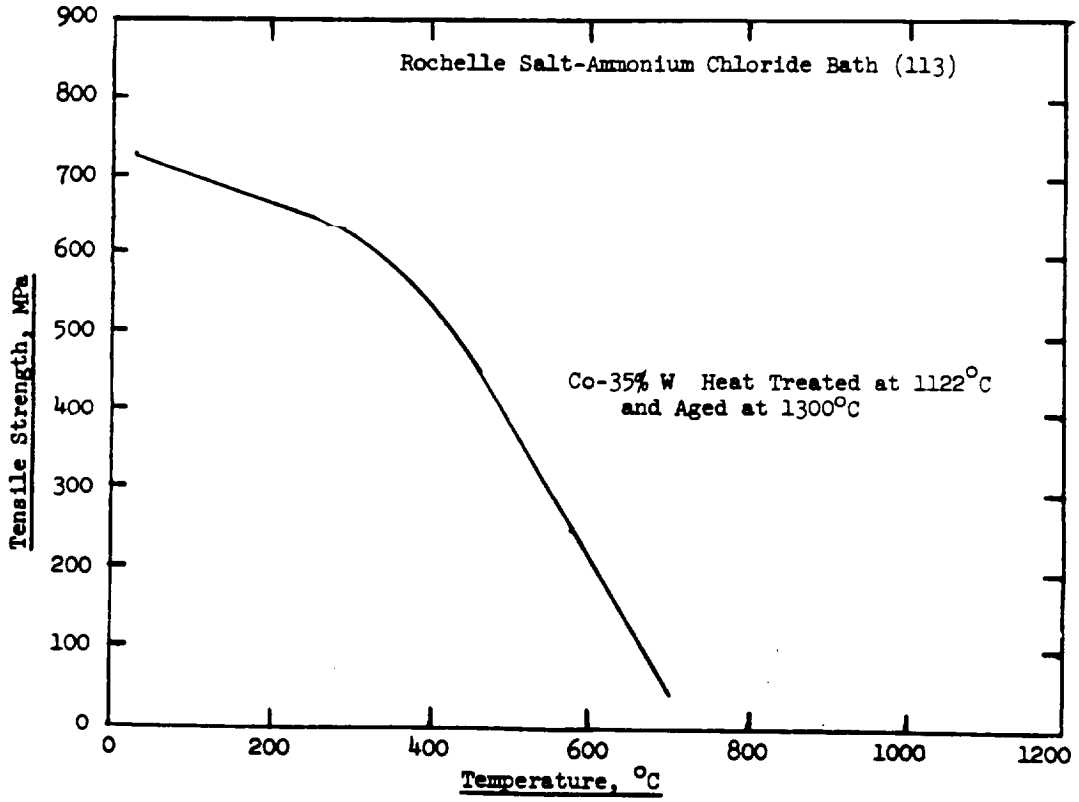

Figure 3.2-24. Tensile Strength at High Temperatures of Heat Treated Cobalt-Tungsten Alloy Electrodeposits (75)

The paper presented by Browning and Turns (76) appears to be mostly a reiteration of the work of Turns and Hildebrand. It does, however, give a critical review of cobalt-tungsten plating baths and their shortcomings. Included in this discussion are the tartaric acid and boric acid bath used by Offermans and Stackelberg, the citric acid bath employed by Clark and Holt, Hoar and Bucklows' citric acid-ammonium chloride bath, Fedot'ev's ammonium sulfate bath, and Brenners Rochelle salt-ammonium chloride bath (which they selected for a suggested or preferred bath). Also of great interest is their discussion of a cobalt-tungsten-nickel ternary alloy bath which will be discussed here due to the low nickel content of the alloy deposits. The bath formulation and operating conditions were given:

$CoSO_4 \cdot 7H_2O$	110 to 115 g/l
$Na_2WO_4 \cdot 2H_2O$	38 to 43 g/l
$NiSO_4 \cdot 6H_2O$	5 to 8 g/l
Rochelle Salts	375 to 385 g/l
NH4Cl	50 to 55 g/l
Wetting Agent	0.5 to 0.8 g/l
pH	8 to 9 using gaseous NH_3
Anodes	Tungsten or tungsten-cobalt
Temperature	87.8°C
Cathode Current Density	4.3 to 5.4 A/dm^2

Deposit compositions ranged from 4.1 to 4.5 percent nickel, 31.1 to 32 percent tungsten, and 62.6 to 63.5 percent cobalt - a small amount of nonmetallic material was present. For a heat treatment at 1140°C for 4 hours and a 4 hour age at 700°C, the alloy exhibited an ultimate strength (average) of 342 MPa (49.6 ksi).

3.2.6.2 Conclusions - EF Nickel-Molybdenum, Nickel-Tungsten, Cobalt-Molybdenum, and Cobalt-Tungsten Alloys

Although it has been demonstrated that these alloys can be electroformed to provide some outstanding mechanical properties at very high temperature, they have serious drawbacks which almost preclude their use on a commercial basis. The electrolytes are highly complexed with organic acids which leads to incorporation of breakdown products in the deposits. pH control requires close attention throughout the electroforming operation. The use of ammonia gas or saturated ammonia solutions to adjust and maintain pH can be physiologically objectionable, particularly where large plating facilities are required. The baths are usually subject to less than 90 percent efficiency which means that solution imbalance is always a problem. The operating temperatures are frequently high which poses a serious problem with respect to electroforming maskants and waxes often employed to protect or provide inert fillers for complex features of the end item.

If the above alone were not enough to discourage use of these baths, the fact that "as deposited" product is extremely brittle offers another problem. Severe heat treatments are invariably required to restore ductility and microstructural features desired. Often the electroform is required on a substrate that is sensitive to these high heat treating temperatures. Also, the deposits are highly stressed. This may require keeping the mandrel in the electroform through the heat treating so as to prevent distortional forces from warping the structure to an extent that it is no longer useful.

3.2.7 EF Nickel and Cobalt Dispersion Strengthened Metals

3.2.7.1 General

There is general agreement among investigators that plastic deformation of metals at elevated temperatures is inhibited by blocking, or at least delaying, the movement of dislocations in the metal matrix. In dispersion strengthened metals, this blocking is due to termination of dislocation movement at inert dispersoid particles as illustrated in Figure 3.2-25. To effectively constrain dislocations, interparticle spacing should be small - preferably less than one micron. This dictates that the particles themselves be extremely small to afford close proximity to one another.

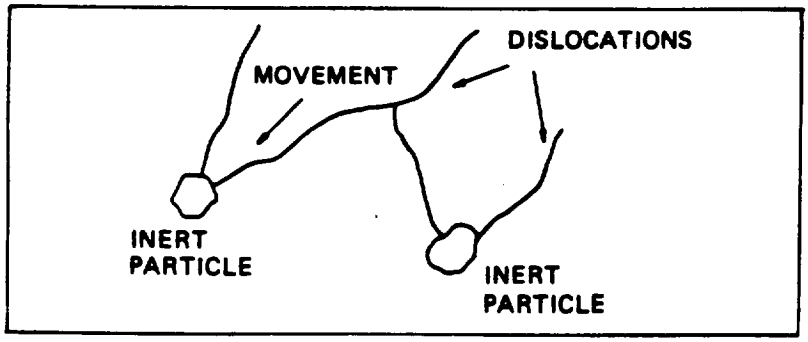

Figure 3.2-25. Mechanism of Dispersion Strengthening in Metals

Wrought dispersion strengthened nickel base alloys such as TD Nickel and TD Nickel-Chromium are usually produced by the powder compaction and sintering method. To obtain best high-temperature properties in the alloys, numerous cycles of warm rolling (reduction) and heat treating in a hydrogen atmosphere are used. This thermo-mechanical history of the alloy is what leads to outstanding high-temperature mechanical properties. Without this microstructural conditioning the beneficial effects of dispersion strengthening are only achieved to a temperature approximately one-half that of the metal melting point,. At lower temperatures (below 0.5 T_m - where T_m equals the melting point), the size and distribution of the dispersion particles are of prime importance in determining the strength (77).

Sautter (78) studied the effects of particle concentration, particle size, and plating conditions on the microstructure and physical properties of aluminum oxide dispersed in nickel deposited from a Watts type electrolyte.

His electrolyte was formulated and operated as follows:

Nickel Sulfate (Hexahydrate)		300 g/l
Nickel Chloride (Hexahydrate)		45 g/l
Boric Acid		30 g/l
Wetting Agent		0.2 vol. %
Aluminum Oxide		Linde Alumina B5125, 0.1 micron particles
	or	Cabot Alumina Alon C, 0.01-0.04 micron particles
Anodes		Rolled nickel, 99.9%
Stirrers		Magnetic
Temperature		50°C
pH		3.5
Current Density		2 A/dm^2

Sautter found that the amount of aluminum oxide incorporated in the nickel deposits was roughly proportional to the concentration in the bath. For a concentration of 50 g/l of aluminum oxide in the bath, he did not note any significant change in concentration of aluminum oxide in the deposit. Likewise, current density had no appreciable effect on alumina content of the deposit. Alumina concentration in the electrodeposited nickel remained fairly constant for pH in the range of 2 to 5. However the content was greatly decreased when the pH changed from 2 to 1.

Figure 3.2-26 illustrates the effect of alumina concentration in the bath on concentration of alumina in the electrodeposited nickel for the given plating conditions.

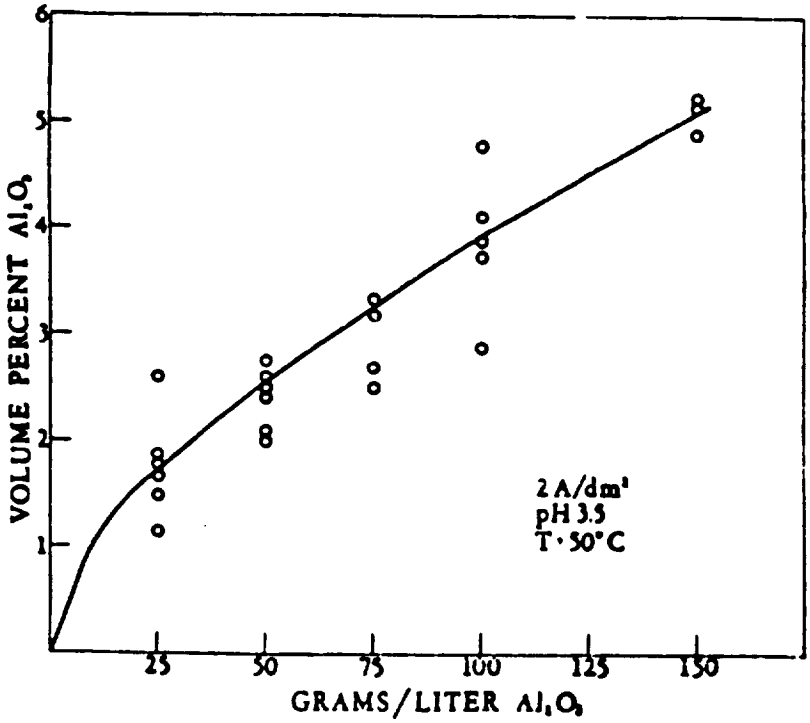

Figure 3.2-26. Oxide Content of Deposit as a Function of Oxide Content of Bath

Figure 3.2-27 shows the effect of pH on the concentration of alumina in the deposit. Sautter investigated the strengthening effect of dispersed alumina in nickel by measuring the yield strength at 0.1 percent offset. All tests were conducted at room temperature. To remove the effect of the plating conditions on the yield strength by different grain structure and orientation, he subjected all specimens to a heat treatment prior to testing by annealing at 800°C for 20 hours in nitrogen. Sautter than assumed a uniform spacing of the particles (verified by electron microscopy), calculated the interparticle spacing based on particle sizes and concentration in the deposit, and plotted the reciprocal spacing values against corresponding yield strengths as shown in Figure 3.2-28. It is seen that the yield strength is a function of the distance between particles.

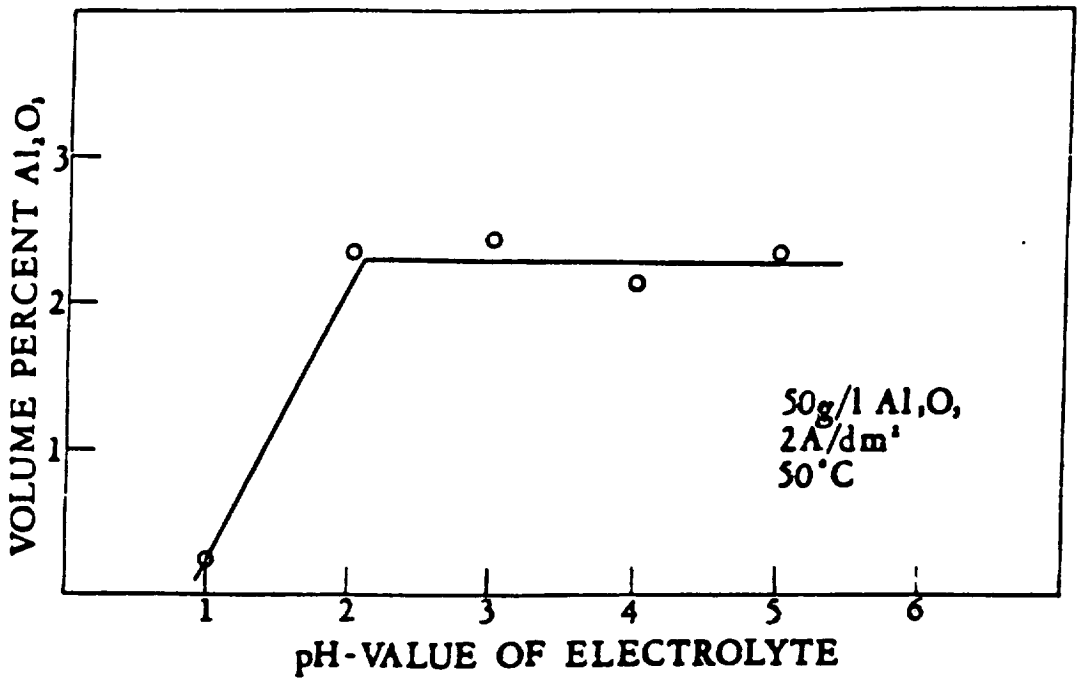

Figure 3.2-27. Effect of the Bath pH Value on Deposit Oxide Content

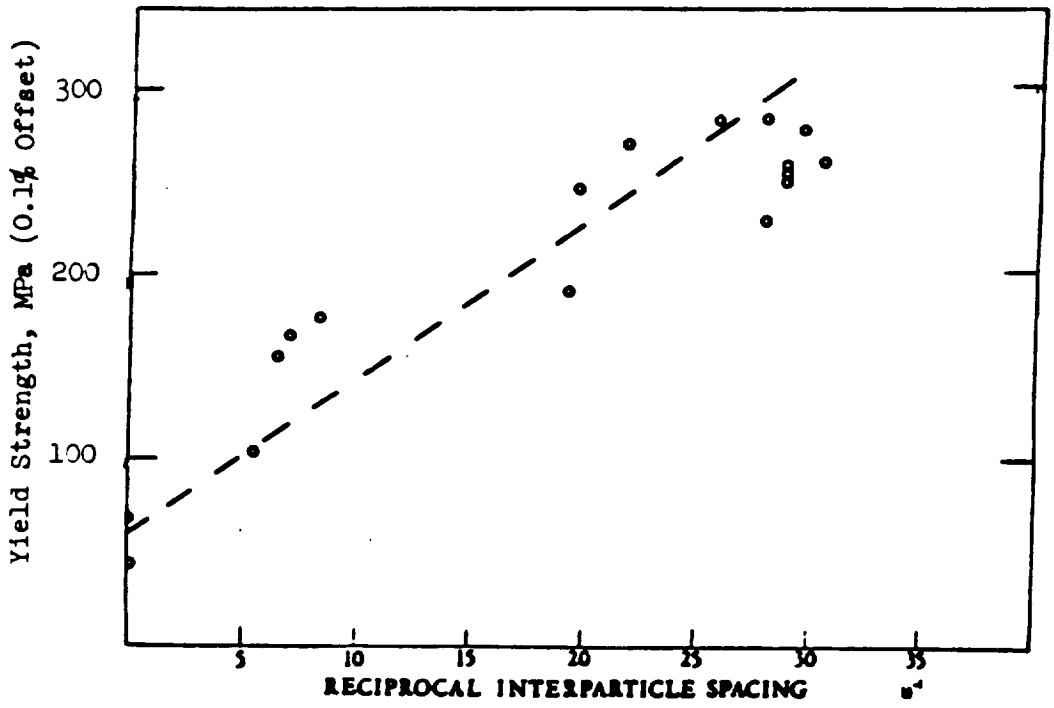

Figure 3.2-28. Yield Strength of Electrodeposited Nickel-Al_2O_3 as a Function of Reciprocal Interparticle Spacing (78)

Lakshminarayanan, Chen, and Sautter (79) examined the effects of alpha and gamma aluminum oxide dissolution on the properties of Co-Al_2O_3 and Ni-Al_2O_3 dispersion strengthened electrodeposits. The alpha form had a nominal particle size of 0.3 micron while the gamma form had a nominal particle size of 0.03 micron. They introduced both forms of aluminum oxide to dilute sulfuric acid solutions, Watts type nickel electrolytes, and Watts type cobalt electrolytes. The gamma form additions produced more significant and immediate changes in pH of all solutions, Figure 3.2-29. This was believed due to the greater surface area per unit of volume of the gamma form and its ability to establish an equilibrium with the potential determining ions (H^+, OH^-). Further pH change was found to occur over long time periods. This was attributed to dissolution of aluminum oxide to produce aluminum ions in the electrolytes, Figure 3.2-30. In Figure 3.2-30, the solid lines correspond to gamma aluminum oxide while the dotted lines represent alpha aluminum oxide. To compensate for the differing surface areas of the two forms of Al_2O_3, the concentrations of aluminum ion shown in Figure 3.2-30 are based on the calculated surface areas and are per square meter of the respective oxide surface area.

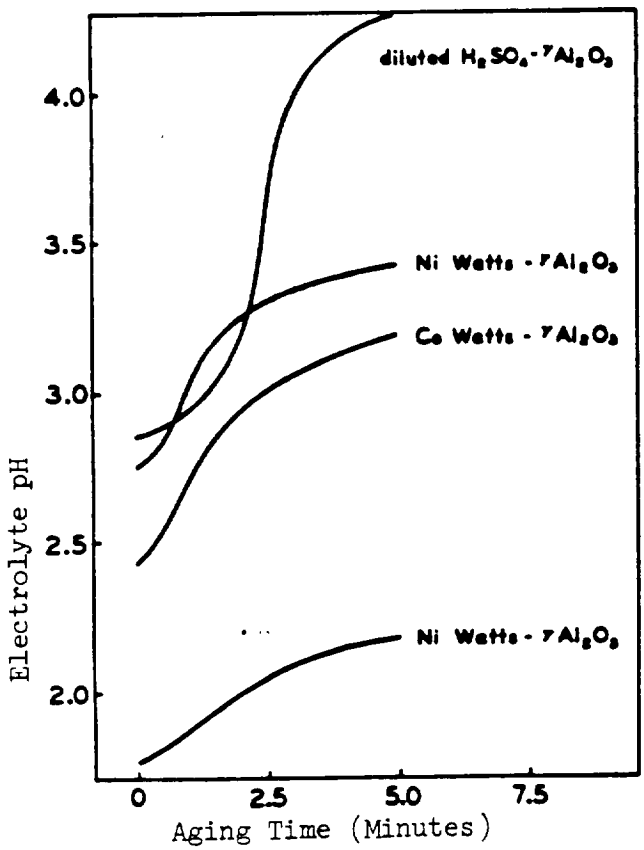

Figure 3.2-29 Effects of 25 g/l Addition of Gamma Al_2O_3 on pH at 25°C for Various Electrolytes with Time

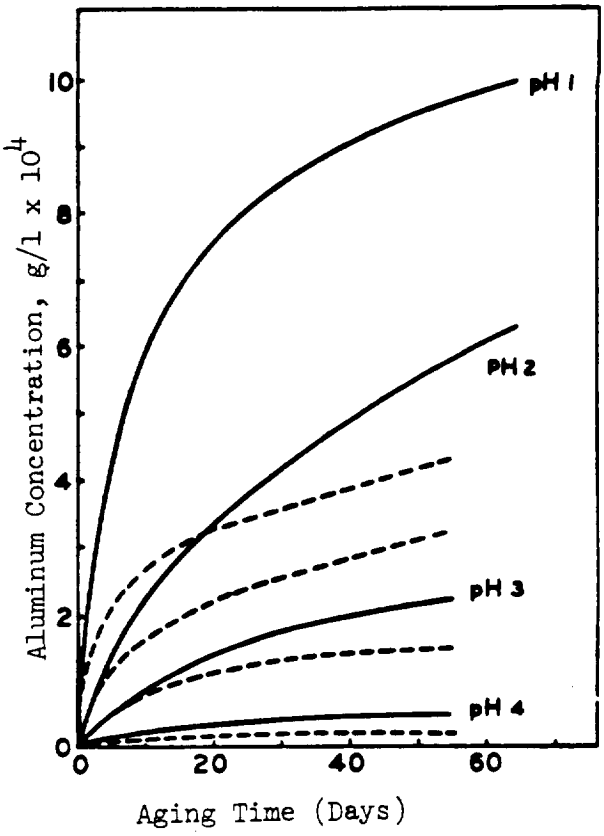

Figure 3.2-30. Effect of Electrolyte pH on Solubility of Gamma and Alpha Al_2O_3 as a Function of Aging Time

They noted that aluminum ion presence in the electrolytes led to a finer grain size in all deposits. This was attributed to the formation of a reaction product, $Al(OH)_3$, at the cathode and possible absorption at active metal grain sites. This may have inhibited grain growth and accelerated the formation of crystallization nuclei. They electroplated mechanical property test specimens from Watts type nickel, Watts type cobalt, Watts type Ni-Al_2O_3, Watts type Co-Al_2O_3, and similar electrolytes containing varied amounts of aluminum ion. Some of the deposits were tested in the "as deposited" condition while others were annealed in hydrogen at 800°C for one hour. Only the yield strengths were reported as this was the primary objective of the investigation. Results are shown in Table 3.2-43.

The investigators noted the different trends in yield strengths resulting from Al_2O_3 and aluminum ion additions to the separate nickel and cobalt Watts type electrolytes. They could offer no explanation of why cobalt deposits from baths to which aluminum ion was added showed increased yield strengths while those for nickel decreased.

TABLE 3.2.43. YIELD STRENGTH DATA FOR DEPOSITS FROM WATTS TYPE PLATING SOLUTIONS OF COBALT AND NICKEL CONTAINING GAMMA Al_2O_3 AND ALUMINUM SULFATE (79)

Plating Solution	Oxide Volume %	Yield Strength Values (0.2% Offset) As Plated MPa	As Plated ksi	Annealed (800°C, 1 Hr) MPa	Annealed (800°C, 1 Hr) ksi
Cobalt Electrodeposits					
Watts Bath	None	341.3	49.5	261.8	38.0
Watts-Al_2O_3 Bath	1.8	473.7	68.7	493.3	71.5
Watts-Al_2O_3-1.5 g/l Aluminum Ion	1.6	521.7	75.7	500.2	72.5
Watts-Al_2O_3-2.5 g/l Aluminum Ion	1.3	509.0	73.8	542.3	78.7
Watts-Al_2O_3-4.5 g/l Aluminum Ion	1.2	499.2	72.4	508.0	73.7
Nickel Electrodeposits:					
Watts Bath	None	313.8	45.5	94.1	13.6
Watts-Al_2O_3 Bath	0.8	310.9	45.1	249.1	36.1
Watts-Al_2O_3-1.5 g/l Aluminum Ion	0.6	306.0	44.4	228.5	33.1
Watts-Al_2O_3-2.5 g/l Aluminum Ion	0.5	282.4	41.0	203.0	29.4
Watts-Al_2O_3-4.5 g/l Aluminum Ion	0.5	274.6	39.8	217.7	31.6

Plating Parameters: Current density was 4 A/dm^2, pH 2.0, nickel bath temperature was 50°C, and cobalt bath temperature was 40°C. Gamma Al_2O_3 concentration in each bath was 25 g/l.

Malone (80) investigated the codeposition of thorium oxide and gamma aluminum oxide in nickel from the Watts type bath and the sulfamate nickel bath. Using sedimentation rate studies, he was able to assess dispersoid particle charge strengths relative to pH of the electrolyte. His findings confirmed those of Sautter and his associates that rapid pH change takes place upon introduction of certain submicron sized refractory oxides to a nickel plating bath. Long term aging of such electrolytes also disclosed further pH changes resulting from the dissolution of Al_2O_3 crystallites; however, such was not the case with thorium oxide. The aluminum oxide used was the gamma form procured under the name "Alon C". Particle size was about 0.03 micron as mentioned by Sautter in his work. The thorium oxide was produced commercially by the sol-gel process and contained crystallites averaging about 0.015 micron.

Malone's initial studies were with nickel sulfamate and Watts type baths operated at pH levels between 3.5 and 4.5. Specimens were electroformed for compositional analysis and mechanical property testing at room and elevated temperatures. The thoria concentration of the electrolyte was varied from 0 to 5 g/l. Table 3.2-44 shows the electroforming parameters used to produce

these samples and the results of room temperature mechanical property tests. Ultimate and yield strengths increased with increasing thorium oxide content while ductility decreased. When subjected to a temperature of 815.6°C (1500°F), these specimens exhibited unsatisfactory mechanical property performance and were brittle.

TABLE 3.2-44. MECHANICAL PROPERTIES OF ELECTRODEPOSITED NICKEL AND THORIUM OXIDE DISPERSION STRENGTHENED NICKEL AT ROOM TEMPERATURE (80)

Bath Temp °C	Current Density A/dm^2	Bath pH	Weight % Thoria in Deposit	Ultimate Strength MPa	Ultimate Strength ksi	Yield Strength MPa	Yield Strength ksi	Elongation in 5.08 cm %
37.8	4.84	3.9	0	359.2	52.1	240.6	34.9	28
37.8	4.84	3.9	0.2	446.8	64.8	280.6	40.7	19
37.8	4.84	4.0	1.0	530.9	77.0	359.2	52.1	12

Electrolyte: Nickel Sulfamate

It was suspected that the poor elevated temperature performance was due to chemisorbed water in the surfaces of the particles. This would be expected to outgas into the grain boundaries at high temperature. The work of Mikhail and Fahim on the thermal removal of chemisorbed water from thoria gel crystallites was reviewed (81). It was found that only 90 percent of this water could be removed by a thermal treatment at 400°C. Even a thermal exposure at 1000°C does not remove all chemisorbed water.

Malone then considered that the "double layer" charge theory might be appropriate to describe the surface chemistry of the thoria crystallites. In this theory it is considered that either an anion or a cation is adsorbed on the crystallite surface at primary adsorption sites. To do this, the particle must have a large surface to volume ratio and be colloidal in size. The type of ion adsorbed depends on the nature of the crystallite. The atomic density and size of the thorium atom in relation to the adjacent oxygen atoms dictates that anions will be adsorbed on the surface. This gives the thoria particle a negatively charged layer. To counter this charge, an outer layer of a cation such as Ni^{++} or H^{+} must be formed. This would explain the pH change noted by Sautter when Alon C was added to a nickel electrolyte.

Noting that Sautter found a great reduction in alumina content of nickel deposits plated from a low pH bath (below pH of 2.0), Malone determined that chemisorbed water and associated anions might be significantly reduced by codeposition from a bath operated at a pH below 2.0. He also considered that a heat treatment might further remove chemisorbed water. He first evaluated the effect of heat treating on Ni-ThO_2 deposits produced from nickel sulfamate electrolytes of normal pH. The results of this study are shown in Table 3.2-45.

TABLE 3.2-45. EFFECT OF HEAT TREATMENT IN OUTGASSING OF CHEMISORBED WATER FROM NICKEL-ThO_2 SAMPLES ELECTROFORMED AT pH 3.9 (80)

Bath Temp °C	Current Density A/dm²	Bath pH	Weight % Thoria in Deposit	Heat Treatment	Mechanical Properties at 1093°C Ultimate Strength MPa	ksi	Yield Strength MPa	ksi	Elongation in 5.08 cm %
37.8	4.84	3.9	1.26	None	6.2	0.9	-	-	3
				538°C, 1 Hr	6.9	1.0	5.5	0.8	4
				1260°C, 2 Hr	18.6	2.7	15.9	2.3	1
37.8	4.84	3.9	0.54	538°C, 1 Hr	10.3	1.5	6.9	1.0	6
				1260°C, 2 Hr	20.0	2.9	19.3	2.8	2

Electrolyte: Nickel Sulfamate

Although the mechanical property test temperature of 1093°C was well above the 0.5 T_m temperature at which dispersion strengthened metal will perform well without prior mechanical hot working and annealing cycles, the Table 3.2-45 results indicate better mechanical properties in the material with the lower thoria content. This indicates that for pH 3.9 electrolytes and deposits with higher thoria contents, one may expect more chemisorbed water to still be present and affect mechanical property performance - even with such severe heat treatments. It was of interest to note that little recrystallization occurred in the alloy with 1.26 percent thoria after the treatment at 1260°C. Significant grain growth was observed in the lower thoria content deposit.

Samples were electroformed from a sulfamate nickel electrolyte operated at various pH levels ranging from 3.2 to 1.6. The purpose of this study was the determination of the effect of pH on the surface residuals of codeposited thoria particles due to chemisorbed water and associated dissolved salts. Table 3.2-46 displays typical results of mechanical property tests at a temperature of 816°C (1500°F). These samples had not been subjected to any preliminary heat treatments.

TABLE 3.2-46. EFFECTS OF NICKEL SULFAMATE ELECTROLYTE pH ON DISPERSOID CONTENT OF Ni-ThO_2 DEPOSITS AND ASSOCIATED STRENGTH AT 816°C

Bath Temp °C	Current Density A/dm²	Bath pH	Electrolyte Thoria Content, g/l	% by Weight Thoria In Deposit	Ultimate Strength MPa	ksi	Elongation in 5.08 cm %
55	3.23	3.2	4.03	1.77	9.0	1.3	Under 1
54	3.23	2.3	4.78	1.75	43.4	6.3	4
51	3.23	1.6	4.58	0.96	75.8	11.0	2

Although Table 3.2-46 shows that decreasing bath pH leads to lower dispersoid content in the electrodeposit, less chemisorbed water and associated ions are present and elevated temperature mechanical strength is much improved. The concept for codepositing such dispersion strengthened metals from low pH electrolytes has received patent status (82). Figure 3.2-31 shows the effects on elevated temperature mechanical strength of employing low pH electrolytes and normal pH baths as functions of thoria content in the deposit. Malone has found similar performance in the nickel Watts type electrolyte and recommends such baths for operation at low pH levels. Sulfamate baths should not be operated at these pH levels for lengthy periods due to hydrolysis of the sulfamate to produce sulfates and objectionable ammonium by-products. He also noted that alumina can be readily substituted for thoria to afford similar properties at high temperatures.

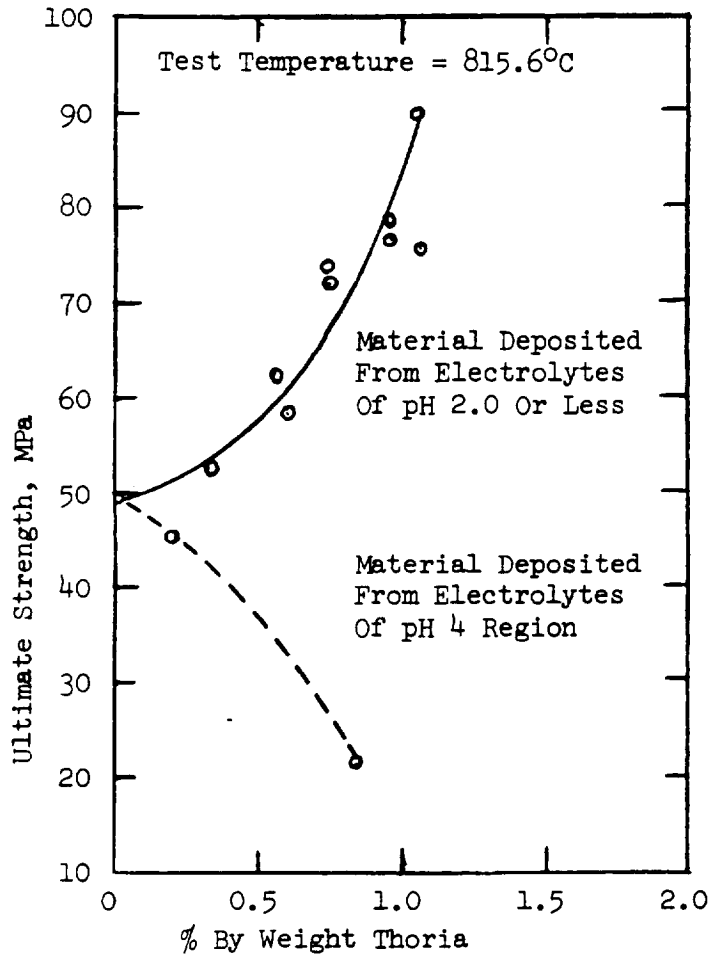

Figure 3.2-31. Typical Mechanical Strength Test Results at 815.6°C for Ni-ThO_2 Dispersion Strengthened Electrodeposits (80)

3.2.7.2 Conclusions - EF Nickel and Cobalt Dispersion Strengthened Metals

Dispersion strengthening of most electrodeposited metals results in a significant retention of yield strength at elevated temperatures. It does not greatly improve ultimate strength at any of the test temperatures studied. Reasons should be readily apparent when one considers that dispersion strengthening does not create a true alloy. The matrix metal will have inherent mechanical strength typical for that metal or alloy - with or without the dispersion phase being present. The benefits derived from a true dispersion strengthening mechanism are:

1. Yield strengths are better retained at elevated temperature through inhibiting, or delaying, dislocation movements by terminating them at ultra fine particles such as refractory oxides uniformly dispersed through the matrix. This is referred to as resistance to slip.

2. Ultimate strengths appear to be slightly better because of the fact that recrystallization at high temperature is inhibited. The oxide dispersions hinder dislocation movements across grain boundaries to minimize coalescence with neighboring grains. This is referred to as resistance to climb such as experienced when a metal anneals.

Dispersion strengthening might prove useful in an electrodeposited alloy such as nickel-cobalt if subject to use at temperatures higher than that at which allotropic changes occur in the lattice cell structure. From the previous discussions it appears that several electroformable alloys are available with sufficiently outstanding mechanical properties at low and moderate regions of temperature so as to remove any need for dispersion strengthening. It should also be noted that dispersion strengthened electrodeposits suffer from ductility problems at high temperature. They generally require a severe heat treatment to relieve side effects from contaminants associated with the codeposited particles. To achieve maximum benefits from a dispersion strengthened alloy, it is necessary to subject the metal to repeated mechanical working and thermal relieving treatments. Such is not possible with electroformed end items because of their complex shapes.

3.2.8 Selection of EF Alloy System for Optimization and Further Study

From the prior reviews of the status of various electroformable alloy or dispersion strengthened systems having potential for providing improved mechanical strength at elevated temperatures, it appears that only the EF nickel-manganese and nickel-cobalt alloys are sufficiently developed products that are greatly superior to conventional EF nickel and potentially competitive with Inconel 718. Both EF alloys can be heat treated at reasonably moderate temperatures and time cycles to afford suitable ductility and high mechanical strength for most structural applications. The EF nickel-cobalt-manganese may eventually prove best from a standpoint of strength retention at elevated temperatures; however, it must be heat treated at a temperature higher than desired to provide adequate ductility. The EF nickel-molybdenum, nickel-tungsten, cobalt-molybdenum, and cobalt-tungsten systems lack

sufficient ductility in the "as deposited" state to provide deposits that would not fracture in electroforming applications. Also, the efficiency and control measures necessary for these baths are not currently practical for commercial or aerospace applications. The benefits of the dispersion strengthened alloys are derived at much higher temperatures than required for the SSME application. These metals do not generally have outstanding strength at lower temperatures. They also require very high heat treatment temperatures to obtain satisfactory ductility.

EF nickel-manganese has been the final selection over EF nickel-cobalt due to the fact that better mechanical properties can be maintained over a much greater temperature range. The electrolyte is chemically much easier to prepare and control. Also, the levels of alloying of EF nickel-manganese are much lower than for EF nickel-cobalt and stress appears to be a slightly smaller problem. Since the objective of this program is to develop and demonstrate an improved electroformable alloy advance aerospace applications in the area of propulsion, it would be desirable to utilize an alloy with a greater range of temperature capabilities than can be obtained with EF nickel-cobalt.

3.3 Phase A - Characterization and Optimization of a High Performance Electroformable Alloy

3.3.1 Introduction

Most of the original work performed at Bell Aerospace Textron with the sulfamate nickel-manganese plating bath was for production of an alloy suitable for application at high temperatures in the region of 482° to 538°C (900° to 1000°F). Conventional EF nickel suffers hot-shortness in this range due to the formation of nickel sulfide which becomes a liquid in this temperature region and wets grain boundaries to decrease grain cohesive strength with resulting intergranular failure under stress. In developing this alloy for high energy chemical laser applications, the mechanical property performance at lower temperature ranges, other than ambient, was not explored. It was found that EF nickel-manganese in the "as deposited" condition had poor ductility from about 93° to 427°C (200° to 800°F). Similar deficiencies in ductility are to be found in "as deposited" nickel-cobalt, as well as most other iron, nickel, or cobalt based EF alloys that have not been heat treated. This problem with EF nickel-cobalt has been resolved as a result of extensive development work by many investigators over a period of over 30 years. The solution was a moderate heat treatment for a long time cycle which restored ductility without excessive loss of mechanical strength. As a result of this extensive attention given EF nickel-cobalt, the optimum composition for best mechanical properties has been found to be 50 to 55 percent by weight cobalt.

Although exploration of EF nickel-manganese began at a similar time, work was brief and did not receive the degree of attention that had been given EF nickel-cobalt. Reasons for this might have been based on the high stresses and cracking noted in some early specimens and the need for a relatively severe heat treatment to restore ductility in the material. Since EF nickel-manganese exhibits better retention of high mechanical strength at high temperatures than EF nickel-cobalt, it was logical to examine and compare these properties at lower temperatures after development of a suitable heat treatment and an optimum manganese content in the alloy.

From the work reported in the literature survey and critique it appeared that certain ranges for EF nickel-manganese bath operating parameters were well established and needed no further development; effects derived from pulse plating needed more attention. A limited amount of work with this method of deposition had shown mechanical property improvements which were not completely defined.

The purpose of pulse plating in this program was to more effectively distribute the manganese distribution in the nickel deposit for strengthening and possibly to reduce the heat treatment temperatures and times required to produce acceptable ductility. In pulse plating there is a high frequency interruption of the current. At each pulse, the voltage - and current - is ramped upwards to a peak value. It is held at this approximate value for a finite time. If there is no superimposed pulse or conventional direct current and periodic current reversal is not being used, the voltage is usually

dropped to zero, and the next pulse is initiated. During the voltage climb chemical reduction reactions take place at the cathode (part being electroformed).

These reactions can vary based on the instantaneous potential and the chemical species available in the zone where reduction occurs. During the near constant portion of the pulse peak, a steady state reaction is occurring as long as all species of ions are present in constant concentrations. As one species is depleted, the alloy composition starts to change. When the voltage is returned to zero, or a potential below the overvoltage required for reduction of the metallic ion species in the electrolyte, chemical diffusion then replenishes the ion concentrations depleted by the current pulse.

3.3.2 Electroforming Facilities, Mandrels, and Solution Maintenance

A 162 liter (42 gallon) plating bath was established for electroforming flat plates of nickel-manganese alloy for testing mechanical properties at ambient and elevate temperatures, before and after heat treatment. Later in the Phase A portion of the program a second facility of identical size was brought into use to increase rates at which specimens could be electroformed under various deposition parameters and manganese concentrations. During this study the alloy plating baths were maintained at compositions in the ranges of 74 to 80 g/l (as metal) of nickel, 30 to 35 g/l of boric acid, and a pH of 3.9 to 4.5. The concentration of manganese was varied intentionally and the values will be mentioned as appropriate in the following discussions. Manganese ions were introduced to the electrolytes as manganous sulfamate. Manganous sulfamate was prepared by mixing molar equivalent amounts of manganous carbonate and sulfamic acid in demineralized water. Mixing was done very slowly as the reaction was exothermic. There was a tendency for some manganese oxides to precipitate to leave the resulting solution acidic from excess sulfamic acid. The resulting solution was filtered to leave a slightly pink colored liquid typical for manganous ion. Analysis for manganese concentration was by means of atomic absorption spectroscopy.

Figure 3.3-1 is a schematic of the facility for specimen electroforming. In the initial studies the specimen mandrels (cathodes) were fixed at stationary positions and solution agitation was obtained entirely by pumped electrolyte flow through 10 micron nominal wound cartridge filters. The filtered solution impinged on the cathode normal to the plane being electroformed. The spray pattern for the electrolyte onto the cathode surface was obtained by means of polyvinyl chloride nozzles. These were available in round cone, square pyramidal, narrow wedge and narrow stream configurations of spray patterns. The pyramidal pattern was used to provide best coverage of the rectangular mandrels used as cathodes in this part of the program. Nozzle openings were kept at a sufficient distance from the part being electroformed so as to assure that general solution movement and displacement was occurring rather than highly localized turbulence which might affect diffusion layer thickness in a non-uniform manner. There was considerable concern over this because the thickness of the diffusion layer resulting from electrolyte agitation has a profound influence on diffusion of ion species into the area where

reduction and deposition takes place - in other words, the rate at which the chemical equilibrium is restored as various ions are consumed in the plating process.

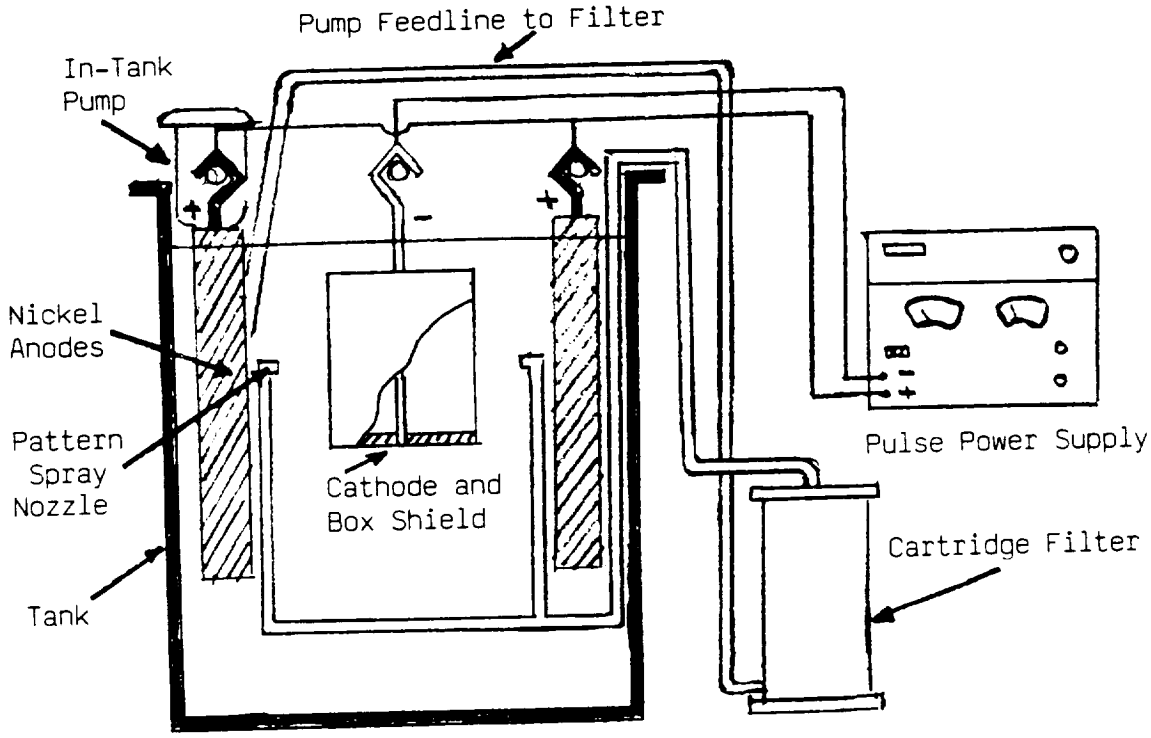

Figure 3.3-1. Schematic Illustration of Flat Specimen Deposition Facility

The mandrels on which alloy deposits were electroformed were stainless steel plate stock, 300 series. The passive surface of stainless steel permitted easy separation of specimens. It was not necessary to dichromate passivate the mandrel surfaces. Both sides of the stainless steel plate were electroformed to produce an adequate amount of material for tensile specimen milling for a variety of tests. This required that the anode to cathode spacings on each side parallel to the mandrel be very accurately equal to assure that one plate surface would not receive a higher current density, and greater thickness than the other. In actual experience it was found that most plates from the same electroforming cycle were within five percent of each other in thickness. Deposit thickness from panel center to various corners and edges generally varied no more than four percent in thicknesses of 0.127 cm (0.050 in.) or more. This control was a result of using "box shields" around the mandrel to obtain reasonably uniform current density. These "box shields" were made from polyvinyl chloride (PVC) thick sheet stock and slotted in a manner that would seal all mandrel edges and shade additional edge of the cathode from full current density. This led to a taper of the deposit to a knife-edge for a distance of about 0.3175 cm (0.125 in.) around all edges. This also eliminated nodules. Figure 3.3-2 shows a typical cathode mandrel installed in a PVC box shield.

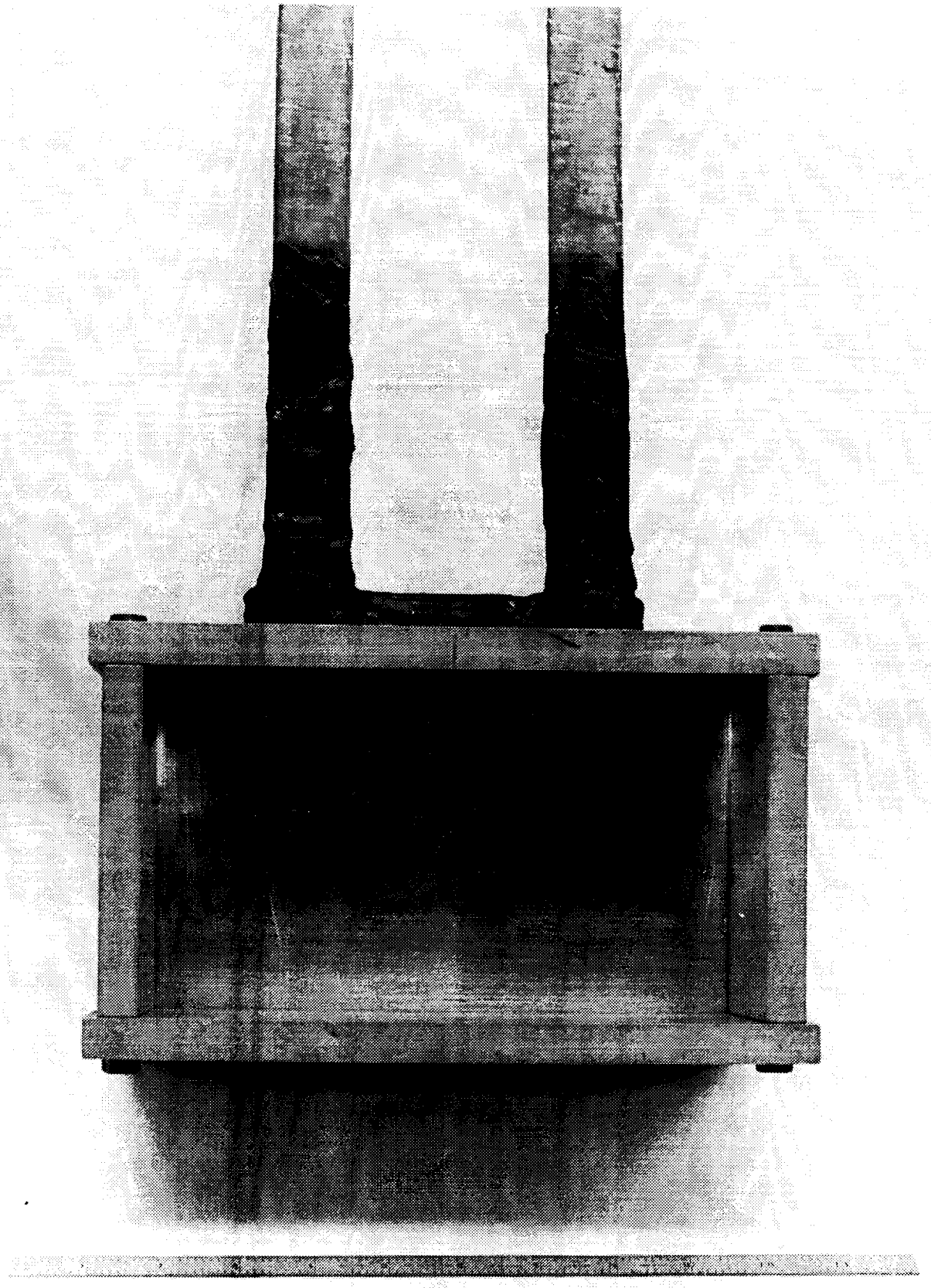

Figure 3.3-2. A Typical Stainless Steel Cathode Mandrel Installed in a PVC Box Shield Fixture

Periodic electrolyte purification by hydrogen peroxide additions and carbon treatment was performed based on ductility results from mechanical tests following heat treatment of deposits. The procedure for the purification of baths was as follows:

1. Remove all metal components such as anodes and anode baskets from the bath to prevent accelerated decomposition of peroxide.

2. Lower the bath temperature to 37.8°C (100°F), or lower, and add about 473 ml of 30 percent hydrogen peroxide to each 378.5 liters (100 gal) of solution being purified. Thoroughly mix to assure complete reaction. Allow the solution to react for about four hours or overnight.

3. Heat the reacted solution to 62.8°C (145°F) and hold at this temperature for one hour to drive off excess hydrogen peroxide.

4. While the solution is cooling, pump it through a carbon pack followed by a filter and back into the original tank. Recirculate the solution in this manner until it cools to 37.8°C (100°F). Hold at this temperature and continue recirculating through the carbon pack overnight. Discard the carbon pack, change the filters, add fresh wetting agent to the bath, and heat the solution to the desired operating temperature.

It was desired that a second electroformable alloy other than conventional nickel-cobalt be examined as an alternate to nickel-manganese should mechanical property data for the latter prove unsuitable for SSME structural applications. At the time this work was undertaken Bell Aerospace Textron was investigating electroformed ternary alloys of the nickel-cobalt-manganese system. Data from this independent research and development project could be made available with no cost or schedule impact on the nickel-manganese program.

Nickel-cobalt-manganese alloy deposition is considerably more complicated than is the case for nickel-manganese. Manganese is controlled in the ternary alloy by simple additions of manganous sulfamate based on instrumental analytical results. As mentioned in the literature review section, nickel-cobalt deposition is of the anomalous type - that is the less noble metal (cobalt) tends to plate out preferentially. As a result, those factors influencing transfer of cobalt ions into the diffusion layer at the cathode where metal reduction is started become critical with regard to the alloy composition in general and to the localized variations of nickel and cobalt ratios from a crystalline lattice plane standpoint. Several methods have been utilized to control cobalt and nickel concentrations in the electrolyte. Rocketdyne has used two separate power supplies to independently control nickel and cobalt anodes by imposing different ampere totals on each anode array. For an electroformed alloy which met all elevated temperature expectations for SSME applications, the concept of independent power source control for cobalt and nickel anodes would be practical with pulse plating. This is possible with the commercial availability of a device which will synchronize two pulse platers for pulse cycle and duration while permitting independent amperage regulation of each supply.

Bell Aerospace Textron has preferred to use a single pulse plating power supply coupled to a periodic reversing unit as shown in Figure 3.3-3. The advantage of such a system will become apparent later in this report as the complications afforded by complex shapes becomes evident.

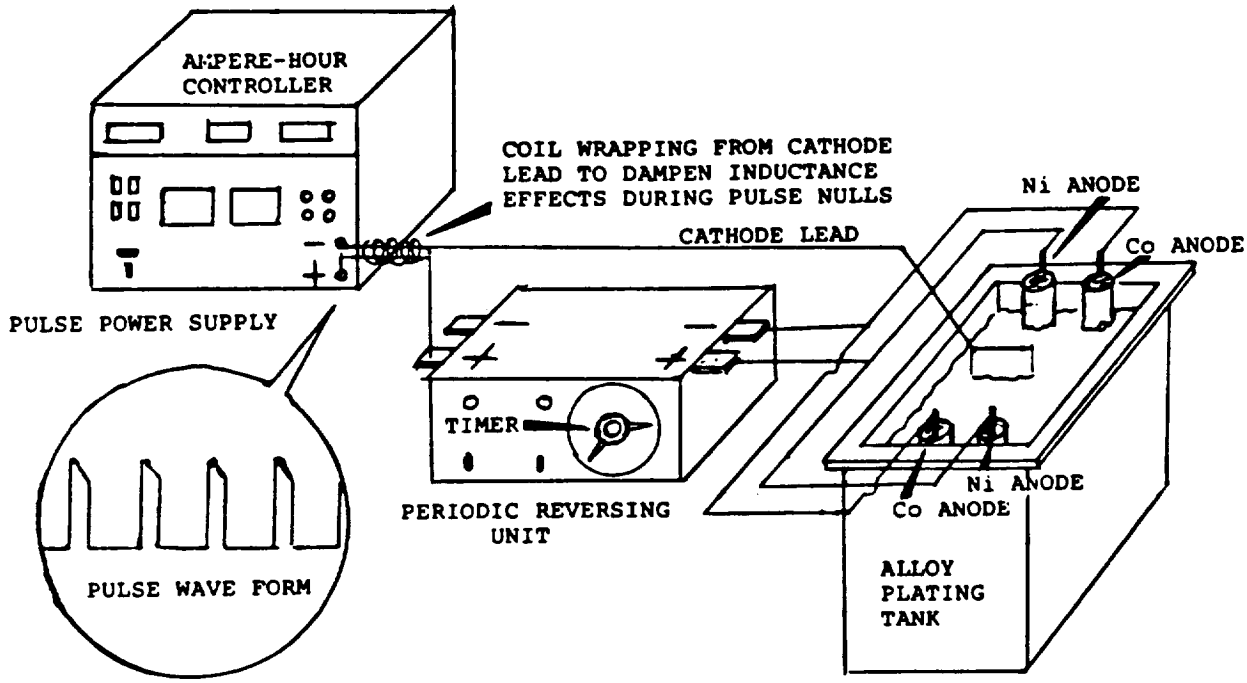

Figure 3.3-3. Diagram of Equipment Arrangment for Pulse Plating Nickel-Cobalt Alloys

Figure 3.3-4 shows the physical layout of the equipment used by Bell Aerospace Textron for nickel-cobalt-manganese electroforming. In this system the pulse plating power supply feeds a pulse of a prescribed frequency and duty cycle to the anode terminal of a periodic reverse plating unit. The negative connection from the pulse plating power supply is directly to the cathode (workpiece). Since there is no cathodic input to the periodic reversing unit, both output terminals become anodic to feed the anode arrays as the timed reversing cycle dictates. One anodic output feeds current to the nickel anode array while the other feeds the cobalt anode array. By adjusting the two-way timer on the periodic reversing unit it was found possible to set a current flow time to nickel anodes while adjusting a different time for the reverse cycle of the timer for current flow to the cobalt anodes. This would provide a precisely controlled current flow to the nickel anodes and to the cobalt anodes to afford an accurate measure of nickel and cobalt ions generated into the electrolyte.

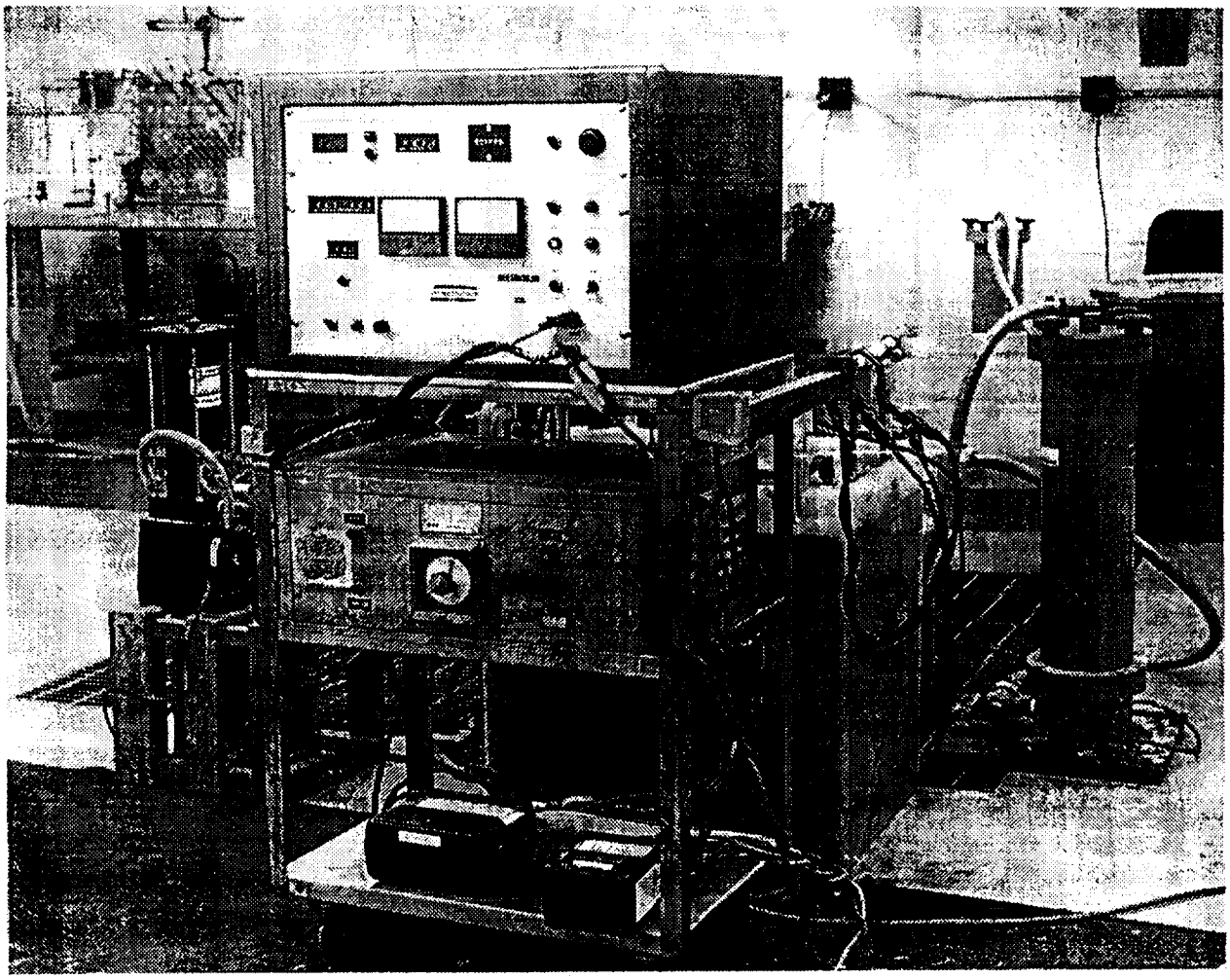

Figure 3.3-4. Facility for Pulse-Periodic Current Shift for Nickel-Cobalt-Manganese Electroforming

By timing the flow of current to each type of metal anode, and repetitively alternating the flow from one type to the other, it was found possible to closely control the metal composition of the electrolyte to produce an electroform having a cobalt content proportionally equal to the fraction of total current passing through the cobalt anodes. As a result, the bath proved to be compositionally self-adjusting. Frequent chemical analyses were not needed.

3.3.3 Optimization of Manganese Alloying Parameters

This effort was devoted to optimizing deposition parameters for making the best combinations of mechanical strength and ductility in the alloys over a temperature range from ambient to 538°C (1000°F) with emphasis on the lower half of this span. Extra specimens of electroformed alloys from previous years of research and development investigations were available for testing in this part of the program. General and moderate heat treatments were used in

this evaluation with the understanding that the finally formulated heat treatment cycle would be dependent on the optimum alloy composition and response to such thermal treatments.

From data and discussions in the literature review, it was established that some form of heat treatment would be required to obtain minimal needed ductility in the alloy deposits. This is true for most electrodeposited alloys based on metals of the iron group which are generally highly stressed and contain significant hydrogen. In the initial portion of this investigation the heat treatment temperature and cycle duration was not established for optimizing electroformed alloys to be used in the SSME shroud application. Therefore, several treatments were applied to provide a better insight as to how the particular alloy specimen might respond once an optimum treatment was selected. As a guide in selecting optimum alloy performance, post heat treatment mechanical properties of about 1400 MPa (200 ksi) for ultimate strength, 1000 MPa (145 ksi) for yield strength, and 10 percent minimum elongation in 2.5 cm (2 in.) were sought.

Where electroformed structures contain internal passages, it is required that the channel be filled with a material which can be made conductive for the electrodeposit close-out and then be removed after fabrication. Waxes are the most commonly used fillers. The temperature range at which such waxes are dimensionally stable places restraints on the temperatures at which the alloy electrolyte can be operated. Since the electroformed alloy in this study is to be applied to a shroud structure (jacket) for the MCC, there will be no wax fillers present. This permits electrolyte temperatures outside of the 48^{o} to 50^{o}C region to be used. However, there are expected to be applications of the EF alloy which might require application over waxes - an example might be in close-out of the regeneratively cooled thrust chamber on the future versions of the SSME or other engines. With this possibility in mind, efforts were concentrated on establishing optimum deposition parameters based on an electrolyte used at a universally acceptable temperature.

Initial studies were conducted using an electrolyte containing about 3 grams per liter of manganous ion. In this series of specimens no stress reducing agent (SNHA) was added to the solution. Table 3.3-1 provides all pertinent fabrication and test data for the first group of specimens deposited at average current densities of 2.15 A/dm^2 and fairly short pulse durations (less than five milliseconds). A second group was electroformed under very similar conditions, except that the average current densities were raised to 3.23 A/dm^2. Pulse plating duty cycle was defined as the pulse "on time" divided by the total pulse time (the "on time" plus the "off time"). A duty cycle of 100% means that the electroforming current was not being pulsed. With the exception of temperatures of 427^{o}C, or higher, all post electroform heat treatment cycles were considered moderate for SSME use. Since nickel based deposits tend to be fine-grained and exhibit localized elongation, the ductility has been measured in 2.54 cm and 5.08 cm gauge lengths. The shorter gauge length provides a better insight as to the ability of the deposit to elongate under plastic deformation.

TABLE 3.3-1. FABRICATION AND MECHANICAL PROPERTY TEST DATA FOR ELECTROFORMED NICKEL-MANGANESE ALLOYS FROM 48°-49°c ELECTROLYTES CONTAINING 3 G/L MANGANESE

Group 1 - 2.15 A/dm^2 Average Current Density, No Stress Reducer

Sample Number	Pulse Plating Information	Bath and Alloy Analytical Data	Test No.	Heat Treatment	Test Temp. (°C)	Mechanical Properties: Ultimate MPa	Ultimate Ksi	Yield MPa	Yield Ksi	Elongation, % in: 2.54 cm	Elongation, % in: 5.08 cm
NM-12	Duty Cycle 100%	Ni Metal 76.1 g/l	A	None	Room	1092	158	819	119	7	4
	Pulse On	Mn Metal 3.0 g/l	B	316°C(24 Hr)	Room	1080	159	958	139	Not Deter.	5
	Pulse Off	Boric Acid 33.3 g/l	C								
	Peak CD 2.15 A/dm^2	SNHA 0 ml/l	D								
	Avg. CD 2.15 A/dm^2	Acidity(pH) 4.36	E								
	Avg. Volts 3.9	Temp 48.3 °C	F	538°C(2 Hr)	Room	862	125	764	111	Not Deter.	7
		Alloy Mn 0.23 %	G	204°C(72 Hr)	Room	1166	169	973	141	Not Deter.	5.5
		Alloy S 14 PPM	H								
NM-13	Duty Cycle 50%	Ni Metal 76.8 g/l	A	None	Room	1133	164	852	124	16	7
	Pulse On 1.0 msec	Mn Metal 2.9 g/l	B	316°C(24 Hr)	Room	1081	157	951	138	Not Deter.	5
	Pulse Off 1.0 msec	Boric Acid 33.3 g/l	C								
	Peak CD 4.30 A/dm^2	SNHA 0 ml/l	D								
	Avg. CD 2.15 A/dm^2	Acidity(pH) 4.13	E								
	Avg. Volts 3.9	Temp 48.3 °C	F	538°C(2 Hr)	Room	850	123	756	110	Not Deter.	7
		Alloy Mn 0.19 %	G	204°C(72 Hr)	Room	1077	156	874	127	Not Deter.	6
		Alloy S 19 PPM	H								
NM-14	Duty Cycle 25%	Ni Metal 77.1 g/l	A	None	Room	1031	150	705	102	14	8.5
	Pulse On 1.0 msec	Mn Metal 2.9 g/l	B	204°C	Room	1023	148	795	115	14	9.5
	Pulse Off 3.0 msec	Boric Acid 32.8 g/l	C	316°C(24 Hr)	Room	1067	155	859	125	14	8
	Peak CD 8.61 A/dm^2	SNHA 0 ml/l	D	427°C(4 Hr)	Room	920	133	788	114	16	9
	Avg. CD 2.15 A/dm^2	Acidity(pH) 4.30	E								
	Avg. Volts 3.8	Temp 48.9 °C	F								
		Alloy Mn 0.21 %	G								
		Alloy S 42 PPM	H								

Group 2 - 3.23 A/dm^2 Average Current Density, No Stress Reducer

Sample Number	Pulse Plating Information	Bath and Alloy Analytical Data	Test No.	Heat Treatment	Test Temp. (°C)	Mechanical Properties: Ultimate MPa	Ultimate Ksi	Yield MPa	Yield Ksi	Elongation, % in: 2.54 cm	Elongation, % in: 5.08 cm
NM-15	Duty Cycle 100%	Ni Metal 76.9 g/l	A	None	Room	Specimen broke in machining.					
	Pulse On	Mn Metal 2.9 g/l	B	204°C(72 Hr)	Room	1431	207	1180	171	8	4
	Pulse Off	Boric Acid 32.9 g/l	C	316°C(24 Hr)	Room	1260	183	1079	157	10	5
	Peak CD 3.23 A/dm^2	SNHA 0 ml/l	D	427°C(4 Hr)	Room	1317	191	1160	168	10	5
	Avg. CD 3.23 A/dm^2	Acidity(pH) 4.30	E	316°C(24 Hr)	149	1329	193	889	129	10	6
	Avg. Volts 5.6	Temp 48.1 °C	F	316°C(24 Hr)	260	1136	165	815	118	14.5	8.9
		Alloy Mn 0.66 %	G	343°C(24 Hr)	149	1186	172	1001	145	8.5	4.5
		Alloy S 25 PPM	H	343°C(24 Hr)	260	996	145	760	110	10	6.5
NM-16	Duty Cycle 50%	Ni Metal 75.6 g/l	A	None	Room	Specimen broke in machining.					
	Pulse On 1.0 msec	Mn Metal 2.9 g/l	B	204°C(72 Hr)	Room	1149	167	914	133	11	7
	Pulse Off 1.0 msec	Boric Acid 32.2 g/l	C	316°C(24 Hr)	Room	1369	199	1178	171	Broke out of gauge.	
	Peak CD 6.46 A/dm^2	SNHA 0 ml/l	D	427°C(4 Hr)	Room	1180	171	1024	149	10	6
	Avg. CD 3.23 A/dm^2	Acidity(pH) 4.28	E	316°C(24 Hr)	149	1156	168	935	136	9.5	5
	Avg. Volts 5.5	Temp 49.4 °C	F	316°C(24 Hr)	260	1049	152	794	115	13	6.8
		Alloy Mn 0.49 %	G	343°C(24 Hr)	149	1070	155	929	135	7	2
		Alloy S 15 PPM	H	343°C(24 Hr)	260	869	126	687	100	11	6
NM-17	Duty Cycle 25%	Ni Metal 75.4 g/l	A	None	Room	1210	175	861	125	10	7
	Pulse On 1.0 msec	Mn Metal 2.9 g/l	B	204°C(72 Hr)	Room	1218	177	806	117	8	6.5
	Pulse Off 3.0 msec	Boric Acid 31.9 g/l	C	316°C(24 Hr)	Room	1159	168	905	131	14	8.5
	Peak CD 12.91 A/dm^2	SNHA 0 ml/l	D	427°C(4 Hr)	Room	976	142	826	120	14	8.5
	Avg. CD 3.23 A/dm^2	Acidity(pH) 4.18	E	316°C(24 Hr)	149	925	134	725	105	12	6.5
	Avg. Volts 5.3	Temp 49.4 °C	F	316°C(24 Hr)	260	853	124	604	88	16.3	11.5
		Alloy Mn 0.26 %	G								
		Alloy S 52 PPM	H								

A comparison of mechanical property test results for Group 1 and Group 2 specimens indicated that higher mechanical strength was obtained in the latter series where the average current density was higher. The Group 1 specimens did not show significant differences in manganese content for the pulse and non-pulse plating conditions employed. Group 2 samples showed varied contents of manganese ranging from high in the non-pulsed alloy to low in the lowest pulse duty cycle specimen. This was unexpected on the basis that the high peak current densities obtained with low duty cycle conditions were previously found to promote higher manganese contents in the deposits. The fact that the manganese content of alloy from specimen NM-17 was less than that of NM-16, and NM-16 was less than NM-15 would indicate that diffusion of manganese ion at the cathode surface is not a composition controlling factor - or, the pulse on/off times were too short in duration for effective diffusion to occur.

All specimens in Groups 1 and 2 had mechanical properties far superior to those of conventionally electroformed nickel. Post heat treatment mechanical strength of test strips from Specimens NM-12 through 14 did not sufficiently approach the 1400 MPa being sought in competition to Inconel 718, so no tests at elevated temperature were conducted. Specimens NM-15 and 16 exhibited promising ultimate strengths and mechanical properties were evaluated at 149°C (300°F) and 260°C(500°F). Although this material mights have been considered acceptable for the MCC shroud application, further improvements through variation of other parameters were deemed possible.

A third group of electroformed alloy specimens was prepared from the same electrolyte as was used for Groups 1 and 2, but the bath temperature was increased to 55.6°C in anticipation that ductility improvements might be obtained. Consumed manganous ion was replaced by bath additions resulting in slightly more manganese than was planned, 3.2 g/l rather than 3.0 g/l. Fabrication and test data for these Group 3 specimens are shown in Table 3.3-2.

Increasing the electrolyte temperature would be expected to improve diffusivity through the liquid layer immediately adjacent to the cathode and result in higher concentrations of manganese in the electroformed alloy if manganous ion transport phenomena governed the reduction reactions which determined deposit composition. A comparison of alloy composition results for Group 2 and Group 3 specimens shows this is not the case. Test data for these two groups indicate that increasing bath temperature, while keeping other parameters the same, results in a lower manganese content in the alloy and generally inferior mechanical properties - with the exception of a small improvement in ductility. If increased electrolyte temperature becomes a necessity in producing an optimum structural alloy, it is apparent that other changes will also be needed to maintain or improve strength. Such changes might include increasing the bath manganous ion concentration or increasing the average current density.

TABLE 3.3-2. FABRICATION AND MECHANICAL PROPERTY TEST DATA FOR ELECTROFORMED NICKEL-MANGANESE ALLOYS FROM 55.6° ELECTROLYTES CONTAINING 3.2 G/L MN ION

Group 3 - 3.23 A/dm^2 Average Current Density, 55.6° Bath, No Stress Reducer

Sample Number	Pulse Plating Information	Bath and Alloy Analytical Data	Test No.	Heat Treatment	Test Temp. (°C)	Mechanical Properties: Ultimate MPa	Ultimate Ksi	Yield MPa	Yield Ksi	Elongation, % in: 2.54 cm	Elongation, % in: 5.08 cm
NM-18	Duty Cycle 100%	Ni Metal 75.9 g/l	A	None	Room	Specimen broke in machining.					
	Pulse On	Mn Metal 3.2 g/l	B	204°C(72 Hr)	Room	Specimen broke in machining.					
	Pulse Off	Boric Acid 31.1 g/l	C	316°C(24 Hr)	Room	Specimen broke in machining.					
	Peak CD 3.23 A/dm^2	SNHA 0 ml/l	D	427°C(4 Hr)	Room	Specimen broke in machining.					
	Avg. CD 3.23 A/dm^2	Acidity(pH) 4.30	E	316°C(24 Hr)	149	1089	158	874	127	14	9
	Avg. Volts 5.1	Temp 55.6°C	F	316°C(24 Hr)	260	974	141	682	99	19	11
		Alloy Mn 0.33%	G	260°C(72 Hr)	149	1172	170	918	133	10.5	6
		Alloy S 11 PPM	H	260°C(72 Hr)	260	992	144	722	105	12.3	6.3
NM-19	Duty Cycle 50%	Ni Metal 76.3 g/l	A	None	Room	1167	169	827	120	BOG*	4.6
	Pulse On 1.0 msec	Mn Metal 3.2 g/l	B	204°C(72 Hr)	Room	1168	169	957	139	BOG*	
	Pulse Off 1.0 msec	Boric Acid 32.1 g/l	C	316°C(24 Hr)	Room	Specimen broke in machining.					
	Peak CD 6.46 A/dm^2	SNHA 0 ml/l	D	427°C(4 Hr)	Room	Specimen broke in machining.					
	Avg. CD 3.23 A/dm^2	Acidity(pH) 4.20	E	316°C(24 Hr)	149	988	143	784	114	13	8
	Avg. Volts 5.1	Temp 55.6°C	F	316°C(24 Hr)	260	903	131	647	94	15	10
		Alloy Mn 0.25%	G	260°C(72 Hr)	149	1083	157	798	116	9	5
		Alloy S 9 PPM	H	260°C(72 Hr)	260	915	133	657	95	18.4	12.2
NM-20	Duty Cycle 25%	Ni Metal 74.9 g/l	A	None	Room	1023	148	689	100	12.5	8.1
	Pulse On 1.0 msec	Mn Metal 3.2 g/l	B	204°C(72 Hr)	Room	1076	156	818	119	BOG*	
	Pulse Off 3.0 msec	Boric Acid 31.9 g/l	C	316°C(24 Hr)	Room	Specimen broke in machining.					
	Peak CD 12.91A/dm^2	SNHA 0 ml/l	D	427°C(4 Hr)	Room	1068	155	883	128	BOG*	5.2
	Avg. CD 3.23A/dm^2	Acidity(pH) 4.20	E	316°C(24 Hr)	149	990	144	760	110	15	8
	Avg. Volts 5.0	Temp 55.6°C	F	316°C(24 Hr)	260	838	122	553	80	18	9.5
		Alloy Mn 0.17%	G								
		Alloy S 20 PPM	H								

Before increasing the electrolyte manganese content to a significantly higher level, an evaluation of formal temperature (48° - 49°C) baths was made using pulse duty cycles with much longer off times compared to on times. From the results show in Table 3.3-3 for these Group 4 specimens it was noted that more manganese was incorporated in the deposit with the lower peak current density (Specimen NM-21) than in the one with the higher peak current density (NM-22) - even though each sample was pulse electroformed with the same duty cycle. It is noted that material from Specimen NM-22 had much better mechanical strength than that from NM-21, although the latter contained more manganese in the alloy. This might support a theory that the amount of manganese present is not as critical as the manner in which it is combined with nickel in a stoichiometric ratio from the aspect of lattice cell structure.

TABLE 3.3-3. FABRICATION AND MECHANICAL PROPERTY TEST DATA FOR ELECTROFORMED NICKEL-MANGANESE FROM 49°C ELECTROLYTES CONTAINING 3.35 G/L MANGANESE AND PULSE PLATED AT LOW DUTY CYCLES

Group 4 - Various Average Current Densities, 49°C Bath, Low Duty Cycles

Sample Number	Pulse Plating Information	Bath and Alloy Analytical Data	Test No.	Heat Treatment	Test Temp. (°C)	Mechanical Properties: Ultimate MPa	Ultimate Ksi	Yield MPa	Yield Ksi	Elongation, % in: 2.54 cm	Elongation, % in: 5.08 cm
NM-21	Duty Cycle 12.5%	Ni Metal 74.1 g/l	A	None	Room	931	135	611	89	BOG*	10
	Pulse On 1.0 msec	Mn Metal 3.35g/l	B	204°C(72 Hr)	Room	932	135	708	103	BOG*	7.8
	Pulse Off 7.0 msec	Boric Acid 31.9g/l	C	316°C(24 Hr)	Room	803	116	622	90	Not Deter.	12
	Peak CD 8.61 A/dm^2	SNHA 0 ml/l	D	427°C(4 Hr)	Room	556	81	417	61	BOG*	27.8
	Avg. CD 1.08 A/dm^2	Acidity(pH) 4.35	E	316°C(24 Hr)	149	633	92	461	67	21	13
	Avg. Volts 2.2	Temp 49.4°C	F	316°C(24 Hr)	260	579	84	395	57	20	11
		Alloy Mn 0.18%	G								
		Alloy S 10 PPM	H								
NM-22	Duty Cycle 12.5%	Ni Metal 74.1 g/l	A	None	Room	1265	183	991	144	5.6	2.6
	Pulse On 1.0 msec	Mn Metal 3.35g/l	B	204°C(72 Hr)	Room	1260	183	901	131	7.5	6.5
	Pulse Off 7.0 msec	Boric Acid 32.1g/l	C	316°C(24 Hr)	Room	1161	168	845	123	15	8.5
	Peak CD 17.22 A/dm^2	SNHA 0 ml/l	D	427°C(4 Hr)	Room	981	142	787	114	BOG*	9.2
	Avg. CD 2.15 A/dm^2	Acidity(pH) 4.47	E	316°C(24 Hr)	149	990	144	714	104	11	6.5
	Avg. Volts 3.7	Temp 49.4°C	F	316°C(24 Hr)	260	819	119	573	83	21	12
		Alloy Mn 0.10%	G								
		Alloy S 8 PPM	H								

*BOG = Broke out of gauge

In electroforming Group 5 specimens, the manganese metal content of the electrolyte was increased to 4.75 g/l and two different average current densities were used for a common pulse duty cycle. No significant improvements in mechanical properties were noted as can be determined from test data in Table 3.3-4. It was noted that the specimen (NM-24) deposited using the higher average current density contained more manganese than NM-23 deposited at the lower average current density. This was contrary to the findings on the Group 4 specimens and is unexplained. It is interesting to note that Specimen NM-14 of Group 1 has a comparable content of manganese to that found in Specimen NM-24, yet the manganese content of the bath from which the latter was deposited contained 60 percent more manganese than the solution used for Group 1 electrodeposition. This indicates that the manganese concentration in the bath, or at least some amount beyond a baseline concentration requirement, may not be of significant influence on the resulting alloy composition and performance as long as other parameters are constant.

The next series of specimens, Group 6, was produced using the higher manganese concentrations in the electrolyte in combination with longer pulse on an off times. Fabrication and mechanical property test data for this series are shown in Table 3.3-5. All specimens exhibited high ultimate and yield strengths. Those samples pulse deposited at duty cycles of 50 percent or higher had significantly better elongation values in 2.54 cm gauge lengths than those pulsed at duty cycles less than 50 percent. Specimens NM-25 and NM-28 had very good combinations of mechanical strength and ductility as

TABLE 3.3-4. FABRICATION AND MECHANICAL PROPERTY TEST DATA FOR ELECTROFORMED NICKEL-MANGANESE FROM 49°C ELECTROLYTES CONTAINING 4.75 G/L MANGANESE AND PULSE PLATED AT LOW DUTY CYCLES

Group 5 - Various Average Current Densities, 49°C Bath, Low Duty Cycles

Sample Number	Pulse Plating Information	Bath and Alloy Analytical Data	Test No.	Heat Treatment	Test Temp. (°C)	Mechanical Properties: Ultimate MPa	Ultimate Ksi	Yield MPa	Yield Ksi	Elongation, % in: 2.54 cm	Elongation, % in: 5.08 cm
NM-23	Duty Cycle 20%	Ni Metal 76.9 g/l	A	None	Room	1068	155	749	109	9	5.5
	Pulse On 1.0 msec	Mn Metal 4.75 g/l	B	316°C(24 Hr)	Room	1037	150	813	118	10	5.5
	Pulse Off 4.0 msec	Boric Acid 31.9 g/l	C	343°C(24 Hr)	Room	929	135	783	113	11	6.5
	Peak CD 12.91 A/dm^2	SNHA 0 ml/l	D	427°C(4 Hr)	Room	809	117	643	93	20	13
	Avg. CD 2.58 A/dm^2	Acidity(pH) 4.13	E								
	Avg. Volts 4.4	Temp 49.4 °C	F								
		Alloy Mn 0.10 %	G								
		Alloy S 10 PPM	H								
NM-24	Duty Cycle 20%	Ni Metal 79.2 g/l	A	None	Room	1153	167	828	120	8	5.5
	Pulse On 1.0 msec	Mn Metal 4.8 g/l	B	316°C(24 Hr)	Room	1187	172	954	138	11	5.5
	Pulse Off 3.0 msec	Boric Acid 33.0 g/l	C	343°C(24 Hr)	Room	1158	168	1001	145	9	5.5
	Peak CD 12.91 A/dm^2	SNHA 0 ml/l	D	427°C(4 Hr)	Room	1083	157	879	127	10	7
	Avg. CD 3.23 A/dm^2	Acidity(pH) 4.13	E	260°C(72 Hr)	149	981	142	772	112	9.5	4
	Avg. Volts 4.2	Temp 49.4 °C	F	260°C(72 Hr)	260	835	121	608	88	10	6.8
		Alloy Mn 0.20 %	G	343°C(24 Hr)	149	897	130	692	100	10	6
		Alloy S 30 PPM	H	343°C(24 Hr)	260	812	118	600	87	16	9

TABLE 3.3-5. FABRICATION AND MECHANICAL PROPERTY TEST DATA FOR ELECTROFORMED NICKEL-MANGANESE FROM 48° - 49°C ELECTROLYTES CONTAINING 4.2-4.7 G/L MANGANESE AND PULSE PLATED WITH LONG DURATION PULSE CYCLES

Group 6 - 2.15 A/dm^2 Average Current Density, Various Long Pulse Cycles

Sample Number	Pulse Plating Information	Bath and Alloy Analytical Data	Test No.	Heat Treatment	Test Temp. (°C)	Mechanical Properties: Ultimate MPa	Ultimate Ksi	Yield MPa	Yield Ksi	Elongation, % in: 2.54 cm	Elongation, % in: 5.08 cm
NM-25	Duty Cycle 50%	Ni Metal 78.9 g/l	A	None	Room	1255	182	940	136	10	6
	Pulse On 20 msec	Mn Metal 4.65 g/l	B	316°C(24 Hr)	Room	1288	187	1077	156	10	5.5
	Pulse Off 20 msec	Boric Acid 32.9 g/l	C	343°C(24 Hr)	Room	1280	186	1096	159	11	5
	Peak CD 4.30 A/dm^2	SNHA 0 ml/l	D	427°C(4 Hr)	Room	1228	178	1096	159	10	6
	Avg. CD 2.15 A/dm^2	Acidity(pH) 4.08	E	260°C(72 Hr)	149	1102	160	883	128	10	7
	Avg. Volts 3.9	Temp 48.9 °C	F	260°C(72 Hr)	260	953	138	696	101	11	6.7
		Alloy Mn 0.36 %	G	343°C(24 Hr)	149	1160	168	932	135	6	4
		Alloy S 24 PPM	H	343°C(24 Hr)	260	944	137	738	107	11	6
NM-26	Duty Cycle 40%	Ni Metal 78.9 g/l	A	None	Room	1460	212	1050	152	5	3
	Pulse On 20 msec	Mn Metal 4.45 g/l	B	316°C(24 Hr)	Room	1558	226	1369	198	8	4.5
	Pulse Off 30 msec	Boric Acid 32.7 g/l	C	343°C(24 Hr)	Room	1556	226	1393	202	7.5	4
	Peak CD 5.38 A/dm^2	SNHA 0 ml/l	D	427°C(4 Hr)	Room	1481	215	1364	198	7	4
	Avg. CD 2.15 A/dm^2	Acidity(pH) 4.16	E	371°C(24 Hr)	Room	1316	191	1128	164	19.5	5.8
	Avg. Volts 3.9	Temp 48.3 °C	F	371°C(24 Hr)	149	1242	180	973	141	6	3.5
		Alloy Mn 0.51 %	G	371°C(24 Hr)	260	1159	168	877	127	9	6
		Alloy S 32 PPM	H								
NM-27	Duty Cycle 25%	Ni Metal 79.2 g/l	A	None	Room	1665	241	1225	178	Broke out of gauge.	
	Pulse On 10 msec	Mn Metal 4.25 g/l	B	316°C(24 Hr)	Room	2018	293	1669	242	4.5	3.5
	Pulse Off 30 msec	Boric Acid 32.8 g/l	C	343°C(24 Hr)	Room	1944	282	1775	257	6	3.5
	Peak CD 8.61 A/dm^2	SNHA 0 ml/l	D	427°C(4 Hr)	Room	1836	266	1496	217	6	4
	Avg. CD 2.15 A/dm^2	Acidity(pH) 4.29	E	371°C(24 Hr)	Room	1627	236	1433	208	5.8	3.8
	Avg. Volts 3.8	Temp 48.6 °C	F	371°C(24 Hr)	149	1379	200	1088	158	Broke out of gauge.	
		Alloy Mn 0.50 %	G	371°C(24 Hr)	260	Specimen broke in machining.					
		Alloy S 49 PPM	H								
NM-28	Duty Cycle 60%	Ni Metal 78.3 g/l	A	None	Room	1200	174	830	120	9	6
	Pulse On 30 msec	Mn Metal 4.2 g/l	B	316°C(24 Hr)	Room	1239	180	1119	162	10	5.5
	Pulse Off 20 msec	Boric Acid 33.0 g/l	C	343°C(24 Hr)	Room	1282	186	1121	163	10	6
	Peak CD 3.57 A/dm^2	SNHA 0 ml/l	D	427°C(4 Hr)	Room	1170	170	1011	147	14	8
	Avg. CD 2.15 A/dm^2	Acidity(pH) 4.13	E								
	Avg. Volts 3.9	Temp 48.3 °C	F								
		Alloy Mn 0.39 %	G								
		Alloy S 10 PPM	H								

deposited, after various moderate heat treatments, and at the desired elevated test temperatures of 149°C and 260°C. From the Group 6 specimen data it will be noted that all of the post electroforming heat treatments resulted in significant increases in ultimate and yield strengths - particularly in the latter. Such changes had also been observed in specimens from prior series but not to this extent. This phenomenon might be considered analogous to age-hardening experienced in some wrought metal alloys where specific thermal cycling causes precipitations or phase separations resulting in strengthening.

It is appropriate at this point to discuss sulfur as a trace impurity in the alloy deposits. Electrolytes considered in electroforming specimens from Groups 1 through 5 have not contained stress reducing agents which decompose to codeposit sulfur with nickel. All of the specimens considered in these groups have contained manganese far in excess of stoichiometric amounts needed to chemically combine with sulfur upon heat treatment. It is also questionable if any, or only part, of the sulfur is chemically combined with manganese as a result of the moderate heat treatment cycles employed. This is not expected to pose a problem with respect to hot shortness in the deposits since the intended application does not entail thermal excursions to 482°C (900°F). Any such exposures to 427°C, or higher, would initiate chemical combination of manganese and sulfur. Prior experience with "as deposited" nickel-manganese alloys has shown that low ductility in the 100° - 316°C range is to be expected. However, this problem surfaced as a decrease in elongation in this temperature range, and the test data for moderately heat treated specimens does not show a deterioration at these elevated test temperatures.

Internal stress of a tensile nature has presented some problems in making flat electroformed alloy specimens for mechanical property testing. The flat sheets are visibly distorted with a slight bow after removing from the stainless steel mandrel. This presented some difficulties in machining and testing some strips since the bow was in the direction of the length of the test bar. The addition of a stress reducer to the electrolyte to counter the residual tensile stress in the deposits was considered. The additional sulfur expected in the deposit as a result of using such an agent was not considered to be detrimental on the basis that a very large excess of manganese would be present to counter the effects of sulfur at elevated temperatures. A proprietary stress reducer, SNHA (Allied Kelite Division of Witco), was used.

Specimens shown as Group 7 in Table 3.3-6 were electroformed with the stress reducer present. Test results were discouraging in that good mechanical properties were not obtained after moderate heat treatments, or good mechanical strength values could not be maintained at test temperatures of 149°C and 260°C. There appeared to be a great fluctuation in manganese and sulfur contents of the alloy samples - more so than electroforming parameters would dictate. Part of the problem might have been due to the high voltage peaks generated in pulse plating and subsequent decomposition of the organic compound of which the stress reducer is composed.

TABLE 3.3-6. FABRICATION AND MECHANICAL PROPERTY TEST DATA FOR ELECTROFORMED NICKEL-MANGANESE FROM 48° - 50°C ELECTROLYTES CONTAINING 4.2-5.0 G/L MANGANESE AND 0.8 TO 1.3 ML/L STRESS REDUCER

Group 7 - Various Average Current Densities, Various Pulse Duty Cycles, Stress Reducer in Electrolyte

Sample Number	Pulse Plating Information	Bath and Alloy Analytical Data	Test No.	Heat Treatment	Test Temp. (°C)	Mechanical Properties: Ultimate MPa	Ultimate Ksi	Yield MPa	Yield Ksi	Elongation, % in: 2.54 cm	Elongation, % in: 5.08 cm
NM-30	Duty Cycle 50%	Ni Metal 78.9 g/l	A	None	Room	1644	238	Not Deter.		Broke out of gauge.	
	Pulse On 20 msec	Mn Metal 4.2 g/l	B	316°C(24 Hr)	Room	1473	214	Not Deter.		1	0.8
	Pulse Off 20 msec	Boric Acid 31.9 g/l	C	343°C(24 Hr)	Room	1413	205	Not Deter.		1	0.8
	Peak CD 6.46 A/dm²	SNHA 0.80 ml/l	D	427°C(4 Hr)	Room	1616	234	1494	217	4	2
	Avg. CD 3.23 A/dm²	Acidity(pH) 4.34	E	371°C(24 Hr)	Room	1677	243	1411	205	4	2
	Avg. Volts 5.5	Temp 48.3 °C	F	371°C(24 Hr)	149	Specimen broke in machining.					
		Alloy Mn 0.68 %	G	371°C(24 Hr)	260	902	131	878	127	4	1.5
		Alloy S 23 PPM	H								
NM-31	Duty Cycle 50%	Ni Metal 77.8 g/l	A	None	Room	1504	218	838	122	13	10.5
	Pulse On 20 msec	Mn Metal 4.45 g/l	B	316°C(24 Hr)	Room	666	97	535	78	Broke out of gauge.	
	Pulse Off 20 msec	Boric Acid 31.3 g/l	C	343°C(24 Hr)	Room	564	82	438	64	42	33.5
	Peak CD 6.46 A/dm²	SNHA 0.80 ml/l	D	427°C(4 Hr)	Room	540	78	441	64	41	36
	Avg. CD 3.23 A/dm²	Acidity(pH) 4.18	E								
	Avg. Volts 5.1	Temp 53.9 °C	F								
		Alloy Mn 0.17 %	G								
		Alloy S 179 PPM	H								
NM-32	Duty Cycle 50%	Ni Metal 78.0 g/l	A	None	Room	1627	236	1031	150	2.5	1.5
	Pulse On 20 msec	Mn Metal 5.0 g/l	B	316°C(24 Hr)	Room	932	135	Not Deter.		1	0.8
	Pulse Off 20 msec	Boric Acid 32.7 g/l	C	343°C(24 Hr)	Room	1077	156	866	126	6	3.5
	Peak CD 6.46 A/dm²	SNHA 1.30 ml/l	D	427°C(4 Hr)	Room	1053	153	730	106	9	4
	Avg. CD 3.23 A/dm²	Acidity(pH) 4.23	E								
	Avg. Volts 5.3	Temp 48.9 °C	F								
		Alloy Mn 0.48 %	G								
		Alloy S 239 PPM	H								
NM-33	Duty Cycle 67%	Ni Metal 78.2 g/l	A	None	Room	1602	232	1054	153	6	4.5
	Pulse On 40 msec	Mn Metal 4.9 g/l	B	316°C(24 Hr)	Room	985	143	719	104	2.5	1.5
	Pulse Off 20 msec	Boric Acid 31.4 g/l	C	343°C(24 Hr)	Room	672	97	552	80	23	15
	Peak CD 4.84 A/dm²	SNHA 1.30 ml/l	D	427°C(4 Hr)	Room	641	93	527	76	31	18.5
	Avg. CD 3.23 A/dm²	Acidity(pH) 4.15	E								
	Avg. Volts 5.35	Temp 50.0 °C	F								
		Alloy Mn 0.32 %	G								
		Alloy S 174 PPM	H								
NM-34	Duty Cycle 100%	Ni Metal 79.8 g/l	A	None	Room	1364	198	998	145	39.5	30.9
	Pulse On	Mn Metal 4.95 g/l	B	260°C(72 Hr)	Room	896	130	729	106	13.3	9.0
	Pulse Off	Boric Acid 31.9 g/l	C	343°C(24 Hr)	Room	552	80	464	67	26.7	10.5
	Peak CD 2.69 A/dm²	SNHA 1.30 ml/l	D	371°C(24 Hr)	Room	532	77	456	66	39.5	30.9
	Avg. CD 2.69 A/dm²	Acidity(pH) 4.28	E	343°C(24 Hr)	149	491	71	471	68	36	26.5
	Avg. Volts 4.9	Temp 49.4 °C	F	343°C(24 Hr)	260	438	64	418	61	29.7	19.4
		Alloy Mn 0.11 %	G	371°C(24 Hr)	149	487	71	478	69	40	28
		Alloy S 902 PPM	H	371°C(24 Hr)	260	426	62	413	60	29.5	21.7
NM-35	Duty Cycle 67%	Ni Metal 78.8 g/l	A	None	Room	1551	225	939	136	13	6.1
	Pulse On 40 msec	Mn Metal 4.85 g/l	B	260°C(72 Hr)	Room	1638	238	1418	206	8	5
	Pulse Off 20 msec	Boric Acid 32.0 g/l	C	343°C(24 Hr)	Room	736	107	633	92	11.7	6
	Peak CD 4.00 A/dm²	SNHA 1.30 ml/l	D	371°C(24 Hr)	Room	788	114	690	100	13	6.1
	Avg. CD 2.69 A/dm²	Acidity(pH) 4.17	E	343°C(24 Hr)	149	1012	147	858	124	5	4
	Avg. Volts 4.8	Temp 49.4 °C	F	343°C(24 Hr)	260	703	102	518	75	7	4.3
		Alloy Mn 0.34 %	G	371°C(24 Hr)	149	646	94	563	82	16.5	7.5
		Alloy S 158 PPM	H	371°C(24 Hr)	260	740	107	531	77	7.5	4.3

During the initial portion of this investigation a companion study was made of electroformed alloys of nickel-cobalt-manganese. Although the details of the electroforming parameters will not be presented here, compositions and mechanical properties are furnished in Table 3.3-7 for comparison with similar data for electroformed nickel-manganese.

TABLE 3.3-7. COMPOSITION AND MECHANICAL PROPERTY TEST RESULTS FOR TYPICAL SPECIMENS OF ELECTROFORMED NICKEL-COBALT-MANGANESE ALLOY

Sample Number	Alloy Composition Nickel (Wt.%)	Cobalt (Wt.%)	Manganese (Wt.%)	Heat Treatment	Test Temp. (°C)	Mechanical Properties Ultimate MPa	Ultimate Ksi	Yield MPa	Yield Ksi	Elongation % in 2.54 cm
NCM-31	73.13	26.80	0.069	None	Room	1387	201	899	130	10
				260°C(72 Hr)	Room	1227	178	1026	149	9.5
				316°C(24 Hr)	Room	1260	183	1063	154	10
				343°C(24 Hr)	Room	1045	152	881	128	14.8
				427°C(4 Hr)	Room	939	136	880	128	15
				260°C(72 Hr)	260	935	136	564	82	12.9
				343°C(24 Hr)	260	852	124	590	86	8.9
NCM-24	67.04	32.80	0.16	None	Room	1670	242	1221	177	3 +
				316°C(24 Hr)	Room	1680	244	1380	200	4 +
				371°C(24 Hr)	Room	1387	201	1192	173	5
				427°C(4 Hr)	Room	1553	225	1309	190	5 +
				371°C(24 Hr)	149	1356	197	1103	160	5.5
				371°C(24 Hr)	260	1246	181	919	133	8.5
NCM-33	59.57	40.40	0.035	None	Room	1489	216	960	139	10
				204°C(72 Hr)	Room	1473	214	1089	158	9.8
				316°C(24 Hr)	Room	1272	185	1050	152	9
				427°C(4 Hr)	Room	932	135	856	124	18
				204°C(72 Hr)	149	1228	178	752	109	18
				204°C(72 Hr)	260	935	136	407	59	25.9
NCM-49	47.08	52.80	0.117	None	Room	1502	218	1024	149	3
				260°C(72 Hr)	Room	1405	204	1120	163	11.6
				316°C(24 Hr)	Room	1387	201	1085	157	15
				343°C(24 Hr)	Room	1268	184	967	140	13
				427°C(4 Hr)	Room	1216	176	972	141	15
				343°C(24 Hr)	149	1162	169	754	109	15.5
				260°C(72 Hr)	260	942	137	496	72	15.3
				343°C(24 Hr)	260	975	141	553	80	23.6
NCM-46	46.82	53.10	0.081	None	Room	1487	216	963	140	3.5
				260°C(72 Hr)	Room	1413	205	1156	168	9.2
				316°C(24 Hr)	Room	1359	197	1031	150	13
				343°C(24 Hr)	Room	1236	179	1067	155	13
				427°C(4 Hr)	Room	1232	179	932	135	14
				343°C(24 Hr)	149	1140	165	787	114	16
				260°C(72 Hr)	260	911	132	457	66	16
				343°C(24 Hr)	260	932	135	580	84	21.6

Most of the electroformed nickel-cobalt-manganese exhibited outstanding ultimate and yield strengths at room temperature before and after heat treatment. After moderate heat treatment, the ductility of this ternary alloy was better than that found in similarly treated nickel-manganese electroformed specimens. However, the mechanical properties of the nickel-cobalt-manganese alloys were more greatly affected at elevated temperatures where significant loss of yield strength was observed. These ternary alloys were also highly stressed - more so than was found with electroformed nickel-manganese. It was also noted that some samples of electroformed nickel-cobalt-manganese alloy having over 0.15% manganese present were among the strongest alloys observed at elevated temperature. However, these same examples exhibited excessively

low ductility. Improvement of this ductility by more severe heat treatments might be possible, but such heat treatments might be unacceptable for MCC application.

3.3.4 Optimization of Manganese Alloying Parameters - Solution Agitation Factors

Before examining the parameter of electrolyte flow and the consequent effects on diffusion layer at the cathode, it is appropriate to summarize various other parameters on mechanical properties of electroformed nickel-manganese alloys:

1. Increasing the manganese concentration in the electrolyte results in an increased manganese content in the alloy, but not to a significant degree unless pulse plating parameters are such that fairly long pulse cycles are used. Increasing the manganese content increases the mechanical strength and decreases ductility (which can often be restored by moderate heat treatments). Manganese contents in deposits exceeding 0.25 weight percent require more prolonged or severe heat treatments while 0.50 weight percent, or more, manganese in the alloy usually results in a brittle and highly tensile stressed "as deposited" metal. The form in which the manganese is codeposited with nickel (i.e., whether in the composition Ni_3Mn, Ni_2Mn, or NiMn) may have an important influence on stress, response to heat treatments, and mechanical properties.

2. Increasing the current density in the conventional dc plating mode, or the average current density in the pulse plating mode, increases manganese concentration in the alloy in an exponential manner. In the pulsed current mode, and for a constant average current density, it appears that increasing the peak current density also increases manganese content and mechanical strength - if the pulse time is sufficiently long. Pulse off times of 10 to 30 milliseconds appear to produce better mechanical properties than lesser times.

3. Electrolyte pH - at least in the normal range of 3.8 to 4.3 - has not been noted to have a significant effect on alloy manganese concentration or mechanical properties. Hydrogen ion may play a part in electron transfer in the reduction of nickel and manganese. In other words, hydrogen may catalyze the reduction of manganese by lowering the reduction potential in some manner. Since hydrogen is reduced, or "plates" at the cathode, the diffusion layer tends to become less acidic. This is easily offset by electrolyte agitation which thins out the cathode diffusion layer and allows quicker hydrogen ion diffusion to restore the proper pH and continuation of the catalyzing process. The use of pulse plating provides an "off" time to enhance the hydrogen replenishment process.

4. Bath temperature increase results in a significant decrease in alloy manganese concentration. Ion migration in the diffusion layer should be easier as the layer temperature increases. However, ion activity increases with temperature. If hydrogen in a monatomic form of protons is crucial to the catalytic process to reduce manganese, then temperature increases would

promote increased proton mobility to promote proton collisions to produce hydrogen molecules of two hydrogen atoms. This would decrease the availability of hydrogen to act as a catalyst for manganese.

5. Deposition voltage is directly related to manganese content in the alloy. High voltages lead to high manganese concentrations in deposits. Since increased current densities are accompanied by increased hydrogen overvoltages on iron group metals such as nickel and cobalt, the increased liberation of hydrogen atoms would promote increased catalyzing activity for manganous ions.

The above discussion has in many cases pointed to electrolyte agitation and the resulting "thinning" of the diffusion layer as an important influence on the catalytic process by which manganous ion is possibly affected through decreasing its reduction potential to promote codeposition with nickel. The serious effects of agitation on alloy composition and mechanical properties became evident during a portion of this investigation where an attempt was being made to duplicate, or improve upon, the mechanical properties of Specimen NM-25 where ultimate strength exceeded 1200 MPa (even after heat treating at 427^{o}C for four hours) and elongation was at least ten percent. The panel fabrication matrix included use of several pulse duty cycles in the 25% to 60% range with low frequencies (long pulse cycles) of 25 to 50 Hz. Long pulse times were being investigated since the off time for Specimen NM-25 was 20 milliseconds.

When a duplicate nickel-manganese electroforming facility was established to increase rate at which specimens could be made, all spray systems in both tanks were overhauled. Single "Fulljet" solid square spray pattern nozzles were installed in each pumped electrolyte outlet perpendicular to the plane of the panel being electroformed. The same spray configurations were placed to provide agitation on each face of the shielded mandrel from which duplicate electroform plates were made. These sprays were 3/8 HH24WSQ with a rated flow of 6.8 liters per minute (1.8 gallons per minute) at 34.5 KN/m^2 (5 psig) and 9.1 liters per minute (2.4 gallons per minute) at 69 KN/m^2 (10 psig). The nozzle-to-mandrel surface distance was 12.7 cm. Panels electroformed under this electrolyte spray condition are denoted by the word "Single" under descriptions in subsequent tables and commentary. A rearrangement of sprays was made where two "Fulljet" solid square spray nozzles pumped electrolyte on each face of each panel being electroformed. This permitted a higher volume flow but at a lower pressure. Such agitation conditions are described as "Double" under the discussions that follow. Any references to "Single Square" mean the same as "Single". All spray nozzles were made from polyvinyl chloride and were obtained from Spray Systems Company, Wheaton, Illinois. Also employed in this study were nozzles composed of open pipe nipples and "Veejet" nozzles. The latter nozzle produces a flat fan shaped spray pattern.

Analytical data and mechanical property test data from a large number of electroformed alloy specimens was obtained using these various spray nozzles and different pulse plating parameters. Center and edge manganese contents were determined for comparison for effects of electrolyte spray agitation on

manganese variation. Table 3.3-8 lists these results and it was observed that manganese did not vary significantly across the individual panels, with the exception of one or two isolated cases.

From the results of tests on the above specimens, additional material was electroformed with slight modifications of current density and the use of more than one heat treatment. Results for NMR-27A, NMR-35, NMR-37, and NMR-38 series were impressive as shown in Table 3.3-9. Although these samples showed borderline elongation values, it was anticipated that results from round bar fabrication might show improvements.

At this time the effects of heat treatment on microstructures and ductility were examined. Figures 3.3-5 and 3.3-6 show how the ductility, in the form of neck-down, is improved by heat treating the "as deposited" alloy which appeared somewhat brittle in the non-heat treated state. The term "brittle" does not infer that the alloy is glass-like; however, as the strength approaches the 1380 MPa (200 ksi) level, the elongation is low in the "as deposited" state. The electroformed nickel-manganese alloys exhibiting the highest strengths have very interesting microstructures as shown in Figures 3.3-7 and 3.3-8. As with electroformed nickel-cobalt alloys, there is a banding present - although not as prominent as in the EF nickel-cobalt alloy. The banding does not disappear with any of the heat treatments used on these samples. The material is also very fine-grained before and after heat treatment, a factor that may help explain the large retention of strength after heat treating and at elevated temperatures.

Of special interest in the above table are the test results for Specimen NMR-27A with a heat treatment at 260°C (500°F) for 72 hours. This material appeared competitive with Inconel 718. The mechanical properties of the EF alloy only differ from those of age-hardened Inconel 718 in the area of ductility where the former exhibited an elongation of 16% in 2.54 cm as opposed to 22% in 5.08 cm for the latter at a test temperature of 149°C (300°F).

3.3.5 Preparation of Electroformed Nickel-Manganese Specimens for Submittal to Marshall Space Flight Center

Although residual stress distortion appeared tolerable in specimens of thicknesses to 1.52 mm (0.060 in), there was concern that electroforming to a thickness of 1.27 cm (0.5 in.) on each face of the mandrel might lead to an accumulative stress with distortion sufficient to separate the electroform from the mandrel and possibly cause cracking or damage to the plastic shield box and fixturing. Therefore, the initial electroform deposit on both sides of the mandrel was bonded to allow induced tensile stresses to counter one another.

TABLE 3.3-8. MANGANESE DISTRIBUTION IN ELECTROFORMED NICKEL-MANGANESE

Sample Number	Cur. Density Average	Cur. Density Peak	Duty Cycle (%)	Milisec. On	Milisec. Off	Bath Mn (g/l)	Electrolyte Spray Config.	Deposit Mn (ppm) Edge	Deposit Mn (ppm) Center	Mechanical Properties (After Heat Treat) Ultimate MPa	Ultimate Ksi	Yield MPa	Yield Ksi	Elongation, % in 2.54 cm
5A1B	2.72	5.44	50	20	20	4.6	Sgl.Sq.Far	3205		1302	189	1134	164	9.3
6A1B	2.72	5.44	50	12	12	4.5	Sgl.Sq.Far	2541		1329	193	1113	161	5.2
6B1B	2.72	5.44	50	12	12	4.7	Dbl.Sq.Far	2443		933	135	825	120	9.8
6C1A	2.72	5.44	50	12	12	4.7	Dbl.Sq.Cls.	3423		1062	154	977	142	7
7A1B	2.72	6.81	40	8	12	4.6	Dbl.Sq.Far	1913	2168	1104	160	949	138	7.5
8A1B	2.18	5.44	40	8	12	4.4	Dbl.Sq.Far	1288	1419	962	140	681	99	13.3
8B1B	2.18	5.44	40	8	12	4.6	Dbl.Sq.Far	1438		920	134	792	115	13
9A1B	2.18	8.71	25	6	18	4.7	Dbl.Sq.Far	1758	1778	1249	181	1089	158	5.8
9B1B	2.18	8.71	25	6	18	4.6	Dbl.Sq.Far	1716		1140	165	982	142	4.6
10A1C	2.18	4.36	50	10	10	4.8	Sgl.Sq.Far	1919	2024	971	141	852	124	10
11A1C	2.18	5.44	40	6.7	10	4.7	Sgl.Sq.Far	1531	1660	1104	160	963	140	8
12A1C	2.18	4.36	50	20	20	4.7	Sgl.Sq.Far	2766	2898	1142	166	856	124	8
13A1C	2.18	5.44	40	13.4	20	4.7	Sgl.Sq.Far	2368	2631	1100	160	1054	153	8
14A1C	2.18	4.36	50	30	30	4.6	Sgl.Sq.Far	3035	3158	937	136	872	126	Broke out of ga.
15A1C	2.18	5.44	40	20	30	4.6	Sgl.Sq.Far	3352	3333	1272	185	1079	157	Broke out of ga.
16A1C	2.18	6.53	33	5	10	4.5	Sgl.Sq.Far	1670	1750	919	133	765	111	10
17A1B	2.18	3.63	60	15	10	4.6	Sgl.Sq.Far	1784	1962	1010	147	829	120	15.6
18A1B	2.18	6.53	33	10	20	4.6	Sgl.Sq.Far	3037	2932	1196	174	1097	159	7.8
19A1B	2.18	4.36	50	10	10	4.6	Sgl.3/8"Pipe	1619	1746	1098	159	940	136	16.2
20A1B	2.18	5.44	40	6.7	10	4.3	Sgl.3/8"Pipe	1705	1825	1096	159	935	136	11
21A1B	2.72	5.44	50	10	10	4.6	Sgl.3/8"Pipe	2975	2930	1308	190	1078	156	10.7
22A1B	2.72	6.81	40	6.7	10	4.8	Sgl.3/8"Pipe	2800	2785	1207	175	1069	155	8.8
23A1B	2.18	4.36	50	20	20	4.6	Sgl.3/8"Pipe	2062	2666	1219	177	1034	150	10.7
24A1B	2.18	5.44	40	13.4	20	4.6	Sgl.3/8"Pipe	3054	2808	1229	178	1060	154	9
25A1B	2.18	4.36	50	20	20	4.3	Sgl.Fan,Cls.	2238	2608	1221	177	1040	151	9.4
26A1B	2.18	4.36	50	20	20	4.3	Sgl.Sq.Cls.	3173	3242	1201	174	1051	152	7.4
25B1B	2.18	4.36	50	20	20	4.3	Sgl.Fan,Cls.	1977		932	135	856	124	10.1
26B1B	2.18	4.36	50	20	20	4.4	Sgl.Sq.Cls.	1904		894	130	814	118	9.8
27A1B	2.18	5.44	40	13.4	20	4.6	Sgl.Fan,Cls.	2280		1291	187	1111	161	7.9
28A1B	2.18	5.44	40	13.4	20	4.6	Sgl.Sq.Cls.	2741		1180	171	1068	155	7.6
29A1B	2.72	5.44	50	20	20	4.6	Sgl.Fan,Cls.	3416		1476	214	1280	186	7.3
30A1B	2.72	5.44	50	20	20	4.8	Sgl.Sq.Cls.	4439		1267	184	Not Determined		5.9
31A1B	2.18	5.44	40	20	30	4.3	Sgl.Fan,Cls	3244		1343	195	1185	172	8.4
32A1B	2.18	5.44	40	20	30	4.3	Sgl.Sq.Cls.	3521		965	140	923	134	8.6

All heat treatments were at 343°C for 24 hours. Sprays described by Sgl.Sq.Far were for a square pattern, one on each side of the panels, and about 12.7 cm from electroformedsurface. Dbl.Sq.Far means that two square spray pattern sprays were used on each side of the panels and at the approximate distance of 12.7 cm from the panels. Cls. means close and the distance to panel was about 7.6 cm. Sgl.3/8"Pipe means an open 3/8" I.D. pipe nipple.

TABLE 3.3-9. FABRICATION AND MECHANICAL PROPERTY TEST DATA FOR ELECTROFORMED NICKEL-MANGANESE ALLOYS FROM 48°C ELECTROLYTES CONTAINING 4.75 G/L MANGANESE AND PULSE ELECTROFORMED USING VARIOUS SPRAYS

Sample Number	Pulse Plating Information	Bath and Alloy Analytical Data	Test No.	Heat Treatment	Test Temp. (°C)	Mechanical Properties: Ultimate MPa	Ultimate Ksi	Yield MPa	Yield Ksi	Elongation, % in: 2.54 cm	Elongation, % in: 5.08 cm
NMR-27A	Duty Cycle 40%	Ni Metal 76.92 g/l	A	None	Room	1276	185	965	140	9.2	4.7
	Pulse On 13.4 msec	Mn Metal 4.6 g/l	B	343°C(24 Hr)	Room	1291	187	1112	161	7.9	4.6
	Pulse Off 20 msec	Boric Acid 30.6 g/l	C	343°C(24 Hr)	149	1116	162	861	125	Broke out of gauge.	
	Peak CD 5.44 A/dm^2	SNHA 0 ml/l	D	343°C(24 Hr)	260	969	141	699	101	12.9	7.6
	Avg. CD 2.18 A/dm^2	Acidity(pH) 4.12	E	260°C(72 Hr)	Room	1351	196	1115	162	10	6.1
	Avg. Volts 4.00	Temp 48.8 °C	F	260°C(72 Hr)	149	1237	179	937	136	16.3	8.4
	Sprays - Single Fan, Close	Alloy Mn 0.23 %	G	260°C(72 Hr)	260	1021	148	708	103	17	9.4
		Alloy S PPM	H								
NMR-35A	Duty Cycle 50%	Ni Metal 78.48 g/l	A	None	Room	1389	201	1157	168	5.3	3.2
	Pulse On 15 msec	Mn Metal 4.9 g/l	B								
	Pulse Off 15 msec	Boric Acid 30.75 g/l	C	343°C(24 Hr)	Room	1432	208	1281	186	7.5	4.2
	Peak CD 5.44 A/dm^2	SNHA 0 ml/l	D								
	Avg. CD 2.72 A/dm^2	Acidity(pH) 3.78	E								
	Avg. Volts 4.70	Temp 48.2 °C	F								
	Sprays - Single 3/8" Pipe Nipples, Close	Alloy Mn %	G								
		Alloy S PPM	H								
NMR-37C	Duty Cycle 40%	Ni Metal 74.92 g/l	A	None	Room	1214	176	968	140	5.2	2.7
	Pulse On 20 msec	Mn Metal 4.8 g/l	B	343°C(24 Hr)	Room	1236	179	1089	158	7.3	5.8
	Pulse Off 30 msec	Boric Acid 30.24 g/l	C								
	Peak CD 5.44 A/dm^2	SNHA 0 ml/l	D								
	Avg. CD 2.18 A/dm^2	Acidity(pH) 4.07	E								
	Avg. Volts 4.00	Temp 48.3 °C	F								
	Sprays - Double Sq., Close	Alloy Mn %	G								
		Alloy S PPM	H								
NMR-38D	Duty Cycle 50%	Ni Metal 74.64 g/l	A	None	Room	1465	212	1080	157	6.3	4.2
	Pulse On 20 msec	Mn Metal 4.7 g/l	B	343°C	Room	1374	199	1188	172	6.7	4.6
	Pulse Off 20 msec	Boric Acid 30.09 g/l	C								
	Peak CD 4.36 A/dm^2	SNHA 0 ml/l	D								
	Avg. CD 2.18 A/dm^2	Acidity(pH) 4.08	E								
	Avg. Volts 3.99	Temp 47.5 °C	F								
	Sprays - Double Fan, Close	Alloy Mn %	G								
		Alloy S PPM	H								
NMR-38B	Duty Cycle 50%	Ni Metal 74.64 g/l	A	None	Room	1386	201	1079	157	7.3	4.8
	Pulse On 20 msec	Mn Metal 4.6 g/l	B	343°C(24 Hr)	Room	1474	214	1319	191	5.2	3.2
	Pulse Off 20 msec	Boric Acid 30.09 g/l	C								
	Peak CD 4.36 A/dm^2	SNHA 0 ml/l	D								
	Avg. CD 2.18 A/dm^2	Acidity(pH) 4.00	E								
	Avg. Volts 3.92	Temp 48.4 °C	F								
	Sprays - Single ½" Pipe Nipples	Alloy Mn %	G								
		Alloy S PPM	H								

Figure 1 - As Deposited Ni-Mn Alloy (7X)

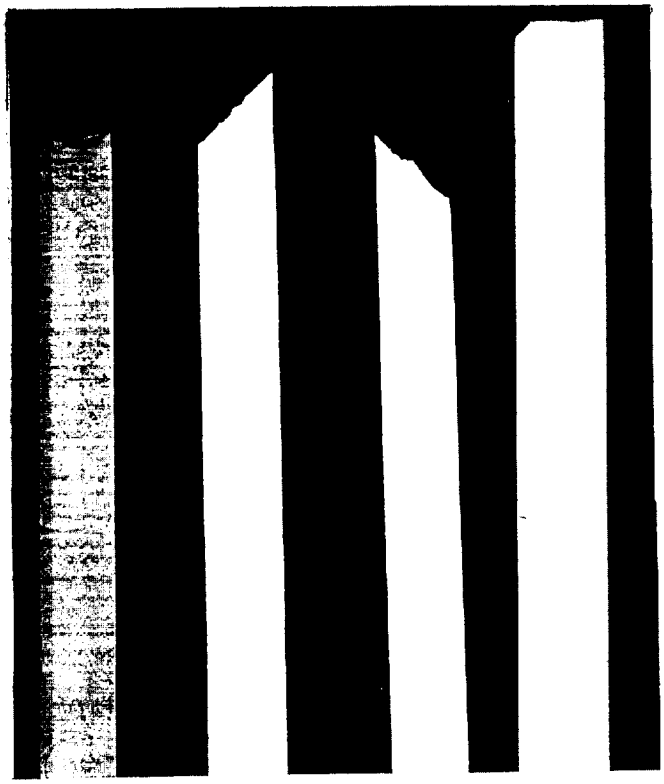

Specimen
NMR-31A1A
Mn = 0.32%
Pulsed:
20 ASF Avg.
50 ASF Peak
20 Msec On
30 Msec Off

Specimen
NMR-29A1A
Mn = 0.34%
Pulsed:
25 ASF Avg.
50 ASF Peak
20 Msec On
20 Msec Off

Specimen
NMR-21A1A
Mn = 0.30%
Pulsed:
25 ASF Avg.
50 ASF Peak
10 Msec On
10 Msec Off

Specimen
NMR-05A1A
Mn = 0.32%
Pulsed:
25 ASF Avg.
50 ASF Peak
20 Msec On
20 Msec Off

Figure 3.3-5. As Deposited Ni-Mn Alloy. Magnification 7X

Figure 2 - Ni-Mn Alloy Heat Treated at 343°C (650°F) for 24 Hours (7X)

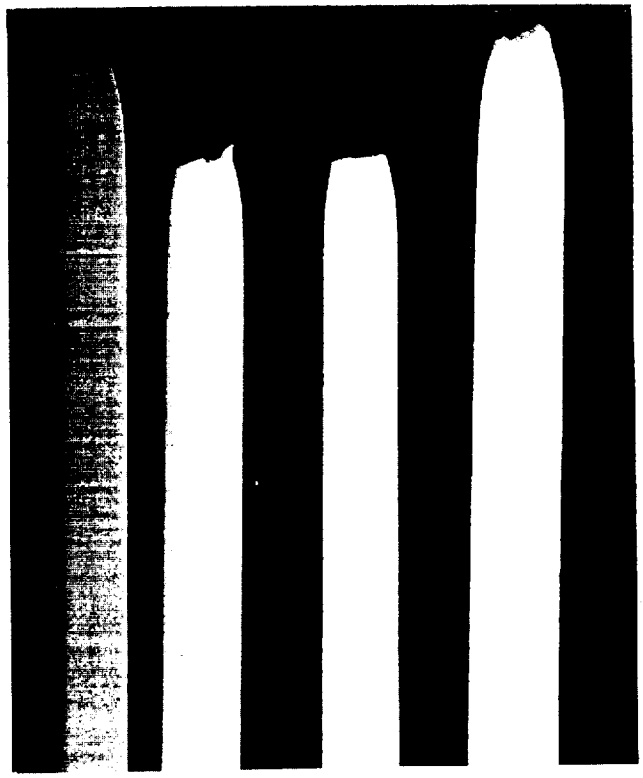

Specimen
NMR-31A1B
Mn = 0.32%
Pulsed:
20 ASF Avg.
50 ASF Peak
20 Msec On
30 Msec Off

Specimen
NMR-29A1B
Mn = 0.34%
Pulsed:
25 ASF Avg.
50 ASF Peak
20 Msec On
20 Msec Off

Specimen
NMR-21A1B
Mn = 0.29%
Pulsed:
25 ASF Avg.
50 ASF Peak
10 Msec On
10 Msec Off

Specimen
NMR-05A1B
Mn = 0.32%
Pulsed:
25 ASF Avg.
50 ASF Peak
20 Msec On
20 Msec Off

Figure 3.3-6. Ni-Mn Alloy Heat Treated at 343°C for 24 hrs. Magnification 7X

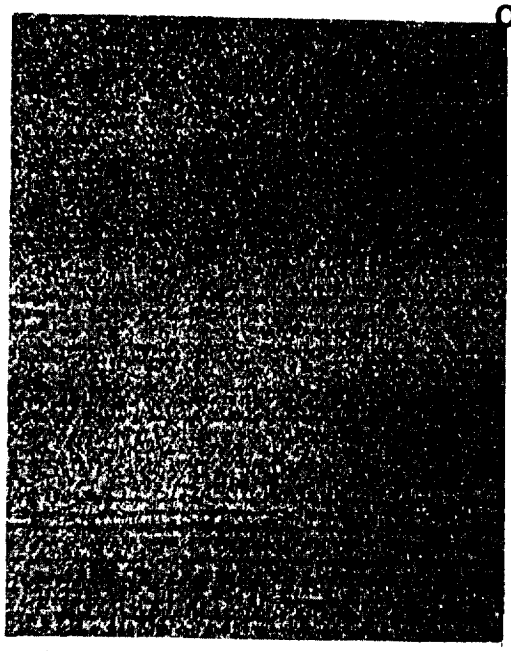

Specimen NMR-05A1A 50X

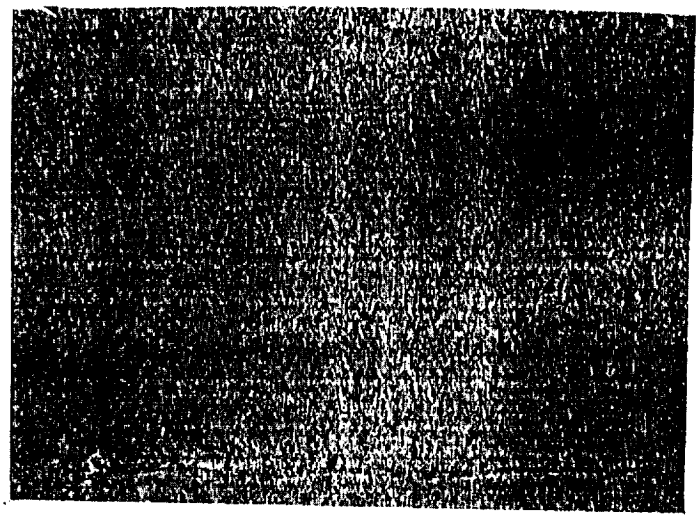

Specimen NMR-05A1A 200X

As deposited condition of EF Ni-Mn alloy with 0.32% by weight Mn. Pulse plated at an average current density of 25 ASF, a peak current density of 50 ASF, and a pulse "on" time of 20 msec. and an "off" time of 20 msec. Cathode agitation was from single Veejet 9510 spray nozzles located about 4 inches from the cathode surface. Mn metal concentration in the bath was 4.6 g/l.

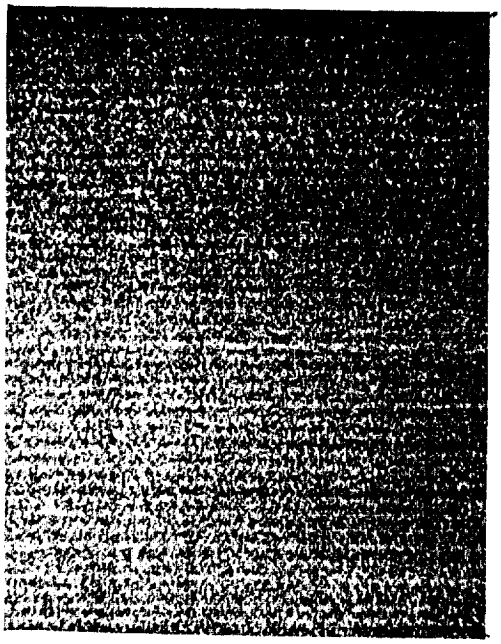

Specimen NMR-05A1B 50X

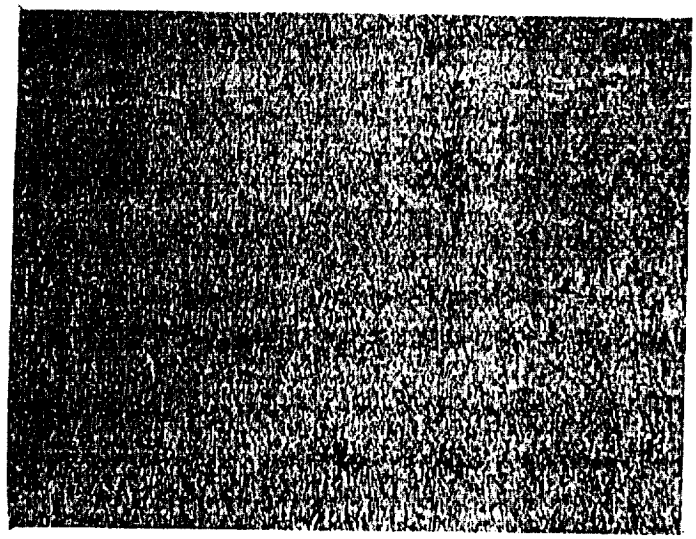

Specimen NMR-05A1B 200X

EF Ni-Mn alloy containing 0.32% by weight Mn after heat treating at 650°F (343°C) for 24 hours. This material was from the same panel from which the NMR-05A1A specimen was obtained. Heat treatment resulted in an age-hardening effect wherein the yield strength increased from 143 to 164 ksi and elongation improved from 7.8 to 9.3 percent in 2.54 cm (1 inch).

Figure 3.3-7. Microstructure of EF Ni-Mn Alloy - Specimen NMR-5A

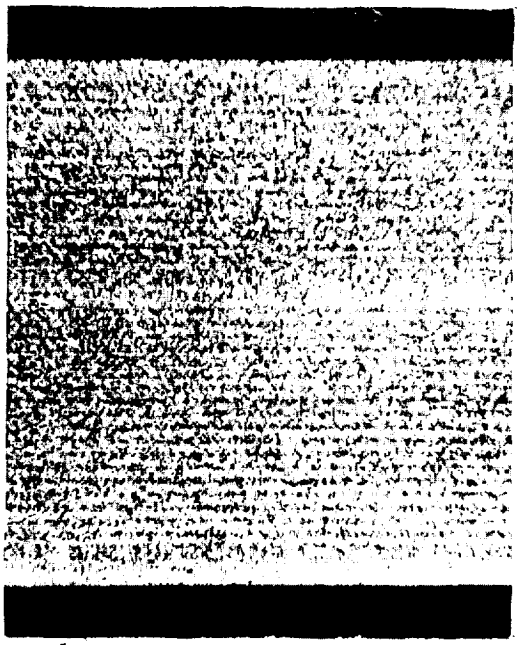

Specimen NMR-21A1A 50X

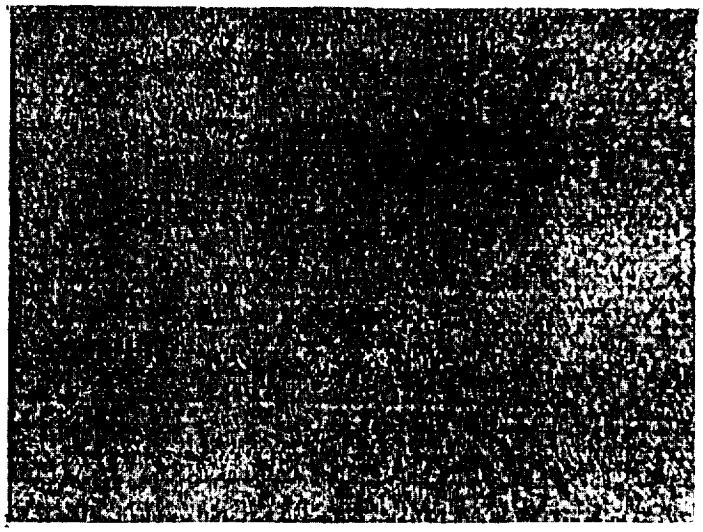

Specimen NMR-21A1A 200X

As deposited condition of EF Ni-Mn alloy with 0.30% by weight Mn. Pulse plated at an average current density of 25 ASF, a peak current density of 50 ASF, and a pulse "on" time of 10 msec. and an "off" time of 10 msec. Cathode agitation was from single open 3/8 inch pipe nipples located about 4 inches from the electroform surface. Mn metal concentration in the bath was 4.6 g/l.

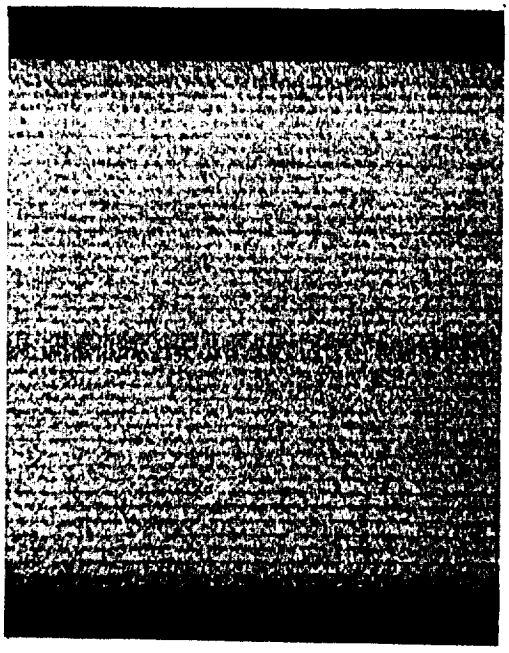

Specimen NMR-21A1B 50X

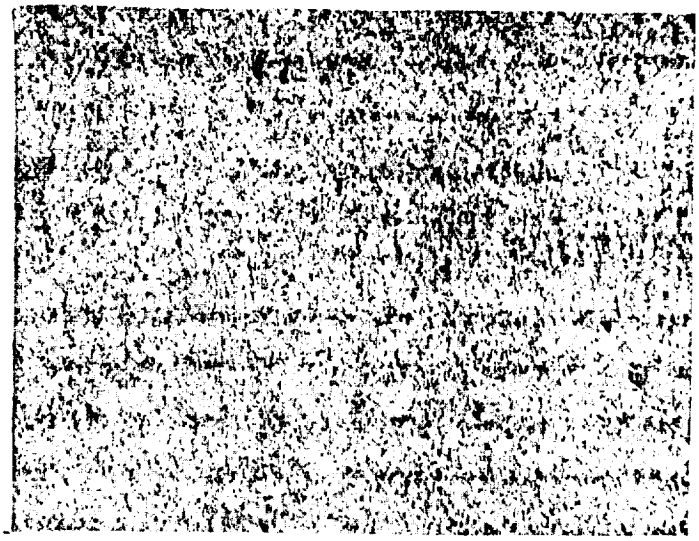

Specimen NMR-21A1B 200X

EF Ni-Mn alloy containing 0.29% by weight Mn after heat treating at 650°F (343°C) for 24 hours. This material was from the same panel from which the NMR-21A1A specimen was obtained. Heat treatment resulted in an age-hardening effect wherein yield strength increased from 139 to 156 ksi and elongation improved from 8.2 to 10.7 percent in 2.54 cm (1 inch).

Figure 3.3-8. Microstructure of EF Ni-MN Alloy - Specimen NMR-21A

The parameters selected for electroforming the thick slab material for machining round bars for mechanical property testing were compromises of the conditions used to deposit the most promising specimens tested and reported under the NMR series of specimen numbers. Selected were an average current density of 2.42 A/dm^2, a peak current density of 4.84 A/dm^2, a pulse plating "on" time of 15 msec., an "off" time of 15 msec., and the use of arrays of Veejet (flat fan) sprays for bath agitation at the cathode surface. The use of these particular sprays was arbitrary, since mechanical property performance of NMR-35 series plates involving many spray combinations showed less spray effect differences than was expected. Bath temperature was maintained in the normal 48^{o} - $49^{o}C$ range. Electroform growth to about 0.89 cm (0.35 in.) was without serious problems. Deposit roughness then became serious, and it was necessary to stop deposition, remove some spike nodules, perform some surface grinding, anodic etch to reduce grinding effects, and activate for bonding and continuation of build-up.

The final slab composed of 1.27 cm thicknesses of EF nickel-manganese alloy bonded to a center plate of wrought copper was cut into two nearly equal parts. One part was heat treated at $260^{o}C$ for 72 hours, and the other portion was heat treated at $343^{o}C$ for 24 hours. Before cutting individual square bars from each section, a macroexamination was made which indicated discontinuous cracking within the alloy. Figure 3.3-9 shows a face of the cross sectional cut after polishing. The cracks were only visible in the upper portion of the slab. Figure 3.3-10 is a 4X enlargement of the region with internal cracking from stress build-up. The problem was discussed with NASA-MSFC personnel and it was agreed that flat test bars would be produced to provide material for verifying mechanical properties.

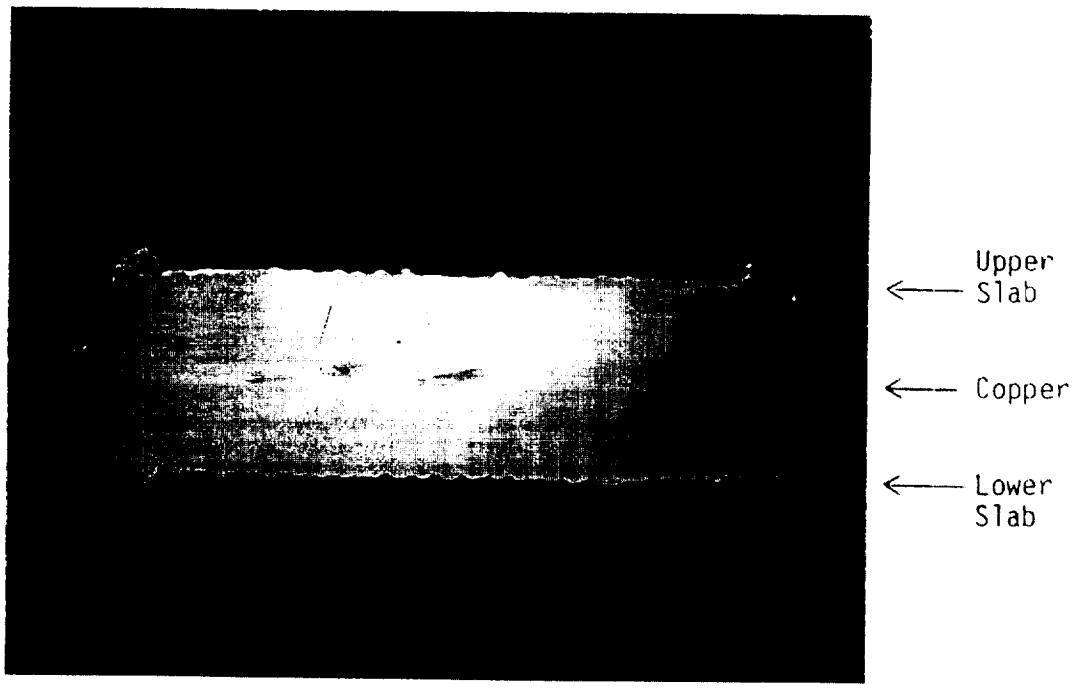

Figure 3.3-9. Cross-section of Electroformed Nickel-Manganese Alloy Slab for the Production of Round Tensile Bars

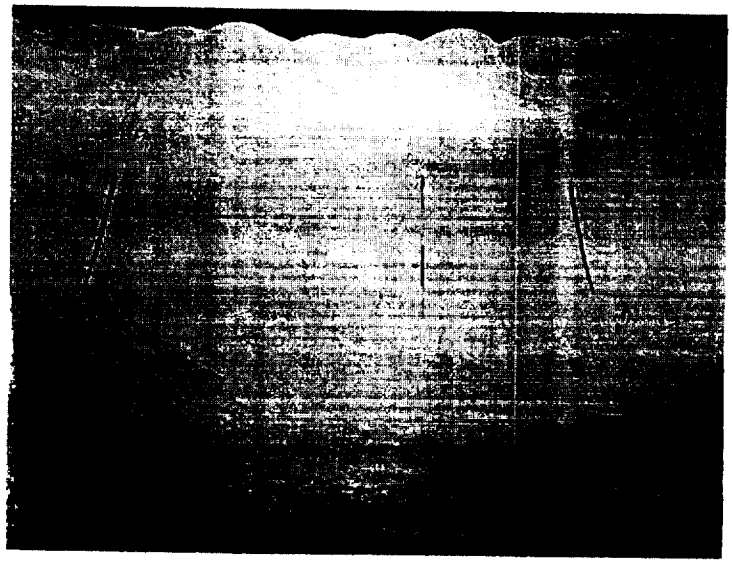

Figure 3.3-10. Cross-section of Electroformed Nickel-Manganese Alloy Slab Showing Isolated Cracking from Stress Build-up

Although the stress problem could be alleviated by stress relieving periodically during electroform build-up, this would not be a satisfactory solution. Very thick alloy electroforms would require too many heat treatments and much manual labor in masking and demasking between electroforming stages. Reducing the manganese content would solve the stress problem, but this would greatly reduce mechanical strength. An alternative possibility was the reconsideration of the use of a stress reducer such as saccharin to eliminate the tensile stress so thick electroforms would be possible. In addition, it was considered essential that effects of cathode bar agitation (reciprocal movement of the flat cathode mandrel back and forth through the electrolyte spray) and rotation of the mandrel (as a cylinder) be evaluated, since these conditions might change agitation conditions, manganese stresses, and resulting mechanical properties.

3.3.6 Alloy Characterization and Optimization - Flat Specimens for Mechanical Property Verification

New flat electroformed plates were produced for mechanical property testing by NASA-MSFC and Bell Aerospace Textron for confirmation of performance of the electroformed alloy. Two different electroforming conditions representing the best known (at the time) parameters for making alloy capable of retaining high mechanical properties after thermal treatment. A separate replication of these panels was made to provide material for comparison of reproducibility and testing at elevated temperatures after various heat treatments. Results and disposition of the specimens from these panels are shown in Table 3.3-10. Photomicrographs of representative alloy from each different specimen are shown in Figures 3.3-11 and 3.3-12.

TABLE 3.3-10. FABRICATION AND MECHANICAL PROPERTY VERIFICATION TEST DATA FOR ELECTROFORMED NICKEL-MANGANESE TEST BARS SUBMITTED TO NASA-MSFC

Sample Number	Pulse Plating Information	Bath and Alloy Analytical Data	Test No.	Heat Treatment	Test Temp. (°C)	Mechanical Properties: Ultimate MPa	Ultimate Ksi	Yield MPa	Yield Ksi	Elongation, % in: 2.54 cm	Elongation, % in: 5.08 cm
NMC-01	Duty Cycle 50%	Ni Metal 78.2 g/l	A	260°C(72 Hr)	Submitted to MSFC						
	Pulse On 15 msec	Mn Metal 4.8 g/l	B	260°C(72 Hr)	Submitted to MSFC						
	Pulse Off 15 msec	Boric Acid 30.8 g/l	C	260°C(72 Hr)	Submitted to MSFC						
	Peak CD 4.91 A/dm^2	SNHA 0 ml/l	D	260°C(72 Hr)	Room	1382	200	1193	173	7	4
	Avg. CD 2.45 A/dm^2	Acidity(pH) 3.90	E	343°C(24 Hr)	Submitted to MSFC						
	Avg. Volts 4.45	Temp 47.8 °C	F	343°C(24 Hr)	Submitted to MSFC						
	Sprays - Double Fan,	Alloy Mn 0.32 %	G	343°C(24 Hr)	Submitted to MSFC						
	Close	Alloy S PPM	H	343°C(24 Hr)	Room	1402	203	1244	180	8	4
NMC-01 (Replicate)	Duty Cycle 50%	Ni Metal 78.6 g/l	A	260°C(72 Hr)[1]	Room	1389	201	1193	173	6	4.5
	Pulse On 15 msec	Mn Metal 4.7 g/l	B	260°C(72 Hr)[2]	149	1122	163	899	130	6	4
	Pulse Off 15 msec	Boric Acid 31.6 g/l	C								
	Peak CD 4.91 A/dm^2	SNHA 0 ml/l	D								
	Avg. CD 2.45 A/dm^2	Acidity(pH) 4.20	E	454°C(2 Hr)	Room	1328	193	1133	164	7	5.5
	Avg. Volts 4.35	Temp 47.2 °C	F	454°C(6 Hr)[3]	149	1101	160	1025	149	8	4.5
	Sprays - Double Fan,	Alloy Mn %	G	427°C(4 Hr)	Room	1359	197	1237	179	9	4
	Close	Alloy S PPM	H	427°C(4 Hr)[4]	149	1204	175	980	142	5	3.5
NMC-02	Duty Cycle 40%	Ni Metal 78.4 g/l	A	260°C(72 Hr)	Submitted to MSFC						
	Pulse On 16 msec	Mn Metal 4.8 g/l	B	260°C(72 Hr)	Submitted to MSFC						
	Pulse Off 24 msec	Boric Acid 31.7 g/l	C	260°C(72 Hr)	Submitted to MSFC						
	Peak CD 5.44 A/dm^2	SNHA 0 ml/l	D	260°C(72 Hr)	Room	1477	214	1298	188	7	4
	Avg. CD 2.17 A/dm^2	Acidity(pH) 4.15	E	343°C(24 Hr)	Submitted to MSFC						
	Avg. Volts 3.95	Temp 47.8 °C	F	343°C(24 Hr)	Submitted to MSFC						
	Sprays - Double Fan,	Alloy Mn 0.34 %	G	343°C(24 Hr)	Submitted to MSFC						
	Close	Alloy S PPM	H	343°C(24 Hr)	Room	1429	207	1342	195	6	3.5
NMC-02 (Replicate)	Duty Cycle 40%	Ni Metal 77.0 g/l	A	260°C(72 Hr)[1]	Room	1528	222	1280	186	7	5
	Pulse On 16 msec	Mn Metal 4.6 g/l	B	260°C(72 Hr)[2]	149	1307	190	1092	158	9	4
	Pulse Off 24 msec	Boric Acid 31.5 g/l	C								
	Peak CD 5.44 A/dm^2	SNHA 0 ml/l	D								
	Avg. CD 2.17 A/dm^2	Acidity(pH) 3.88	E	454°C(2 Hr)	Room	-1480	215	1206	175	8	4
	Avg. Volts 3.95	Temp 48.3 °C	F	454°C(6 Hr)[3]	149	1351	196	1126	163	3	1.5
	Sprays - Double Fan,	Alloy Mn %	G	427°C(4 Hr)	Room	1548	225	1299	188	7.5	4.1
	Close	Alloy S PPM	H	427°C(4 Hr)[4]	149	1323	192	1106	160	6	3.5

Notes: 1 - Followed by additional heat treatment at 343°C for 24 hours.
2 - Followed by additional heat treatments at 343°C for 24 hours and 454°C for 4 hours.
3 - Followed by additional heat treatment at 454°C for 4 hours with cooling between cycles.
4 - Followed by additional heat treatment at 454°C for 4 hours.

The mechanical properties shown in Table 3.3-10 indicate an electroformable alloy with mechanical and yield strengths comparable to Inconel 718 (at moderate test temperatures) and far superior to conventional electroformed nickel. This holds true after moderate and prolonged heat treatments; however, a disappointing aspect of this data is the fact that ductility is not as good as would be desired. It was preferred to obtain an elongation of at least ten percent in 2.54 cm. The concept of superimposing additional heat treatments to those originally applied was only partially successful. It is probable that more severe thermal treatments would be necessary to obtain the sought ductilities. Such treatments could be risk inducing with respect to the properties of the materials in the MCC such as the copper-zirconium-silver alloy of the liner.

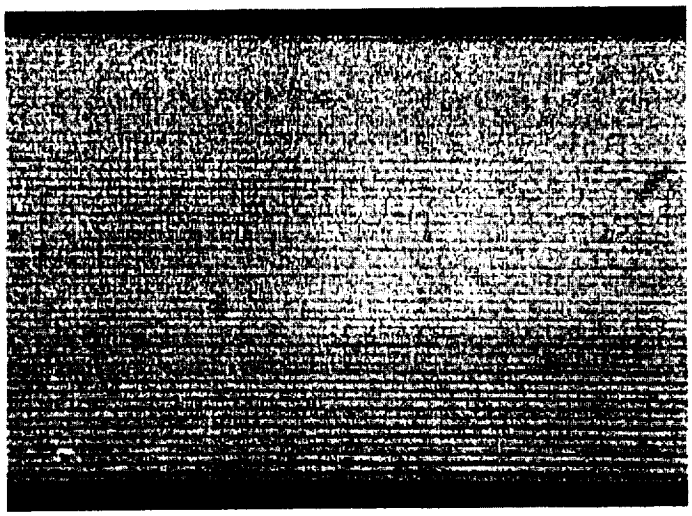

Specimen NMC-01A Magnification 33X

Specimen NMC-01 was heat treated at 260°C for 72 hours. Banding appears at a regular frequency and was retained after heat treating.

Specimen NMC-01A Magnification 200X

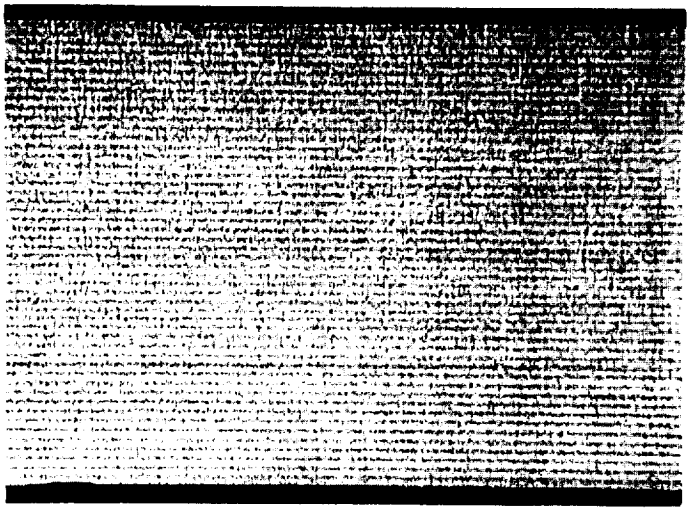

Specimen NMC-01B Magnification 33X

The above specimen was heat treated at 343°C for 24 hours. Banding is similar to that found in the specimen illustrated at the top of this figure.

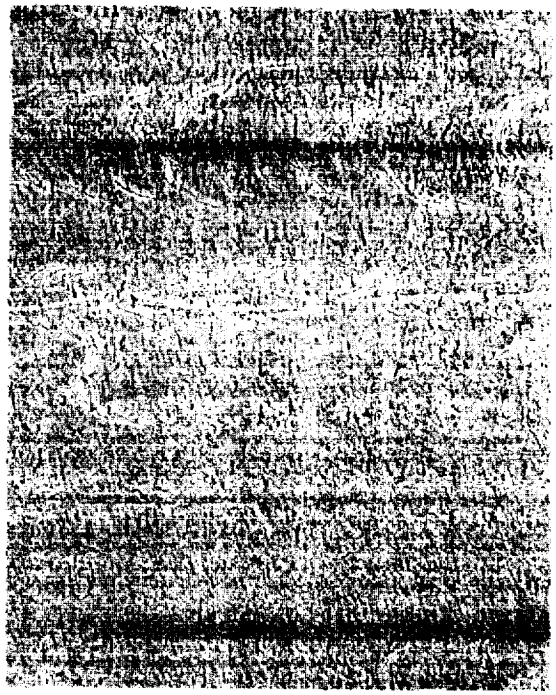

Specimen NMC-01B Magnification 200X

FIGURE 3.3-11. PHOTOMICROGRAPHS OF PULSE ELECTROFORMED NICKEL-MANGANESE ALLOY - DUTY CYCLE 50%, MANGANESE CONTENT 0.31-0.33 WT. %, 2.45 A/dm^2 AVERAGE CURRENT DENSITY

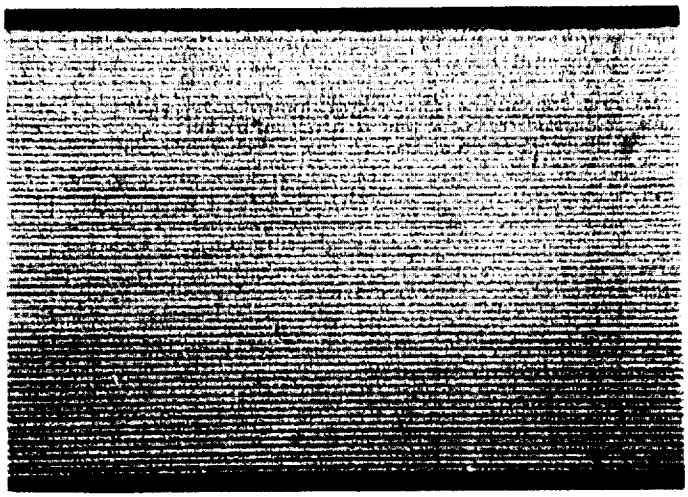

Specimen NMC-02A Magnification 33X

Specimen NMC-02 was heat treated at 260°C for 72 hours. Banding appears at a regular frequency and was retained after heat treating.

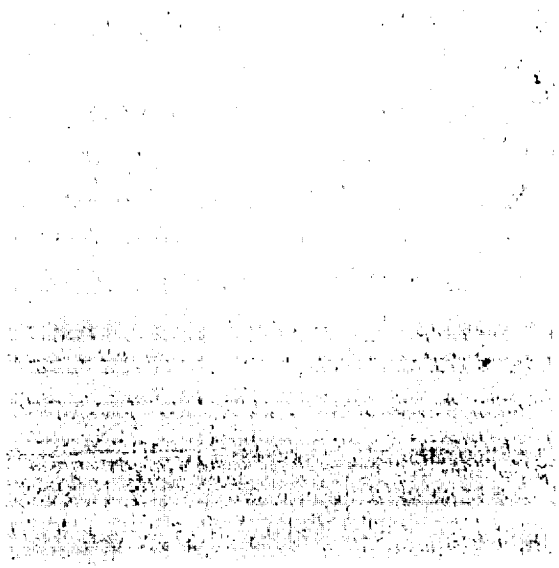

Specimen NMC-02A Magnification 200X

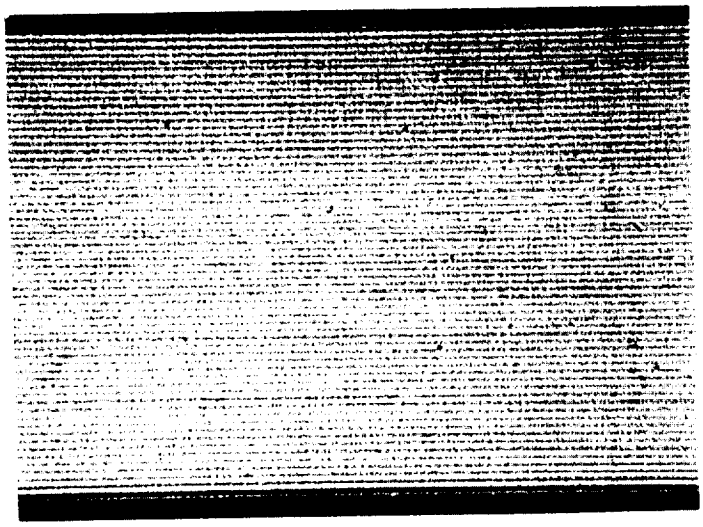

Specimen NMC-02B Magnification 33X

The above specimen was heat treated at 343°C for 24 hours. Banding is similar to that found in the specimen illustrated at the top of this figure.

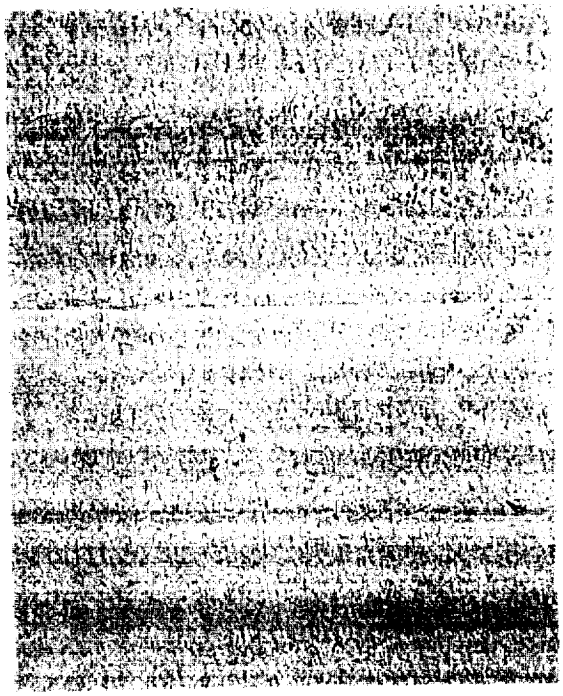

Specimen NMC-02B Magnification 200X

FIGURE 3.3-12. PHOTOMICROGRAPHS OF PULSE ELECTROFORMED NICKEL-MANGANESE ALLOY - DUTY CYCLE 40%, MANGANESE CONTENT 0.32-0.36 WT. %, 2.17 A/dm^2 AVERAGE CURRENT DENSITY

The microstructures shown in the following pages for the alloy samples submitted to NASA-MSFC are very interesting in that they illustrate alloys with extremely fine grain sizes and banding which repeats at a regular frequency. This banding is also found in examples of other high strength nickel base electroformed alloys such as nickel-cobalt, nickel-tungsten, and nickel-iron. It is not known with certainty what actually causes the banding. However, it appears to be retained in the electroformed nickel-manganese after heat treating, and this may provide an indicator of the ability of the alloy to retain high strength at elevated temperatures.

3.3.7 Additional Optimization Studies to Improve Ductility - Cathode Movement

At the time the flat specimen test pieces were submitted to NASA-MSFC it was realized that further improvements in "as deposited" ductility would be needed to enable electroforming to the large thicknesses required in many of the structural applications to which the alloy would be intended. It was recognized that many parts to be electroformed would be symmetric in shape and would lend themselves to rotation in an electroforming bath. Work thus far in this program had involved flat specimens housed in a shield-box with electrolyte agitation provided by a spray of pumped electrolyte. The shield-box may possibly trap some of the electrolyte at corners and along edges so that recirculation occurs rather than the continuous, and more uniform, replacement of electrolyte that would likely be obtained under open flow conditions expected with a rotating part shielded only at the top and bottom.

Although the shield box could not be eliminated in the procedures for the electroforming of flat specimens (because of thickness control considerations) it was possible to reciprocally move the shield box back and forth through the electrolyte spray field. This appeared to provide a better "averaging" of cathode surface agitation effects. Table 3.3-11 presents mechanical property test data for some representative specimens from this additional study. The numbers of the samples are coded so that the third letter describes the electrolyte operating temperature. "L" means that the bath temperature was below the normal 48.9°C. "N" refers to a normal bath temperature, and "H" designates a higher than normal solution temperature.

Data for Specimen NML-03 indicates that moving the sprays to a greater distance from the cathode has some effect on "as deposited" mechanical properties. For this specimen, samples A through D were from the mandrel side that was slightly further from the sprays than the opposite side was. In general, it appeared that the use of a heat treatment at 343°C provided better mechanical properties (particularly with respect to ductility) than did 260°C for the heat treatment times used. The use of pulse duty cycles of 50 percent or higher and long pulse cycles appears beneficial.

TABLE 3.3-11. FABRICATION AND MECHANICAL PROPERTY TEST DATA FOR ELECTROFORMED NICKEL-MANGANESE ALLOYS FROM ELECTROLYTES OPERATED UNDER A VARIETY OF DEPOSITION PARAMETERS WITH CATHODE BAR AGITATION

Sample Number	Pulse Plating Information	Bath and Alloy Analytical Data	Test No.	Heat Treatment	Test Temp. (°C)	Mechanical Properties: Ultimate MPa	Ultimate Ksi	Yield MPa	Yield Ksi	Elongation, % in: 2.54 cm	Elongation, % in: 5.08 cm
NML-03	Duty Cycle 40%	Ni Metal 77.0 g/l	A	None	Room	1446	210	1050	152	5.5	4.5
	Pulse On 10 msec	Mn Metal 3.6 g/l	B	260°C(72 Hr)	Room	1325	192	1095	159	8.4	5.5
	Pulse Off 15 msec	Boric Acid 32.3 g/l	C	343°C(24 Hr)	Room	1290	187	1111	161	10.9	6.1
	Peak CD 5.44 A/dm²	SNHA 0 ml/l	D	260°C(72 Hr)	149	1136	165	902	131	8	6
	Avg. CD 2.18 A/dm²	Acidity(pH) 4.08	E	None	Room	1291	187	960	139	9.1	6
	Avg. Volts 3.95	Temp 45.7°C	F	260°C(72 Hr)	Room	1337	194	1109	161	7.8	5.2
	Sprays - Single Sq.	Alloy Mn 0.27 %	G	343°C(24 Hr)	Room	1389	201	1199	174	7.3	4.4
	Far(A-D),Close(E-H)	Alloy S PPM	H	260°C(72 Hr)	149	1298	188	1014	147	6	4
NML-11	Duty Cycle 67%	Ni Metal 80.0 g/l	A	None	Room	1172	170	1113	161	2	2
	Pulse On 30 msec	Mn Metal 3.4 g/l	B	260°C(72 Hr)	Room	1380	200	Not Determined		6.4	5.1
	Pulse Off 15 msec	Boric Acid 32.3 g/l	C	343°C(24 Hr)	Room	1361	197	1073	156	9.2	5.2
	Peak CD 3.92 A/dm²	SNHA 0 ml/l	D	260°C(72 Hr)	149	1223	177	979	142	8.2	5
	Avg. CD 2.61 A/dm²	Acidity(pH) 4.14	E	427°C(4 Hr)	Room	1236	179	1019	148	8.7	5.8
	Avg. Volts 4.72	Temp 45.9°C	F	454°C(2 Hr)	Room	1224	177	1031	150	11	6.5
	Sprays - Double Fan,	Alloy Mn 0.52 %	G	343°C(24 Hr)	343	899	130	669	97	18	9
	Close	Alloy S PPM	H	343°C(24 Hr)	538	385	56	211	31	Not Determ.	16.3
NML-15	Duty Cycle 60%	Ni Metal 78.5 g/l	A	None	Room	1346	195	1144	166	Broke out of gauge.	
	Pulse On 45 msec	Mn Metal 3.5 g/l	B	260°C(72 Hr)	Room	1467	213	1270	184	8.6	4.8
	Pulse Off 30 msec	Boric Acid 32.4 g/l	C	343°C(24 Hr)	Room	1397	203	1052	153	8	5
	Peak CD 3.63 A/dm²	SNHA 0 ml/l	D	427°C(4 Hr)	Room	1318	191	1117	162	9	6
	Avg. CD 2.18 A/dm²	Acidity(pH) 4.05	E	260°C(72 Hr)	149	1299	188	1006	146	8.4	6.2
	Avg. Volts 4.04	Temp 45.7°C	F	343°C(24 Hr)	149	1239	180	1011	147	9.5	4.8
	Sprays - Double Fan,	Alloy Mn 0.46 %	G	343°C(24 Hr)	343	970	141	747	108	12	7.5
	Close	Alloy S PPM	H	343°C(24 Hr)	538	379	55	153	22	49	28
NMH-04	Duty Cycle 50%	Ni Metal 80.5 g/l	A	None	Room	1306	189	945	137	5	4.5
	Pulse On 30 msec	Mn Metal 4.7 g/l	B	260°C(72 Hr)	Room	1440	209	1245	181	11	6.1
	Pulse Off 30 msec	Boric Acid 33.7 g/l	C	343°C(24 Hr)	Room	1366	198	1141	165	12	6.4
	Peak CD 5.16 A/dm²	SNHA 0 ml/l	D	427°C(4 Hr)	Room	1259	183	1097	159	9	6.5
	Avg. CD 2.58 A/dm²	Acidity(pH) 4.02	E	260°C(72 Hr)	149	1237	179	1024	149	Broke out of gauge.	
	Avg. Volts 4.28	Temp 51.7°C	F	343°C(24 Hr)	149	1243	180	981	142	11.4	5.7
	Sprays - Single Sq.	Alloy Mn 0.44 %	G	343°C(24 Hr)	343	982	142	710	103	18	12
	Close	Alloy S PPM	H	343°C(24 Hr)	538	375	54	142	21	22.5	15
NMN-03	Duty Cycle 62.5%	Ni Metal 83.1 g/l	A	None	Room	1169	169	927	134	7	3.5
	Pulse On 25 msec	Mn Metal 3.3 g/l	B	260°C(72 Hr)	Room	1270	184	1086	157	9	5
	Pulse Off 15 msec	Boric Acid 30.0 g/l	C	343°C(24 Hr)	Room	1247	181	1086	158	10	5
	Peak CD 4.18 A/dm²	SNHA 0 ml/l	D	427°C(4 Hr)	Room	1155	167	984	143	10	6
	Avg. CD 2.61 A/dm²	Acidity(pH) 4.12	E	260°C(72 Hr)	149	963	140	809	117	8	4.5
	Avg. Volts 4.45	Temp 49.1°C	F	343°C(24 Hr)	149	1165	169	986	143	9	4.5
	Sprays - Single Sq.	Alloy Mn 0.33 %	G	343°C(24 Hr)	343	1552	225	1242	180	11	6
	Close	Alloy S PPM	H	343°C(24 Hr)	538	394	57	200	29	45	24

4.0 PHASE B - PROTOTYPE STRUCTURAL JACKET ELECTROFORMING

4.1 Introduction

The purpose of this phase of the high performance alloy electroforming program was to demonstrate the practical application of the alloy optimized in Phase A and to highlight and resolve problems associated with the fabrication of complex configuration hardware such as the structural jacket used on the SSME Main Combustion Chamber (MCC). It had been planned to perform this demonstration exercise on a surplus, or rejected MCC liner fabricated from a copper-zirconium-silver alloy. However, there was no liner available at the

time, and the task planning was changed to substitute a one-half scale model of the MCC machined from aluminum. This was subsequently fixtured and used in numerous trials to electroform structural jacket samples for evaluation of compositional, thickness, and hardness distributions based on anode configurations, anode placement, shielding designs, bath agitation, and other parameters.

It was originally planned to evaluate heat treatment of electroformed alloys and the effects on resulting mechanical properties in this phase of the program. Most of this work had necessarily been performed in the characterization and optimization study under Phase A. This task was redirected to solving problems related to conversion of electroforming from flat panels with typical box shielding for thickness distribution control to cylindrical sections being rotated in an electrolyte with totally different shielding considerations. The scope of Phase B is shown below:

1. Studies of Alloy Composition and Mechanical Property Control on Rotating Cylindrical Mandrels (Section 4.2).

2. Tooling for Electroforming of Prototype SSME Structural Jackets (Section 4.3).

3. Preparations for Electroforming Prototype Structural Jackets (Section 4.4).

4. Electroforming Operations (Section 4.5)

4.2 Studies on Rotating Cylindrical Mandrels

4.2.1 Introduction

In various trials in which thick specimens were being electroformed for subsequent machining into round test bars, significant problems were encountered with respect to accumulated stress and distortion when alloy of a flat configuration was made. Some of these specimens had thicknesses to 1.27 cm (0.5 in.) Since most thick applications of electroforms involving the high performance nickel-manganese alloy would be cylindrical or symmetrical in shape, it was considered essential that continued development and optimizing be performed on such configurations of material.

4.2.2 Status of Thick Flat Electroforms of Alloy

Electroforming of thick flat slabs of electroformed nickel-manganese alloy in shield box fixturing encountered many difficulties due to stress accumulations, distortion, and surface roughness (or nodule formations). However, thicknesses to about 1.067 cm (0.42 in.) were electroformed in two cases involving unbonded deposits on a stainless steel mandrel. At a thickness of about 0.635 cm (0.25 in.), smooth and vertical nodules began to grow near the shield box walls. Each time this occurred it was necessary to remove the slab and mechanically remove the more prominent growths. A standard anodic and cathodic sulfuric acid etch-activation was used to restart the

electroforming process to assure a good bond of new alloy. One slab was produced from an electrolyte operated at 46°C and the other at 52°C, and this rework procedure was necessary on each electroform.

Although each slab thus produced was curved from accumulated stress distortion, it was possible to cut square bars and machine most of them into usable round mechanical property test specimens. As a general observation, the material from the 46°C electrolyte appeared sounder than the 52°C alloy based on the number of round bars produced without crack defects. This may have been related to the amount of mechanical rework needed when nodules became significant. This association with rework was based on the fact that cracks perpendicular to the plating direction were located exactly where the restart was made. Generally, specimens from the central region of each slab machined well with no problems. It was possible to produce round bars with 0.635 cm (0.25 in.) diameter test sections and 0.953 cm (0.375 in.) grip sections. Threading was not necessary, since self-locking jaws were used in the Instron Test Machine. Fabrication data and mechanical property test results for the thick slabs electroformed in the flat condition were as follows:

Flat Slab 125-1

This slab was pulse plated at a duty cycle of 56.67% with the pulse on for 34 msec and off for 26 msec. The peak current density was 4.19 A/dm^2, and the average current density was 2.37 A/dm^2. Single square pattern PVC spray nozzles an cathode bar agitation were used to provide good electrolyte movement at the cathode surface. The bath temperature was 52°C, and the bath manganese concentration was 4.2 g/l. An average of two tests indicated the following mechanical properties:

Ultimate Strength	1189 MPa	(172.5 ksi)
Yield Strength	967 MPa	(140.2 ksi)
Elongation in 1.27 cm	11.5%	
Reduction in Area	53%	

Flat Slab 115-1

This slab was pulse plated at a duty cycle of 64% with the pulse on for 32 msec and off for 18 msec. The peak current density was 3.36 A/dm^2, and the average current density was 2.15 A/dm^2. Also employed were single square spray pattern nozzles, cathode bar agitation, and a bath temperature of 40°C (115°F). Bath manganese concentration was 3.3 g/l. Deposit mechanical properties were:

Ultimate Strength	1166 MPa	(169.1 ksi)
Yield Strength	955 MPa	(138.5 ksi)
Elongation in 1.27 cm	13%	
Reduction in Area	56%	

From the flat slab studies it was concluded that electroforming nickel-manganese alloys in large flat thicknesses must be performed with the material under some form of restraint such as bonding to the mandrel. This prompted electroforming thick alloy in a cylindrical form which was expected to be self-restraining.

4.2.3 Thick Cylindrical Electroforms Using Nickel-Manganese Alloy

The mandrel for electroforming cylindrical thick alloy was fabricated as a 15.24 cm diameter aluminum ring of 12.7 cm height. Outside surface machining provided a six mil taper to permit an easier removal of the thick alloy deposit. Plexiglas shields were applied on the top and bottom of the ring to improve current distribution and thickness uniformity. The first thick specimen was electroformed using a bath temperature of 46°C (115°F) and a cathode rotational speed of 8 RPM. Four square spray pattern electrolyte sprays were used at 90 degree intervals to assure good solution flow deemed necessary from flat slab work. The average current density was 2.4 A/dm^2 and the pulse duty cycle was 64 percent with a pulse on time of 32 msec and an off time of 18 msec. Although the cylinder was electroformed to full thickness, a number of cracks developed after about ten days of plating. These cracks appeared almost equally spaced by sensing with a gloved hand during the actual electroforming. Upon removal of the cylinder from the bath and dismantling the shields, the deposit separated into about five major segments. The inside area (the initial deposit) was cracked extensively but not excessively deep. Figure 4.2-1 illustrates the stainless steel mandrel with shields for electroforming thick cylinders.

It was obvious that the rotational speed of the cathode was imparting a higher degree of agitation to the electrolyte than anticipated. Adding this to the fairly severe spray nozzle agitation probably resulted in excessive manganese codeposition for a bath at 46°C (115°F). For the second thick cylinder, the bath temperature was raised to 48.9°C (120°F) and the spray nozzles were removed and replaced with open short pipe nipples. This was expected to provide an adequate electrolyte volume turn-over without seriously disrupting the cathode diffusion layer so critical to manganese ion diffusion rate. The actual rotational speed was maintained at 8 RPM. The pulse duty cycle, pulse on time, and pulse off time were not changed. The average current density used as 2.15 A/dm^2 and the peak current density was 3.36 A/dm^2. This cylinder was electroformed to a thickness of 1.067 cm without difficulties. The use of the four open pipe nipples to supply fresh electrolyte provided high volume at low pressure appeared to alleviate the high turbulence which caused stress problems on the prior cylinder deposit. The electroform from this run, Cylinder 120-1, was machined to produce round bars and each bar was heat treated at 343°C for 24 hours and four specimens were tested with the following results:

Cylinder 120-1

Ultimate Strength	1347 MPa	(196.8 ksi)
Yield Strength	1126 MPa	(161.2 ksi)
Elongation in 4 Dia. Length	5.8%	
Reduction of Area	25.5%	

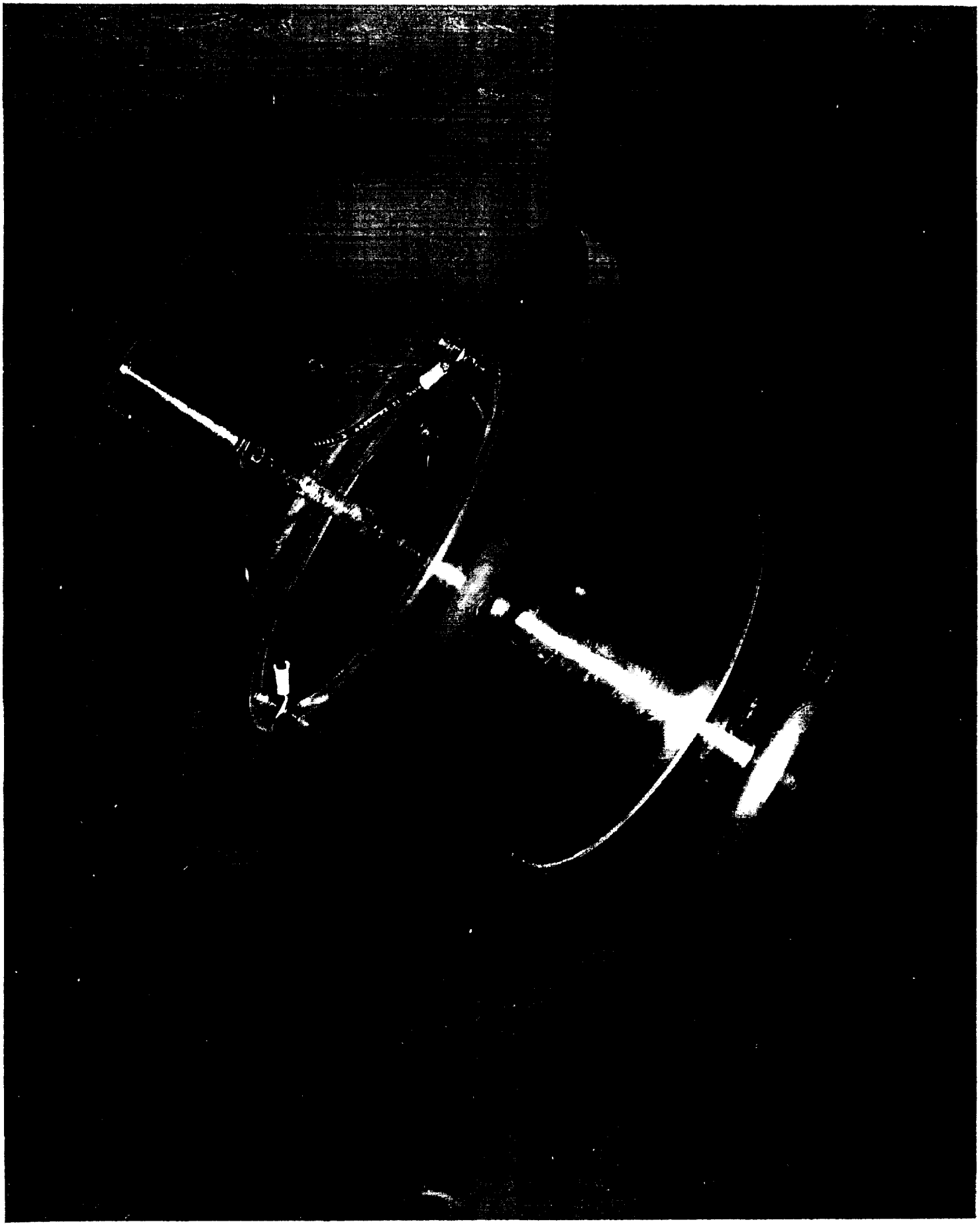

Figure 4.2-1. Thick Cylinder Electroforming Fixture

Another cylinder, Cylinder 120-2, was electroformed from the same bath using a lower pulse duty cycle of 56%. For the same average current density of 2.15 A/dm^2, the lower duty cycle resulted in a higher peak current density of 3.86 A/dm^2. This tended to increase tensile strength and slightly decrease ductility. Had the test data for the prior cylinder been available before starting this part, the parameters would have been different. Cylinder 120-2 cracked into four pieces before completion.

To improve ductility at some sacrifice of ultimate strength, the alloy bath temperature was raised to 51.7°C (125°F) and Cylinder 125-1 was electroformed. The pulse duty cycle for this higher bath temperature was set at 56%. Through over 80 percent of the electroforming cycle, the cylinder was determined to be smooth and uniform. However, an unusually straight vertical crack occurred which resulted in termination of the plating test. Figure 4.2-2 shows the vertical crack in Cylinder 125-1. We suspect that certain electroforming conditions leading to high manganese contents results in very high stresses and fine cracking which relieves the stress temporarily. This fine crack can not be felt with a gloved hand during the electroforming until such time as stress accumulates to a value sufficient to propagate the defect through to the mandrel. The straightness of the crack was surprising. We anticipate that the solution to this problem is to shift the pulse duty cycle to a higher percentage such as 64% or more and/or back off the electrolyte spray pressure a small amount.

Cylinder 125.2 was next made and showed no stress cracks as deposited and after heat treating at 343°C for 24 hours. This cylinder was electroformed from a bath operated at 51.7°C (125°F), a pulse duty cycle of 4%, a pulse on time of 32 msec, an off time of 18 msec, and an average current density of 2.15 A/dm^2. Four open pipe nipples from a pump output system were used for solution spray agitation. The part was rotated at 8 rpm. Specimens cut from this cylinder and heat treated at 343°C for 24 hours furnished the following room temperature mechanical properties:

Cylinder 125-2

Ultimate Strength	1242 MPa	(180.0 ksi)
Yield Strength	982 MPa	(142.4 ksi)
Elongation in 4 Dia. Length	8.75 %	
Reduction in Area	43%	

To determine if we could improve the ductility, Cylinder 125-3 was started through electroforming with the same electroforming parameters, except that the sprays were aimed tangential to the rotating cathode surface rather than directly at the surface. This cylinder and a subsequent cylinder, 125-4, exhibited cracking early in the process.

At the period of time when the cracking problem was found on these cylinders, we were in the process of evaluating a high performance ion chromatography system for rapid analysis of plating baths. An unusual peak was occurring at a very short retention time after test start. This was confirmed to be from the deionized water supplied as electrolyte make-up and level control for the tanks. The water goes through a carbon bed prior to

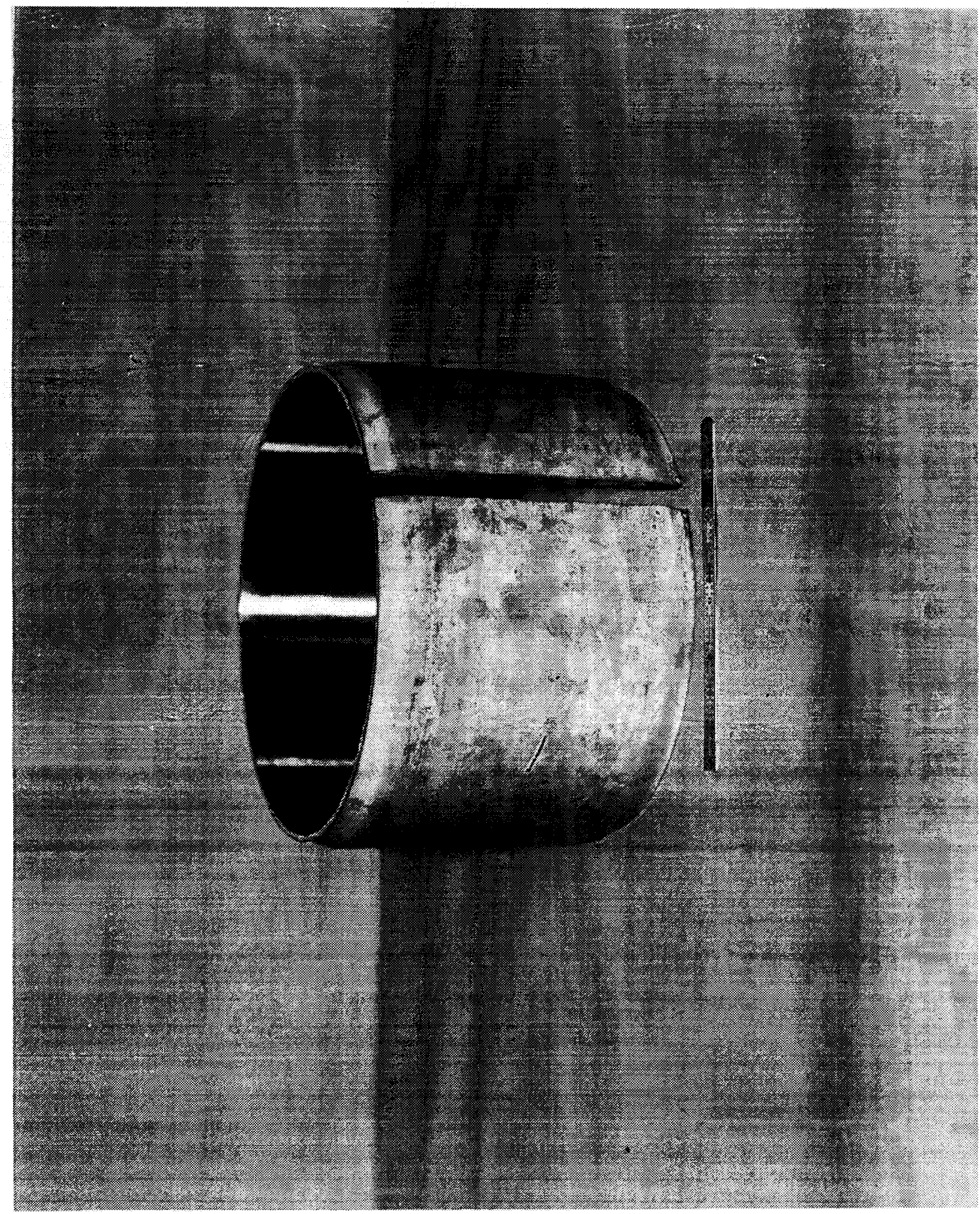

Figure 4.2-2. Vertical Crack in Ni-Mn Alloy Cylinder

entering the tanks as a means of removing organics such as decomposed algae. The chromatograph indicated that aldehydes might be getting into the electrolytes due to depletion of the carbon bed. Although the carbon had been changed prior to the fabrication of the last several cylinders, the accumulated organic matter might have been responsible for high internal stress in the deposits which led to cracking.

Prior to electroforming Cylinder 125-6, the production tank was peroxide treated to decompose organics, excess peroxide was boiled off, and the electrolyte was double carbon treated. The electrolyte wetting agent was replaced and a new thick cylinder, Cylinder 125-6, was produced with no stress cracking. Parameters for this cylinder were bath temperature of 51.7°C (125°F), a pulse plating duty cycle of 64 percent, an average current density of 2.15 A/dm^2 (20 ASF), and a rotational speed of 8 rpm. The electrolyte sprays remained positioned near the tank walls. The alloy was found to contain 1,574 ppm by weight manganese. Round bar specimens were machined from the cylinder and heat treated at 343.3°C (650°F) for 24 hours and provided the following room temperature mechanical properties (results are an average of three tests):

Cylinder 125-6

Ultimate Strength	1071.2 MPa	(155.36 ksi)
Yield Strength	878.1 MPa	(127.36 ksi)
Elongation, % in 4 Dia.	16.17	
Reduction of Area, %	57.33	

Cylinder 120-4 was electroformed from a Ni-Mn alloy bath operated at 48.9°C (120°F), a pulse plating duty cycle of 64%, an average current density of 2.15 A/dm^2 (20 ASF), and a rotational speed of 8 rpm. The electrolyte sprays were positioned near the tank walls. The alloy contained 1,902 ppm of manganese by weight. Round bar specimens machined from this cylinder and heat treated at 343.3°C (650°F) for 24 hours were found to have the following mechanical properties at room temperature (average of three tests):

Cylinder 120-4

Ultimate Strength	1162.1 MPa	(168.54 ksi)
Yield Strength	964.9 MPa	(139.94 ksi)
Elongation, %	13.67	
Reduction of Area, %	50.03	

For Cylinder 120-5, the pulse duty cycle was decreased from 64% to 56% - all other parameters remained the same. Decreasing the pulse duty cycle, for a fixed average current density, requires that the peak current density increase. This increases the amount of manganese codeposited and increases ultimate and yield strengths. This electroformed alloy cylinder contained 2,512 ppm by weight of manganese. Round test bars were machined and heat treated at 343.3°C (650°F) for 24 hours. Three extra round bars were made, but not heat treated, and supplied to NASA-MSFC for verification of our test results. Based on an average of four tests, the following room temperature mechanical property test results were obtained:

Cylinder 120-5

Ultimate Strength	1230.4 MPa	(178.44 ksi)
Yield Strength	994.5 MPa	(144.25 ksi)
Elongation, %	11.75	
Reduction of Area, %	56.00	

These properties are reasonably competitive with ace-hardened Inconel 718 at room temperature. It is probable that even higher mechanical strength can be obtained by (1) reducing the pulse duty cycle to 50% or less, and (2) increasing the average current density from 2.15 A/dm^2 (20 ASF) to 2.58 A/dm^2 (24 ASF). Under these conditions we anticipate ultimate strength to increase to about 1310 MPa (190 ksi) and elongation to be about 10% in a 4D gauge length.

4.3 Tooling for Electroforming of Prototype SSME Structural Jackets

Based on drawings provided by NASA-Marshall Space Flight Center personnel, new drawings were produced from which a one-half scale MCC mandrel was made. The material from which the two-piece mandrel was machined was 6061 Aluminum. The two-piece design was intended to permit assembly and separation of the mandrel for reuse on various electroforming trials. The two separate parts were designed with alignment pins and locking bolts to provide a smooth throat transition with minimal leakage gaps. The aluminum sections were zincated and chromium plated for minimization of corrosion for reuse.

An existing strongback with variable speed gear motor drive was modified for support and rotation of the subscale mandrel. Electrical transfer to the rotating shaft was by means of a mercury well. An illustration of the device with the subscale mandrel and shielding installed is found in Figure 4.3-1. The top and bottom surfaces of the mandrel were drilled to accommodate round acrylic plates by means of screws. The acrylic plates were drilled and threaded at the edges to accommodate variable end shields to control edge current density.

4.4 Preparation for Electroforming Prototype SSME Structural Jackets

The purpose of this portion of the effort was to conduct electroforming trials using the subscale MCC mandrel and associated tooling. The initial trials were to develop information on primary metal distribution and what shielding modifications would be needed for subsequent work. The factors governing electroform thickness and compositional distribution over an object of complex shape, such as the Space Shuttle MCC include close control of spacing of the anode and cathode (primary current loss due to solution resistance), and agitation which affects the solution to part interface or double layer (secondary current distribution effects). With conventional EF Ni there is a need to selectively control current density distribution so that the growth rate at the throat region of the MCC or Structural Shroud is approximately the same as at the forward and aft ends of far greater diameters. Another reason for controlling the localized current density in EF Ni is the fact that mechanical properties change with current density. Generally, a significant increase in current density lowers tensile and yield strength while slightly increasing elongation.

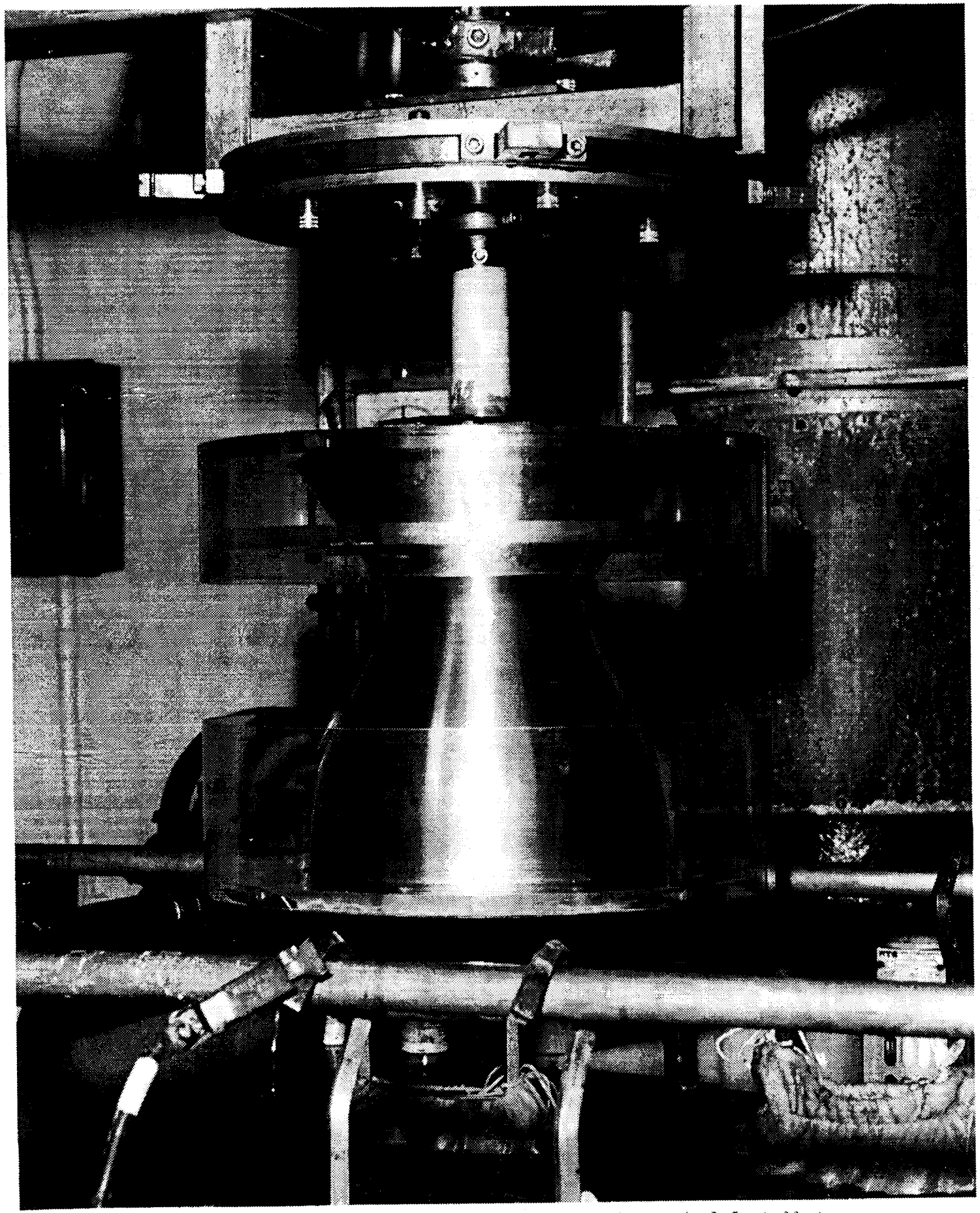

Figure 4.3-1. Fixturing for Rotation with Subscale Mandrel Installed

EF Ni-Mn alloy deposition requires additional considerations since mechanical property relationships are primarily dependent on manganese content of the alloy and the manner in which it is dispersed or codeposited with nickel. Since the high thermal strength of EF Ni-Mn alloy is derived from a small controlled percentage of manganese, the importance of compositional uniformity and distribution cannot be over-emphasized.

Factors affecting manganese codeposition with nickel include principally the concentration of manganese in the electrolyte, manganese valence (or oxidation state), current density, electrolyte temperature, and agitation of the solution adjacent to the electroform surface. The concentration of manganese in the alloy is a rapidly increasing non-linear function of current density (see Figure 4.4-1). Therefore, current density differences from improper primary and secondary current distribution control can lead to greatly varied mechanical properties. Total manganese content in the electrolyte and solution temperature are readily controlled. The need exists to maintain the divalent Mn concentration and all operating parameters during tests. The manganese content of the alloy increases with both manganese concentration in the solution and current density, and decreases with increased electrolyte temperature. Agitation of the electrolyte is a secondary effect equally important to shielding in control of manganese distribution in the alloy.

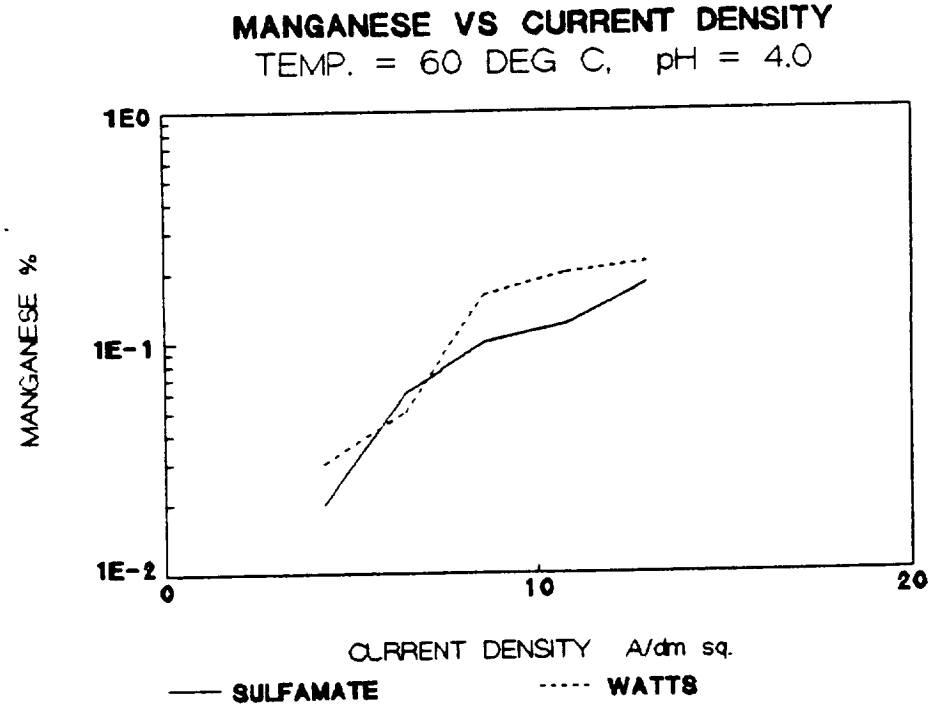

Figure 4.4-1. Manganese vs. Current Density

In Trial Run No. 1 only the acrylic end plates were mounted on the aft and forward ends of the subscale MCC mandrel. This was to determine if pulse plating would by itself promote reasonable deposit uniformity. Using a typical pulse plating setting of 50 percent duty cycle and an average current density of 2.15 A/dm^2, the mandrel was electroformed for two days and evaluated. The alloy deposit was found to be splitting at both forward and aft ends of the subscale mandrel. It was concluded that end plates alone would not reduce end edge current density enough to prevent high current density accompanied by high manganese content in the alloy at these locations. Such high manganese contents lead to abnormally high stress and low ductility.

A second trial was made with ring-shields mounted on the acrylic end-plates. Both ring-shields were made from 38.1 cm diameter acrylic tubing. The forward end shield had a length of 5.08 cm and the length of the aft end ring-shield was 7.62 cm. Identical pulse plating conditions were used for the first and second trials. The electrolyte manganese concentration in both trials was 3.5 g/l. At the end of Trial Run No. 2 it was noted that alloy cracking was eliminated at the forward end. Cracking was still observed at the aft end, and this was thought to be due to high current density encroachment through small hydrogen outgassing holes intentionally drilled in the acrylic end-plate. These holes were plugged and a hydrogen gas relief pipe installed to prevent high current density through the end-plate. This improved the condition on Trial Run No. 3, but cracking was not entirely eliminated. An illustration of the end shielding used for the third run is found in Figure 4.4-2.

It had been intended to bring the manganese ion concentration to 4.6 g/l in this study to equal the concentrations used in flat specimen electroforming in prior tasks. It was decided to limit this concentration to 3.5 g/l as a result of the cracking experienced on subscale mandrels being rotated at slow speeds in the large 960 liter production tanks.

For Trial Run No. 4 the top shield (aft end) was modified by making the acrylic cylinder section longer so that a series of fastener holes could be drilled at different stations (if required) to make the effective length over the mandrel adjustable. A further current density distribution control was provided by adding a "choke". This consisted of an acrylic ring which could be attached to the inside of the top shield. By adjusting the location at which this ring was attached to the top shield, the opening between the "choke" and the mandrel could be changed to limit the flow of current. An illustration of this shielding and modifications after attaching to the mandrel is found in Figure 4.4-3. Before the modifications of the shielding, cracking of the deposit was very severe. Once cracks started in the thicker (more highly stressed) end locations adjacent to the shield plates, they appeared to propagate through the thinner alloy at the middle of the mandrel until they extended to the full mandrel length as shown in Figure 4.4-4.

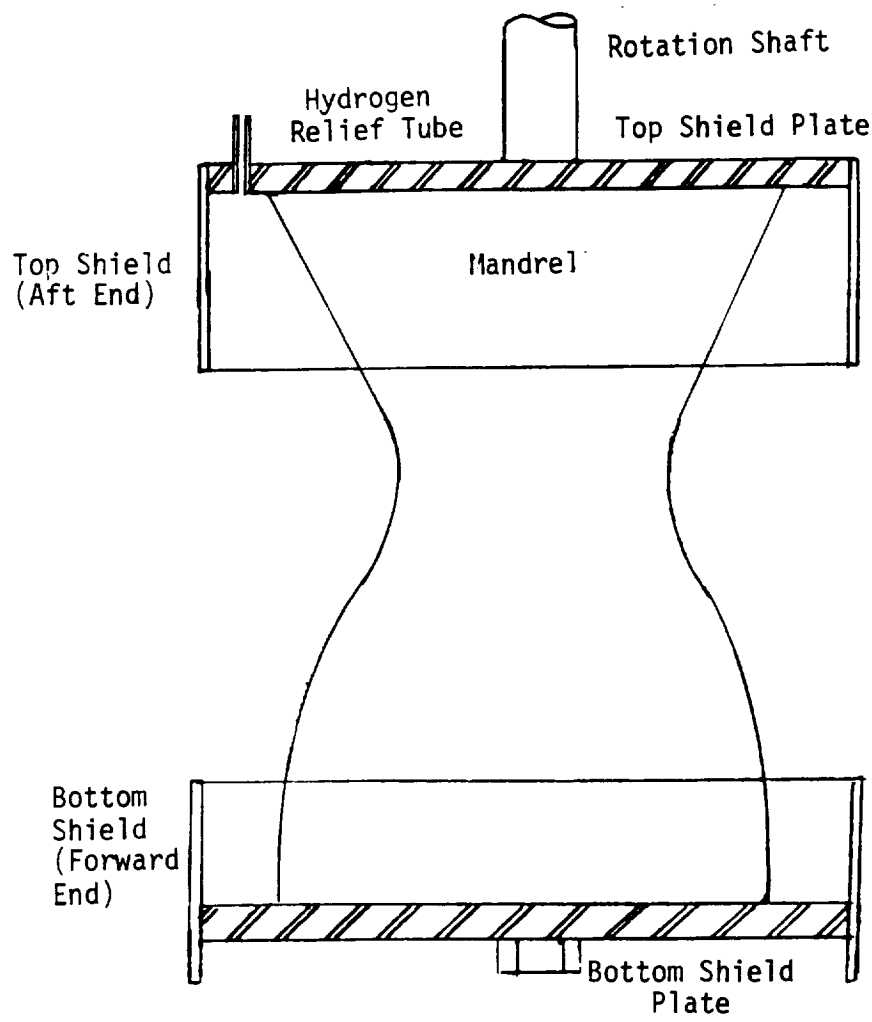

Figure 4.4-2. Shielded Mandrel for Run No. 3

By means of micrometer readings it was determined that Trial Run No. 4 produced a structural jacket having a typical thickness of 0.203 cm at the forward end but with less than 0.102 cm thickness at the throat. It was not possible to make a clean separation of the two-piece mandrel from the shell that was electroformed in this trial. The shell had to be removed by dissolving the alloy in nitric acid. The mandrel was remachined to provide a three degree draft at the forward end for easier separation.

One of the problems that had to be resolved in this preparatory effort for the subsequent task of structural jacket electroforming was that of pulse plating rectifier capacity. The particular pulse plating power supplies on hand were of 30 ampere maximum average current capacity. The area of the subscale mandrel was 0.166 m^2 (16.6 dm^2). Using only one power supply would only permit a current density to 1.81 A/dm^2. It was possible to electrically tie two such power supplies in a parallel circuit to provide a 60 ampere maximum average current. A special electronic circuit board (available from the manufacturer) could be inserted in each unit to allow one power supply to time the pulse frequency and duty cycle in each unit for synchronization. An illustration of this combination is found in Figure 4.4-5.

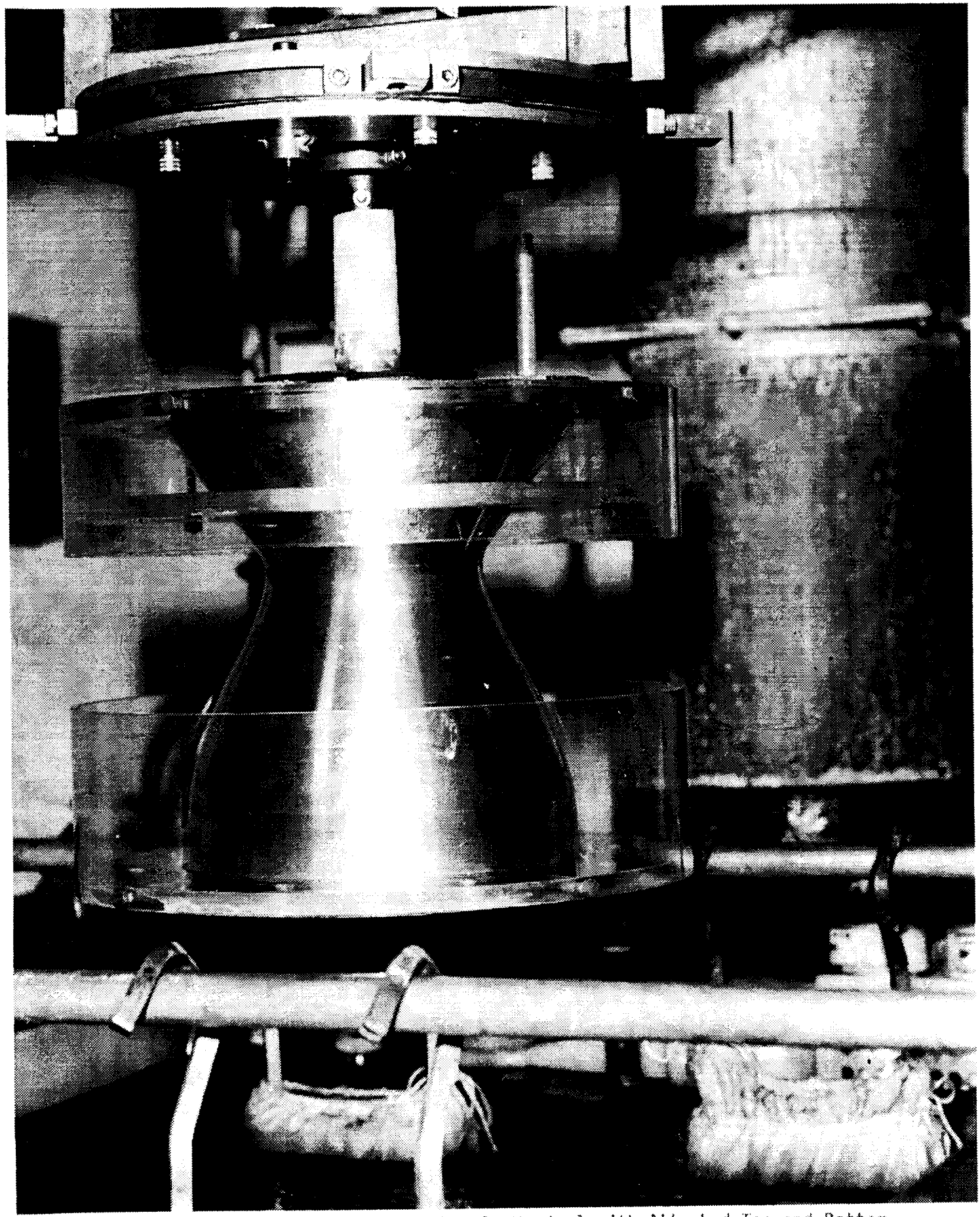

Figure 4.4-3. Fixtured Subscale Mandrel with Attached Top and Bottom Plexiglas Shields

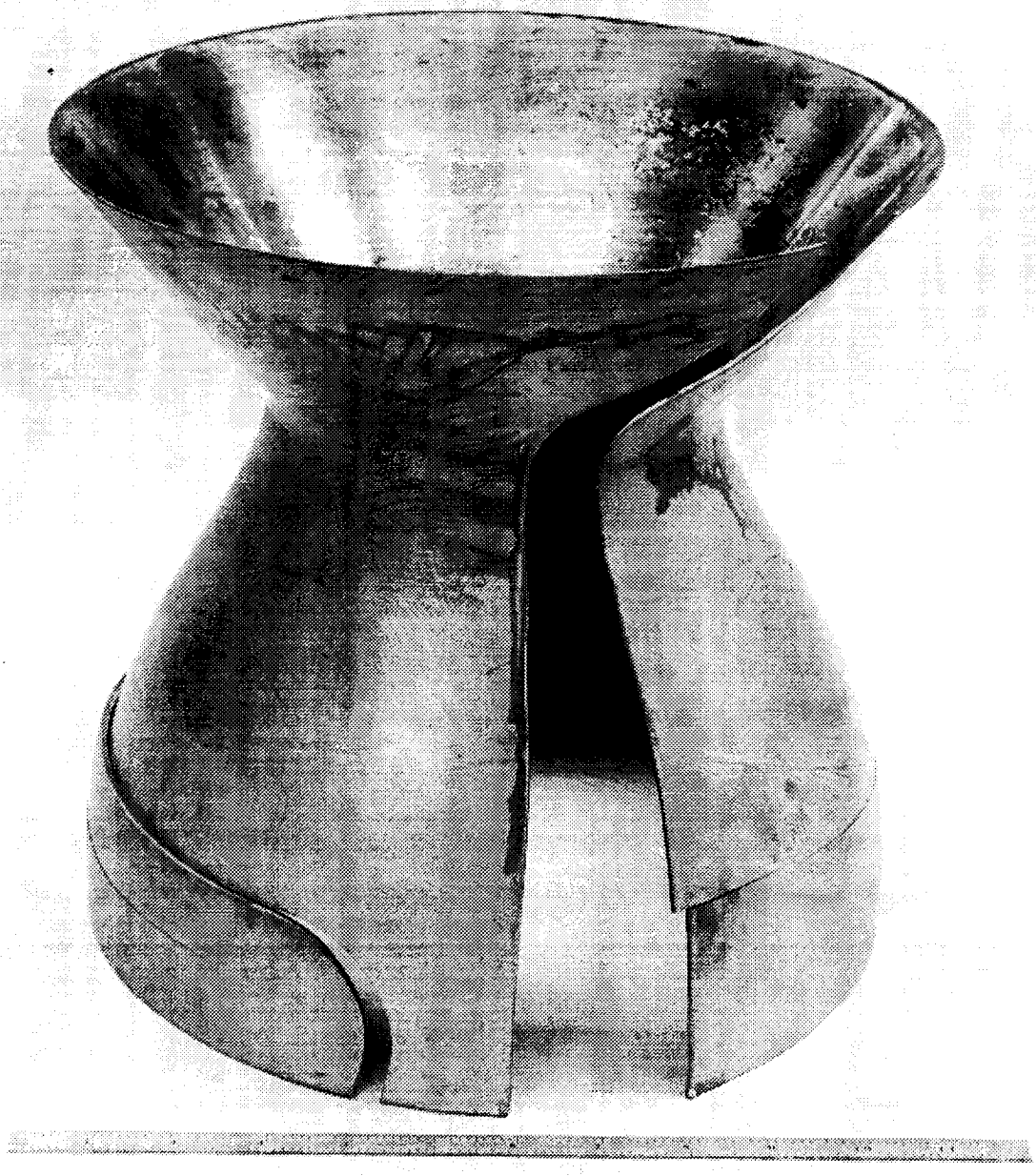

Figure 4.4-4. Cracking in Alloy Shell Structure Resulting from Inadequate Current Distribution Control

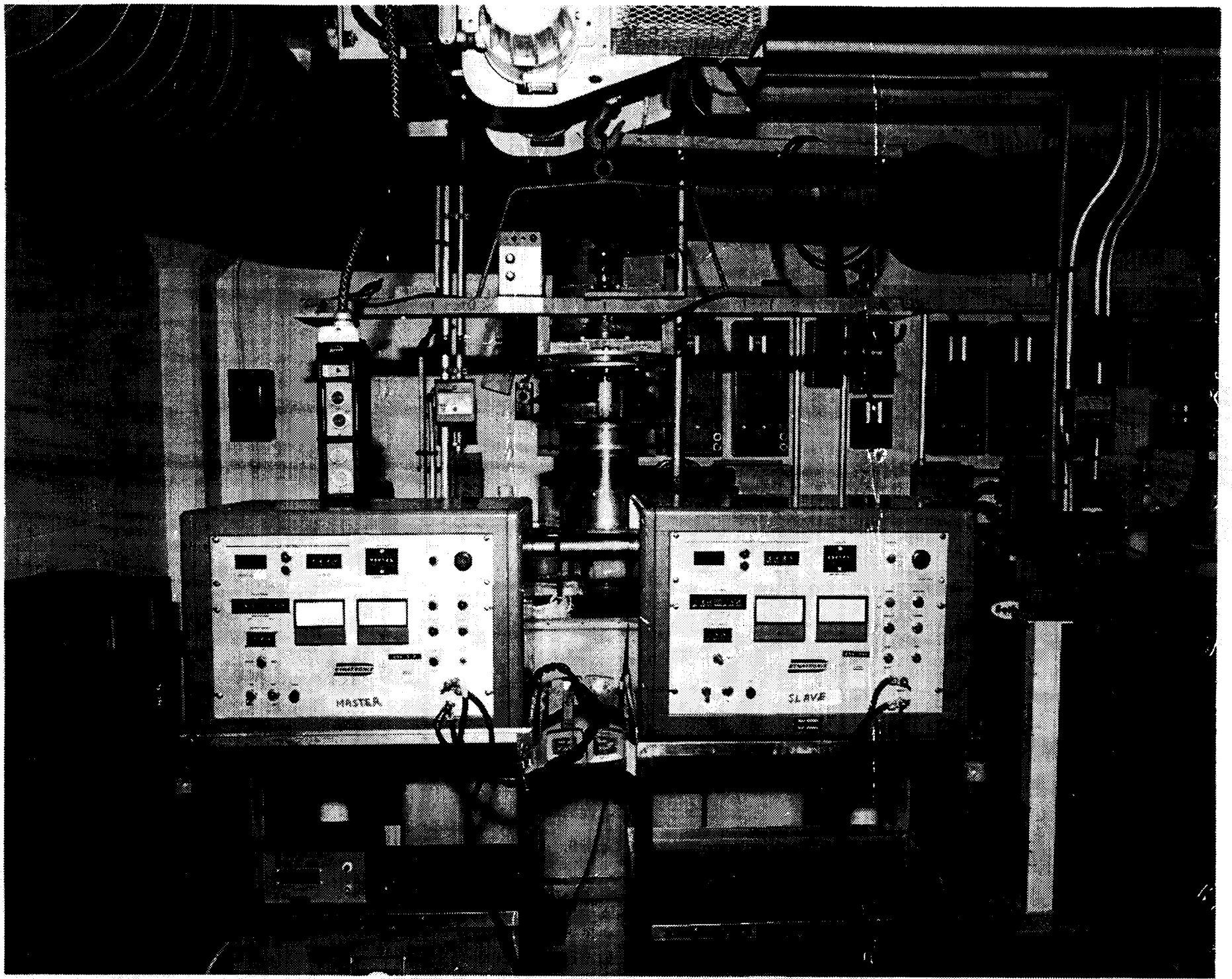

Figure 4.4-5. Illustration of Facility with Parallel Pulse Plating Power Supplies and Fixtured Mandrel

From the results of the fixturing and basic shield trial runs in this part of the electroforming study it was concluded that edge cracking of the alloy could be prevented by shielding control to inhibit excessive manganese codeposition at what would normally be high current density regions. Simple shielding does not sufficiently control primary current distribution on the complex shapes typical of the MCC profile and wide ranges of alloy composition may be expected with consequent differences with regards to mechanical properties. A more sophisticated approach to shielding and current distribution was considered (see Section 4.5).

4.5 Electroforming Operations for SSME Structural Jackets

The use of simple ring shields failed to provide adequate primary current distribution in electroforming a reasonably uniform wall thickness on the trial structural jackets runs previously described. Alternate shielding techniques had to be evaluated, and the first of these was the serrated shield employed on actual MMC electroformed nickel close-outs over the thin copper electrodeposits hydrogen barrier layer over cooling channels in the copper-silver-zirconium liner alloy. Two such serrated cylindrical shields are used in this electroforming process - one is located at the aft end of the liner, and the other is positioned at the forward end. The design of these shields is based on mathematical calculations furnished in Rocketdyne Materials Laboratory Technical Bulletin No. 1053. From the formula for plotting incremental area ratios, distance ratios, plotting factors, and shield design factors, the individual shield serrations and distances between each can be determined. The shields can be made in 90 degree segments and four segments cemented after thermally bending to provide a radius at least 5.08 cm greater than the radius of the aft (or forward) end of the chamber being shielded.

It should be noted that the serrated, or scalloped, shield is not fastened to the acrylic end plates secured to the forward and aft ends of the mandrel. The mandrel must be free to rotate independently of the scalloped shields so that all areas of the mandrel are equally exposed to the openings provided in the shield configuration. Failure to make this provision would lead to a deposit of alloy which was alternately thick and thin in the same pattern as the shields. The rotation device employed to drive the subscale mandrel was equipped with a drive gear mounted on the primary drive shaft. Two thin plates mounted above and below this gear supported a second gear which drove an internally geared ring. This resulted in a ring rotation in a direction opposite that of the primary drive shaft. By attaching the scalloped shields to the gear driven ring, the shields could be made to rotate in a direction opposed to that in which the mandrel rotated.

Figure 4.5-1 shows the subscale mandrel with the scalloped shields in place and ready for immersion into the alloy plating bath. Figure 4.5-2 is another view of the mandrel with scalloped shielding with more detail of the drive mechanism and anode arrangement for the electroforming trial. Using the same pulse plating parameters previously described for these trial runs, a "thin" jacket was electroformed for evaluation. A strip was cut from aft to forward ends and measured for thickness at selected stations. Chips were milled from each station and analyzed for manganese by atomic absorption spectroscopy. Figure 4.5-3 shows the jacket profile and test results at each

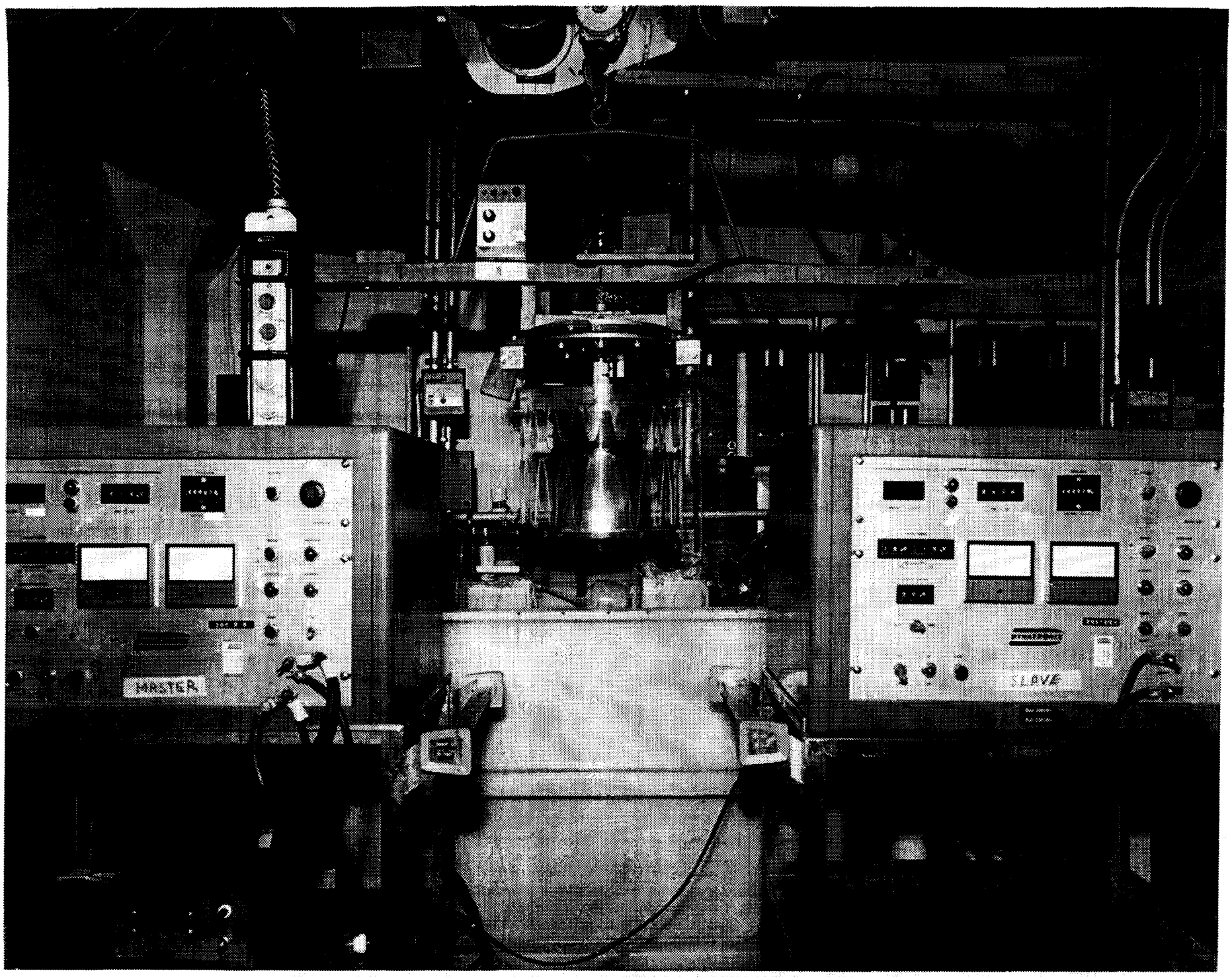

Figure 4.5-1. View of Subscale Mandrel with Scalloped Shields Installed and the Alloy Electroforming Facility

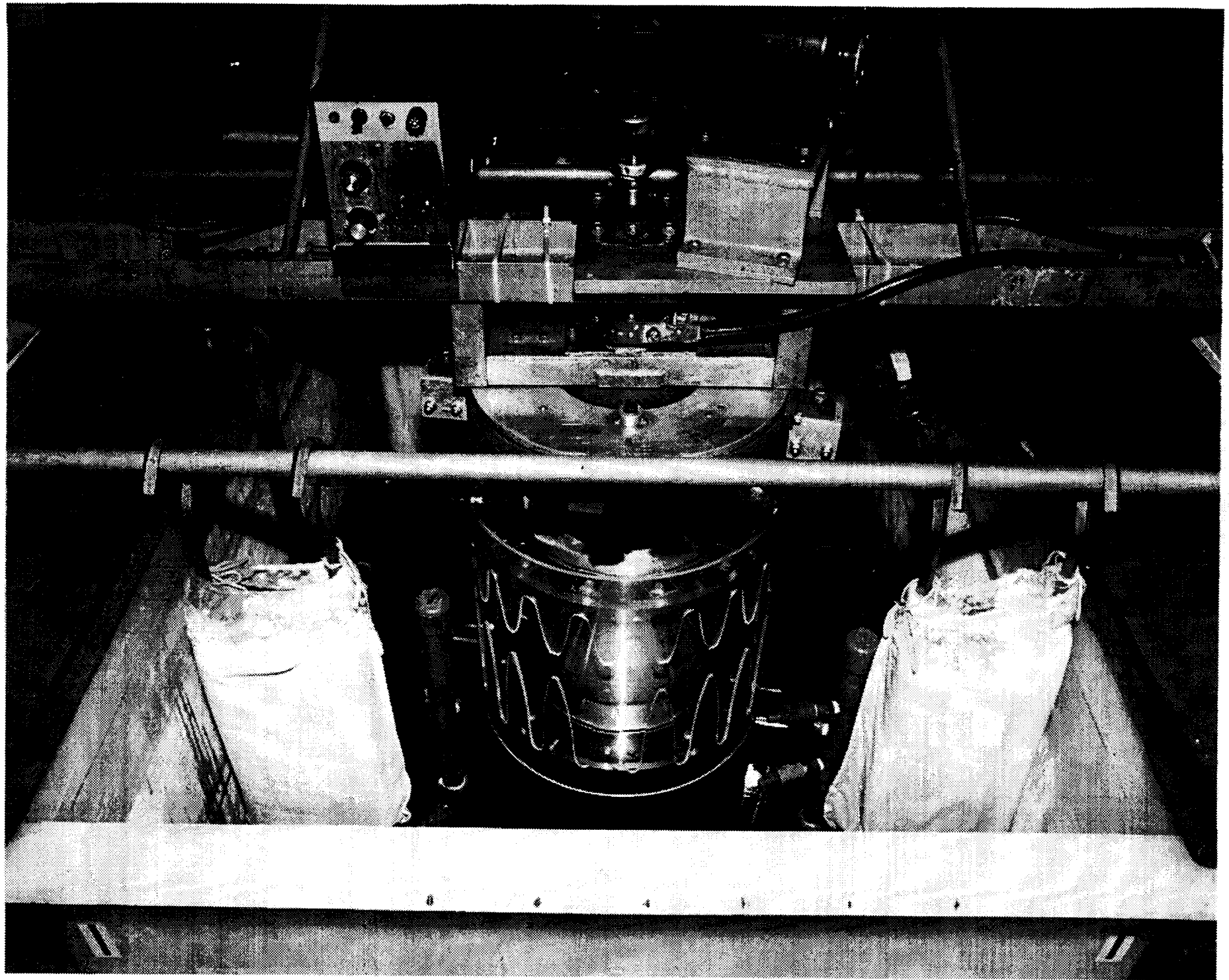

Figure 4.5-2. Partially Emptied Electroforming Tank Showing Shielded Mandrel and Spray Relationship

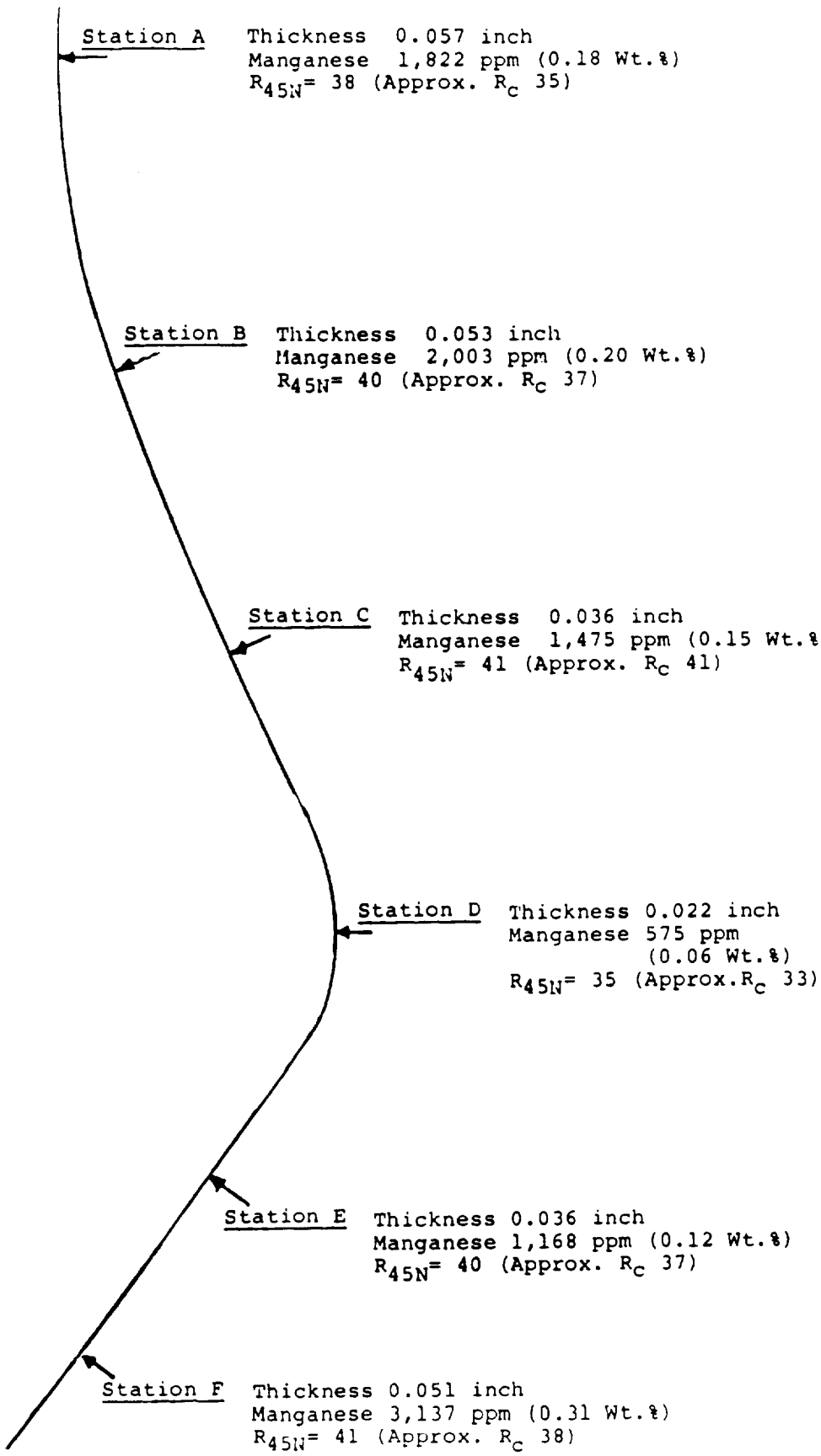

Figure 4.5-3. Test Results from Electroformed Ni-Mn Alloy Shell from Subscale MMC Mandrel Using Scalloped Shields

station. The Rockwell C indentor could not be used over the entire profile due to thickness constraints at the throat. Where this situation existed, coupons were cut from the strip and subjected to Rockwell 45N scale testing with a superficial indentor. Results were converted to Rockwell C readings. From thickness measurements it was noted that the serrated shields such as used on conventional nickel close-outs on production MCC hardware did not provide adequate thickness distribution for alloy electroforming. The throat area experienced only about one-half, or less, of the average build-up found on the forward and aft sections. It was noted that manganese concentrations in the alloy were not directly proportional to the measured thicknesses. This was to be expected based on the fact that thickness is a function of current density, and manganese concentration increases exponentially with increasing current density. It is also possible that manganese concentration deviations could be partially due to cathode surface agitation differences imposed by the shields.

Diameters vary from station to station on the subscale MCC mandrel. Since the mandrel is rotated, the resulting tangential surface velocities at each station will be different and the surface agitation governing cathode diffusion layer thickness will be affected to different degrees. This indicates that a more complex system for control of primary current distribution may be needed. Such a system might involve separate anode arrays spaced in such a manner as to provide more optimum anode cathode spacing with respect to both the MCC throat area and the forward and aft regions. Separate pulse power supply units (with pulse synchronization) might provide means of simultaneously varying current densities at regions of greatest solution agitation differences. This would possibly promote more uniform manganese compositions at the throat and extremities. Such an approach was considered and evaluated in Phase C efforts as an extension of this task.

5.0 PHASE C - EVALUATION OF ELECTROFORMING MATERIALS AND PROCESSES

5.1 Introduction

In Phase C of this program, the alloy system and processing procedures developed during the preceding phases were further evaluated and improved. This phase was divided into four tasks:

Task 1 - Additional Material Data

Development of additional electroformed alloy material data and comparisons with electroformed nickel and Inconel 718.

Task 2 - Process Development

Process development and verification studies to assure that the electroformed alloy can be bonded to other materials of construction used in the Space Shuttle main combustion chamber (MCC).

Task 3 - Shield Development

Expanded shield design studies in order to improve the electroform thickness and compositional distribution over an object of complex shape such as the Space Shuttle MCC.

Task 4 - Design Refinement

A feasibility study on the design changes required to change from a welded structural jacket to an electroformed jacket.

5.2 Task I - Additional Material Data

5.2.1 Introduction

In order to perform the special evaluations of this task, it was necessary to electroform nickel-manganese alloy to a thickness of 0.4 inches for fabrication of round test bars. In addition to reporting the conventional mechanical properties obtained the following tests were all made from this one sample (Cylinder 120-5):

1. Thermal Fatigue
2. Notch Sensitivity
3. Creep or Stress Rupture
4. Hydrogen Embrittlement
5. Thermal Secondary Fabrication Processes (i.e., welding)

5.2.2 Fabrication of Test Material

Nickel-manganese alloy was electroformed on a cylindrical stainless steel mandrel in order to simulate real Space Shuttle Main Engine (SSME) hardware where deposition is on a rotating mandrel. Figure 5.2-1 illustrates the mandrel with shields. The thick electroformed alloy for fabricating test specimens is shown in Figure 5.2-2.

Cylinder 120-5 was produced from a nickel-manganese alloy bath operated at 48.9°C (120°F), a pulse plating duty cycle of 56% (28 msec on, 22 msec off), and an average current density of 2.15 A/dm^2 (20 ASF). The peak current density was 3.84 A/dm^2 (35.68 ASF). Four equally spaced electrolyte sprays were used to provide fresh solution at the mandrel surface. A cathode rotational speed of 8 rpm was used. The bath was operated with 75 g/l nickel metal, 38 g/l boric acid, 3.1 g/l manganese metal at a pH of 4.15-4.35.

The electroformed alloy cylinder contained 2,512 ppm by weight of manganese. Round test bars were machined and heat treated at 343.3°C (650°F) for 24 hours to stress relieve the material. For comparison round test bars of conventional EF nickel were machined and heat treated at 343.3°C (650°F) for one hour. Inconel 718 in the age-hardened condition was also provided for comparison of properties to that of the electroformed nickel-manganese alloy.

Tensile tests for EF nickel-manganese, EF nickel, and age-hardened Inconel 718 were performed over the temperature range of 20°C to 204.4°C (68°F to 400°F). Test results for all three materials are compared graphically in Figure 5.2-3.

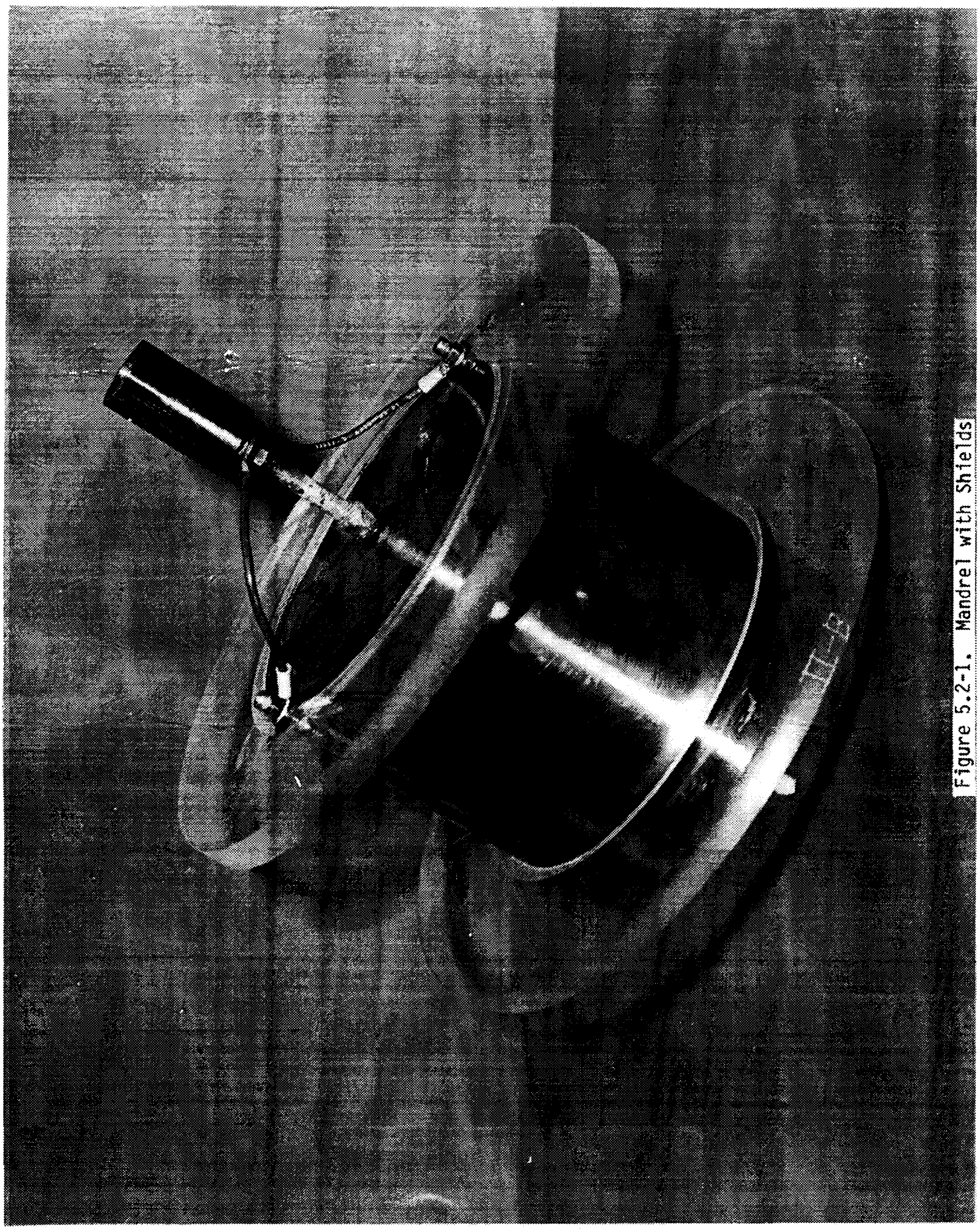

Figure 5.2-1. Mandrel with Shields

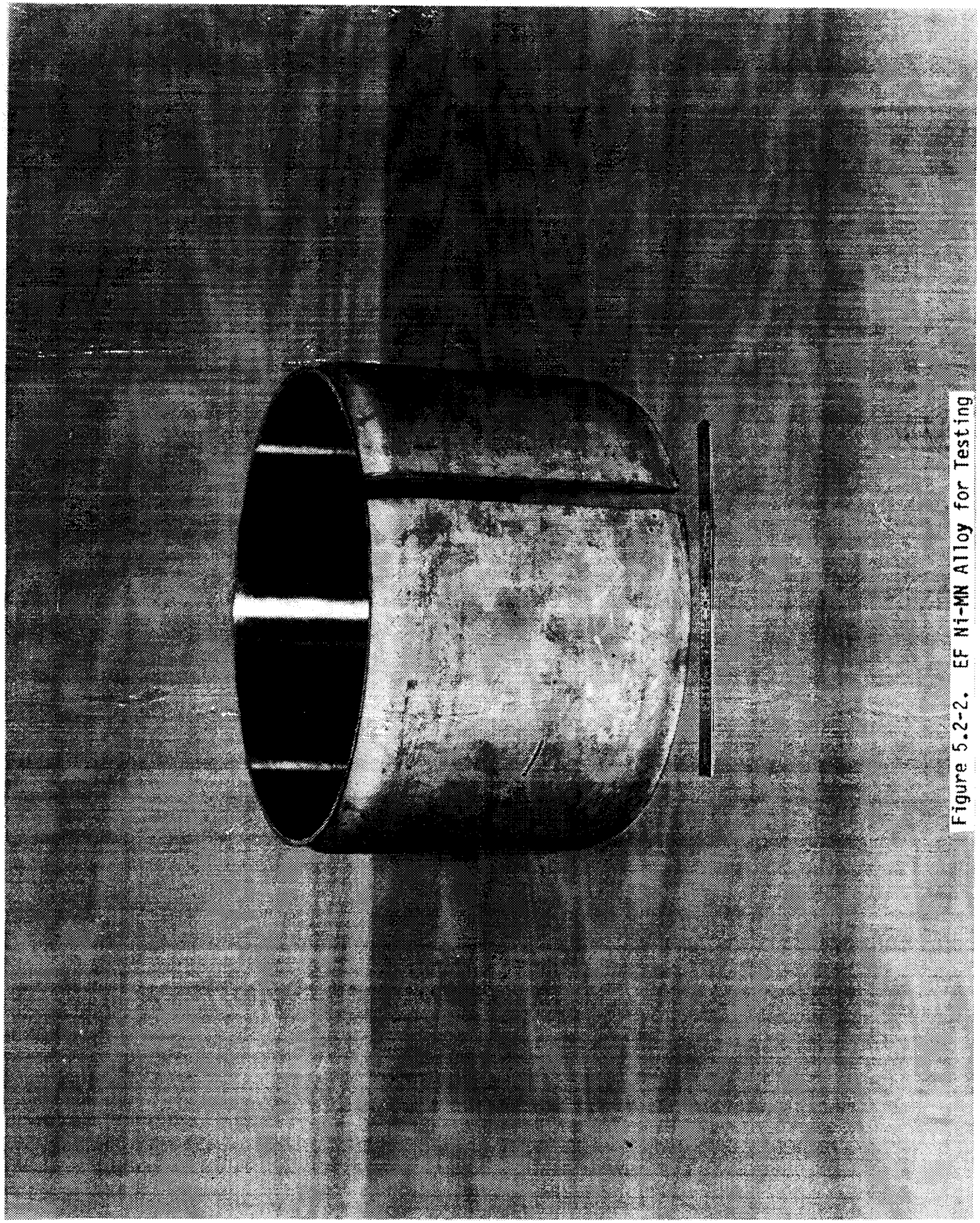

Figure 5.2-2. EF Ni-MN Alloy for Testing

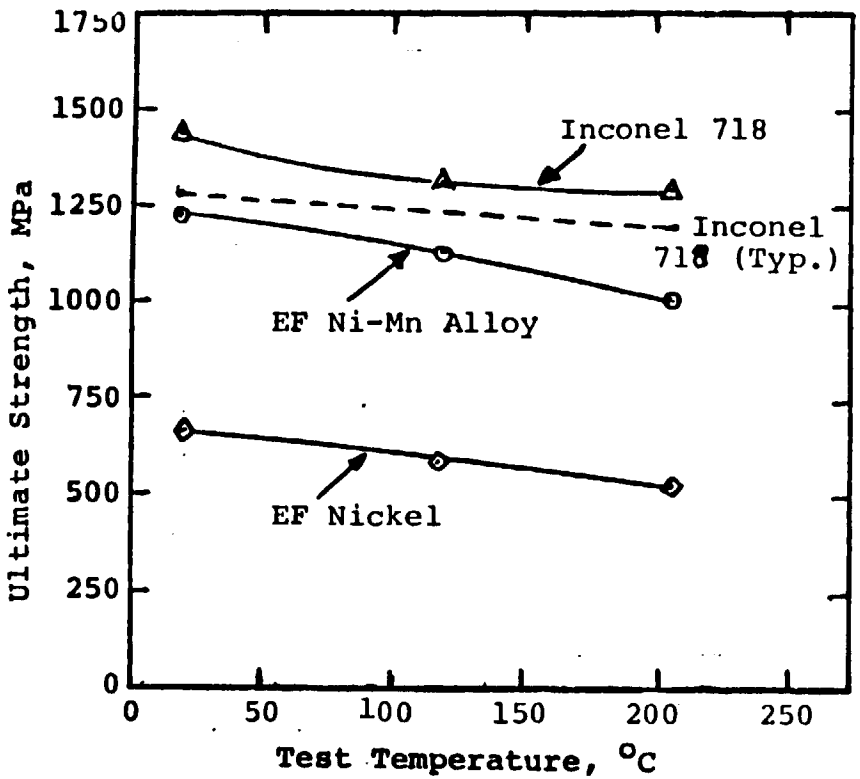

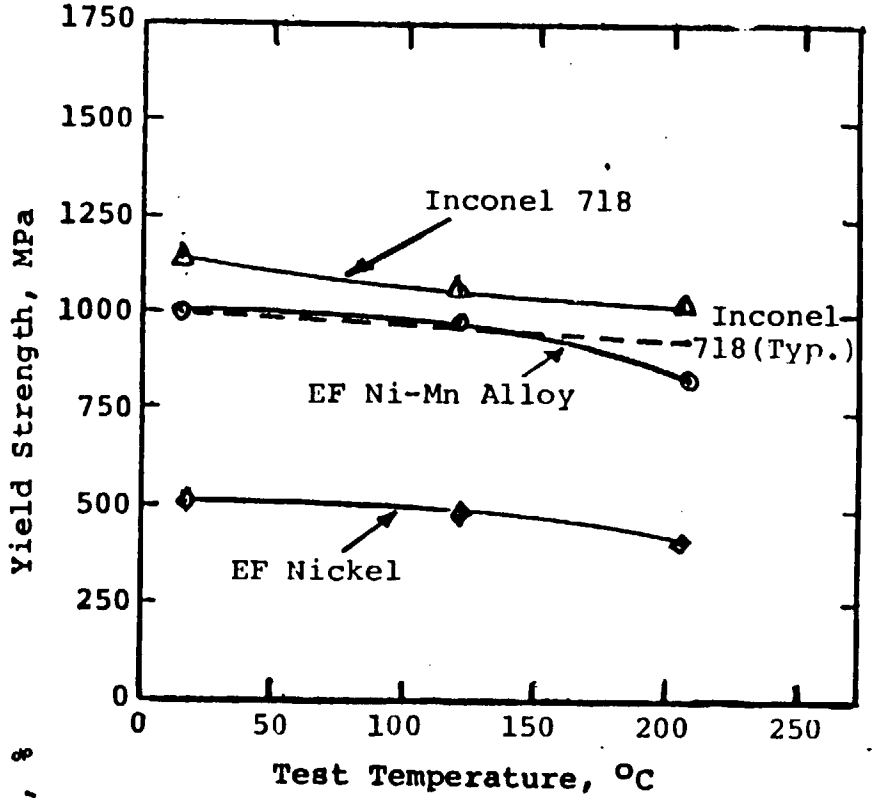

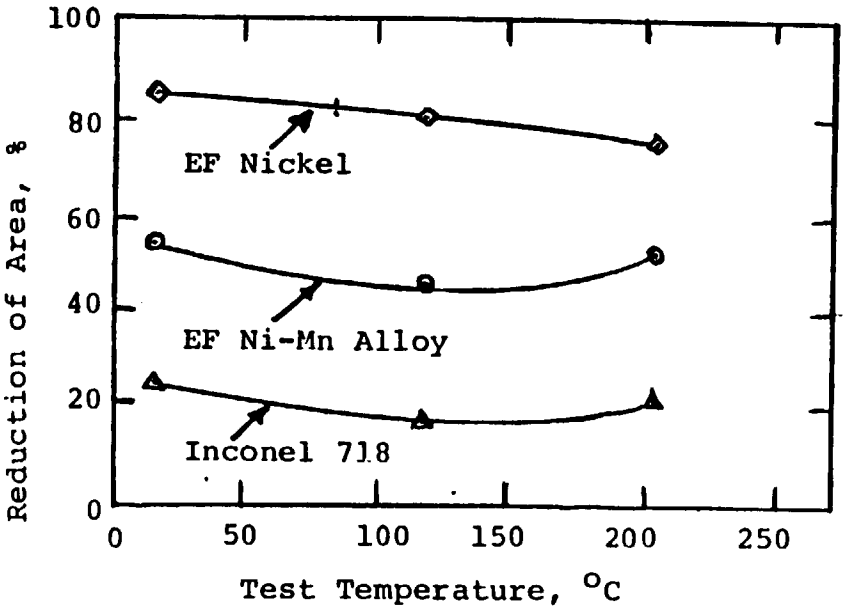

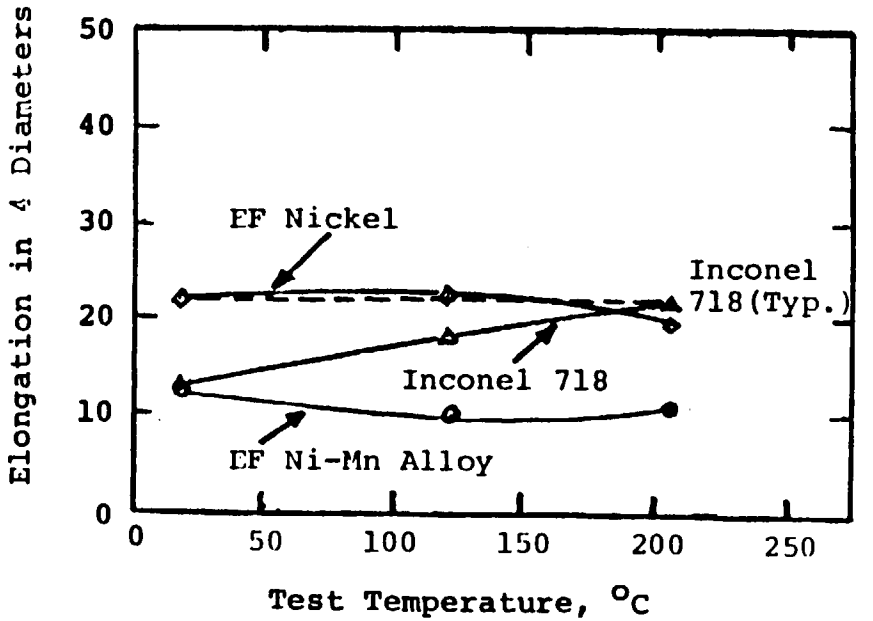

Figure 5.2-3. Comparisons of Mechanical Properties of EF Nickel, EFNi-Mn and Inconel 718

The test results shown for the Inconel used in this study appeared rather high and may not represent the typical mechanical properties expected. This may be due to minor variations in chemistry or aging treatment. Dotted lines are shown in Figure 5.2-3 for Inconel 718, mill annealed sheet aged at 1325^{o}F for 16 hours (as reported from Alloy Digest, April 1961).

The yield and ultimate strength of the electroformed nickel-manganese is about twice that of conventionally electroformed nickel, and very nearly approaches that of age-hardened Inconel 718. The EF Ni-MN alloy ductility was such that the elongation remained above 10% in a 4D gauge length.

5.2.3 Thermal Fatigue of Electroformed Nickel - Manganese Alloy

Critical to the continued, reliable operation of the Space Shuttle Main Engine or any other re-usable rocket engine is the ability of the material to survive multiple cycles of stress (fatigue) at the temperatures of interest. Even in an efficiently cooled engine structure such as the SSME, variations in temperature, both within the engine at any one time, and over the firing time cycle, will produce significant stresses on all portions of the structure, with those stresses often exceeding the yield strength of the material in tension and in compression. In order to obtain a preliminary judgment on the potential improved performance of this electroformed nickel-manganese alloy under these severe conditions of high strain (post-yield) fatigue, a series of reversed strain fatigue tests of both the alloy electroform and conventional nickel electroform were conducted.

The testing was conducted using threaded end, cylindrical shaped tensile samples of the same configuration previously described. As already mentioned, these test samples were unique in being fabricated from thick walled cylinders of electroformed material. Thus the material closely simulated the material that would be in an SSME chamber of this alloy, and yet the specimens, being cylindrical, gave properties much more representative of true material properties than would have been obtained from flat sheet samples. In all significant aspects, this fatigue testing followed the ASTM Specification E606, "Standard Recommended Practice for Constant Amplitude Low Cycle Fatigue Testing". The uniform profile, or cylindrical sample type was used and all testing was performed on an MTS 20 KIP electrohydraulic closed loop testing machine, with strain being monitored by a strain-gaged longitudinal extensometer, which also served as the controlled parameter for the testing machine. Where tests were performed at 121^{o}C (250^{o}F) or 204^{o}C (400^{o}F), an RI quartz tube radiant heater was used for controlled heating of the sample, and the extensometer was shielded and cooled so that its active elements (strain gages) continued to give accurate and calibrated output. All tests were conducted per the ASTM E606 practice of using fully reversed tensile/compression stressing, and were continued until specimen failure.

A tabulation of all data obtained from the low cycle fatigue testing of nickel-manganese alloy electroform, conventional nickel electroform and heat treated Inconel 718 are given in Table 5.2-1. The limited number of Inconel 718 tests were included to provide a reference to a common high strength material used in thrust chamber design and construction. Data includes the total strain range, cycles to failure (defined as complete separation),

TABLE 5.2-1. TEST RESULTS FOR LOW CYCLE/HIGH STRAIN FATIGUE TESTING OF ELECTROFORMED NICKEL

Material Type	Sample No.	Test Temp.	Total Strain Range (Constant thru Test)	Cycles to Failure	Max Stress At Start of Test KSI	Max Stress At Start of Test % of Yld.	Max Stress At Mid Life (KSI)
Nickel-Manganese Alloy Electroform	A-14	Room Temp. (21°C/70°F)	0.010 (±0.005)	2,175	125	87%	109
	A-15		0.016 (±0.008)	353	147	102	127
	A-16		0.008 (±0.004)	2,820	107	75	103
	A-17		0.004 (±0.002)	15,080	69	48	67
Conventional Nickel Electroform	N-8		0.020 (±0.010)	242	89	120	68
	N-9		0.011 (±0.0055)	1,130	81	109	62
	N-12		0.008 (±0.004)	2,337	68	91	66
	N-14		0.008 (±0.004)	2,526	68	91	64
	N-13		0.008 (±0.004)	2,708	64	86	60
	N-15		0.004 (±0.002)	23,861	51	68	44
Inconel 718 (Double Aged)	I-4		0.016 (±0.008)	343	177	105	158
Nickel-Manganese Alloy Electroform	A-18	121°C/250°F	0.016 (±0.008)	162	143	101	116
	A-19		0.010 (±0.005)	1,100	129	92	104
	A-20		0.004 (±0.002)	19,100	66	47	65
Conventional Nickel Electroform	N-16		0.016 (±0.008)	62	79	110	66
	N-17		0.010 (±0.005)	729	73	103	58
Inconel 718 (Double Aged)	I-5		0.016 (±0.008)	299	181	115	152
	I-6		0.008 (±0.004)	3,386	122	78	116
Nickel-Mn Alloy Electroform	A-23	204°C/400°F	0.010 (±0.005)	295	127	103	113
	A-24		0.016 (°0.008)	110	129	105	112
Conventional Nickel Electroform	N-19		0.010 (±0.005)	324	66	105	43
	N-20		0.016 (±0.008)	95	62	98	55

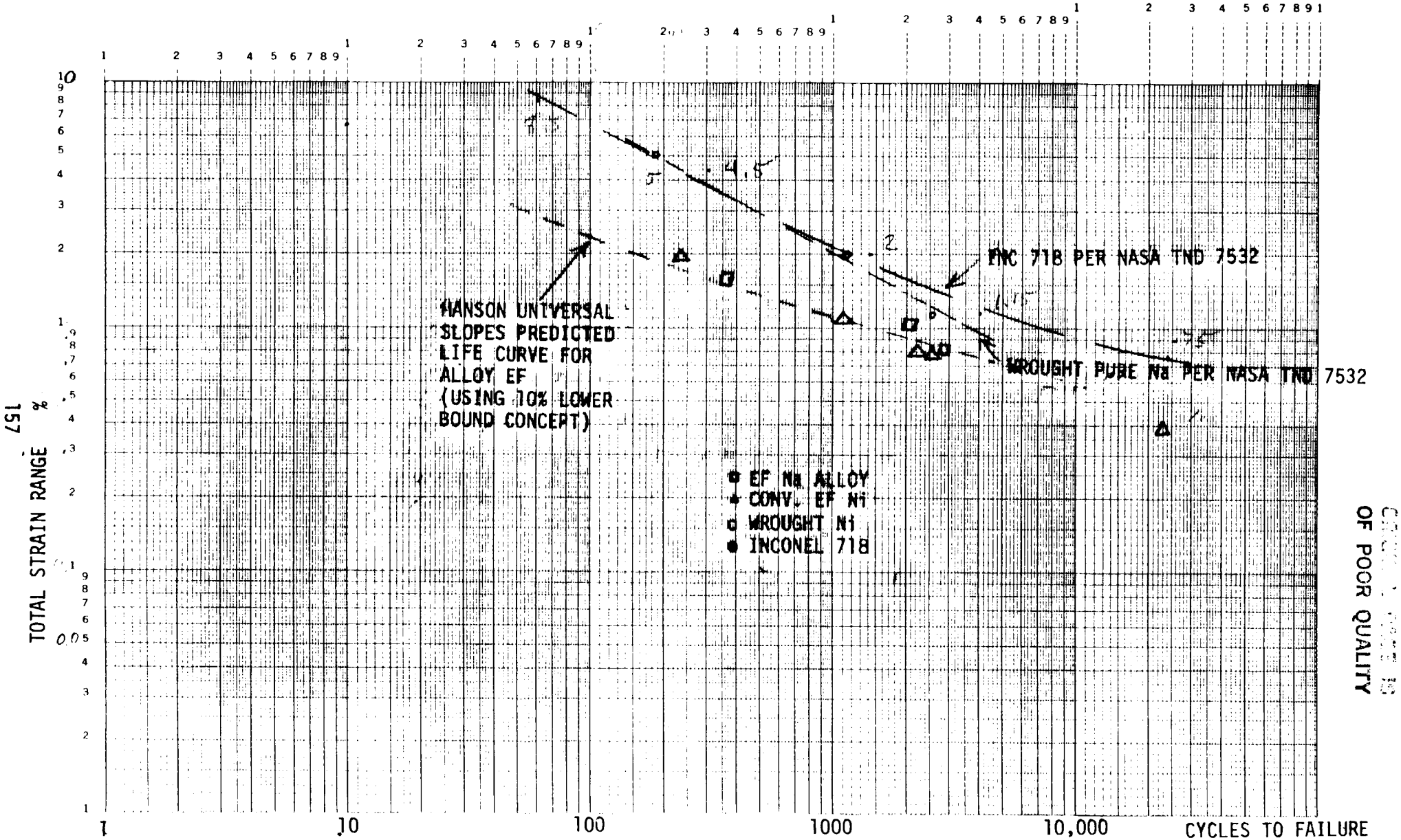

Figure 5.2-4. Test Data and Life Prediction Curve for Room Temperature Low Cycle/Hi Strain Fatigue

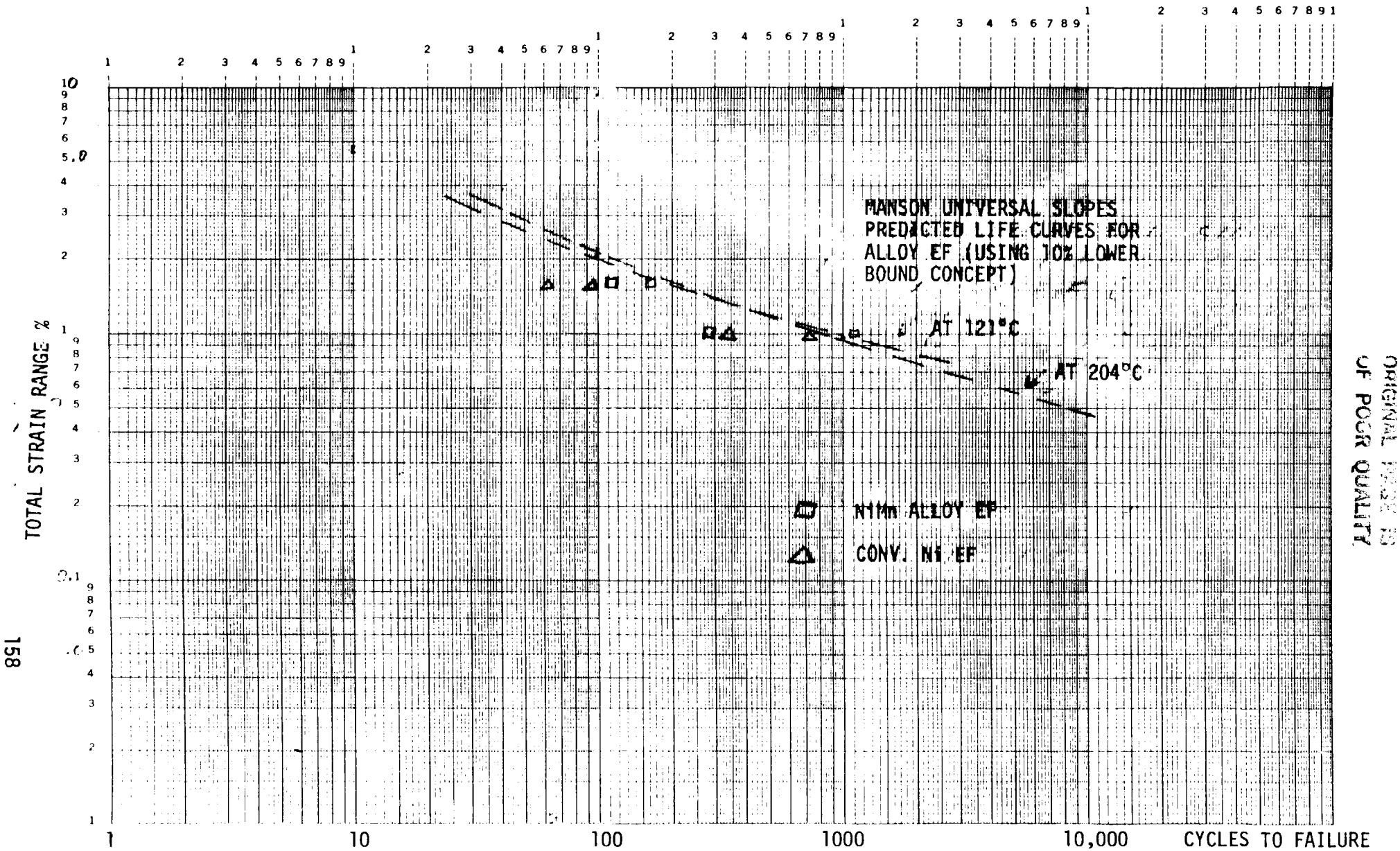

Figure 5.2-5. Test Data and Life Prediction Curves for Warm (121 or 204°C) Low Cycle/Hi Strain Fatigue

maximum stress at the start of cycling and at mid-life. This data is then plotted as strain range vs. cyclic life in Figures 5.2-4 and 5.2-5, using the typical log/log plotting method. These curves cover a small portion of the probable strain/life behavior of the material, since it was not possible in this limited data gathering program to cover either extreme of life. To properly test a very high strain/short cyclic life conditions, "hourglass" samples and diametral strain monitoring would have been required, neither of which were planned for this program. In a similar manner low strain/very long cyclic life tests would have required specimen redesign to avoid the possibility of failure in the threaded grip region. However within the confines of this limited program, it is felt that the data in Figures 5.2-4 and 5.2-5 do show the proper trend and range of behavior for this material.

In a complex thermal/mechanical environment such as thermal fatigue represents, it is vital to develop some method of correlating, rationalizing and summarizing what limited data is available, and presenting equations or other devices which could aid in design of components using these materials. As had been outlined in the proposal for this work, it was felt that for this preliminary study of properties, one of the earliest and simplest of the correlating equations for thermal fatigue, Manson's "Universal Slopes Method", would be most appropriate.

While some progress is being made in many advanced areas of design and material analysis such as finite element structural analysis with plastic behavior formulations, and strain range partitioning of complex material behavior waveforms, the most useful technique available for the past 20 years remains low cycle fatigue analysis by the Manson "Universal Slopes Method". As described in many of his papers, such as Reference 1 below, analysis of the fatigue behavior of most metals under high strain conditions showed that the fatigue behavior (cycles to failure for a given applied cyclic strain) followed a relation that was a composite of the behavior under elastic, and under plastic, conditions. These could be expressed mathematically as follows:

$$\Delta\epsilon_{TOT} = \frac{3.5 \times \sigma_u}{E} \times N_F^{-0.12} + D^{0.6} \times N_F^{-0.6}$$

$\Delta\epsilon_{TOT}$ = Total cyclic strain range

N_F = Cycles to failure

σ_u = Ultimate tensile strength

E = Elastic modulus

D = Logarithmic ductility = $\ln \frac{100}{100 - R \text{ of } A}$

It can be seen that the terms in this equation require only the knowledge of reliable tensile properties (elastic modulus, ultimate strength and reduction of area) in order to solve for expected cyclic life as a function of applied cyclic strain or the reverse. For conservative design practice, Manson suggested using a Lower Bound value for cyclic life of 10% of the cyclic life found by the above equations.

Ref. 1 - "Interfaces Between Fatigue, Creep and Fracture" by S.S. Manson, International Sources of Fracture Mechanics, 1966 Vol. 2, p. 327

Curves representing the predicted life using the Manson Universal Slopes equation (and the lower bound 10% life version of it) calculated using the material property data generated in this program at the various temperatures of interest, are also included in Figures 5.2-4 & 5.2-5. A comparison of the 10% life suggested lower bound of Manson to the available data shows a very reasonable fit. Thus it seems appropriate to offer the following equations as a good first approximation of the high strain fatigue life of the nickel-manganese alloy electroform at the temperatures covered by this test program.

At Run Temp.

$$\Delta\epsilon_{TOT} = \frac{3.5 \times 178{,}000}{29 \times 10^6} \times (N_F)^{-0.12} + 0.621^{0.6} \times N_F^{-0.16}$$

At 121°C

$$\Delta\epsilon_{TOT} = \frac{3.5 \times 163{,}000}{28 \times 10^6} \times (N_F)^{-0.12} + 0.616^{0.6} \times N_F^{-0.16}$$

At 204°C

$$\Delta\epsilon_{TOT} = \frac{3.5 \times 146{,}000}{27.5 \times 10^6} \times (N_F)^{-0.12} + 0.777^{0.6} + N_F^{0.16}$$

After computing a strain/life relationship using the above equations the lives should be reduced by a factor of ten to adhere to the Manson suggestion of a Lower Bound Life at 1/10 that originally calculated.

Behavior of the alloy electroform remained tough and relatively ductile through all of this type of fatigue testing. To illustrate this, Figure 5.2-6 shows a comparison of fractured specimens from tensile, low cycle fatigue and creep tests, showing that there was no brittle, flat crack growth in any of these types of tests, nor was there any brittle intergranular fracture observed in any of the testing.

5.2.4 Notch Sensitivity

Tensile tests were performed on notched round bar specimens of EF nickel-manganese alloy and conventional EF nickel. Figure 5.2-7 shows a drawing of an edge-notched tension specimen.

Ultimate strengths on the order of 1,800 MPa (261 ksi) were observed for the notched EF nickel-manganese bars when tested at room temperature. The ultimate strength of an unnotched bar of EF Ni-Mn was 1,230 MPa (178 ksi) at room temperature. Since the notched specimen strength is greater than that of the unnotched specimen, the ratio of notch strength to tensile strength is greater than 1.0. This indicates that the alloy is not notch sensitive at the ambient test temperature employed. This also shows that the alloy is non-brittle.

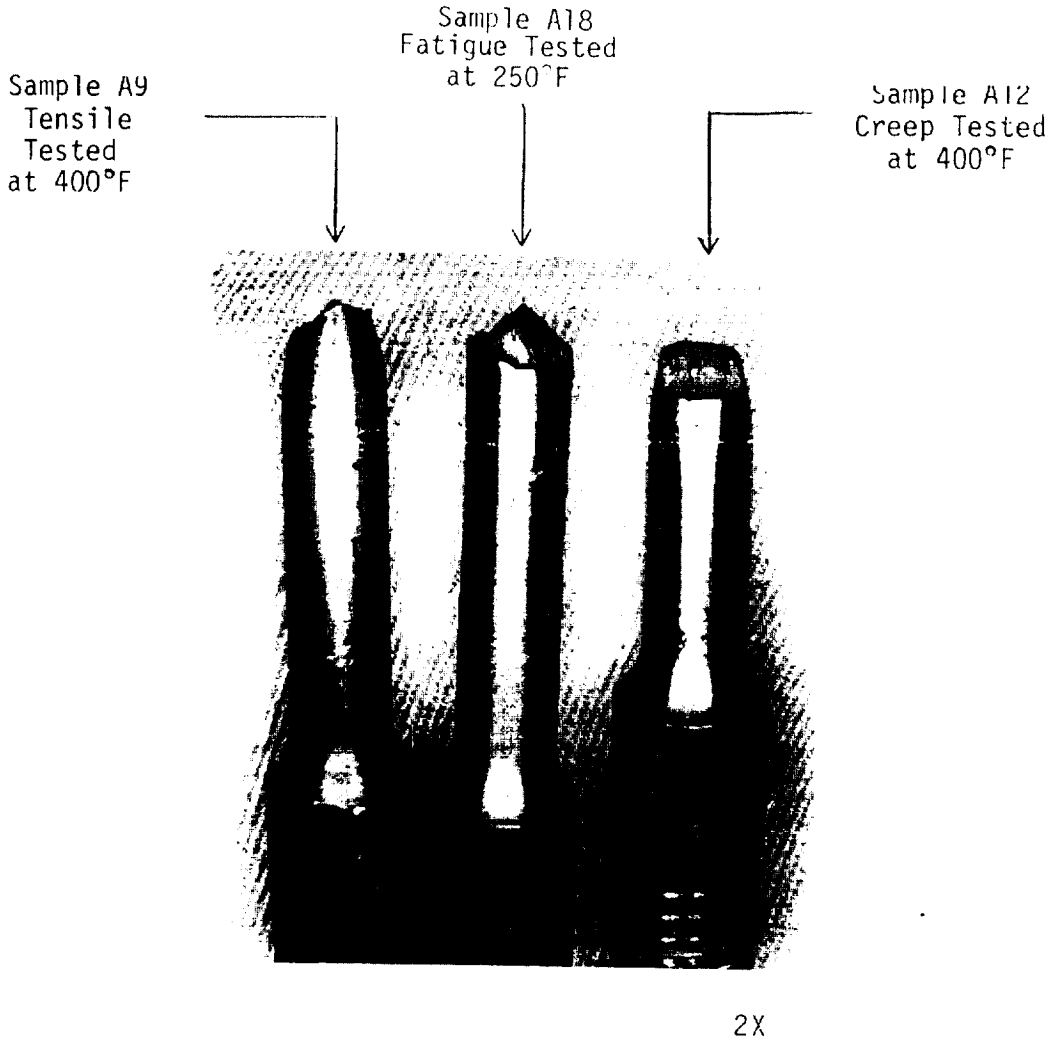

Figure 5.2-6. Photomacrograph of fractured samples of Nickel-Manangese alloy electroform tested warm using the three different testing techniques. All samples show some ductility, even the hi-strain low cycle fatigue one, a test which often shows very limited ductility or even flat fracture.

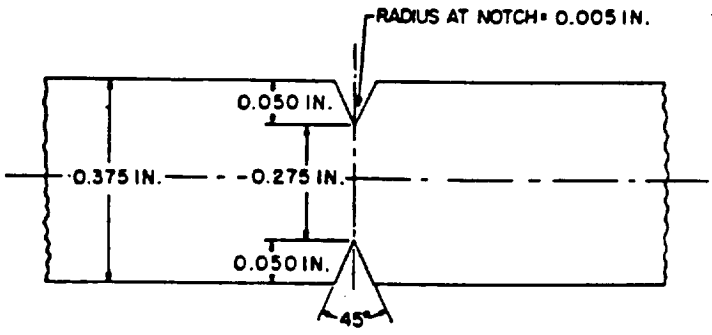

Figure 5.2-7. Edge-Notched Tension Specimen

Ultimate strengths for the notched nickel bars were on the order of 1,350 MPa (196 ksi) at room temperature. Since the ratio of notch strength to tensile strength is again greater than 1.0, the same conclusions can be drawn for the conventionally electroformed nickel.

5.2.5 Effects of Welding on Mechanical Properties

Short round specimens of EF nickel-manganese alloy have undergone TIG welding, which imposes a "worst case" effect on properties and microstructures. Cross-sections taken at the weld zone disclosed that grain growth was greatly restricted in the heat affected zones.

Additional round bars of EF nickel-manganese and EF nickel were TIG welded and then machined into tensile bars to determine mechanical strength retention after the severe thermal exposure of welding.

The conventional EF nickel bars had been heat treated at 343.3°C (650°F) for one hour prior to welding. The following room temperature mechanical properties were obtained at the welded section:

Ultimate strength	223.6 MPa	(32.43 ksi)
Yield strength	103.3 MPa	(14.98 ksi)
Elongation in 4 dia.	8.7 %	
Reduction of area	12.25 %	

The EF nickel-manganese bars were heat treated at 343.3°C (650°F) for 24 hours prior to welding. They provided the following room temperature mechanical properties at the welded section:

Ultimate strength	418.1 MPa	(60.64 ksi)
Yield strength	134.4 MPa	(19.48 ksi)
Elongation in 4 dia.	35.8 %	
Reduction of area	63.6 %	

The mechanical strength of both conventional EF nickel and EF Ni-Mn decreased proportionally due to welding. The EF nickel-manganese showed significant improvement in post-weld strength over conventional EF nickel. Much

of this improvement is believed due to inhibition of grain growth which results in heat affected zones of low strength. Figure 5.2-8 shows the microstructures of the welded specimens.

5.2.6 Creep/Stress Rupture Testing

A very limited set of tests was conducted at the higher of the two "warm" temperatures used for testing of the electroformed material to demonstrate what the creep or constant load behavior of the materials would be. This testing was concentrated at high applied stresses (85 - 94% of the tensile strength) with rupture failures occurring in times ranging from less than one hour to just over five hours. This type of data would be the starting point for design and material selection of moderate life, reusable thrust chambers. The test equipment used and sample configuration was exactly the same as that used for the thermal fatigue testing. The data from the tests of both nickel-manganese alloy electroform, and conventional nickel electroform are given in Table 5.2-2 An example of the rupture curve for the alloy electroform at 204^{o}C is given in Figure 5.2-9. Because of the limited amount of data collected, it is not possible to draw conclusions or generalizations from this data. As with the low cycle, thermal fatigue tests, the best observation is that brittle or grain boundary separation failures did not occur under these test conditions. This is shown in an example of fracture test specimen included in Figure 5.2-6.

5.2.7 Tensile Tests in a Pressurized Hydrogen Atmosphere

In order to assess the susceptibility of this high strength alloy electroformed nickel to strength/ductility degradation in a hydrogen atmosphere, a series of tensile tests of notched and unnotched tensile tests were performed. A chamber shown in Figure 5.2-10 was available which allows vacuum and inert gas purging, followed by pressurizing with up to 3.45 MN/m^2 (500 PSI) purified hydrogen 2.76 MN/m^2 (400 PSI) gas pressure was used for these tests). The welded chamber, consisting of high integrity stainless steel pipe, contains a sliding, double 'O' ring seal for the movable end. By using vacuum purging, both the explosion hazard of hydrogen/air mixture is eliminated and the maximum effect of the hydrogen gas (if any) on the sample is assured. Past work by other researchers indicated that small amounts of oxygen or water vapor tended to nullify the aggressive behavior of hydrogen on many metal surfaces. With the cleaned metal tensile sample threaded into the pull rods and the assembly closed, two vacuum purges, with low pressure hydrogen admitted between them, assures that the final pressurizing with 2.76 MN/m^2 (400 PSI) hydrogen gas will produce a clean, aggressive hydrogen atmosphere. The pressurizing chamber was mounted in a universal tensile machine, enclosed with a safety shroud to exhaust any leaking gas, similar to the one shown in Figure 5.2-11. Even at modest pressures of 2.76 MN/m^2 (400 PSI) it was necessary to correct the pressure effect on the pull rod, which adds 1.07 KN (240 lbs.) of force to the tensile force on the specimen, a force not sensed by the tensile machine load cell.

3/8" dia. rod of alloy electroformed nickel

3X

a) Overall View of Cross Section Thru ℄ of Weld

WELD METAL

HEAT AFFECTED EF MAT'L 100X

b) Microstructure at edge of fusion. EF material has some grain enlargement from original deposit.

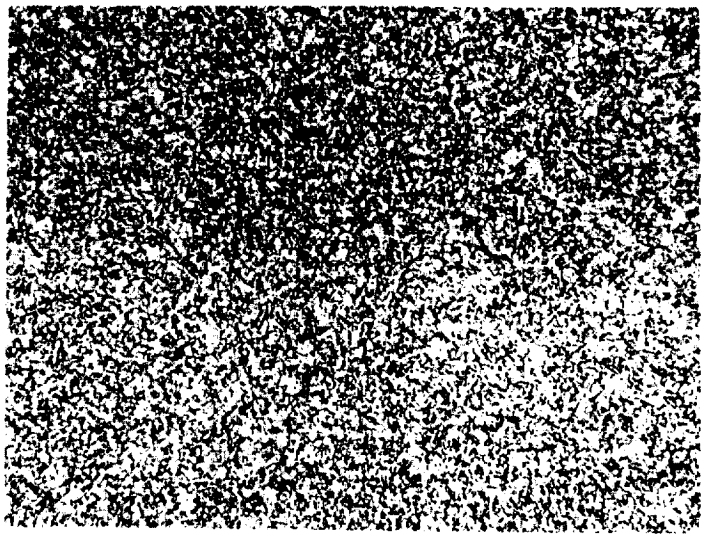

100X

c) Microstructure of alloy EF away from weld, showing extremely fine grain.

Figure 5.2-8. Weld Joining Rods of Electroformed Nickel

TABLE 5.2-2. TEST RESULTS FOR CREEP/STRESS RUPTURE TESTING OF ELECTROFORMED NICKEL

Material Type	Sample No.	Test Temp.	Applied Stress KSI	Applied Stress % of UTS	Time to Failure Min.	Elongation at Failure %
Nickel-Manganese Alloy Electroform	A-11	204°C/400°F	137	94	16.5	6.5
	A-12		123	85	320	8
Conventional Nickel Electroform	N-25		70	90	120	7
	N-26		72.5	93	94	7.5

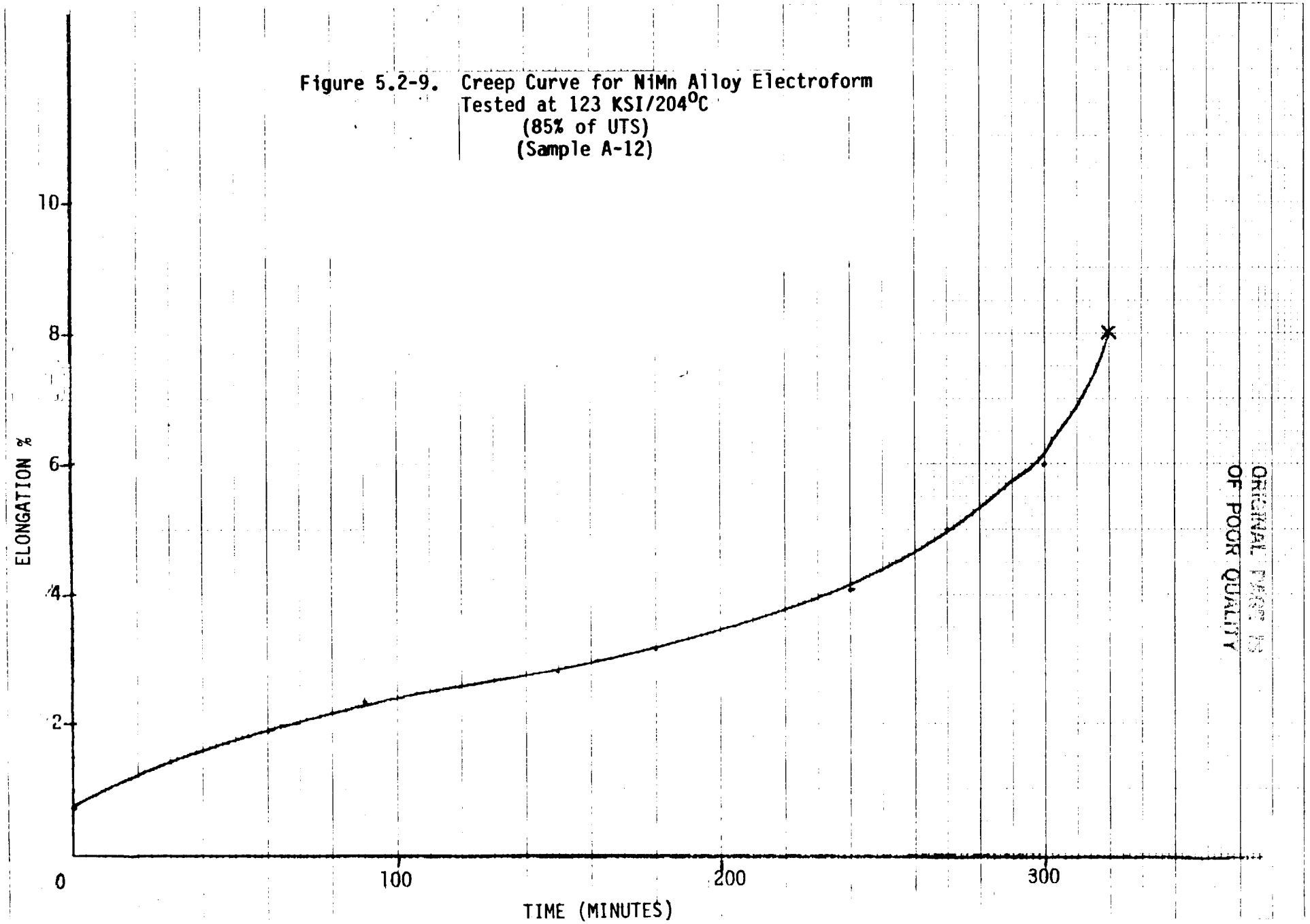

Figure 5.2-9. Creep Curve for NiMn Alloy Electroform Tested at 123 KSI/204°C (85% of UTS) (Sample A-12)

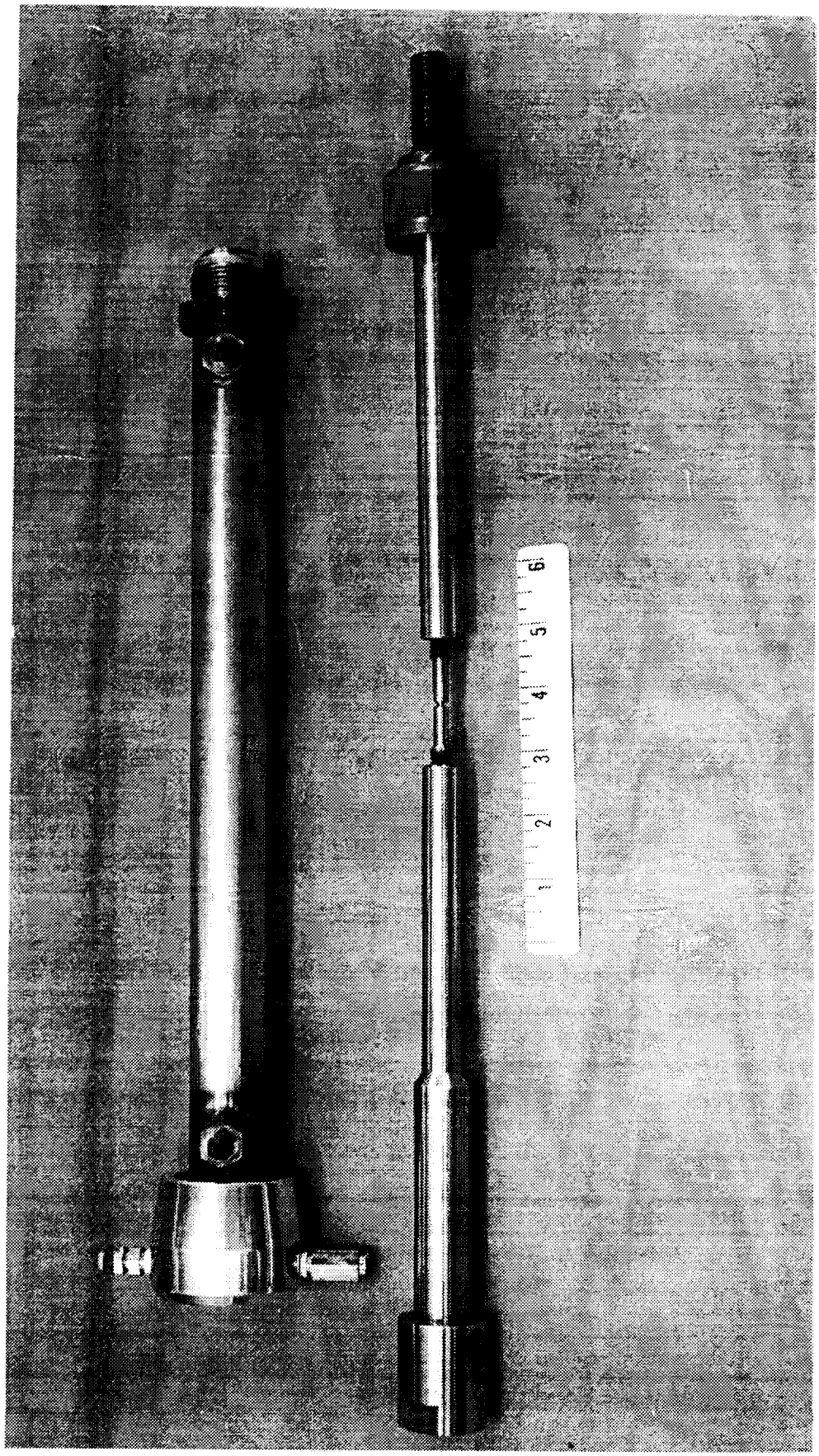

Figure 5.2-10. Presurized Hydrogen Exposure Chamber for Tensile Testing Shown in Unassembled Condition with Notched Sample in Place

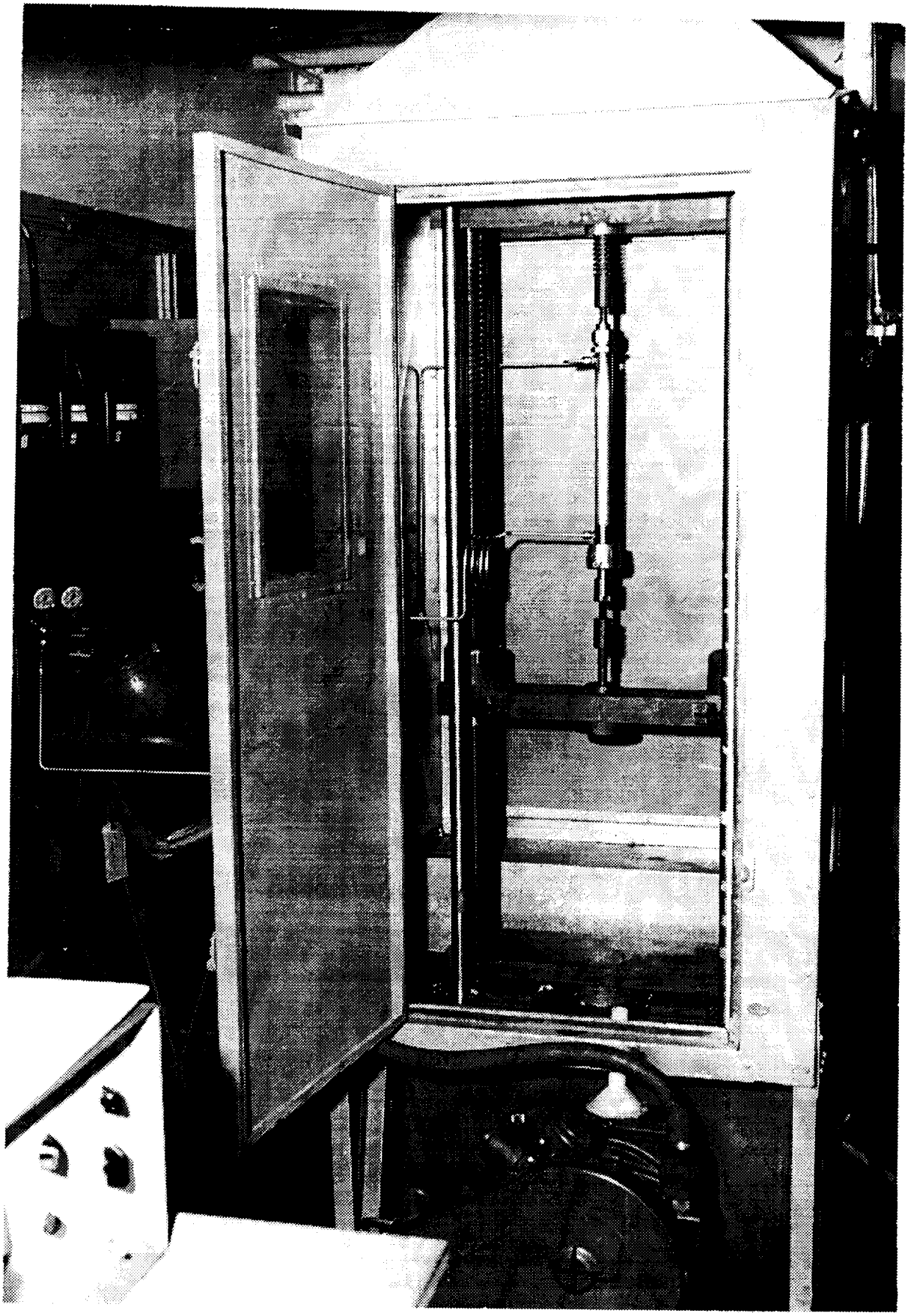

Figure 5.2-11. Pressurized Hydrogen Exposure Chamber Set Up in Tensile Machine Inside Explosive Proof Exhaust Hood, with Vacuum Purge Pump and Hydrogen Source Tank Visible

The data obtained from the four tests of the alloy electroform are shown in Table 5.2-3. All specimens were cylindrical samples, machined from the specially produced heavy wall cylinders of electroformed Nickel - Mn alloy and stress relieved at 343°C (650°F) for 24 hrs. before testing. A nominal diameter of 7.62 mm (0.300 in.) OD for the notched bars with 5.08 mm (0.200 in.) notch diameter and 0.1 mm (0.004 in.) root radius gave notch concentration factors (K_t) of 4 to 6. Specific dimensions for the test specimens, and the resultant properties and K_t values are given in Table 5.2-3. A shadowgraph of the notch and root radius region of one typical sample in Figure 5.2-12 shows the smooth and sharp notch obtained.

The unnotched specimens tested in pressurized hydrogen produced consistent failure in the threaded ends of the specimens, and therefore the equivalent notch conditions for the thread region were computed and are shown in Table 5.2-3. The root of the threads had a notch concentration factor of approx. 3.5, and it is thus not surprising that failures occurred in the threads. Stress in the cylindrical section of the specimen was 344.7 MPa (50 ksi) to 620.5 MPa (90 ksi), still below the yielding stresses of the alloy electroform. It is only when yielding of the metal surface begins that hydrogen begins to produce its degrading effects.

The test results shown in Table 5.2-3 demonstrate that this high strength alloy electroformed material has significant loss in notched strength capability in a pressurized hydrogen atmosphere. A previous section of this report showed that in air atmosphere, this alloy electroform is NOT sensitive to notches (notched strength 1.5 times unnotched strength for a K_t of 3 - 5. In a hydrogen atmosphere the notched strength is 30% for the unnotched (air) strength, such that the loss in notched strength is 80% from notched air values to notched hydrogen values. Also included in Table 5.2-3 are values taken from the literature for the effect on notched properties in hydrogen for wrought nickel and Inconel 718. Those data show that for somewhat more severe conditions 69 MN/m^2 (10,000 PSI) H_2 pressure and notch K_t of 8.4), wrought nickel loses 30% of its notched strength and Inconel 718 loses 54% of its strength. Although the alloy electroform shows somewhat greater degradation in hydrogen than the Inconel 718, there should still be a role for this very high strength alloy electroformed material to play in rocket engine thrust chamber fabrication, because of that high strength and the unique processing advantages that pulsed plating techniques offer.

5.2.8 Cryogenic Mechanical Properties of Electroformed Nickel-Manganese Alloy

Mr. John Kasaroff, NASA-LeRC, expressed an interest in the alloy being electroformed in this program from the standpoint of cryogenic applications. He was also curious as to the potential for this alloy to show good combustion resistance in pure oxygen environments. Material from Cylinder No. 125-6 was available as excess material to the test requirements of this program. Twelve round test bars were made and supplied to NASA-LeRC. All specimens were heat treated at 343°C for 24 hours prior to testing. NASA-LeRC performed room temperature and cryogenic tests on the electroformed alloy and compared the results with those from Inconel 718. Cryogenic testing was in liquid nitrogen at -195.8°C. Results are shown in Table 5.2-4.

TABLE 5.2-3. TENSILE PROPERTIES OBTAINED IN TESTS OF ALLOY ELECTROFORM IN 2.76 MN/m^2 (400 PSI) PRESSURIZED HYDROGEN

SAMPLE ID	NOTCH CONC. FACTOR K_T	NOTCHED TENSILE STR. MPA	NOTCHED TENSILE STR. KSI	REDUCTION IN NOTCH STR NOTCH AIR / NOTCH H_2	NOTCH RATIO NOTCHED H_1 / UNNOTCH AIR
AN-5	4.4*	363	52.7	79%	0.30
AN-8	6.0*	318	46.2	82%	0.26
A30	SMOOTH, UNNOTCHED SPECIMEN, BUT FAILED IN THREADS AT K_T OF 3.5	254	36.8**		
A31	SAME AS A30	418	60.7**		
LITERATURE VALUES FOR					
WROUGHT N_iVO	8.4	372	54	30%	
INCONEL 718 (DOUBLE AGED)	8.4	869	126	54%	

TAKEN FROM:

BATTELLLE DMIC REPORT S-31
"Effect of Hydrogen Gas on Metals at Ambient Temperature" by J. E. Campbell, Table 14, April 1970

* Nominal Specimen Dimensions were:
Outer Diameter: 7.62 mm (0.300 inch)
Notch Diameter: 5.08 mm (0.200 inch)
Root Radius: 0.1 mm (0.004 inch)
specific requirements of each specimen produced K_T's shown

** Stress in smooth test area 6.35 mm (0.025 inch diameter) was 345 610 MPa at time of failure in thread

Figure 5.2-12. Shadowgraph Showing Sharpness and Smooth Notch Walls in a Notched Alloy Electroformed Specimen Ready for Tensile Test

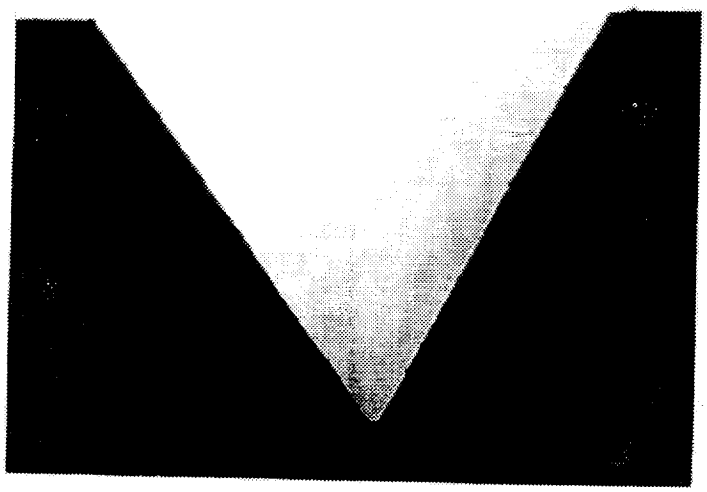

Mag: 50X

TABLE 5.2-4. A COMPARISON OF MECHANICAL PROPERTIES FOR EF NI-MN ALLOY AND INCONEL 718 (AGE-HARDENED) AT 20°C AND -195.8°C TEST TEMPERATURES

	EF Ni-Mn Alloy		Inconel 718	
	20°C	-195.8°C	20°C	-195.8°C
Tensile Strength (MPa)	1034	1241	1241	1620
(Ksi)	150	180	180	235
Yield Strength (MPa)	827	945	1007	1207
(Ksi)	120	137	146	175
Elongation in 4D, %	13	17	30	32
Reduction of Area, %	55-58	63	48	39
Modulus ($\times 10^{-6}$)	29.5	31	29.5	31

5.3 Task II - Process Development

5.3.1 Introduction

The ability to metallurgically bond the EF alloy to various metallic substrates without the use of thermal joining techniques is of importance. This is to insure that mechanical properties of all joined metals are maintained at the highest possible level and unfavorable microstructual changes are not introduced with severe thermal treatments. Bond strength data of the EF nickel-manganese alloy to itself, to EF copper, and to Inconel 718 was generated. Response of these bonds to elevated temperatures characteristic of those encountered during fabrication and operation of the MCC was investigated.

5.3.2 Bonding Techniques

5.3.2.1 Bond Testing

To test for bond integrity the electrodeposit under study was electroformed on both sides of a flat plate of the substrate metal of concern. By electroforming to a total plate thickness of about 0.5 inch it is possible to EDM from this plate a series of cylindrical plugs similar to core samples wherein two bondlines will exist near the midpoint of the cylinder lengthwise. These plugs are then machined into conical head bond test specimens of a design shown in Figure 5.3-1.

These conical head test samples are subsequently heat treated and pulled to failure generating tensile results. Photomicrographs document bond integrity after test to material failure.

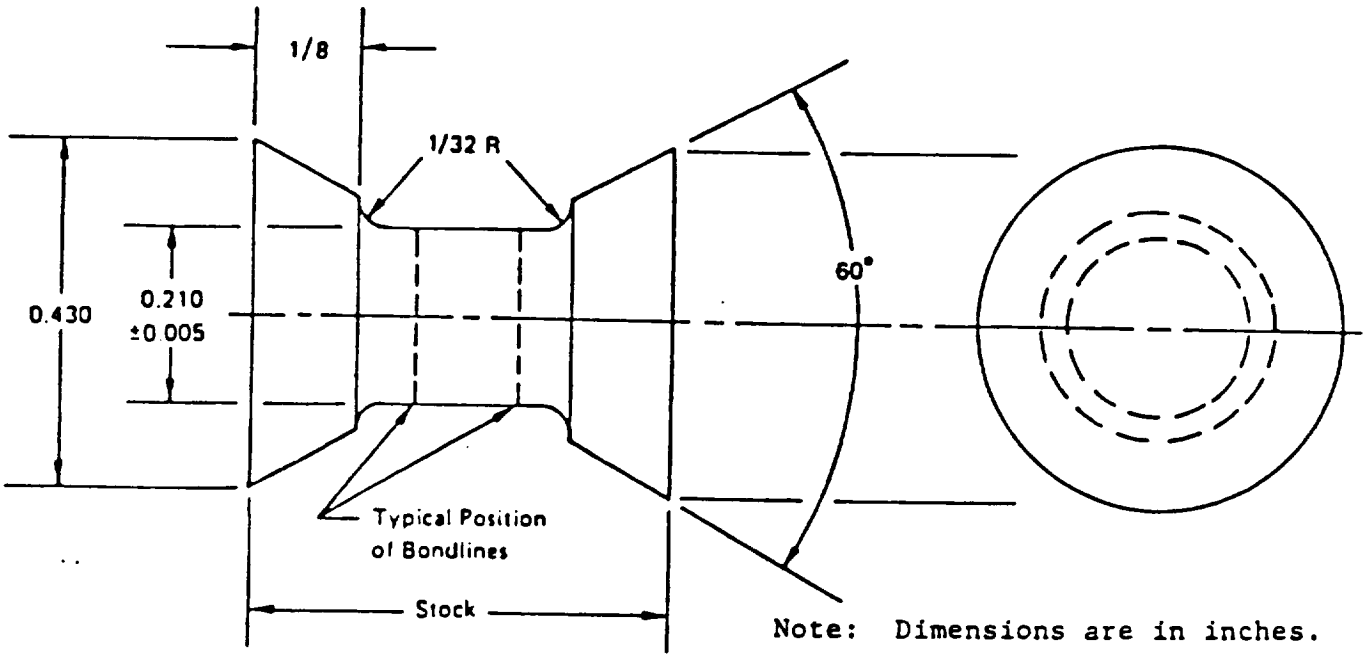

Figure 5.3-1. Conical Head Bond Test Specimen

5.3.2.2 Bonding EF Ni-Mn to EF Copper

The first bond study performed was that of EF Ni-Mn alloy bonded to EF copper which was, in turn, bonded to a wrought copper substrate. Presently, EF Ni is bonded to EF copper which is used as a hydrogen barrier in the initial close-out of the coolant passages in the copper base alloy liner (NARloy-Z). The EF Ni-Mn alloy developed may be substituted for EF Ni as a liner structural close-out, due to superior strength and resistance to thermally induced microstructual changes. Therefore bond strength of the alloy to EF copper needed to be evaluated. The following procedure was followed:

A. Preparation of wrought copper substrate for plating.

1. Wash plate with alconox-detergent and pumice scrub until obtaining water break.

2. Activate anodically in 75 percent by volume phosphoric acid at room temperature, 7 to 9 volts for 4 minutes.

3. Rinse in tap water followed by second rinse in demineralized water.

4. Activate cathodically in 30 percent by volume sulfuric acid at room temperature. Current density is set to a minimum of 10 A/dm^2 (100 ASF) for 3 minutes.

5. Double rinse in demineralized water.

6. Place part in cooper plating tank with voltage applied at 2-2.5 A/dm^2 (20-25 ASF).

B. Plating of Initial Cooper Layer

1. Plate for 20 minutes at 2-2.5 A/dm^2 (20-25 ASF).

2. Turn periodic reversal unit on and run at 21 seconds forward and 7 seconds reverse.

3. Raise current density to 4-5 A/dm^2 (40-50 ASF) and plate until a thickness of 0.025 mm (0.001 inch) is obtained.

C. Preparation of Cooper Plated Panel for Alloy Bonding

1. Wash panel with alconox-solution to obtain water break.

2. Activate anodically in 75 percent by volume phosphoric acid at room temperature. Set voltage 7 to 9 volts, one minute.

3. Rinse in tap water followed by second rinse in demineralized water.

4. Activate cathodically in 30 percent by volume sulfuric acid at room temperature. Current density is set to 10 A/dm^2 (100 ASF) for 3 minutes.

5. Double rinse in demineralized water.

6. Place part in alloy electroforming tank with voltage applied at 0.5 A/dm^2 (5 ASF).

D. Plating of Thick EF Ni-Mn Alloy Layer

1. Begin plating using conventional rather than pulse plating and only 0.05 A/dm^2 (5 ASF).

2. Gradually increase current density to 2 A/dm^2 (20 ASF). Gradually decrease duty cycle from 100% to 64%.

3. Electroform to desired thickness.

The resulting Conical head bond test specimens were tested at room temperature, 204.4^{o}C (400^{o}F) and 538^{o}C (1000^{o}F). The following values reported are average bond strengths for each test temperature.

Room Temperature	255.2 MPa	(37.02 ksi)
202^{o}C (400^{o}F)	119.8 MPa	(17.38 ksi)
538^{o}C (1000^{o}F)	59.8 MPa	(8.67 ksi)

The above values are expected for these test temperatures based on the mechanical properties of typical wrought OFHC copper and conventional EF acid sulfate copper. At room temperature failure occurred in the wrought copper while both bond types, EF Ni-Mn to EF Cu and EF Cu to wrought OFHC Cu, remained intact. This indicates that the strength of these bonds are at least equivalent to the ultimate strength of the wrought copper at room temperature. At 204.4°C (400°F) and 538°C (1000°F), failure occurred at the wrought copper to EF copper interface. However, the bonds between the EF copper and EF Ni-Mn remained intact. This indicates that the bonds of the EF nickel alloy are once again at least as strong as the bonds between the wrought Cu and EF copper materials at these temperatures.

5.3.2.3 Bonding of EF Ni-Mn to EF Ni-Mn and EF NI-Mn to Inconel 718

The second bond study performed was that of EF Ni-Mn alloy bonded to itself, which was in turn, bonded to an age-hardened Inconel 718 substrate. Occasionally electroforming must be interrupted when fabricating hardware by this technique. Interruptions may be due to power failures or by intent where an in-process inspection is desired. It thus becomes necessary to activate the previously electroformed surface in such a manner that a metallurgically sound bond is produced as electroforming is resumed. Should a flaw or unsound metal be observed, it may be necessary to machine away the defect and repair by electroforming. Ability to bond an electroformed alloy to like material is therefore, essential. Since certain components such as manifolds may be of a different material such as age-hardened Inconel 718, it is necessary to demonstrate a process whereby sound bonds can be made with the electroformed alloy. The response of such bonds to elevated temperatures was also evaluated. This study provided test specimens with Ni-Mn alloy bonded to itself and Ni-Mn alloy bonded to Inconel 718 in combination. The following procedure was followed:

A. Plating of Ni-Mn Onto Inconel Substrate

1. Plate Ni-Mn onto Inconel 718 substrate at 2 A/dm^2 (20 ASF) in order to obtain a minimum of 0.025 mm (0.001 inch) of EF Ni-Mn.

2. Remove panel for reactivation of Ni-Mn alloy.

B. Preparation of Ni-Mn Plated Panel for Reactivation

1. Wash panel with alconox solution to obtain water break.

2. Activate anodically in 30 percent by volume sulfuric acid at room temperature. Set current density to a minimum of 10 A/dm^2 (100 ASF) for 2 minutes.

3. Turn power supply off and allow part to soak in sulfuric acid for 2 minutes to dissolve any manganese oxide on the surface.

4. Rinse in tap water followed by second rinse in demineralized water.

5. Activate cathodically in 30 percent by volume sulfuric acid at room temperature. Current density is set at 15 A/dm^2 (150 ASF) for 2 minutes minimum.

6. Double rinse in demineralized water.

7. Place part in alloy electroforming tank with voltage applied at 2 A/dm^2 (20 ASF).

C. Plating of Thick EF Ni-MN Alloy Layer

1. Place at a current density of 2 A/dm^2 (20 ASF).

2. Use duty cycle of 64%.

3. Electroform to desired thickness.

The resulting conical head bond test specimens were tested at room temperature, 202°C (400°F) and 538°C (1000°F). The following values indicate the strength of the bonds obtained for each temperature:

Room Temperature	1,079.9 MPa	(156.62 ksi)
202°C (400°F)	855.0 MPa	(124.00 ksi)
538°C (1000°F)	352.6 MPa	(51.14 ksi)

Since failure occurred in the electroformed alloy while the bonds remained intact, the strength of the bonds are at least equivalent to the ultimate strength of the EF nickel-manganese. The fact that the ultimate strength of the EF nickel-manganese samples from these particular round test bars was lower than samples produced from an electroformed cylinder was not unexpected. The bond panel was produced in a 42 gallon development bath using a flat mandrel (the substrate), a different electrolyte agitation system, and plating parameters designed to codeposit less manganese to minimize distortion and possible cracking on very thick deposits.

In conclusion, this study demonstrated the ability to produce high integrity bonds by electroforming. This was clearly demonstrated for the electroformed Ni-Mn alloy which was bonded to previously deposited Ni-Mn samples, electroformed copper, and age-hardened Inconel 718.

5.4 Task III - Shield Development

As discussed in Sections 4.4 and 4.5, the development of a proper shielding system to control pulsed electroforming current distribution uniformly over the complex curved surfaces of the MCC mandrel is essential.

Proper shielding consists of non-conductive pieces of acid stable plastic which are cut and shaped to normalize the effects of solution resistance (IR) effects. The proper shielding for this task included pieces designed to reduce the current density at the large ends of the biconical shaped SSME/MCC mandrel. The necessary control also included assembly of a spray nozzle

system which allowed close control of the plating solution agitation. The proper control of plating bath parameters, is also essential in order to provide an EF Ni-MN alloy shell with uniform thickness, composition, microstructure, tensile strength and hardness.

The prototype subscale MCC mandrel was assembled and Plexiglas shields attached as rings fastened to end-plates. The forward end ring-shield is 38.1 cm (15 in.) in diameter and extends 7.62 cm (3 in.) from the end-plate towards the throat of the MCC mandrel. The aft end ring-shield has the same diameter and extends for 2.54 cm (1 in.) from the end-plate towards the middle of the mandrel. A Plexiglas ring was also mounted inside the aft end ring shield in order to taper the material deposited at the extreme end. This end, because of its linear sloped contour, becomes a very high current density location and must be heavily shielded. Figure 5.4-1 illustrates the subscale mandrel after the first electroforming trial and shows the shielding details.

The anodes were arranged in the electroforming tank to include four (4) 15.24 cm (6 inch) wide nickel chip baskets to mainly deposit on the forward and aft sections of the mandrel. There were also four (4) 7.62 cm (3 inch) diameter cylinder baskets for nickel chips to direct current to the throat section of the mandrel. These cylindrical baskets were shielded with Plexiglas boxes with boxed openings at a position corresponding to the mandrel throat. A similar boxed opening was attached to the backside of the shielded anode baskets to provide solution circulation. The physical shielding is better illustrated in Figure 5.4-2 wherein the tank had been partially emptied to show relative locations of all anodes and the electrolyte spray positions.

All of the anodes were placed approximately 34.29 cm (13.5 in.) from the vertical axis of the MCC mandrel, Figure 5.4-3. Two pulse plating power supplies were linked electronically in order to synchronize the pulses while both were in simultaneous operation. One pulse unit was used to drive the large anodes, and the other was powered to drive the small shielded anodes, Figures 5.4-4.

A prototype alloy jacket, MCC-01, was electroformed to a thickness of about 0.127 cm (0.050 in.) under the same parameters used to electroform Cylinder 120-5 from which mechanical property studies were based. The Ni-Mn alloy bath was operated at 48.9°C (120°F), a pulse plating duty cycle of 64%, electrolyte sprays positioned near the tank walls, and a cathode rotational speed of 8 rpm. In this first trial an average current density of 1.81 A/dm^2 (16.8 A/ft^2) was used due to a maximum current restriction on the power supply driving the large anodes. Figure 5.4-5 shows the profile electroformed with the thickness distribution indicated. It should be noted that actual thicknesses for jackets would be much greater than those being obtained on these trial electroforms. We were limiting the deposit thickness to 1) conserve nickel, 2) make separation simpler from the mandrel, and 3) to save time in obtaining results (thus permitting more trials).

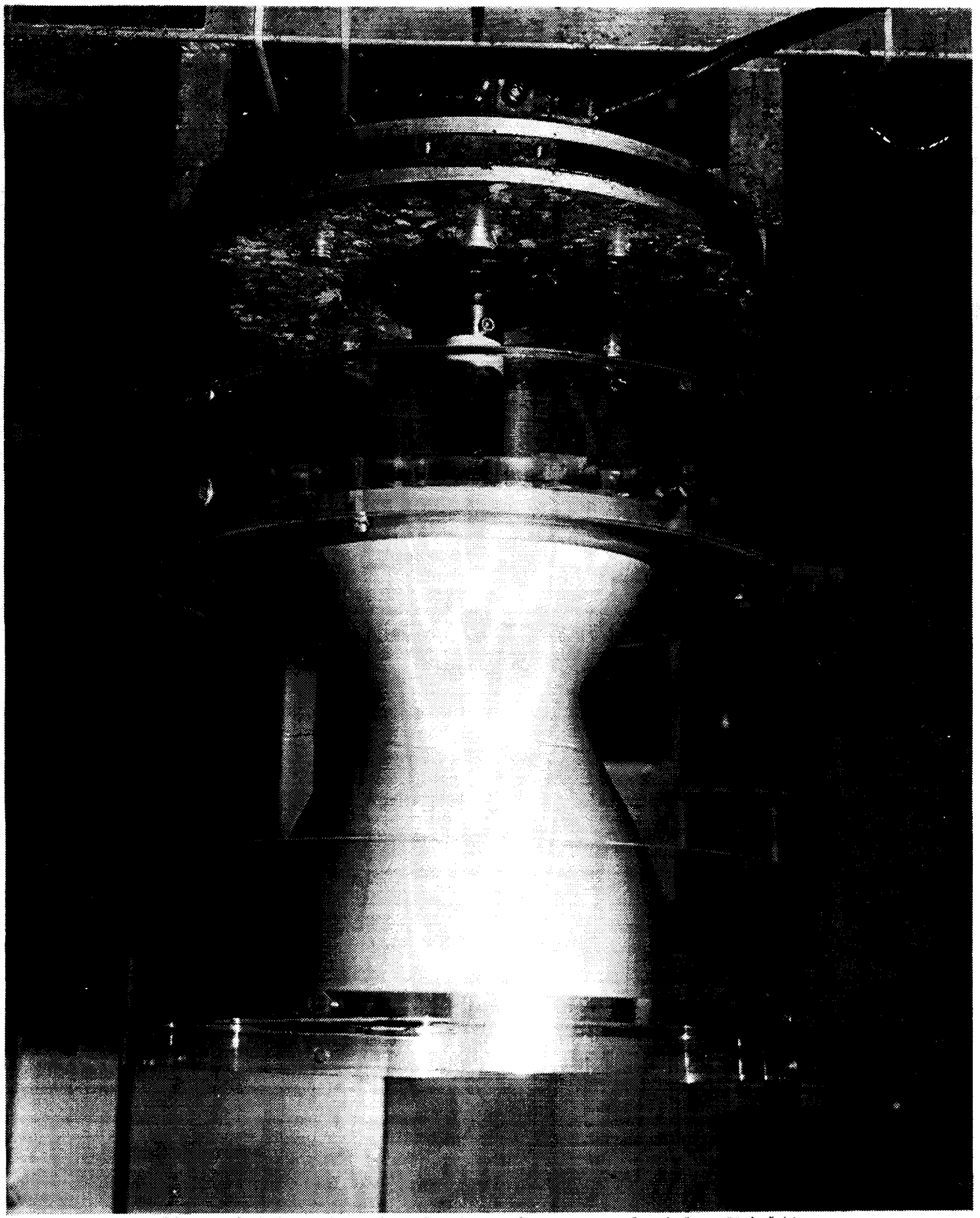

Figure 5.4-1. MCC Subscale Mandrel Showing Plexiglas Shielding

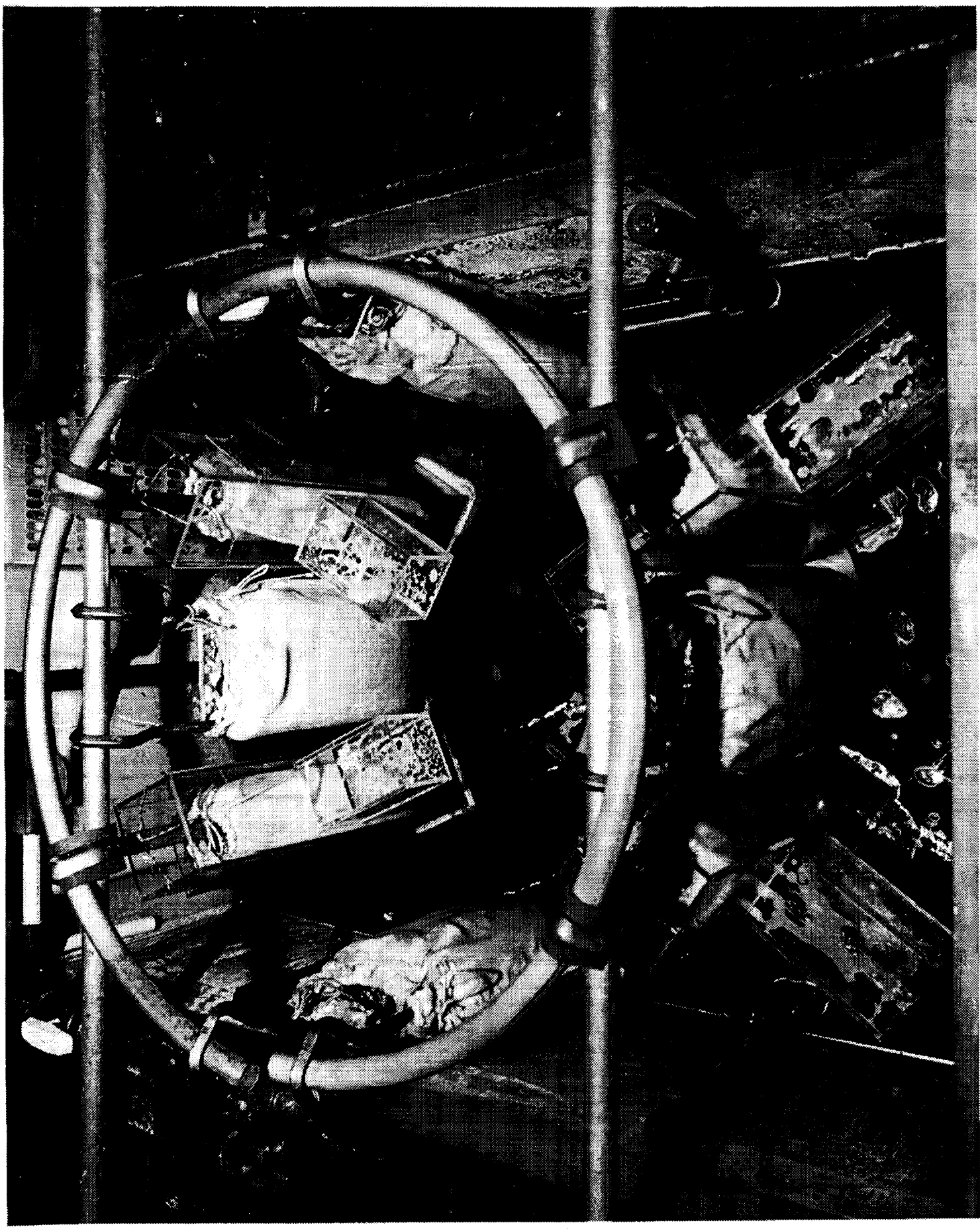

Figure 5.4-2. Relative Locations of Alloy Electroforming Anode Arrays

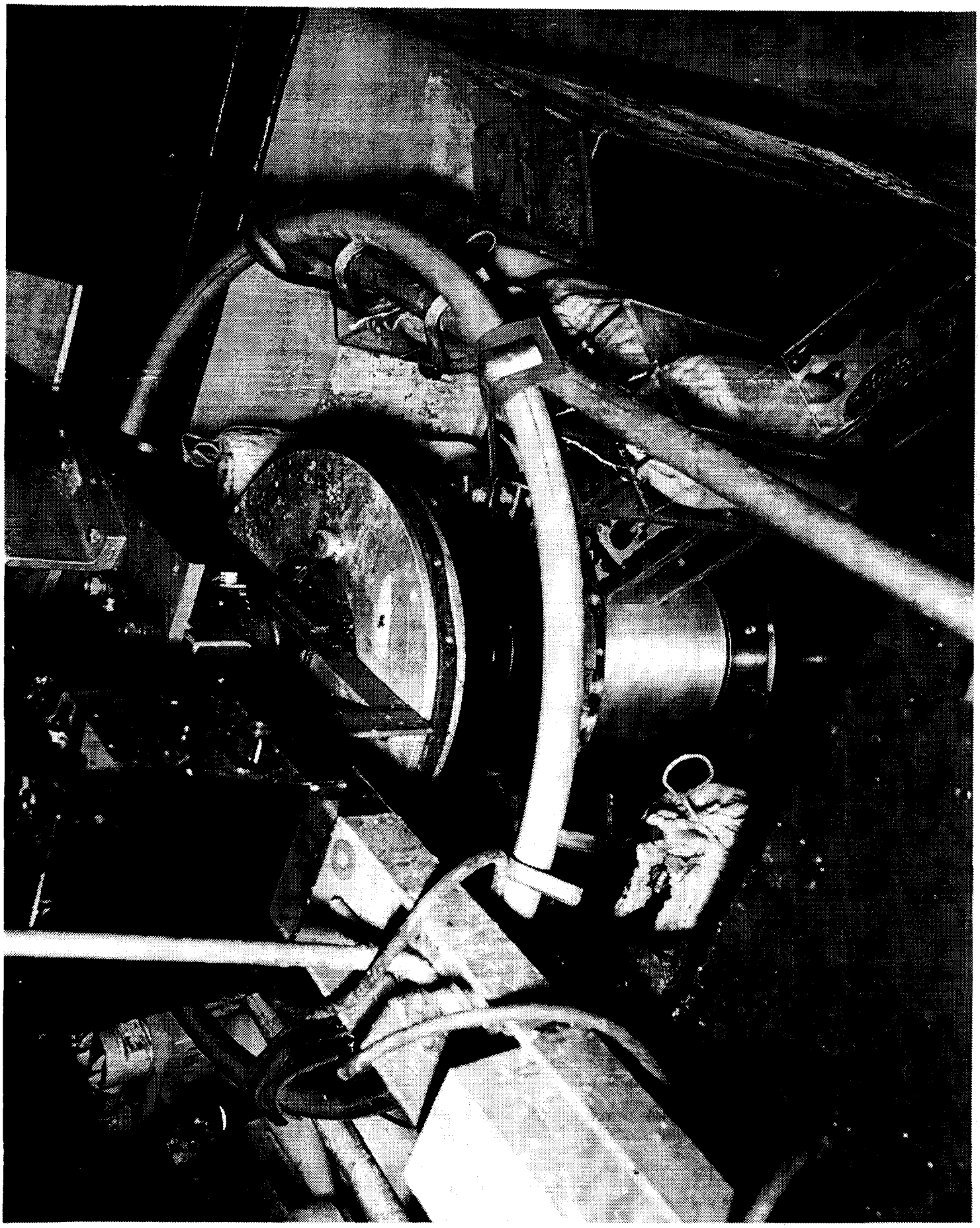

Figure 5.4-3. Relationship of Subscale MCC Mandrel to Anode Arrays

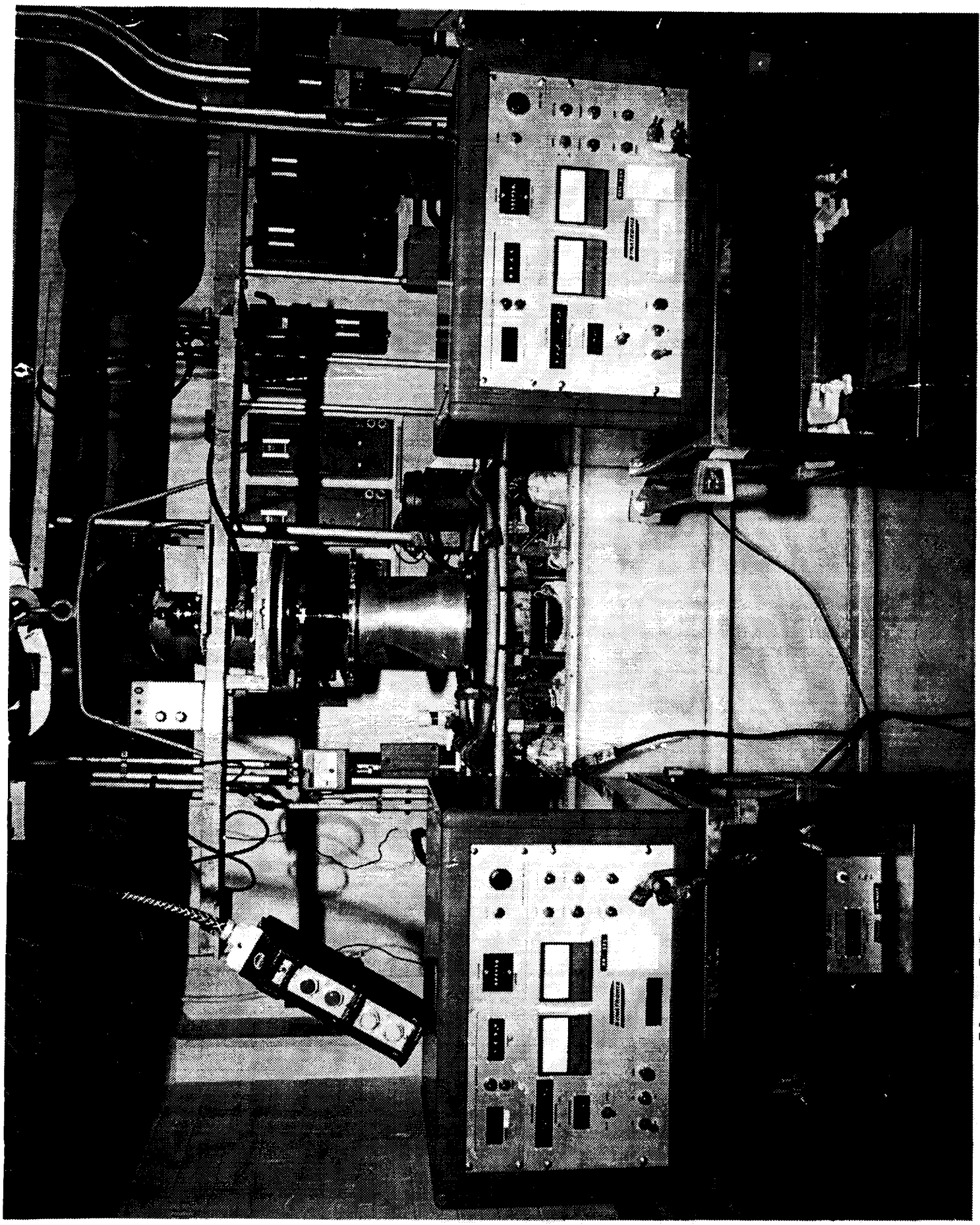

Figure 5.4-4. Electroforming Facility With Synchronized Pulse Power Supplies

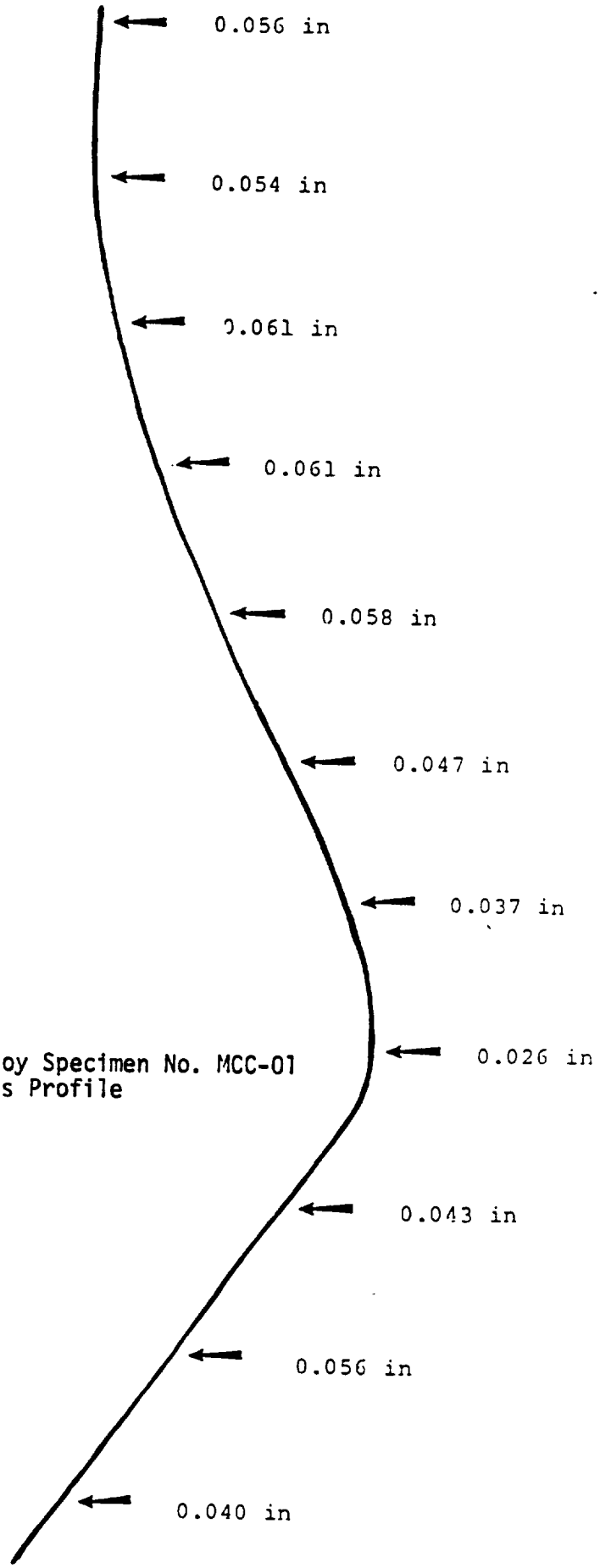

Figure 5.4-5. EF Alloy Specimen No. MCC-01 Thickness Profile

In electroforming a second prototype alloy jacket, MCC-02, the four large anodes were moved back so that they were an average of 10.8 cm (4.25 in.) further away from the mandrel. Three of these large anodes were driven by Pulsed Power Supply No. 1, and the fourth large anode was linked electrically with the small shielded anode array feeding the MCC throat area and driven by Pulsed Power Supply No. 2. Since the aft end of the alloy jacket from Trial MCC-01 tapered too far from the edge, the aft end ring-shield and inner ring were moved up 0.95 cm (0.375 in.) from the middle of the mandrel - leaving a 1.59 cm (0.625 in.) extension from the end-plate to the middle of the mandrel.

The nickel-manganese alloy bath was operated again at 48.9°C (120°F), a pulse plating duty cycle of 64%, electrolyte sprays positioned near the tank walls, and a cathode rotational speed of 8 rpm. Pulsed Power Supply No. 1 was operated at 21.25 amperes while Pulsed Power Supply No. 2 ran at 14.75 amperes. This resulted in an overall average current density of 2.15 A/dm^2 (20 A/ft^2). These were the parameters used to electroform Cylinder 120-5 from which acceptable mechanical properties were obtained.

Figure 5.4-6 shows the profile electroformed with the thickness distribution indicated. Adjusting the position of the aft-end ring-shield improved the thickness distribution at that end. Overall, the thickness distribution became slightly worse. The ratio between the thickest and thinnest sections on Trial MCC-01 was 2.35 to 1. On Trial MCC-02 this ratio increased to 2.45 to 1. This could be due to the fact that an anode with a greater cross-sectional area, and therefore less resistance, was driven by the same power supply as the four smaller shielded anodes. This may cause current to preferentially flow through the large anode rather than the small anodes designated to deposit alloy at the throat section of the mandrel. The result was a deficient deposit at the throat.

The next subscale EF alloy jacket, Trial MCC-03, was electroformed with the four large anodes driven by Pulsed Power Supply No. 1 with the four small shielded anodes driven by Pulsed Power Supply No. 2. Current from Power Supply No. 1 was decreased from 21.25 amperes to 18.0 amperes. Power Supply No. 2, which supplies current to the throat region, was increased from 14.75 amperes to 18.0 amperes. All other bath parameters, mandrel shielding, and anode distances from the mandrel remained the same. Figure 5.4-7 shows the profile electroformed with the distribution of thicknesses indicated for comparable stations as shown in previous profiles. The ratio of the thickest to thinnest sections improved slightly to 2.15 to 1.

To further improve the thickness distribution, Trial MCC-04 was electroformed with a modification to the four shielded anodes. Previously the boxed openings extending towards the mandrel throat had 7.62 cm (3 in.) by 7.62 cm (3 in.) openings located 6.35 cm (2.5 in.) from the mandrel throat. For this trial, these openings were modified to produce a slot in each anode shield that was 2.54 cm (1 in.) high by 7.62 cm (3 in.) wide and extending to a position only 2.54 cm (1 in.) from the mandrel throat. All other bath parameters and anode distances from the mandrel were the same as before. The resulting thickness distribution in the profile of EF alloy is shown in Figure 5.4-8. The thickness ratio improved only slightly to 2.13 to 1. We suspect

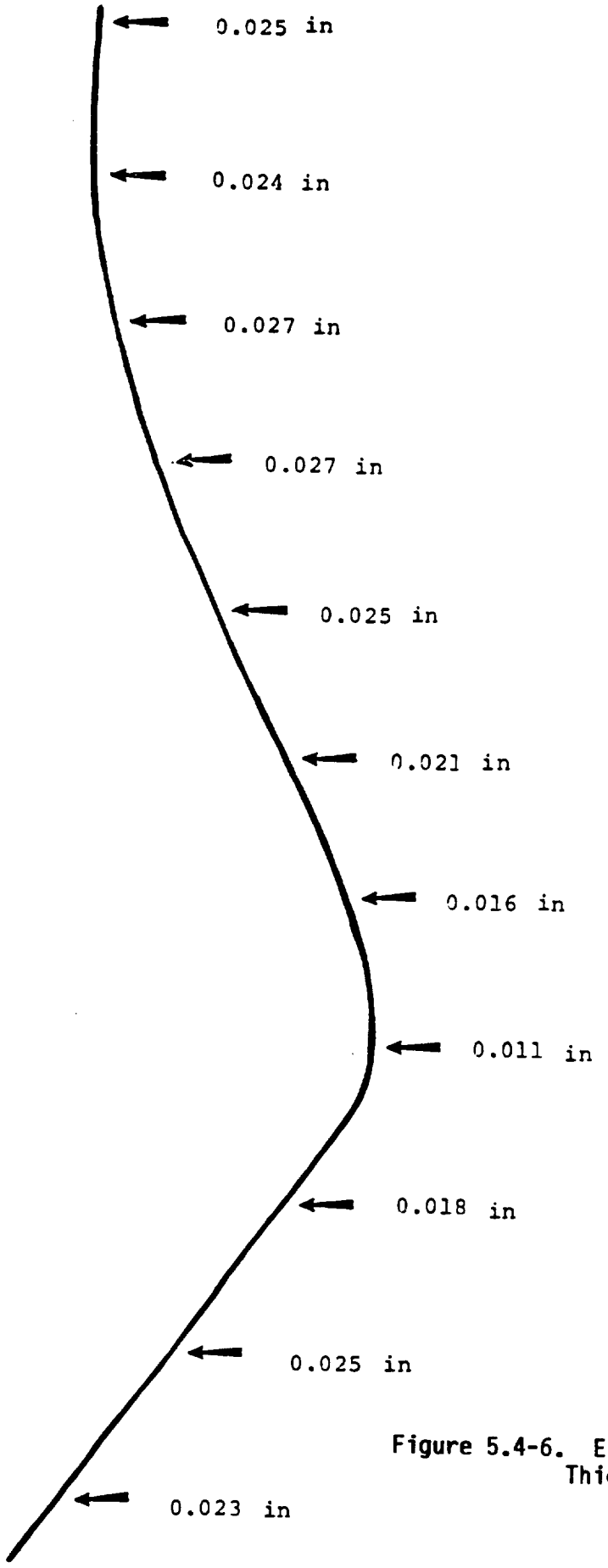

Figure 5.4-6. EF Alloy Specimen No. MCC-02 Thickness Profile

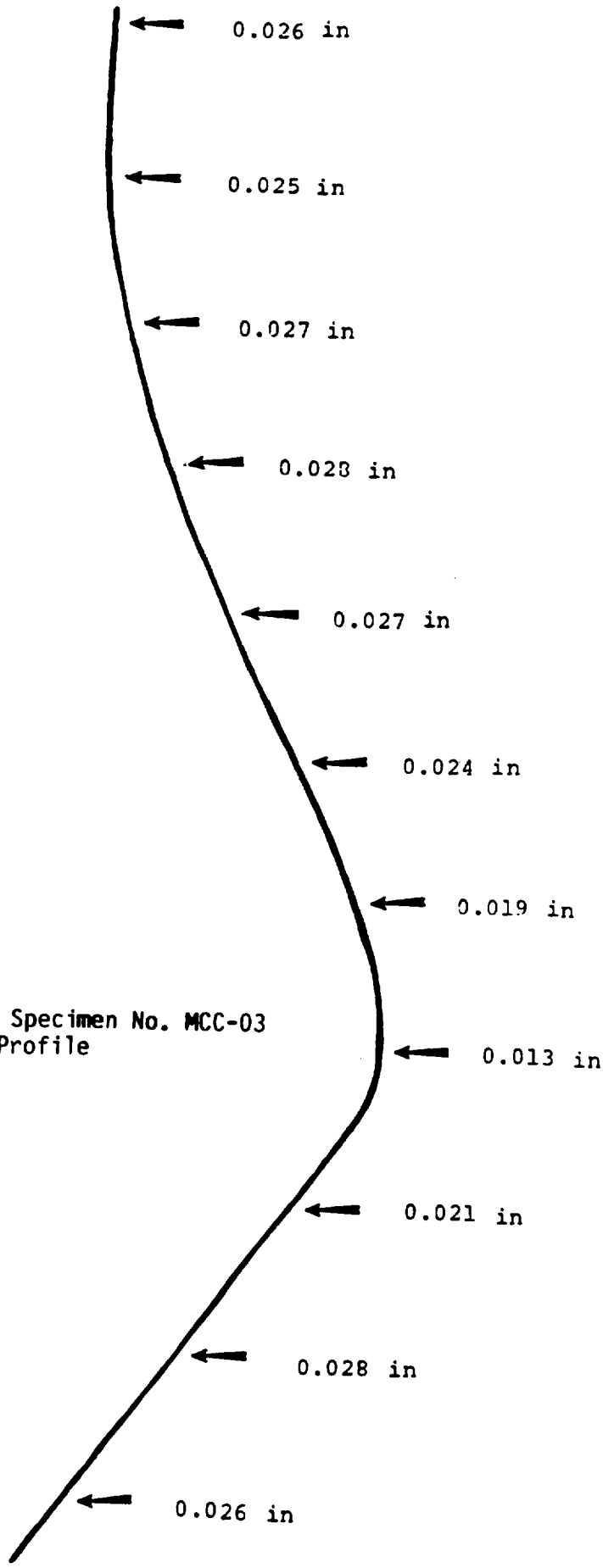

Figure 5.4-7. EF Alloy Specimen No. MCC-03 Thickness Profile

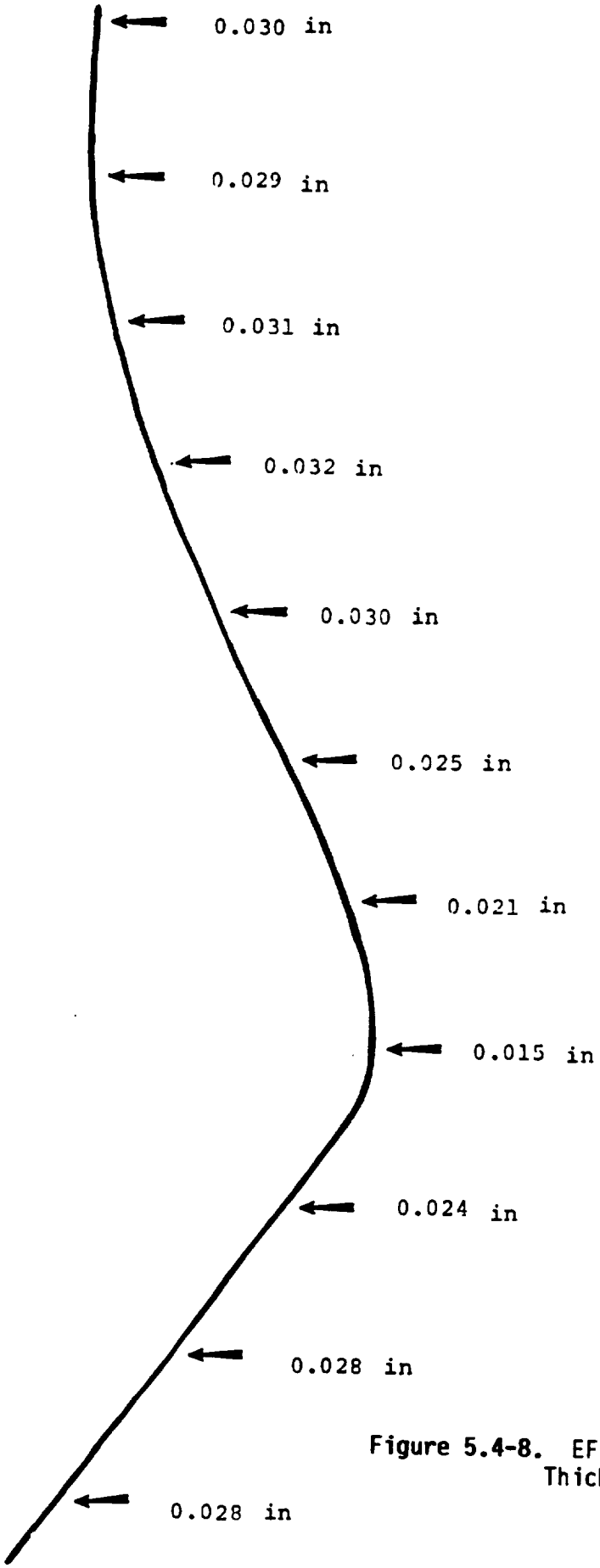

Figure 5.4-8. EF Alloy Specimen No. MCC-04 Thickness Profile

this lack of significant improvement to be due to increased resistance imposed on the small shielded anodes by the smaller boxed openings which may have caused a larger proportion of current from these anodes to flow from the back-side openings facing the tank walls.

In order to improve the thickness distribution obtained from a prototype alloy jacket, MCC-5 was electroformed under a modification in the anode distances. The four small shielded anodes were placed 8.9 cm (3.5 in.) closer to the mandrel, resulting in an overall distance of 25.4 cm (10.0 in.) from the anode basket to the vertical axis of the MCC mandrel. This decreased the distance between nickel chips and the mandrel throat to 15.24 cm (6 in.) while a 2.54 cm (1 in.) separation was maintained between the shielding boxed opening and the mandrel throat. The four large anodes were all placed approximately 8.3 cm (3.25 in.) further away from the mandrel, resulting in an overall distance of 53.3 cm (21.0 in.) from the anode to the vertical axis of the MCC mandrel. Mandrel shielding remained the same as that used in the previous three trials.

As in previous trials, the nickel manganese alloy bath was operated at 48.9°C (120°F), a pulse plating duty cycle of 64%, electrolyte sprays positioned near the tank walls, and a cathode rotational speed of 8 rpm. Pulsed Power Supply No. 1 and Pulsed Power Supply No. 2 were both operated at 1.94 A/dm^2 (18.0 A/ft^2) resulting in an overall average current density of 2.15 A/dm^2 (20.0 A/ft^2). These were the parameters used to electroform Cylinder 120-5 from which acceptable mechanical properties were obtained.

Figure 5.4-9 shows the profile electroformed with the thickness distribution indicated. The ratio between thickest section and thinnest section on the last prototype alloy jacket electroformed (MCC-4) was 2.13 to 1. The thickness ratio improved considerably on this trial to that of 1.65 to 1.

In an attempt to further improve the thickness distribution, MCC-6 was electroformed with a change in the power supply current outputs. Power Supply No. 1, which drives the four large anodes, was decreased from 18.0 amperes to 13.0 amperes. Power Supply No. 2, which supplies current to the shield anodes plating primarily at the mandrel throat, was increased from 18.0 amperes to 23.0 amperes. All other bath parameters, mandrel shielding, anode shielding, and anode distances from the mandrel remained the same. Figure 5.4-10 shows the profile electroformed with the thickness distribution indicated. The thickness ratio improved to 1.56 to 1 with this trial.

Bringing the small shielded anodes in closer to the mandrel throat provided the most improvement on the thickness distribution for the alloy jacket. The next prototype alloy jacket, MCC-7 was electroformed with a decrease in the distance between the shielded nickel anodes and the mandrel throat. Since the shielded anodes could not be moved any closer to the MCC mandrel, this was accomplished by extending the nickel chips into the boxed openings. The nickel chips were extended 7.62 cm (3 in.) closer to the throat of the mandrel by filling the 7.62 cm (3 in.) by 7.62 cm (3 in.) boxed extension section with nickel anode chips. Figures 5.4-11 shows a cross-sectional view of one of the shielded anode baskets with the nickel chips in the extension. When the anodes were placed in the bath around the mandrel there was

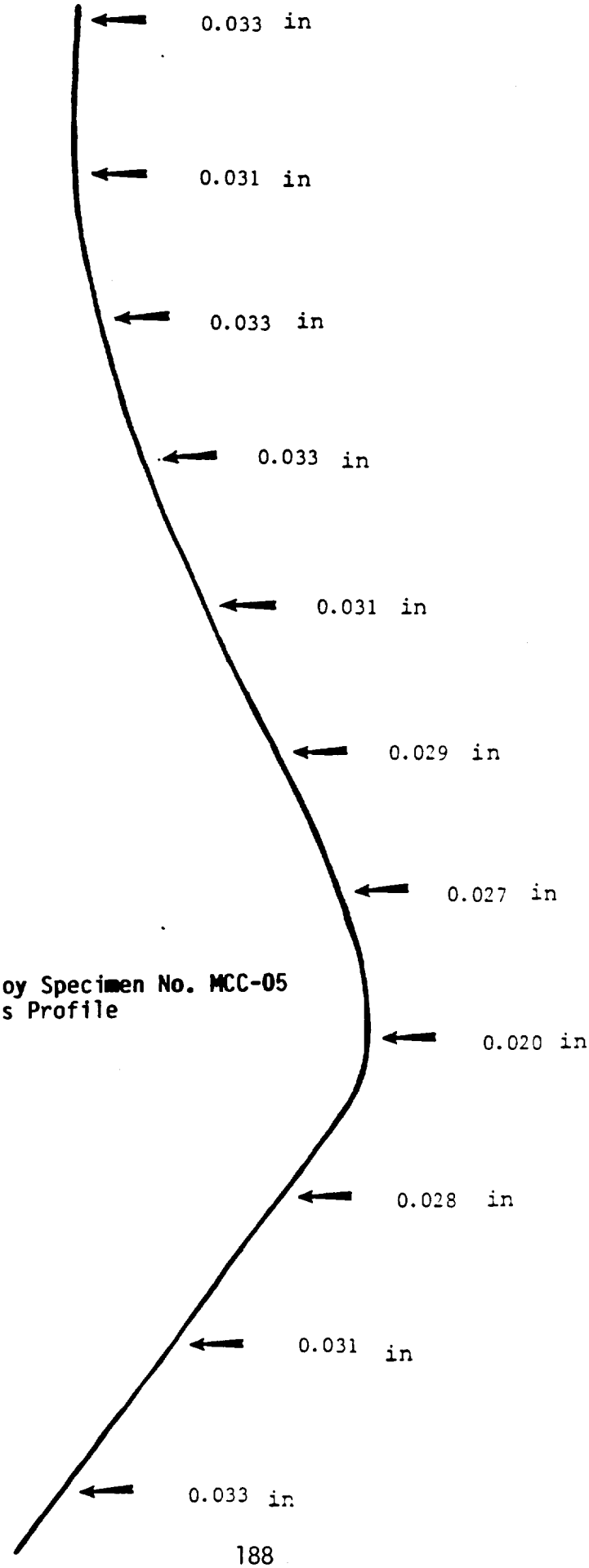

Figure 5.4-9. EF Alloy Specimen No. MCC-05
Thickness Profile

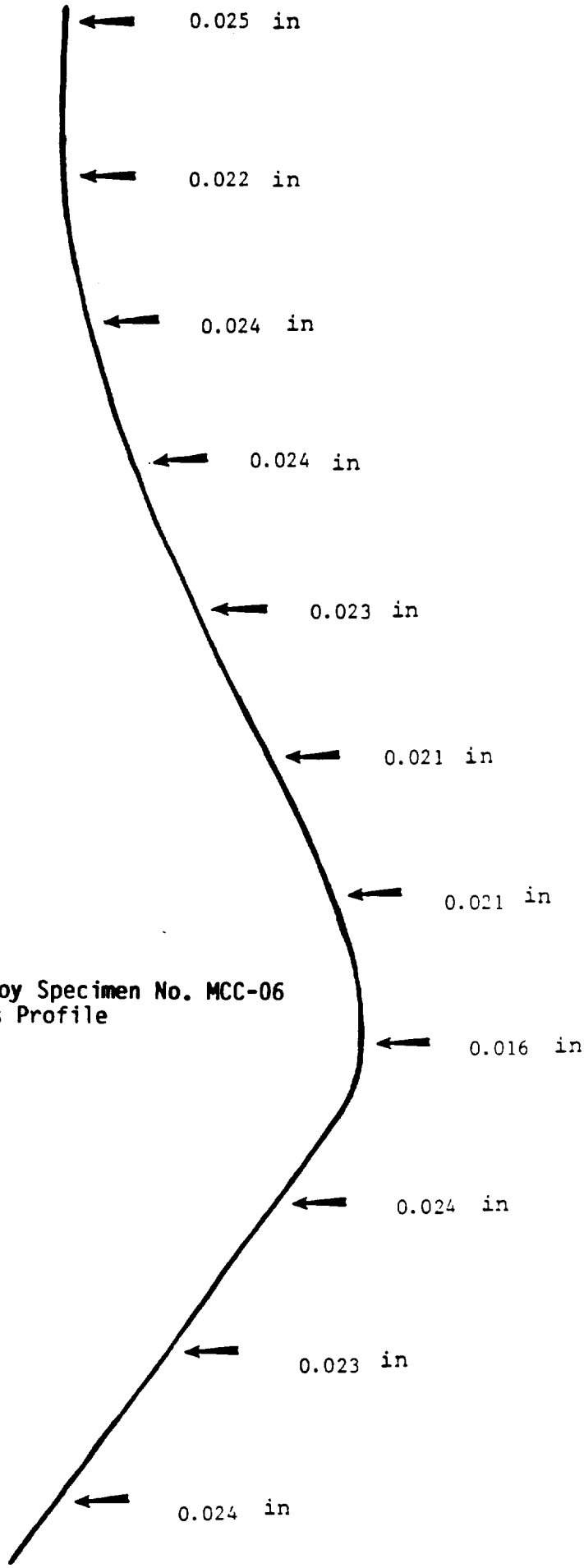

Figure 5.4-10. EF Alloy Specimen No. MCC-06 Thickness Profile

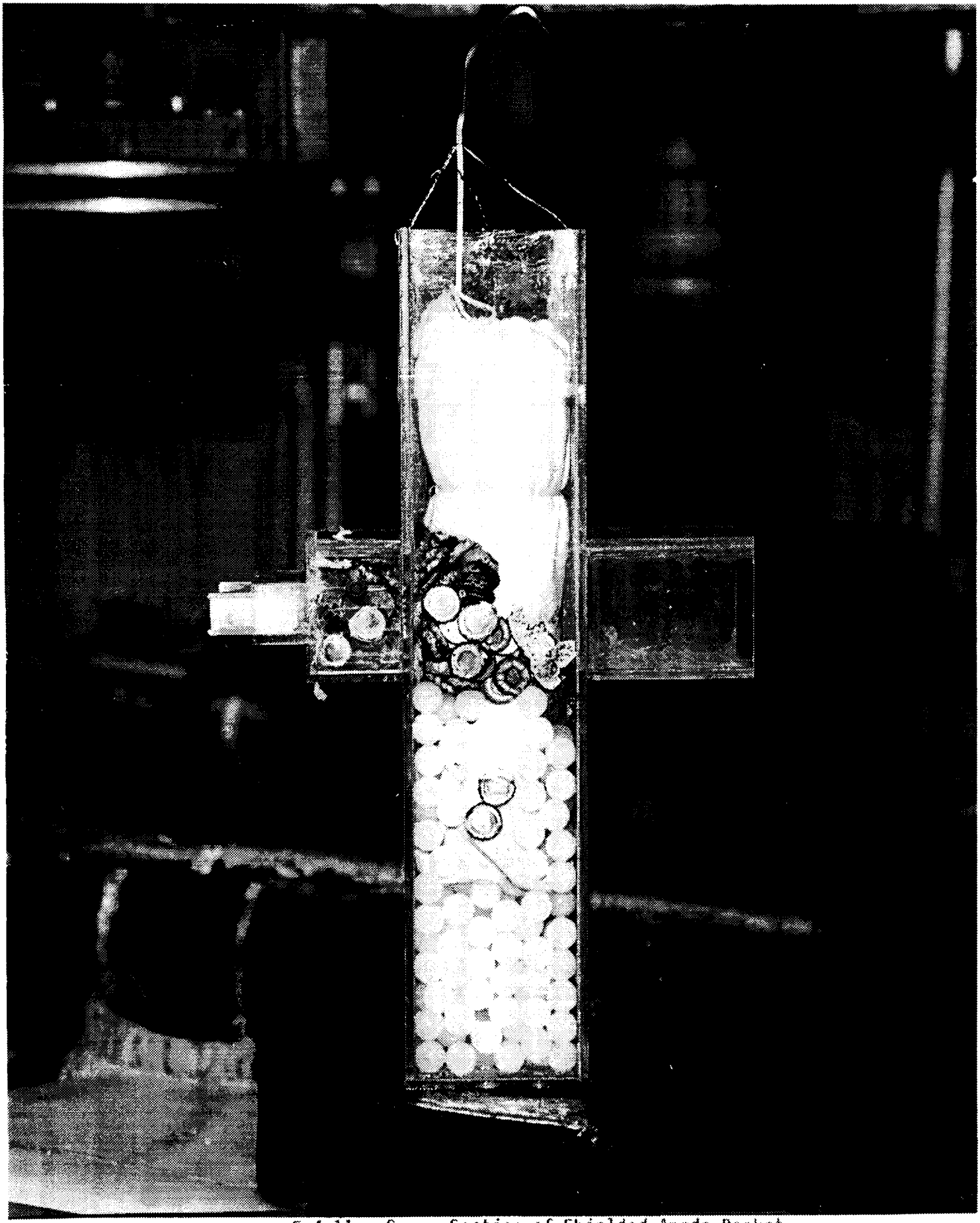

Figure 5.4-11. Cross Section of Shielded Anode Basket

only a 7.62 cm (3 in.) gap between the nickel chips (anode) and the throat of the mandrel (Cathode). Beyond the nickel chips was the 2.54 cm (1 in.) high by 7.62 cm (3 in.) wide plexiglas boxed extension which stopped 1.91 cm (3/4 in.) from the mandrel throat. All other bath parameters, mandrel shielding, anode shielding, anode distances from the mandrel, and power supply current outputs remained the same. Figure 5.4-12 shows the profile electroformed with the thickness distribution indicated. The thickness ratio improved to 1.43 to 1 with this trial. It can also be noted that for the first time the thinnest section was not at the mandrel throat. Also indicated in Figure 5.4-12 is the distribution of manganese deposition and the approximate Rockwell Hardness number on the C scale as obtained from a 10 kg Vickers Hardness Test.

In a final attempt to further improve the thickness distribution along with the manganese and hardness distribution, MCC-8 was electroformed. The only change that was made was to the 2.54 cm (1 in.) high by 7.62 cm (3 in.) wide by 5.72 cm (2-1/4 in.) long extension that extended to within 2.54 cm (1 in.) of the mandrel throat. The square window opening was replaced with a plexiglas insert that was contoured in order to follow the shape of the cylindrical mandrel throat. The top and bottom of this opening were also contoured independently so that they imaged the forward and aft end of the MCC mandrel. This allowed for the opening to be equally distanced from the MCC mandrel along the equal potential lines of plating.

Figure 5.4-13 shows the shielded anode used with the new extension and Figure 5.4-14 shows a close-up of the plexiglas insert used to extend close to the mandrel throat. Figure 5.4-15 shows the profile electroformed with the thickness, manganese, and hardness distribution indicated. The thickness ratio (ratio between the thickest and thinnest sections) improved once again to that of 1.30 to 1. This thickness distribution is twice as good as that of the first trial run. The distribution of manganese along with the hardness distribution along the cross-section of the MCC shroud also improved considerably to a more uniform distribution. For the first time the amount of manganese deposited at the throat and the hardness at the throat is actually higher than in most other areas.

These results show that the thickness, manganese concentration and hardness of the alloy at the throat of the shroud can be brought up consistent with the forward and aft ends. The evolution of the shielded anodes indicates that custom built conformal anodes need to be used to plate at the throat section of the MCC. This along with a fine tuning of the other bath and shielding parameters would provide for a SSME MCC with uniform thickness, composition, microstructure, tensile strength and hardness.

5.5 Task IV - Design Change Considerations

5.5.1 Introduction

The design change recommendations were prepared on the premise that the suggested options would be equally applicable to advanced engine designs - as well as SSME Main Combustion Chamber. The design of the structural jacket allowing for the substitution of electroformed nickel-manganese alloy for the

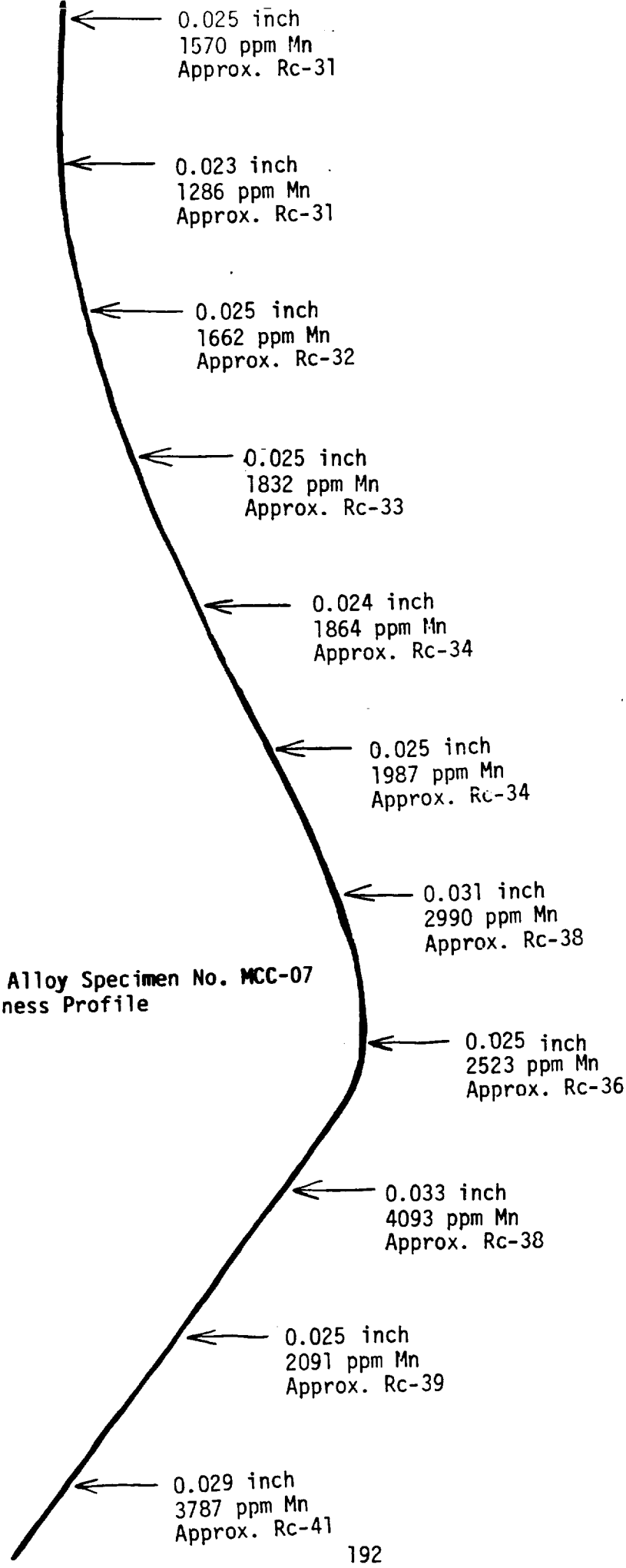

Figure 5.4-12. EF Alloy Specimen No. MCC-07 Thickness Profile

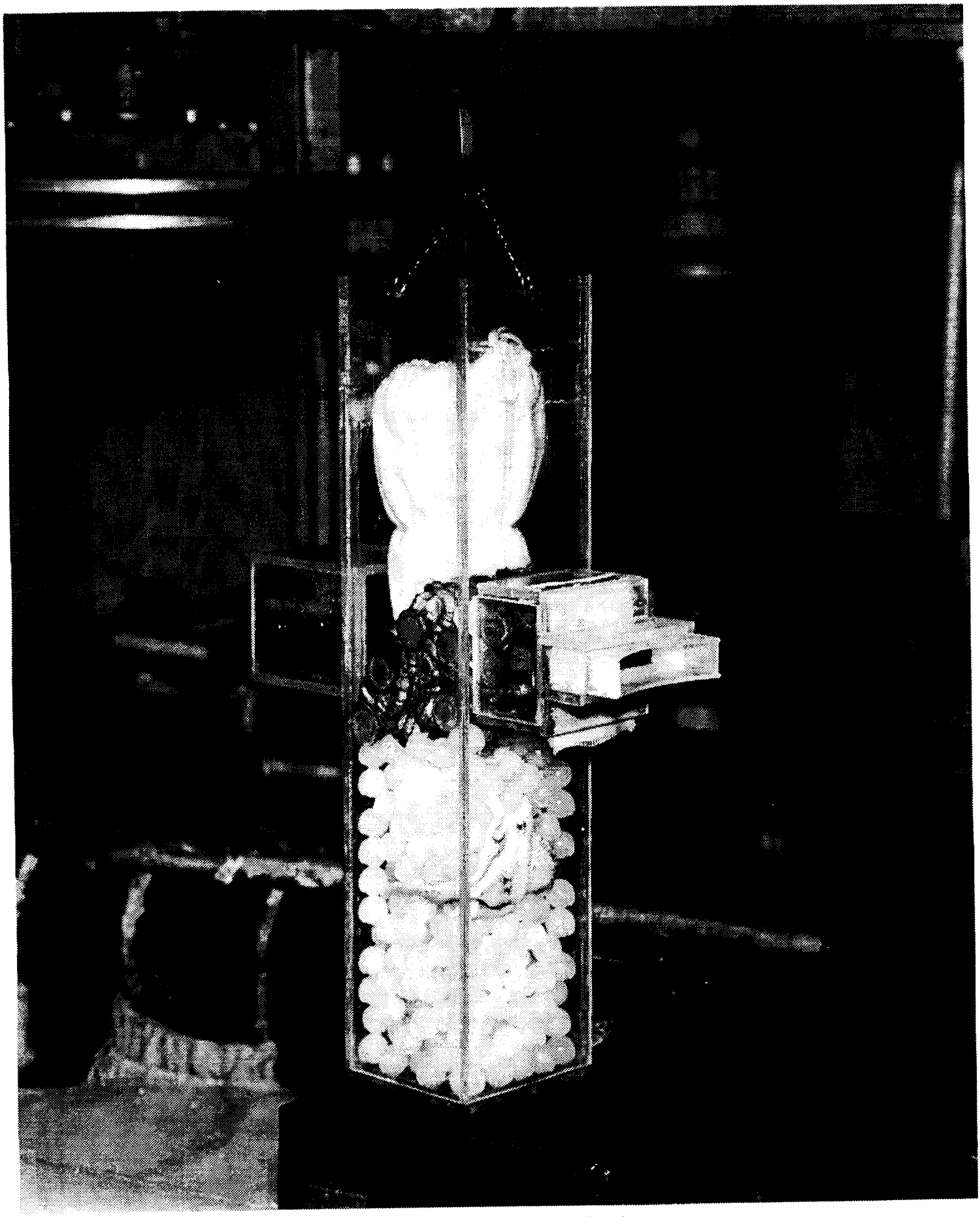

Figure 5.4-13. Shielded Anode Basket

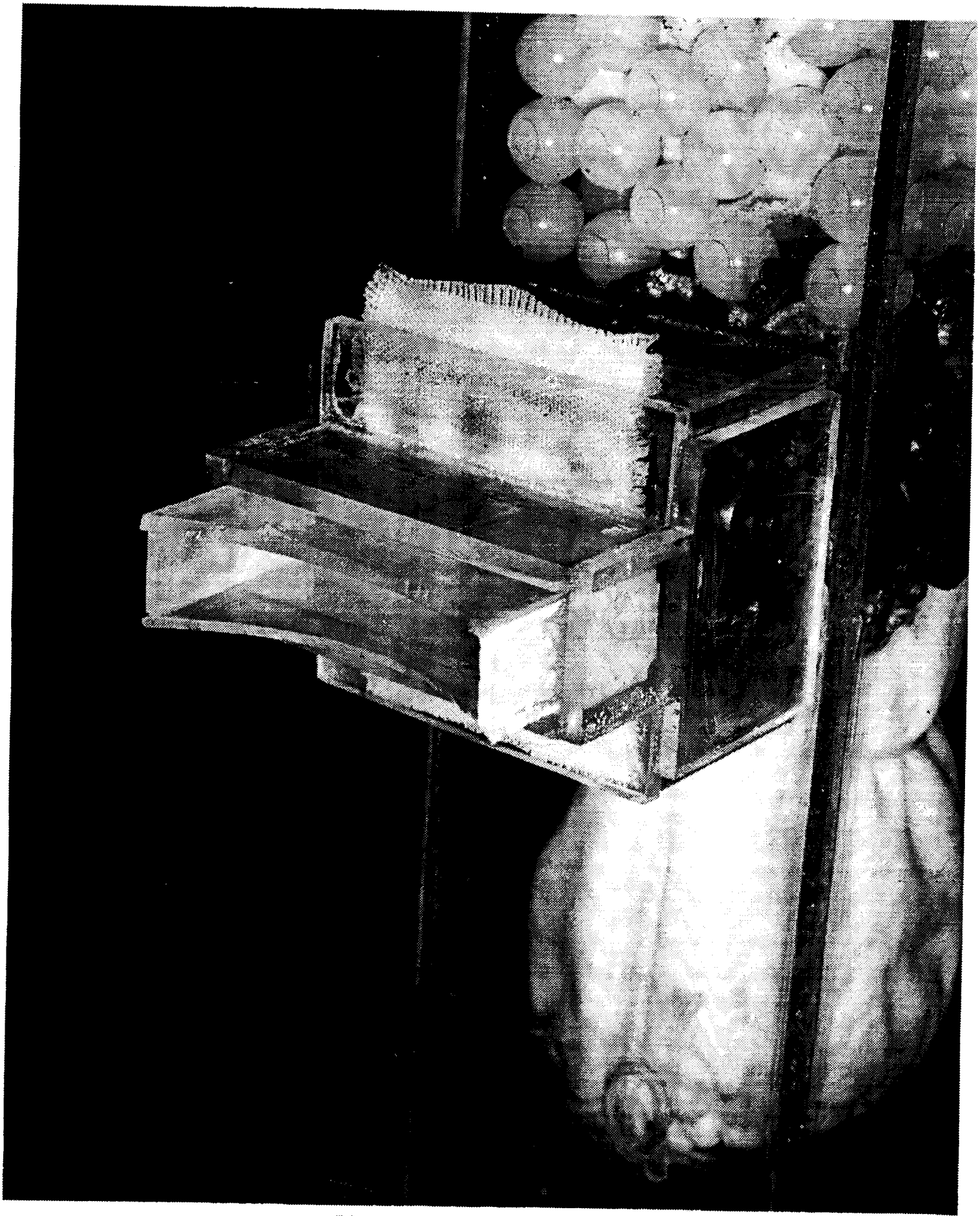

Figure 5.4-14. Plexiglas Insert

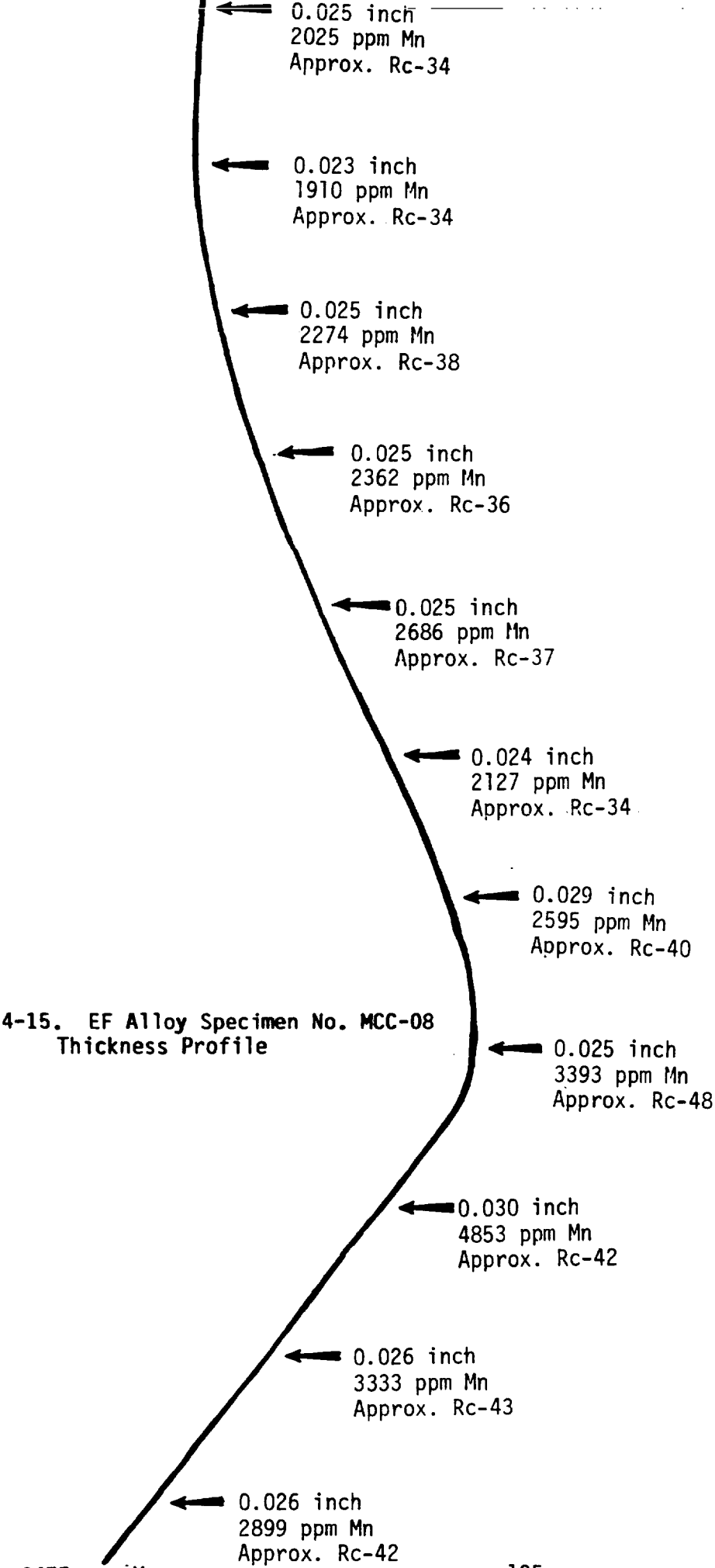

Figure 5.4-15. EF Alloy Specimen No. MCC-08 Thickness Profile

presently used Inconel 718 would partially depend on what material had been used to close out the cooling passages on the Main Combustion Chamber (MCC). At present this close-out consists of a thin hydrogen barrier of electroformed copper followed by a thicker (approximately 0.33 cm) layer of conventional electroformed nickel. If the conventional nickel were replaced with the currently considered electroformed nickel-manganese, the structural requirements of the structural jacket would be diminished to some degree.

There appears to be two general design options for the structural jacket using electroforming as the primary fabrication technique. Each option involves processing sequences and the order in which they are applied.

5.5.2 Option No. 1

The outer cylindrical portion of the current jacket design does not offer any serious problems in that anode-cathode distances are constant from top to bottom. The conformal (inner) member varies continuously in anode-cathode distance. The use of single conformal anodes in an array would provide an inner member of reasonably uniform thickness. However, as the mandrel (MCC) on which the jacket is being electroformed is rotated, there is a difference in surface velocity at different stations. For example, the surface velocity at the MCC throat region compared to the aft end of the nozzle is the ratio of the diameters at these same stations. This means that there is a difference in turbulence and the amount of manganese codeposited. If an array of single conformal anodes were used, it would be necessary to develop a complex spray manifold to compensate for the different turbulences developed at each station. This system would permit use of the present design without the need to increase material thickness at any region to compensate for welds and subsequent heat affected zones.

Conversely, the current design (excluding any extra thicknesses for heat affected zones) could be used with a general electrolyte spray from a remote location if two or more conformal anode arrays were used which could be operated independently. For example, one array would be shaped and positioned to feed pulsed current only to the throat region. A second (or second and third) array would be shaped and positioned to supply pulsed current to the chamber and nozzle areas of the MCC. Power supplies operating each anode array would be pulse synchronized, but each would be capable of operating to supply separate currents to better control current density and desired manganese levels in the deposits. Since manganese concentration in the deposit is not the single factor in achieving the desired mechanical properties (stoichiometric ratios in lattice cells appear to be more influential), the current densities from the two pulse power supplies may still necessarily be different. This would mean that the build up at the nozzle or chamber end might be complete before the desired throat thickness is achieved. In this event, the throat build-up could be continued using the appropriate controlling power supply for some period of time after the other power supply was shut down. A machining step would then restore the required thickness to the entire length of the inner (conformal) part of the jacket. The outer (cylindrical) shell would be added as a simple electroform on top of a wax mandrel cast over the inner codeposit.

5.5.3 Option No. 2

This method would require a design change and is favored because it accommodates the solutions necessary to the problems of variable current density which so often trouble alloy electroforming. This option involves staged type electroforming and greatly reduces the problems of low current density in regions such as the throat of the MCC jacket. In the first stage, Figure 5.5-1, the top and bottom portions of the MCC are masked to prevent deposition, and only the throat is exposed. Anode-cathode distance deviation is reduced so that current density variations are not significant. This permits greater thicknesses to be deposited without greatly differing mechanical properties. In the second stage a straight cylindrical section can be deposited to strengthen the throat part of the shroud. By electroforming two cylindrical sections, each cylinder thickness can be decreased to provide equivalent strength. The advantage in this approach is the thinner walls do not have excessive accumulated internal stress which might cause premature cracking or distortion before heat treating. The cylinder wall is deposited on machinable wax which is conductivized with silver powder. A small hole(s) is drilled into the wall to melt out the wax.

In the third stage the throat cylinder section is masked (except at the edges where bonding is desired). Top and bottom shields are applied, and the top and bottom portions of the conformal part of the jacket are electroformed. Regions requiring bonding to the MCC close-out shell are masked, and a thin layer of alloy (about 0.127 mm) is deposited. The masking at the areas to be bonded is removed. The entire exposed surface is activated for bonding and the electroforming continued. In the final (fourth) stage, a cylinder is electroformed over conductivized wax to support the upper and lower parts of the shroud. An added advantage of this design concept is the fact that the thicknesses of the conformal portion of the jacket and the two cylindrical sections can be varied to provide the strongest structure utilizing the least weight.

6.0 CONCLUSIONS AND RECOMMENDATIONS

This study has demonstrated that an electroformable alloy of nickel-manganese can be deposited in complex shapes to provide vastly superior mechanical properties to those obtainable with conventional electroformed (EF) nickel (Figure 6.0-1). Although the mechanical strength obtained is not superior to that of the complex chemistry superalloy Inconel 718, the electroformed alloy can be produced with strength equivalence to Inconel 718 for test temperatures as high as 260°C (500°F). This makes applications to hardware such as the structural jacket of the Main Combustion Chamber (MCC) on the Space Shuttle Main Engines of practical significance.

EF nickel-manganese alloys generally do not have optimum mechanical properties as deposited; however, they respond to moderate heat treatments that are expected to be compatible to hardware integrity of the SSME (or other advanced engine hardware) in which they might be used. These alloys are susceptible to hydrogen embrittlement, and direct exposure to pressurized hydrogen coolants in cryogenic engines should be avoided where possible.

EF nickel-manganese alloy can be bonded to itself, to conventional nickel, to EF copper, and to Inconel 718 in the age-hardened condition. This permits easily staged electroforming sequences for complex hardware build-up in which electroforms can be joined to electroforms or to wrought metal components. Another favorable factor in the electroformable alloy is the weldability without experiencing cracking, loss of ductility, or abnormally high loss of strength from excessive grain growth.

Disadvantages in the alloy exist in the sensitivity to stress and low ductility when electroforming parameters are not within an optimum range. These problems can be avoided by carefully planned electroforming stages or use of several independently controlled anode arrays. Pulsed deposition appears to enhance mechanical properties by enabling complex electrochemical reactions to occur at the cathode surface. Excessive electrolyte turbulence must be avoided during the electroforming process to avoid localized high tensile stresses and possible formation of internal defects such as cracks. Use of stress reducing additives, especially when pulse electroforming, is not recommended. Slow rotation of the part being electroformed appears to provide suitable electrolyte agitation and cathode diffusion layer control.

The electroforming of this alloy in complex geometries can be accomplished by two general techniques:

1. Complex surface shapes can be theoretically divided into regions of similar anode-to-cathode distance and separately powered arrays of anodes used for each region. Conformal anodes can be used provided the proximity of the array nearest to the cathode does not create a solution turbulence problem which would affect manganese codeposition. Where separate anode arrays are used with independent power supplies, pulse plating can be used by electronically synchronizing the power supplies. Each power supply can be used to supply a different level of pulsed current to independently control current density (and alloy composition) for each region of the electroform served by a separate anode array.

2. The electroform can be analyzed as to logical areas (or sections) which individually have some common factor to make deposition more simplistic. For example, the throat section of a thrust chamber is analogous to a narrow circular band or region of low current density. By isolating the first electroforming stage to this region (as suggested in Section 5.5), many of the problems of current density variation and solution agitation effects can be minimized to produce the required structural properties. This analysis and regional isolation is made step-by-step until the entire part is electroformed as a single continuous structure.

It is recommended that investigation of the electroformable alloy be continued with emphasis on applying the two general techniques for complex geometries and developing further process details essential to electroforming actual hardware. Details concerning the superiority of one technique over the other (or when one technique should be used in preference to the other) could be better defined.

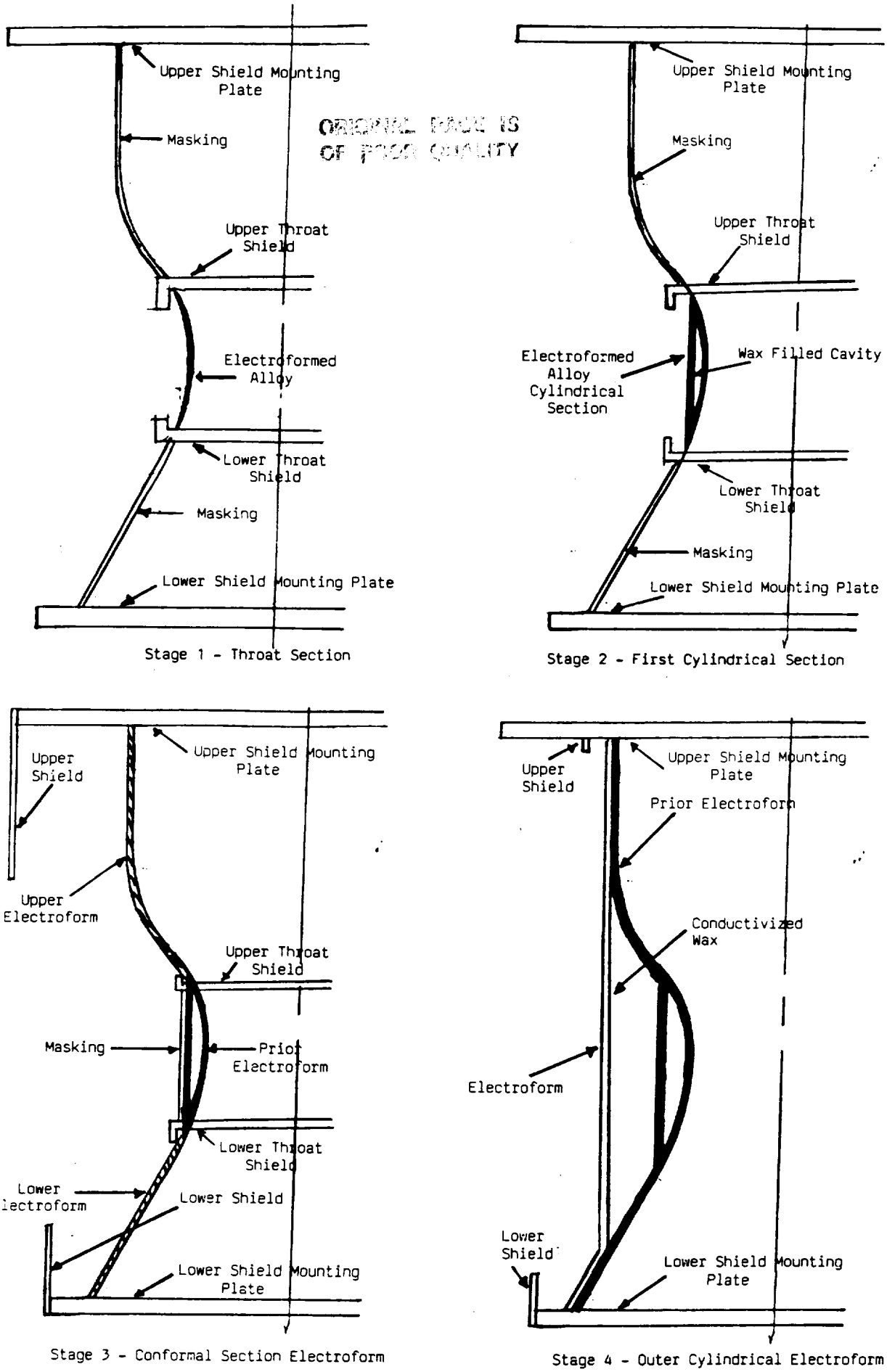

Figure 5.5-1. Design Change for Multi-Stage Electroforming of Shroud

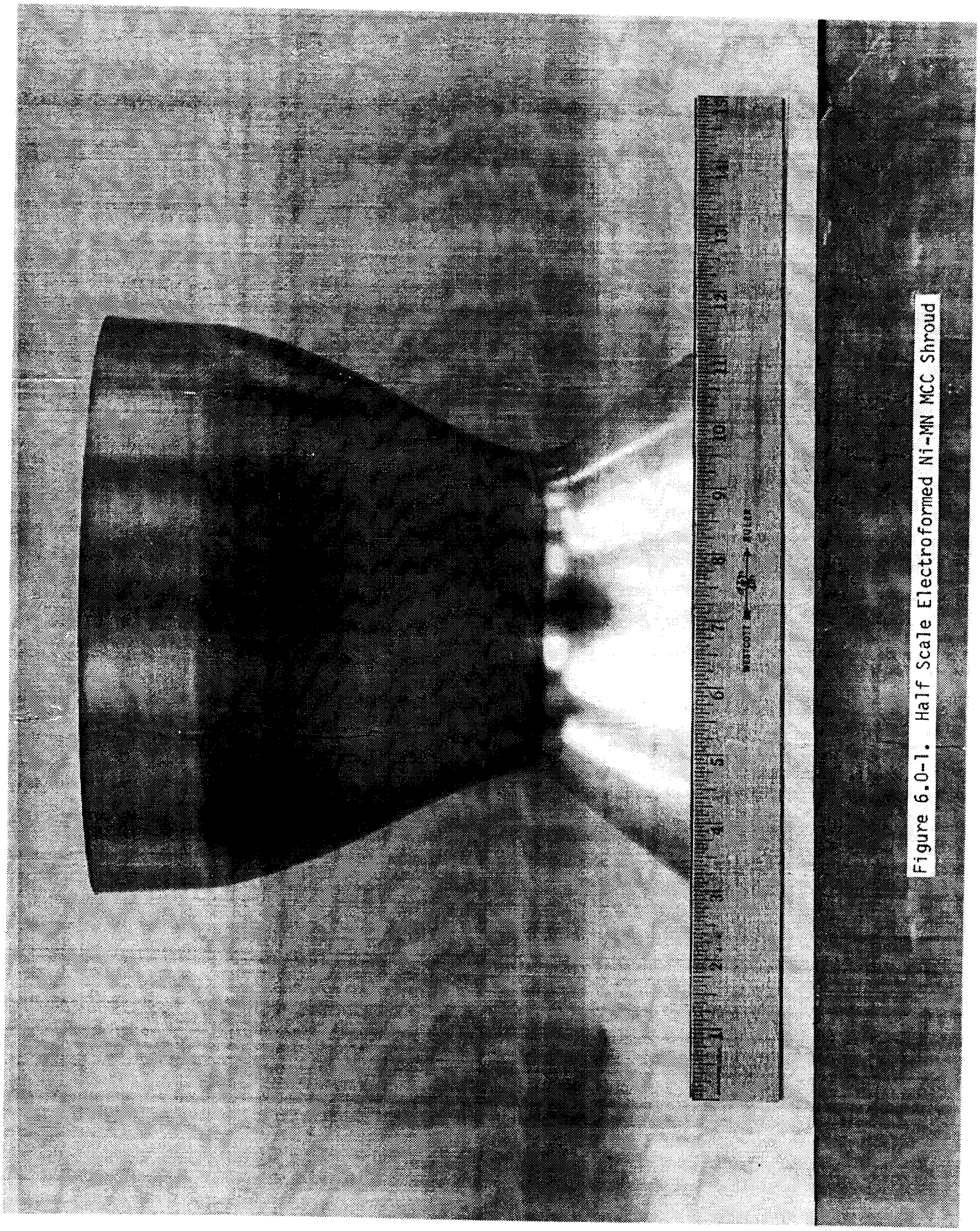

Figure 6.0-1. Half Scale Electroformed Ni-MN MCC Shroud

7.0 REFERENCES

(1) Diggen, M. B., "Modern Electroforming Solutions and Their Applications", ASTM Special Technical Publication No. 318 (1962) pp. 10-26.

(2) Savage, F. K. and Bommerscheim, C. H., "Electroforming Supersonic Pitot-static Tubes", ASTM Special Technical Publication No. 318 (1962) pp. 150-158.

(3) International Nickel Company, "Nickel Plating - Processes and Properties of Deposits (1967).

(4) Brenner, A.; Jennings, C. W.; and Zentner, V., "Physical Properties of Electrodeposited Metals - 1. Nickel", American Electroplater's Society Research Report Serial No. 20 (1952).

(5) ASTM Committee B-8, "Recommended Practice for Use of Copper and Nickel Electroplating Solutions for Electroforming", American Society for Testing and Materials Specification B503-69 (1969).

(6) Safranek, W. H., The Properties of Electrodeposited Metals and Alloys, American Elsevier Publishing Company, New York, NY (1974).

(7) Jenkins, W. D.; Digges, T. G.; and Johnson, C. R., "Tensile Properties of Copper, Nickel, and 70-Percent-Copper-30-Percent-Nickel and 30-Percent-Copper-70-Percent-Nickel Alloys at High Temperatures", Journal of Research of the National Bureau of Standards, 58:4, pp. 201-211 (April 1957).

(8) Sample, C. H. and Knapp, B. B., "Physical and Mechanical Properties of Electroformed Nickel at Elevated and Subzero Temperatures", ASTM Special Technical Publication No. 318 (1962) pp. 32-43.

(9) Greenwood, J.D., Heavy Deposition, Robert Draper, Ltd., Teddington, England (1970).

(10) Safranek, W. H., The Properties of Electrodeposited Metals and Alloys, American Elsevier Publishing Company, New York, NY (1974), p. 242.

(11) Yang, L., "Electrolytic Hexagonal Nickel", Journal of the Electrochemical Society, 97:8, pp. 241-244 (August 1950).

(12) Lowenheim, F. A., Modern Electroplating, 3rd Ed., John Wiley and Sons, New York, NY (1963), p. 316.

(13) Struyk, C. and Carlson, A. E., "Nickel Plating from Fluoborate Solutions", Plating 37, pp. 1242-1246, 1263-1264.

(14) Barrett, R. C., "Nickel Plating from the Sulfamate Bath", Plating 41, pp. 1027-1033 (September 1954).

(15) Asher, R. K. and Harding, W. B., "Mechanical Properties of Electroformed Nickel Produced in Sulfamate Solutions", Plating 49, pp. 783-788 (July 1962).

(16) Klingenmaier, O. J., "The Effect of Anode Efficiency on the Stability of Nickel Sulfamate Solutions", Plating 52, pp. 1138-1141 (November 1965).

(17) Knapp, B. B., "Notes on Nickel Plating from Sulfamate Solutions", Plating 58, pp. 1187-1193 (December 1971).

(18) Rocketdyne Division of North American Rockwell, "Nickel Sulfamate Electrolyte (Concentrate)", September 1974, private correspondence.

(19-20) Rocketdyne Division of North American Rockwell, "Electrodeposited Nickel, Structural", September 1974, private correspondence.

(21) Rocketdyne Materials Bulletin RA1609-017, "Electrodeposited Nickel, Class B", March 1974, private correspondence.

(22) Rocketdyne Division of North American Rockwell, "Tensile Strength - ED Nickel from Space Shuttle Main Combustion Chamber Samples", 4 September 1974, private communication from Mr. G. A. Fairburn, Rocketdyne to Mr. G. A. Malone, Bell Aerospace Textron.

(23) Dederra, H. and Seidel, A., "Typical Mechanical Properties of Sulfamate Nickel Deposits - Messerschmitt-Bolkow-Blohm", private communication to Mr. W. Gisel, Bell Aerospace Textron (September 1974).

(24) Safranek, W. H., The Properties of Electrodeposited Metals and Alloys, American Elsevier Publishing Company, New York, NY (1974), pp. 272-274.

(25) DiBari, G. A., "Nickel Plating", Metal Finishing Guidebook 52d Ed, Metals and Plastics Publications, Inc., Hackensack, NJ (1984) pp. 278-284.

(26) Pinkerton, H. L., and Carlin, F. X., "Electroforming", Electroplating Engineering Handbook 3d Ed, A. K. Graham (Editor), Van Nostrand Reinhold Company, New York, NY (1971), pp. 523-524.

(27) Kura, J. G.; Barth, V. D.; Safranek, W. H.; Hall, E. T.; McCurdy, H.; and McIntire, H. O., "The Making of Nickel and Nickel-Alloy Shaped by Casting, Powder Metallurgy, Electroforming, Chemical Vapor Deposition, and Metal Spraying", NASA Technical Memorandum NASA TWX 53430, pp. 134-155 (October 1965).

(28) Technical Bulletin, "Electroforming with Nickel", International Nickel Company, Inc. (1964).

(29) Fialkoff, S. and Hammer, S. S., "Development of Electroforming Techniques for the Fabrication of Injectors", Final Report, NASA Contract NAS 9-6177 (May 1967).

(30) Hanson, T. N.; Dupree, D. G.; and Lui, K., "Structural Electroforming - Applications and Developments", Plating 55, pp. 347-350 (April 1968).

(31) Such, T. E., "The Physical Properties of Electrodeposited Metals", Metallurgia 56, pp. 61-66 (August 1957).

(32) McCandless, L. C. and Davies, L. G., "Development of Improved Electroforming Techniques", Final Report - NASA CR134480 (November 1973).

(33) Malone, G. A.; Vecchies, L.; and Wood, R., "Nondestructive Tests of Regenerative Chambers", Final Report - NASA - CR-134656 (June 1974).

(34) Malone, G. A., "Investigation of Electroforming Techniques", Bell Aerospace Textron Report No. D8756-953001 (April 1974).

(35) Moeller, C. E. and Schuler, F. T., "Tensile Behavior of Electrodeposited Structure", SAMPE Space Shuttle Materials Conference, October 5-7, 1971, Huntsville, Alabama.

(36) "Inconel 718", Engineering Alloys Digest, Upper Montclair, NJ, Sheet No. Ni-65, April 1961.

(37) Brenner, A., Electrodeposition of Alloys, Vol II, Academic Press, New York, NY (1963), pp. 137-149.

(38) Stephenson, W. B. (Jr.), "Development and Utilization of a High Strength Alloy for Electroforming", Plating 53:2, pp. 183-192 (February 1966).

(39) United States Patent No. 3,244,603, "Electrodeposition of a Nickel-Manganese Alloy", April 5, 1966.

(40) Dini, J. W.; Johnson, H. R.; and Helms, J. R., "High Strength Nickel-Cobalt Deposits for Electrojoining Applications", Report SCL-DR-720090, Sandia Laboratories, Livermore, California, pp. 27-28 (March 1973).

(41) Dini, J. W., and Johnson, H. R., "High-Temperature Ductility of Electrodeposited Nickel", Report SAND77--8020, Sandia Laboratories, Livermore, California, pp. 15-24 (July 1977).

(42) Wearmouth, W. R. and Belt, K. C., "Electroforming with Heat-Resistant, Sulfur-Hardened Nickel", Plating and Surface Finishing 66:10, pp. 53-57 (October 1979).

(43) Dini, J. W.; Johnson, H. R.; and West, L. A., Plating and Surface Finishing 65:2, p. 36 (February 1978).

(44) Patent Specification 1,524,748 (United Kingdom), "Improvements In or Relating To the Production of Hard, Heat-Resistant Nickel-Base Electrodeposits", Inventor: W. R. Wearmouth (13 September 1978).

(45) United States Patent 4,108,740, "Hard, Heat-Resistant Nickel Electrodeposits", W. R. Wearmouth, Assigned to International Nickel Company, New York, NY (August 22, 1978).

(46) Lichtenberger, J., "High Temperature Electroformed Metal Characterization", Independent Research and Development Project No. 8007, Bell Aerospace Textron Report No. 0500-927015, March 31, 1980.

(47) Malone, G. A., "Improvement of High-Temperature Mechanical Properties in Nickel-Manganese Electrodeposits", Independent Research and Development Project No. 8260, Bell Aerospace Textron Report No. 0500-927026, March 31, 1982.

(48) Malone, G. A., "Electroforming for Severe Environmental Conditions", Independent Research and Development Project No. 8360, Bell Aerospace Textron Report No. 0500-927040, March 31, 1983.

(49) Johnson, H. R.; Dini, J. W.; and Stoltz, R. E., "The Mechanical Properties of Sulfamate Nickel Electrodeposits", Report SAND77-8042, Sandia Laboratories, Livermore, California, pp. 20-21 (March 1978).

(50) Johnson, H. R.; Dini, J. W.; and Stoltz, R. E., "The Mechanical Properties of Sulfamate Nickel Electrodeposits", Report SAND77-8042, Sandia Laboratories, Livermore, California, p. 23 (March 1978).

(51) Brenner, A., Electrodeposition of Alloys, Vol II, Academic Press, New York, NY (1963) p. 239.

(52) Barrett, R. C., "Plating of Nickel, Cobalt, Iron, and Cadmium from Sulfamate Solutions", Proceedings of the American Electroplaters' Society, 47, p. 173 (1960).

(53) Walker, R. and Cruise, W., "The Use and Production of Electrodeposited Cobalt", Metal Finishing 76:6, pp. 45-47 (June 1978).

(54) Morral, F. R., "Electrodeposition of Cobalt", Metal Finishing 62:6, pp. 82-87 (June 1964).

(55) Endicott, D. W. and Knapp Jr., J. R., "Electrodeposition of Nickel-Cobalt Alloy: Operating Variables and Physical Properties of the Deposits", Plating 53:1, pp. 43-60 (January 1966).

(56) Brenner, A.; Zentner, V.; and Jennings, C. W., "Physical Properties of Electrodeposited Metals: I. Nickel", Plating 39, pp. 865-927 (1952).

(57) Hansen, M., Constitution of Binary Alloys, 2d Ed., McGraw-Hill Book Company, New York, NY (1958) pp. 485-486.

(58) McFarlen, W. T., "Electroformed Nickel-Cobalt Alloy Deposits: An Evaluation", Plating 57:1, pp. 46-50 (January 1970).

(59) Safranek, W. H., "A Survey of Electroforming for Fabricating Structures", Plating 53:10, pp. 1211-1216 (1966).

(60) Dini, J. W.; Johnson, H. R.; and Helms, J. R., "High Strength Nickel-Cobalt Deposits for Electrojoining Applications", Report SCL-dr-720090, Sandia Laboratories, Livermore, California, pp. 12-26 (March 1973).

(61) Belt, K. C.; Crossley, J. A.; and Kendrick, R. J., "Properties of Electrodeposits from a Concentrated Nickel Sulfamate Solution", Interfinish 68, Hanover, May 1968, pp. 222-228.

(62) Schuler, F. T., "Properties of Electrodeposited Nickel-Cobalt (22-50%) Alloys", International Conference on Metallurgical Coatings, San Francisco, California, April 5-8, 1976.

(63) Walter, R. J., "Alloy Plating", American Electroplaters' Society 66th Annual Technical Conference, Atlanta, Georgia, June 25, 1979.

(64) Bockris, J. O'M.; and Reddy, A. K. N., Modern Electrochemistry Vol. 2, Plenum Press (1976) pp. 1223-1227.

(65) Malone, G. A., "Electroforming Technology", Independent Research and Development Project No. 8460, Bell Aerospace Textron Report No. 0500-927052, March 31, 1984.

(66) Brenner, A., Electrodeposition of Alloys, Vol. II, Academic Press, New York, NY (1963), p. 345.

(67) Brenner, A., "The Transfer of Polarization in Induced Codeposition", Fall Meeting of the Electrochemical Society, Wrightsville, North Carolina (1953).

(68) Seim, H. J.; and Holt, M. L.,"The Electrodeposition of Molybdenum Alloys", Transactions of the Electrochemical Society 96:4, pp. 205-213 (1949).

(69) Frantsevich, I. N.; Frantsevich-Zabludovskaya, T. F.; and Zhelvis, E. F., "Electrolytic Production of Nickel and Molybdenum Alloys", Zhur. Priklad. Khim 25, pp. 350-361 (1952).

(70) Rama Char, T. L., Procedures of the American Electroplaters' Society 46, p. 80 (1959).

(71) Brenner, A., Electrodeposition of Alloys Vol II, Academic Press, New York, NY (1963), pp. 348-408.

(72) Gol'tz, L. N.; and Kharlamov, V. N., "Electrolytic Deposition of Alloys of Tungsten, Nickel, and Copper from Water Solutions", Zhur. Priklad. Khim. 9, pp. 640-652 (1936).

(73) Brenner, A.; Burkhead, P.; and Seegmiller, E., "Electrodeposition of Tungsten Alloys Containing Iron, Nickel, and Cobalt", Research Paper RP1834, Journal of Research of the National Bureau of Standards 39, pp. 351-383 (October 1947).

(74) Safranek, W. H., The Properties of Electrodeposited Metals and Alloys, American Elsevier Publishing Company, New York, NY (1974), pp. 75-80.

(75) Turns, E. W.; and Hildebrand, J. F., "Electroforming Refractory Metal Alloys", Proceedings of the American Electroplaters' Society 51, pp. 150-162 (1964).

(76) Browning, M. E.; and Turns, E. W., "Alloy Electroforming for High-Temperature Aerospace Applications", Symposium on Electroforming - Applications, Uses and Properties of Electroformed Metals, ASTM Special Technical Publication No. 318, pp. 107-121 (1962).

(77) Fraser, R. W.; Meddings, B.; Evans, D. J. J.; and Mackiw, V. N., "Dispersion-Strengthened Nickel by Compaction and Rolling of Powder Produced by Pressure Hydrometallurgy", 1965 International Powder Metallurgy Conference, New York, New York, June 14-17, 1965.

(78) Sautter, F. K., "Electrodeposition of Dispersion-Hardened Nickel-Al_2O_3 and Engineering Division, Watervliet, New York (February 1962).

(79) Lakshminarayanan, G. R.; Chen, E. S.; and Sautter, F. K., "The Effect of Oxide Dissolution on the Electrodepositing of Dispersion-Hardened Co and Ni-Al_2O_3 Alloys", Journal of the Electrochemical Society 122:12, pp. 1589-1594 (December 1975).

(80) Malone, G. A., "Electrodeposition of Dispersion Strengthened Alloys", Proceedings of the 1973 Symposium on Electrodeposited Metals for Selected Applications, Battelle Columbus Laboratories, Columbus, Ohio, MCIC Report 74-17, pp. 49-55 (April 1974).

(81) Mikhail and Fahim, "Thermal Treatment of Thorium Oxide Gel at Low Temperatures", Journal of Applied Chemistry 17 (May 1967).

(82) U.S. Patent No. 3,883,402, "A Process for Electroforming Nickel Containing Dispersed Thorium Oxide Particles Therein", G. A. Malone.

(83) Browning, M. E.; Leavenworth, Jr., H. W.; Webster, Jr., W. H.; and Dunkerley, F. J., "Deposition Forming Processes for Aerospace Structures", Technical Documentary Report No. ML-TDR-64-26, Final Report Under Contract AF 33(657)-7016, American Machine and Foundry Company, Alexandria, Virginia (January 1964), pp. 60-72.